



Europhysics
conference
abstracts



UNIVERSITY OF GOTHENBURG
Gothenburg Sweden 9-13 July 2012

EGAS



44th Conference of
the European Group
on Atomic Systems

Volume Editor

Dag Hanstorp, Gothenburg

Henrik Hartman, Malmö/Lund

Lars Engström, Lund

Hampus Nilsson, Lund

Sten Salomonson, Gothenburg

Volume number: 36 C

N° ISBN: 2-914771-75-4

Series editor: Prof. Pick, Paris

Managing editor: P. Helfenstein, Mulhouse

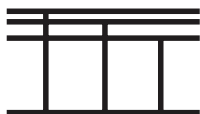


Europhysics
conference
abstracts



UNIVERSITY OF GOTHENBURG
Gothenburg Sweden 9-13 July 2012

EGAS



44th Conference of
the European Group
on Atomic Systems

Volume Editor

Dag Hanstorp, Gothenburg
Henrik Hartman, Malmö/Lund
Lars Engström, Lund
Hampus Nilsson, Lund
Sten Salomonson, Gothenburg

Volume number: 36 C

N° ISBN: 2-914771-75-4

Series editor: Prof. Pick, Paris

Managing editor: P. Helfenstein, Mulhouse

Contact

Dag Hanstorp

Department of Physics
University of Gothenburg
SE - 412 96 Gothenburg
Sweden
dag.hanstorp@gu.se

Henrik Hartman

Department of Applied Mathematics
Malmö University
SE - 205 06 Malmö
Sweden
henrik.hartman@mah.se

Copyright and cataloging information

© 2012, European Physical Society.

Reproduction rights reserved.

Europhysics Conference Abstracts are published by the European Physical Society. This volume is published under the copyright of the European Physical Society. We wish to inform the authors that the transfer of the copyright to the EPS should not prevent an author to publish an article in a journal quoting the original first publication or to use the same abstract for another conference. The copyright is just to protect the EPS against using the same material in similar publications.

This book is not a formal publication. The summaries of talks contained in it have been submitted by the authors for the convenience of participants in the meeting and of other interested persons. The summaries should not be quoted in the literature, nor may they be reproduced in abstracting journals or similar publications, since they do not necessarily relate to work intended for publication. Data contained in the summaries may be quoted only with the permission of the authors.

Welcome to the 44th Conference of the European Group on Atomic Systems!

Gothenburg, Sweden 9-13 July 2012



Framtidens klassrum...

Interaktiva lösningar, en programvara i världsklass och utvärderingsverktyg.



Unika frågor och lektioner
anpassad efter dina behov



Garantera framsteg
med frekvent utvärdering



Allt du behöver är en enhet
med internetuppkoppling



Nästa generation av
utvärderingsverktyg



Hidden Products for UHV and Surface Science

For 30 years Hiden Analytical has been a global leader in the design and manufacture of scientific instruments for research, development and production applications. In vacuum, gas, surface and plasma processes our Quadrupole Mass Spectrometers have gained world wide recognition for their precision and outstanding performance.



UHV Science

For precision analysis in UHV Science Applications the **3F/PIC** Series of triple filter mass spectrometers.

- **PIC** for fast event UHV gas studies.
- **EPIC** for radicals analysis and time resolved measurements.
- **IDP** for electron/photon/laser stimulated desorption studies and mass analysis of low energy ions.



Affordable Research Grade SIMS

High performance SIMS with the **MAXIM** range of secondary ion mass spectrometers.

- High transmission sector field energy filter
- Raster Control for enhanced depth profiling
- Positive and Negative Ion Counting

Fully integrates into Hiden's **SIMS Workstations** and **Surface/Interface Analysis** packages.



Residual Gas Analysis and Vacuum Diagnostics

The fast and precise **RC-RGA** Series with multimode program function for:

- Residual Gas Analysis
- Vacuum Diagnostics
- Ion Implantation
- Vacuum Heat Treatment
- Leak Detection
- MBE
- Vacuum Fingerprinting
- Bake-out Studies

www.HiddenAnalytical.com

surface
science

HIDEN
ANALYTICAL

Hidden Analytical Ltd.
420 Europa Boulevard, Warrington
WA5 7UN, ENGLAND

Tel +44 (0)1925 445 225
Fax +44 (0)1925 416 518
Email: info@hidden.co.uk

Photonics Tools

- Optomechanics
- Motion Controls
- Tunable Lasers
- Advanced Imaging
- OCT Systems
- Optics
- Fibers



Come and see us at the EGAS Conference
10 - 13 July 2012 in Gothenburg

You Speak, We Listen.....

THORLABS

www.thorlabs.com
scandinavia@thorlabs.com

Partners, exhibitors och sponsors

Partners



Exhibitors

Azpect

CVI Melles Griot

Gammadata Instrument AB

Hiden Analytical

IOP Publishing

Laser 2000 GmbH

TOPTICA Photonics AG

Sponsors

European Physical Society

City of Gothenburg

Nano Connect Scandinavia

National Resource Centre for
Physics Education

Royal Swedish Academy of
Sciences

Swedish Research Council

University of Gothenburg

Other support

Scienta

Springer EPJ

RoentDek

Local Organizing Committee

Dag Hanstorp (chair)	Gothenburg
Rose-Marie Wikström (coordinator)	Gothenburg
Klavs Hansen	Gothenburg
Ann-Marie Pendrill	Gothenburg
Sten Salomonson	Gothenburg
Lars Engström	Lund
Henrik Hartman	Malmö/Lund
Hampus Nilsson	Lund
Anne L'Huillier	Lund
Eva Lindroth	Stockholm
Sven Mannervik	Stockholm
Jan-Erik Rubensson	Uppsala

EGAS Board

Prof. Guglielmo M. L. TINO (CHAIR)

Prof. Henri BACHAU

Prof. Peter BARKER

Prof. Mike CHARLTON

Prof. Michael DREWSSEN

Dr Gleb GRIBAKIN

Prof. Nikolay KABACHNIK

Prof. Jose R. Crespo LOPEZ-URRUTIA

Prof. Tilman PFAU

Prof. Laurence PRUVOST

Prof. Xavier URBAIN

Dr. Wim VASSEN

Prof. Nikolay V. VITANOV

Prof. Marc J.J. VRAKKING

Prof. Antoine WEIS

EGAS 44 Schedule

	Monday	Tuesday	Wednesday
08.30-08.45		Opening ^{GD}	^{GD}
08.45-09.00		^{GD}	PL5: Stringari
09.00-09.15		PL1: Krausz	
09.15-09.30			^{GD}
09.30-09.45		^{GD}	PL6: Grimm
09.45-10.00		PL2: Berrah	
10.00-10.15			Coffee EPJ is Coffee break sponsor
10.15-10.30		Coffee	EPJ .ORG your physics journal
10.30-10.45			^{GD} PR3: Kellerbauer
10.45-11.00			^{Eu} PR4: Jochim
11.00-11.15		^{GD} PR1: Johansson	^{GD} CT9: Glöckner
11.15-11.30		^{Eu} PR2: Tastevin	^{Eu} CT12: Billy
11.30-11.45		CT1: van der Hart	CT10: Schioppo
11.45-12.00		CT2: Hultgren	CT13: Gorceix
12.00-12.15		CT3: Guénot	CT11: Grumer
12.15-12.30		CT4: Dahlström	CT14: Benseny
12.30-12.45			
12.45-13.00			Packed lunch
13.00-13.15		Lunch in Volvo-foajén	
13.15-13.30		Coffee in Exhibition area	
13.30-13.45			
13.45-14.00			
14.00-14.15		^{GD} PL3: Campbell	
14.15-14.30			
14.30-14.45			
14.45-15.00		^{GD} PL4: Meijer	
15.00-15.15			Excursion
15.15-15.30			
15.30-15.45			
15.45-16.00			
16.00-16.15			
16.15-16.30		Coffee and poster	
16.30-16.45		Coffee and poster	
16.45-17.00			
17.00-17.15			
17.15-17.30			
18.00-21.00	Registration	18.30-20.30 Reception at city hall	19.30-21.00 Theatre and refreshments

■ Plenary talks

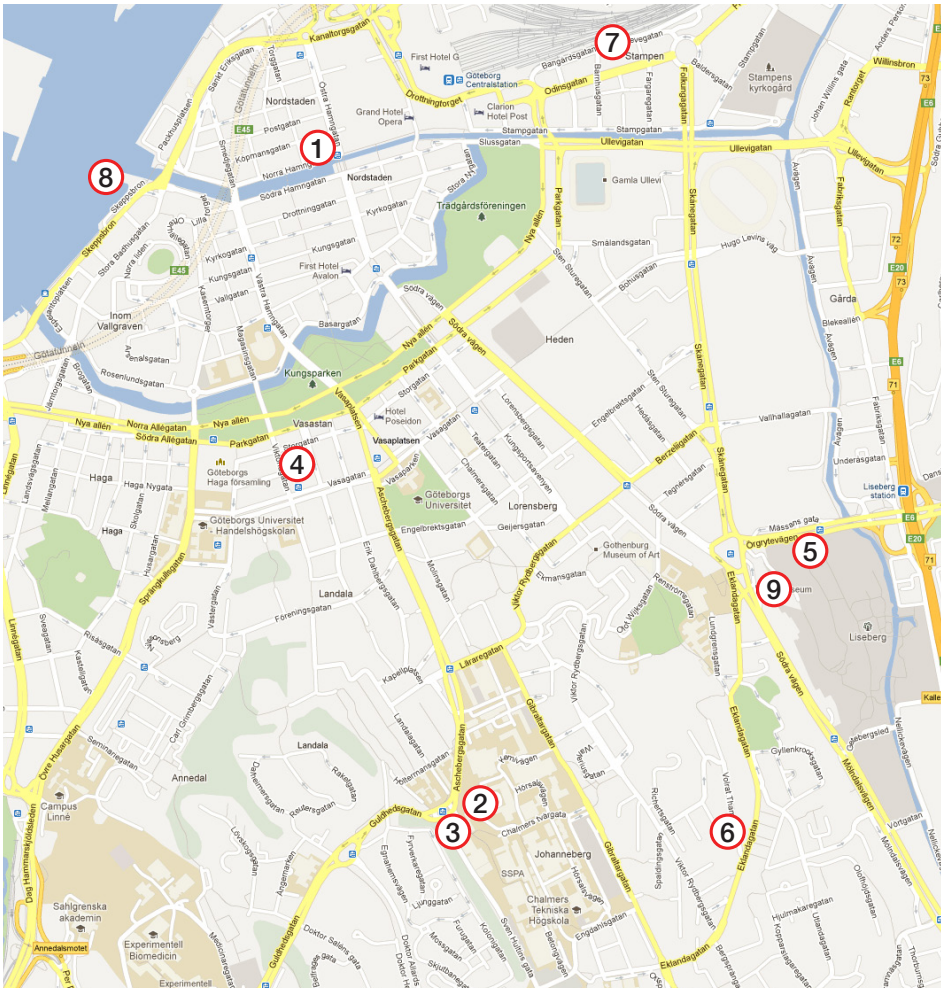
■ Progress reports

■ Contributed talks

■ Social events

Lecture halls: Gustaf Dahlén (GD), Euler (Eu), FB, RunAn

Gothenburg City Map



1. Börser (reception in the City Hall)
2. Department of Physics
3. Chalmers Volvo foajén (Chalmers konferens)
4. Hotel Vasa
5. Lisebergsteatern (play, "Remembling Miss Meitner")
6. Quality Hotel Panorama
7. Rica Hotel Göteborg No 25
8. Stenpiren (departure for boat trip)
9. Universeum (conference dinner)

Practical Information

The Conference will be held at the Department of Physics, located at Chalmers Campus Johanneberg.

Find your way to Chalmers Campus Johanneberg

By tram or by bus: The following buses are operating Chalmers: 58, 16, 158 and 753. In addition, the trams 6, 7, 10 and 13 are operating Chalmers.

By car: Follow signs to Sahlgrenska University Hospital, see map.

By train: At Drottningtorget, outside the railway station in the city center, you can choose tram 7, direction Tynnered to Chalmers.

By air: Airport bus from Landvetter Airport to Korsvägen in the city center. From Korsvägen tram 6, direction Länsmansgården or tram 8, direction Frölunda Torg, are operating Chalmers.

Registration

Conference Registration will take place at Department of Physics, see enclosed map on page XIV, no: 2. Opening hours:

- Monday July 9, 18.00-20.00
- Tuesday July 10, 08.00-16.00
- Wednesday July 11, 08.00-12.00
- Thursday July 12, 08.00-12.00
- Friday July 13, 08.00-13.00

Social program

Pre-reservations must be made for all social events.

July 9, 18.00: **Welcome Reception at the Department of Physics** (University of Gothenburg). The evening before the conference begins you are welcome to the Welcome Reception at the Department of Physics. Participation is included in the congress fee. See enclosed map on page XIV, no: 2.

July 10, 18.30: **Reception at Börsen** (The City Hall, Gustaf Adolfs Torg). Tuesday evening you are invited to a reception by the Lord Mayor in the meeting hall of the City Council. It is in the city centre close to the harbor (a 25 min walk from the Conference venue). This is the historic heart of Gothenburg, with the statue of Gustaf II Adolf (Gustavus Adolphus), the founder of Gothenburg in 1621. See enclosed map on page XIV, no: 1.

July 11, 13.30: **Excursion**. Chartered boat trip in the Archipelago of Gothenburg with the boat St Erik. The boat leaves from Stenpiren. A small bar will be open on the boat during the trip. See enclosed map on page XIV, no: 8.

July 11, 19.30: **Play – “Remembering Miss Meitner”** at Lisebergsteatern in the amusementpark Liseberg. Performed by actors from the Gothenburg City Theatre. Entrance to the right of the main entrance follow the signs. See enclosed map on page XIV, no: 5.

July 12, 19.00: **Tour and Conference Dinner at Universeum**. Conference dinner in the Aquarium Hall of Universeum, the largest science centre in Northern Europe. The dinner will start with a guided tour of the centre. The dinner is served at 20.30. See enclosed map on page XIV, no: 9.

General Information

Badge. For safety reasons we ask you to please wear your name badge during the conference and during the social events.

Internet. There is wireless access at the conference venue. Your username and password will be printed on your name badge.

Taxi. We recommend you to use the following taxi companies:

- Taxi Göteborg, +46 (0) 31 65 00 00
- Taxi Kurir, +46 (0) 31 27 27 27
- VIP Taxi, + 46 (0) 31 27 16 11
- Minitaxi, + 46 (0) 31 14 01 40

Monday, July 9

18.00-21.00 ***Registration and Welcome Reception (Fysikgården)***

20.00- Meeting EGAS board (Lunch room level 8 “Forskarhuset fysik”)

Tuesday, July 10

- 08.00- **Registration (Fysikgården)**
- 08.30-08.45 **Opening (GD)**
- 08.45-10.15 **Plenary session (GD), Chair: Hartmut Hotop**
- 08.45-09.30 PL1: Ferenc Krausz – *Attosecond Physics: The First Decade*
- 09.30-10.15 PL2: Nora Berrah – *Probing Matter from Within Using Ultra-Intense and Ultra-Fast X-Rays from the LCLS Free Electron Laser*
- 10.15-11.00 **Coffee break**
- 11.00-12.30 **Parallel sessions:**
- Session A (GD), Chair: Henri Bachau**
- 11.00-11.30 PR1 (*Selected as Hot Topic*): Per Johnsson – *Photoelectron Diffraction Imaging of Molecular Dynamics*
- 11.30-11.45 CT1: Hugo van der Hart – *Multi-electron dynamics in time-dependent R-matrix theory*
- 11.45-12.00 CT2: Hannes Hultgren – *Visualization of electronic motion in carbon atoms*
- 12.00-12.15 CT3: Diego Guénot – *Photoionization time-delay measurements and calculations in various gases*
- 12.15-12.30 CT4: Marcus Dahlström – *Theory of attosecond delays in laser-assisted photoionization: Including electron–hole interactions*
- Session B (Euler), Chair: Laurence Provost**
- 11.00-11.30 PR2: Geneviève Tastevin – *50 Years of ^3He Optical Pumping: “When Only the Best Will Do”*
- 11.30-11.45 CT5: Stanislav Tashenov – *Spin dynamics of electrons in strong fields studied via bremsstrahlung from a polarized electron beam*
- 11.45-12.00 CT6: Wolfgang Ernst – *Alkali atoms on superfluid helium droplets - laser excitation of an exotic Rydberg complex*

- 12.00-12.15 CT7: Christian Seiler – *Decay of Rydberg hydrogen atoms and molecules after Rydberg-Stark deceleration and off-axis trapping*
- 12.15-12.30 CT8: Julian Berengut – *Optical transitions in highly charged ions for atomic clocks with enhanced sensitivity to variation of fundamental constants*
- 12.30-14.00 ***Lunch (Volvo foajén)***
- 14.00-15.30 ***Plenary session (GD), Chair: Gleb Gribakin***
- 14.00-14.45 PL3: Eleanor Campbell – *Rydberg Fingerprint Spectroscopy: Probing the Excited States and Ionisation Dynamics of Fullerenes*
- 14.45-15.30 PL4: Gerard Meijer – *Taming Molecular Beams*
- 15.30-17.30 ***Poster session and coffee***
- 18.30-20.30 ***Reception at “Börsen”, (the City Hall)***

Wednesday, July 11

- 08.30-10.00 **Plenary session (GD), Chair: Guglielmo Tino**
- 08.30-09.15 PL5: Sandro Stringari – *Dynamic Behavior of Ultra Cold Atomic Gases*
- 09.15-10.00 PL6: Rudolf Grimm – *New Frontiers in Ultracold Quantum Gases*
- 10.00-10.45 **Coffee break**
- 10.45-12.00 **Parallel sessions:**
- Session A (GD), Chair: David Pegg**
- 10.45-11.15 PR3: Alban Kellerbauer – *Towards Laser Cooling of Atomic Anions*
- 11.15-11.30 CT9: Rosa Glöckner – *Sisyphus cooling of polyatomic molecules*
- 11.30-11.45 CT10: Marco Schioppo – *A compact laser-cooling strontium source for a transportable optical lattice clock*
- 11.45-12.00 CT11: Jon Grumer – *Theoretical and experimental studies of In I, Sn II, Sb III, and Te IV atomic properties*
- Session B (Euler), Chair: Wim Vassen**
- 10.45-11.15 PR4: Selim Jochim – *Deterministic Few-Fermion Quantum Systems*
- 11.15-11.30 CT12: Juliette Billy – *Confinement-induced collapse of a dipolar Bose-Einstein condensate in an optical lattice*
- 11.30-11.45 CT13: Olivier Gorceix – *The anisotropic excitation spectrum of a dipolar Bose-Einstein Condensate*
- 11.45-12.00 CT14: Albert Benseny – *Are relativistic corrections needed to describe the adiabatic passage of matter waves?*
- 12.00-13.30 **Lunch (Packed lunch)**
- 13.30-16.30 **Excursion (Chartered boat trip, leaves from “Stenpiren”)**
- 19.30-20.30 **Theatre play “Remembering Miss Meitner” at Lisebergsteatern**
- 20.30- **Refreshments Lisebergsteatern**

08.30-10.00 **Plenary session (RunAn), Chair: Ann-Marie Mårtensson-Pendrill**

08.30-09.15 PL7: Jonathan Tennyson – *Molecular Line Lists for the Opacity of Exoplanet and Other Atmospheres*

09.15-10.00 PL8: Eric Mazur – *Confessions of a Converted Lecturer*

10.00-10.30 **Coffee break**

10.30-10.45 **Group photo (outside coffee area)**

10.45-12.00 **Parallel sessions:**

Session A (GD), Chair: Eva Lindroth

10.45-11.15 PR5: Zheng-Tian Lu – *Atom Trap, Krypton-81, and Global Groundwater*

11.15-11.30 CT15: Yoshihiko Arita – *Optical manipulation of microparticles in vacuum*

11.30-11.45 CT16: Jonas Rodewald – *A universal matter-wave interferometer in the time-domain*

11.45-12.00 CT17: Geoffrey Duxbury – *Renner-Teller coupling in H₂S⁺: A comparison of theory with optical spectra and recent PFI and MATI experimental results*

Session B (Euler), Chair: Jan-Erik Rubensson

10.45-11.15 PR6: Alexei Grum-Grzhimailo – *Two- and Three-Photon Atomic Double Ionization by Intense FEL Pulses*

11.15-11.30 CT18: Gabriel Karras – *Multi-electron dissociative ionization of clusters under ps and fs laser irradiation: the case of alkyl-halide clusters*

11.30-11.45 CT19: Erik Månsson – *Photo-double ionization on the attosecond time scale*

11.45-12.00 CT20: Per Linusson – *Double photoionization of Kr and Ar*

**Session C, “Symposium on Teaching Quantum Physics” (FB) Chair:
Lars Engström**

- 10.45-11.15 PR7: Robert Marc Friedman – *“Remembering Miss Meitner”: History, Memory, and the Future of Physics*
- 11.15-11.45 PR8: Reidun Renström – *Why Do Recognized Textbooks in Physics Represent a Quasi-History of Planck’s, Einstein’s and Bohr’s Development of Quantum Physics?*
- 11.45- Lab visits
- 12.00-12.30 **General assembly (GD)**
- 12.30-14.00 **Lunch (Volvo Foajé)**
- 14.00-15.15 **Parallel sessions:**
- Session A (GD), Chair: Nikolay Kabachnik**
- 14.00-14.30 PR9: Michael Tarbutt – *Is the Electron Round?*
- 14.30-14.45 CT21: Gabrieli Rosi – *The MAGIA experiment: status and prospects*
- 14.45-15.00 CT22: Joseph Borbely – *Frequency metrology in quantum degenerate helium*
- 15.00-15.15 CT23: Pablo Cancio Pastor – *Determination of nuclear parameters and fundamental constants by frequency metrology in low-lying triplet states of He*
- Session B (Euler), Chair: José Crespo**
- 14.00-14.30 PR10: Hans Jakob Wörner – *High-Harmonic Spectroscopy of Electronic Dynamics in Molecules*
- 14.30-14.45 CT24: Vasily Strelkov – *Resonant high-order harmonic generation: beyond the three-step model*
- 14.45-15.00 CT25: Anthony Starace – *Analytic Description of High-Order Harmonic Generation by an Intense Few-Cycle Laser Pulse*

- 15.00-15.15 CT26: Francesca Shearer – *Photodetachment dynamics of H- by few-cycle laser pulses*
- Session C, “Symposium on Teaching Quantum Physics” (FB)***
Chair: Sven Mannervik
- 14.00-14.30 PR11: Eric Mazur – *The Scientific Approach to Teaching: Research as a Basis for Course Design*
- 14.30-14.45 CT27: Gunnar Ohlén – *Teaching Quantum Mechanics using Nanoscience*
- 14.45- Lab visits
- 15.15-17.30 ***Poster session and coffee***
- 19.00- ***Conference dinner (Universeum)***
- 19.00-20.30 Tour at Science Centre and refreshments
- 20.30 Dinner served

Friday, July 13

08.30-09.15 **Plenary session (GD), Chair: Frederic Merkt**

PL9: Per Delsing – Is Vacuum Really Empty?

09.20-11.40 **Parallel sessions:**

Session A (GD), Chair: Tilman Pfau

09.20-09.50 PR12: Ralf Röhlsberger – *Electromagnetically Induced Transparency via Cooperative Emission in a Cavity*

09.50-10.05 CT28: Florin Constantin – *Photomixing for Precision Measurements in the Terahertz Regime*

10.05-10.20 CT29: Daniel Sprecher – *Schemes for high-precision measurements of the ionization and dissociation energies of molecular hydrogen*

10.20-10.55 **Coffee**

10.55-11.10 CT30: Natasa Vujicic – *Polarization effects on multilevel rubidium atoms induced by optical frequency comb*

11.10-11.25 CT31: Anastasios Dimitriou – *Wavelength dependence of Photoelectron Angular Distributions from four- and five-photon ionization of Mg in the vicinity of the 4-photon excited $3p^2\ ^1S_0$ state*

11.25-11.40 CT32: Hicham Agueny – *Interference effects for electron transfer in ion-molecule keV.u-1 collisions*

Session B (Euler), Chair: Xavier Urbain

09.20-09.50 PR13 (Selected as Hot Topic): Andreas Mooser – *Direct Observation of Spin Flips with a Single Isolated Proton*

09.50-10.05 CT33: Alex Gingell – *Internal ground state preparation of molecular ions in a cryogenically-cooled ion trap with a combination of rotational laser-cooling and state-selective dissociation*

10.05-10.20 CT34: Victor Flambaum – *Chaos-induced enhancement of resonant multi- electron recombination in highly charged ions: Statistical theory*

10.20-10.55 **Coffee**

10.55-11.10 CT35: Martino Trassinelli – *Investigation of (quasi) symmetric slow collisions between highly charged ions and free atoms*

11.10-11.25 CT36: Adèle Hilico – *A trapped atom interferometer for the measurement of short range forces*

11.25-11.40 CT37: Richard Thomas – *DESIREE: a unique cryogenic electrostatic storage ring*

Session C, “Symposium on Teaching Quantum Physics” (FB) Chair: Antoine Weis

09.20-09.50 PR14: Christine Lindstrøm – *Exploring The Knowledge Structure of Introductory Quantum Mechanics*

09.50-10.20 PR15: Klaus Wendt – *Particle Traps in Modern Physics Education*

10.20-10.55 **Coffee**

Chair: Anne-Sofie Mårtensson

10.55-11.25 PR16: Judy Hardy – *Not What It Seems? Teaching and Learning Introductory Quantum Physics*

11.25-11.40 CT38: Ann-Marie Mårtensson-Pendrill – *Drama as part of quantum physics teaching*

11.45-12.30 **Plenary session (GD), Chair: Peter Baker**

PL10: Jeffrey Hangst – *The ALPHA Experiment at CERN: Physics with Trapped Antihydrogen*

12.30-13.00 **Closing**



The EPS poster prize will be awarded to the best student poster presented at the conference. The poster must be produced and presented by a student.

The prize jury consists of members of the EGAS board. The winner of the prize, which consists of a diploma and €250, will be announced during the closing ceremony of the conference.

This book contains all abstracts accepted as of June 1, 2012. The abstracts representing talks are identified by

PL for Plenary Lecture

PR for Progress Report

CT for Contributed Talk

each followed by contribution number.

Poster abstracts are sorted by category and alphabetically by the last name of the author. Posters are indicated by **PO** followed by a contribution number. Odd numbered posters are presented on Tuesday, whereas even numbered posters are presented on Thursday.

Contents

PL: Plenary Lectures	1
PL-001 F. Krausz	
Attosecond physics: the first decade	2
PL-002 N. Berrah	
Probing Matter from Within using Ultra-Intense and Ultra-Fast X- Rays from the LCLS Free Electron Laser	3
PL-003 E.E.B. Campbell	
Rydberg Fingerprint Spectroscopy: Probing the Excited States and Ionisation Dynamics of Fullerenes	4
PL-004 G. Meijer	
Taming molecular beams	5
PL-005 S. Stringari	
Dynamic behavior of ultra cold atomic gases	6
PL-006 R. Grimm	
New frontiers in ultracold quantum gases	7
PL-007 Jonathan Tennyson	
Molecular line lists for the opacity of exoplanets and other atmo- spheres	8
PL-008 E. Mazur	
Confessions of a converted lecturer.	9
PL-009 P. Delsing	
Is Vacuum Really Empty?	10
PL-010 J. Hangst	
The ALPHA Experiment at CERN: Physics with Trapped Antihy- drogen	11
PR: Progress Reports	13
PR-001 P. Johnsson	
Photoelectron diffraction imaging of molecular dynamics	14
PR-002 G. Tostevin	
50 years of ^3He optical pumping: “When only the best will do” . .	15
PR-003 Alban Kellerbauer	
Towards laser cooling of atomic anions	16
PR-004 Selim Jochim	
Deterministic few-fermion quantum systems	17
PR-005 Z.T. Lu	
Atom Trap, Krypton-81, and Global Groundwater	18
PR-006 A. N. Grum-Grzhimailo	
Two- and Three-Photon Atomic Double Ionization by Intense FEL Pulses	19

PR-007	R.M. Friedman	Remembering Miss Meitner: History, Memory, and the Future of Physics	20
PR-008	R. Renström	Why do recognized textbooks in physics represent a quasi-history of Planck's, Einstein's and Bohr's development of quantum physics?	21
PR-009	M. R. Tarbutt	Is the electron round?	22
PR-010	H. J. Wörner	High-harmonic spectroscopy of electronic dynamics in molecules	23
PR-011	E. Mazur	The scientific approach to teaching: Research as a basis for course design.	24
PR-012	R. Röhlsberger	Electromagnetically Induced Transparency via Cooperative Emission in a Cavity	25
PR-013	A. Mooser	Direct Observation of Spin Flips with a Single Isolated Proton	26
PR-014	C. Lindström	Exploring the knowledge structure of introductory quantum mechanics	27
PR-015	K.D.A. Wendt	Particle Traps in Modern Physics Education	28
PR-016	J. Hardy	Not what it seems? Teaching and learning introductory quantum physics.	29
CT:	Contributed Talks		31
CT-001	H.W. van der Hart	Multi-electron dynamics in time-dependent R-matrix theory	32
CT-002	H. Hultgren	Visualization of electronic motion in carbon atoms	33
CT-003	D. Guénot	Photoionization time-delay measurements and calculations in various gases	34
CT-004	J. M. Dahlström	Theory of attosecond delays in laser-assisted photoionization: Including electron-hole interactions	35
CT-005	S. Tashenov	Spin dynamics of electrons in strong fields studied via bremsstrahlung from a polarized electron beam	36

CT-006	Wolfgang E. Ernst	Alkali atoms on superfluid helium droplets - laser excitation of an exotic Rydberg complex	37
CT-007	Ch. Seiler	Decay Of Rydberg Hydrogen Atoms And Molecules After Rydberg-Stark Deceleration And Off-Axis Trapping	38
CT-008	J.C. Berengut	Optical transitions in highly charged ions for atomic clocks with enhanced sensitivity to variation of fundamental constants	39
CT-009	R. Glöckner	Sisyphus Cooling of Polyatomic Molecules	40
CT-010	M. Schioppo	A compact laser-cooling strontium source for a transportable optical lattice clock	41
CT-011	J. Grumer	Theoretical and experimental studies of In I, Sn II, Sb III, and Te IV atomic properties	42
CT-012	J. Billy	Confinement-induced collapse of a dipolar Bose-Einstein condensate in an optical lattice	43
CT-013	O. Gorceix	The anisotropic excitation spectrum of a dipolar Bose-Einstein Condensate	44
CT-014	A. Benseny	Are relativistic corrections needed to describe the adiabatic passage of matter waves?	45
CT-015	Y. Arita	Optical manipulation of microparticles in vacuum	46
CT-016	J. Rodewald	A universal matter-wave interferometer in the time-domain	47
CT-017	G. Duxbury	Renner-Teller Coupling In H_2S^+ : A Comparison Of Theory With Optical Spectra And Recent Pfi And Mati Experimental Results	48
CT-018	G. Karras	Multi-electron dissociative ionization of clusters under ps and fs laser irradiation: the case of alkyl-halide clusters	49
CT-019	E. P. Månsson	Photo-double ionization on the attosecond time scale	50
CT-020	P. Linusson	Double photoionization of Kr and Ar	51
CT-021	G. Rosi	The MAGIA experiment: status and prospects	52

CT-022	Joe Borbely	Frequency metrology in quantum degenerate helium	53
CT-023	P. Cancio Pastor	Determination of nuclear parameters and fundamental constants by frequency metrology in low-lying triplet states of He	54
CT-024	V. Strelkov	Resonant high-order harmonic generation: beyond the three-step model	55
CT-025	Anthony F. Starace	Analytic Description of High-Order Harmonic Generation by an In- tense Few-Cycle Laser Pulse	56
CT-026	S. F. C. Shearer	Photodetachment dynamics of H^- by few-cycle laser pulses	57
CT-027	G. Ohlén	Teaching Quantum Mechanics using Nanoscience	58
CT-028	Florin Lucian Constantin	Photomixing for Precision Measurements in the Terahertz Regime	59
CT-029	D. Sprecher	Schemes for high-precision measurements of the ionization and dis- sociation energies of molecular hydrogen	60
CT-030	N. Vujicic	Polarization effects on multilevel rubidium atoms induced by optical frequency comb	61
CT-031	A. Dimitriou	Energy dependence of photoelectron angular distributions from two- photon ionization of Strontium in the proximity of the $5p^2\ ^1S_0$ dou- bly excited state	62
CT-032	Hicham Aguey	Interference effects for electron transfer in ion-molecule $\text{keV}\cdot\text{u}^{-1}$ collisions	63
CT-033	A. D. Gingell	Internal ground state preparation of molecular ions in a cryogenically- cooled ion trap with a combination of rotational laser-cooling and state-selective dissociation	64
CT-034	V.V. Flambaum	Chaos-induced enhancement of resonant multi- electron recombina- tion in highly charged ions: Statistical theory	65
CT-035	M. Trassinelli	Investigation of (quasi) symmetric slow collisions between highly charged ions and free atoms	66
CT-036	A. Hilico	A trapped atom interferometer for the measurement of short range forces	67

CT-037	R. D. Thomas	
	DESIREE: a unique cryogenic electrostatic storage ring facility for merged ion-beams studies	68
CT-038	A.-M. Mårtensson-Pendrill	
	Drama as part of quantum physics teaching	69
Contributed Posters (PO)		71
PO: AMO at large facilities		73
PO-001	Y. Dicle	
	Electron Spin Resonance and Molecular Motion of the $CH_3\dot{C}HCO-NH_2.HCl$ Radical In Gamma Irradiated L-Alanine Hydrochloride Compound	74
PO-002	Y. Dicle	
	Influence of Ionizing Radiation Effect on 2-Thiouracil: an EPR Study	75
PO-003	M. Godefroid	
	Mass and field isotope shift parameters for the $2s - 2p$ resonance doublet of lithium-like ions	76
PO-004	N. M. Kabachnik	
	Effect of partial coherence of the FEL pulses in two-colour multiple ionization of atoms	77
PO-005	L. Rading	
	Angle-resolved photoelectron spectra from two-color XUV+IR photoionization at FLASH	78
PO-006	J.-E. Rubensson	
	Resonant Inelastic Scattering Spectra of Free Molecules with Vibrational Resolution	79
PO-008	N. Walsh	
	Fragmentation of NH_3 investigated using a multi-coincidence ion momentum imaging spectrometer	80
PO: Applications of AMO Physics		81
PO-009	J.C. Angulo	
	A generalized relative complexity: application to atomic one-particle densities	82
PO-010	H. Bahri	
	Primary and secondary kinetic isotope effects on the gas phase reactions $H_2O_2 + X$ ($X=H, Cl$)	83
PO-011	M. Bassi	
	Electron-Impact study of AlO using the R-matrix method	84
PO-012	H. Bohachov	
	Electron excitation of the $1s2sns(nd)$ LiI^{**} states	85

PO-013	M. A. Bolorizadeh	Excitation cross sections in the collision of protons with He atoms at intermediate and high energies under a three body formalism . . .	86
PO-014	M. A. Bolorizadeh	Potential scattering devised to calculate the capture cross sections for the collision of proton with methane	87
PO-015	M. A. Bolorizadeh	Daubechies-3 wavelet basis applied to study the three body proton hydrogen scattering under a Faddeev formalism	88
PO-016	A. Cininsh	Hyperfine structure of laser-dressed atomic states	89
PO-017	M. Fertl	A UV frequency-quadrupled diode laser system for the mercury co-magnetometer in the nEDM experiment	90
PO-018	I. Fescenko	Dark resonances for systems with large J studied in potassium diatomic molecules	91
PO-019	G. F. Gribakin	Statistical multimode resonant annihilation of positrons in molecules	92
PO-020	U. Kalninch	Modeling of coherent atomic excitation including energy distribution within laser profile	93
PO-021	H.-C. Koch	Optical cesium magnetometers for high precision magnetic field measurements	94
PO-022	L. Kalvans	Coherent and non-coherent magneto-optical effects in the $5P_{3/2}$ state of atomic Rubidium	95
PO-023	P. Quinet	Radiative parameters for lowly charged tungsten ions of interest in fusion plasma research	96
PO-024	T. Scholtes	Sensitivity optimization of an optically pumped magnetometer with miniaturized Cs cell at earth's magnetic field strength	97
PO-025	V. Schultze	Atomic magnetometer pumped with intensity-modulated light . . .	98
PO-026	I. Silander	NICE-OHMS – A Spectroscopic Technique for Detection of Molecular Species Down to the 10^{-12} cm^{-1} Range	99
PO-027	J. Singh	Electron-impact study of B_2 molecule: R -matrix method	100

PO-028	A. Spiss	Level-crossing spectroscopy of atomic rubidium at D_2 excitation in the presence of a non zero magnetic field	101
PO-029	J. Wang	Dicke Narrowing and Speed-dependent Effects in Dispersion Mode of Detection – Theory and Experimental Verification by NICE-OHMS	102
PO-030	J. Westberg	Analytical expressions for fast real-time fitting of modulated dispersion line shapes	103
PO-031	S. Y. Yousif Al-Mulla	Elastic scattering of electrons from Lithium and Potassium.	104
PO-032	N. Zvereva-Loöte	Highly correlated multi-state and multi-reference <i>ab initio</i> study of the potential energy surface for the $N(^2D) + CH_4$ reaction	105
PO: Cold atoms, Molecules, Ions and Quantum Gases			107
PO-033	A. Alkauskas	Transition rates for states of the $2s^22p^5$ and $2s2p^6$ configurations in fluorine-like ions between Si VI and W LXVI	108
PO-034	M.T. Bouazza	Transport properties of Li(2s) and Li(2p) diffusing in ground sodium	109
PO-035	K. L. Butler	Towards a quantum gas of polar YbCs molecules	110
PO-036	S. Chervenkov	A Centrifuge Molecular Decelerator for Polar Molecules	111
PO-037	S. J. Curran	Complete ionisation of the neutral gas: why there are so few detections of 21-cm hydrogen in high redshift radio galaxies and quasars	112
PO-038	E. Gazazyan	Formation of Feshbach resonance in laser radiation field in case of two interconnected resonance phases.	113
PO-039	M. Hamamda	Inelastic quantum diffraction of slowed atoms near a surface	114
PO-040	G. Kregar	Characterization and dynamics of rubidium magneto-optical trap induced by pushing beam	115
PO-041	A. Mansouri	1b2 study in (e,3e) oriented water molecule	116
PO-042	V. Meshkov	Fourier transform spectroscopy, direct potential fit, and radiative properties calculation on the shelf-like $E(4)^1\Sigma^+$ state of RbCs molecule	117

PO-043	E. S. Mironchuk	Collisional quenching of Rydberg atomic states by the ground-state alkaline-earth atoms	118
PO-044	T. Mullins	Controlling large molecules at kHz repetition rates	119
PO-045	E. Pazyuk	The revised deperturbation analysis of the $A \sim b$ complex of the Cs_2 dimer based on Fourier transform measurements	120
PO-046	L. Pruvost	Vibrational quantum defect coupled to improved LeRoy-Bernstein formula for a precise analysis of photoassociation spectroscopy . .	121
PO-047	P. Rynkun	On the energy difference between $1s^2 2s^2 2p^2 P^o$ and $1s^2 2s 2p^2 \ ^4P$ terms in Boron	122
PO-048	S. M. Skoff	Buffer gas cooling of YbF molecules	123
PO-049	F. Talbi	Theoretical determination of the potassium far-wing photo-absorption spectra	124
PO-050	O. O. Versolato	Cryogenic Paul trap for experiments on cold HCl's	125
PO-051	T. P. Wiles	Bose-Einstein condensation of ^{85}Rb by direct evaporation in an optical dipole trap	126
PO:	High-resolution Spectroscopy		127
PO-052	P. Bengtsson	Energy structure and transition rates in the Ne-like sequence from relativistic CI calculations	128
PO-053	J.C. Berengut	Searching for cosmological spatial variations in values of fundamental constants using laboratory measurements	129
PO-054	J.C. Berengut	Testing time-variation of fundamental constants using Th and U nuclear clocks	130
PO-055	L. Busaite	Modelling of electromagnetic radiation group velocity reduction . .	131
PO-056	S. Chattopadhyay	Development of perturbed relativistic coupled-cluster theory for the calculation of dipole polarizability of closed-shell systems	132
PO-057	H.-S. Chou	Relativistic calculations of the transition rates for the Be-like and the Zn-like ions	133

PO-058	J. Dembczyński	Semiempirical procedure of parametrization of the oscillator strengths for electric dipole transitions	134
PO-059	A. Drozdova	Study of the spin-orbit coupled $A^1\Sigma_u^+ \sim b^3\Pi_u$ states of the Rb ₂ dimer: laser spectroscopy and refined coupled-channel treatment	135
PO-060	J. Ekman	Spectral properties of In II, Sn III, Sb IV, and Te V in the Cd-sequence from large scale MCDHF and RCI calculations	136
PO-061	A. Er	New classifications of unclassified lines in Niobium Fourier transform spectra	137
PO-062	V.V. Flambaum	Astrophysical evidences for the variation of fundamental constants and proposals of laboratory tests	138
PO-063	V.V. Flambaum	Parity and time reversal violation in atoms and search for physics beyond the Standard Model	139
PO-064	T. A. Florko	Theoretical determination of the transition energies and probabilities in spectra of EuI and HgII	140
PO-065	P. Głowacki	Critical analysis of the methods of interpretation in the hyperfine structure for the chromium atom	141
PO-066	M. Godefroid	Relativistic effects on the hyperfine structures of $2p^4(3P)3p^2D^o$, $4D^o$ and $2P^o$ in F I	142
PO-067	M. Godefroid	Isotope shift parameters, hyperfine interaction constants and Landé factors along the Be, B, C and N isoelectronic sequences	143
PO-068	M. Godefroid	A Partitioned Correlation Function approach for atomic properties	144
PO-069	A. Grochola	The $A^1\Sigma^+$ electronic state of KLi molecule	145
PO-070	Z. D. Grujić	Algebraic model and experimental verification of magnetic resonance induced by amplitude-modulated light	146
PO-071	F. Güzelçimen	Experimental determination of magnetic dipole hyperfine structure constants for levels of the configuration $3d^44p$ of atomic Vanadium	147
PO-072	H. Hartman	Investigations of VUV transitions of iron for astrophysical applications using synchrotron radiation	148

PO-073	J. Ketter	Towards a $^3\text{H}/^3\text{He}$ Mass-Ratio Measurement with THE-Trap . . .	149
PO-074	O. Yu. Khetselius	Quantum structure of electro-weak interaction in heavy atomic systems and Parity nonconservation effect	150
PO-075	O. Yu. Khetselius	Laser electron-gamma-nuclear spectroscopy of heavy atoms and NEET effect in heavy atomic/nuclear systems.	151
PO-076	J. Komasa	Rovibrational levels of hydrohelium cation	152
PO-077	A. Kortyna	Hyperfine-resolved polarizability measurement of the Cs $9s\ ^2S_{1/2}$ state	153
PO-078	P. Kowalczyk	Polarisation labelling spectroscopy of the $2^1\Pi$ state of NaLi	154
PO-079	J. Manrique	Measurements of Stark Widths of Fe II lines by laser induced breakdown spectroscopy	155
PO-080	R. Mirzoyan	Modification of Initially Forbidden Atomic Transitions of Rb D_2 line in Magnetic Field	156
PO-081	O. Nikolayeva	Fourier Transform Spectroscopy of $B^1\Pi$ State in RbCs	157
PO-082	V.A. Polischuk	Semiempirical calculation of energies spectra configurations $2p3p4p$ Cl, $3p4p5p$ SiI and Π , $4p5p6p$ GeI and gyromagnetic ratios . . .	158
PO-083	M. Puchalski	Calculations of energy levels of the beryllium atom	159
PO-084	A. Sargsyan	Hyperfine Paschen-Back regime study using Rb Nano-Thin Cell .	160
PO-085	A. Sargsyan	N-Resonance Formation in Micrometric-Thin Cell Filled with Rubidium and Buffer Gas	161
PO-086	M. Tamanis	Fourier transform spectroscopy of KCs and potential construction of ground $X^1\Sigma^+$ and $a^3\Sigma^+$ states at large internuclear distance . .	162
PO-087	R. Tymchyk	Electron-impact excitation of the $(4p^54d5s)^4P_J$ autoionizing states in Rb atoms	163
PO-088	X. Urbain	Rotationally resolved predissociation lifetimes of the $c\ ^3\Pi_u^+$ state of D_2	164
PO-089	R. Zafar	New odd levels of Pr I	165

PO-090	M. Vogel	Precision Spectroscopy of Highly Charged Ions in Penning Traps	166
PO-091	B. Yapıcı	Investigation of the hyperfine structure of the configuration $3d^34s4p$ of atomic Vanadium with Fourier transform spectroscopy	167
PO-092	A. Stolyarov	The KCs and RbCs $A \sim b$ complex revisited by means of extensive FT high resolution spectroscopy	168
PO: Mesoscopic Systems			169
PO-093	D.U. Matrasulov	Heat capacity of nanoconfined ideal gas	170
PO-094	H. Nadgaran	Modeling of plasmon-molecule interaction based on nano-particles of sphere, bar, and cube shapes	171
PO-095	H. Nadgaran	Interaction of electromagnetic waves with carbon nano tubes (CNT)	172
PO-096	Kh.Yu. Rakhimov	Energy losses of fast highly charged ions in the collisions with carbon nanotubes	173
PO-097	Kh.Yu. Rakhimov	Nonlinear Dynamics of the Kicked Screened Atom	174
PO: Photoionization/Photodetachment, anions			175
PO-098	P. Andersson	Spectroscopic analysis of the blue light emitted from Middleton type Cesium sputter negative ion sources.	176
PO-099	D. Ayuso	Vibrationally resolved photoionization spectra of small molecules	177
PO-100	C. Blondel	Evolution of the accuracy of electron affinity measurements	178
PO-101	K.C. Chartkunchand	Velocity-Map Imaging spectroscopy of negative ion photodetachment	179
PO-102	A. Dimitriou	Wavelength dependence of Photoelectron Angular Distributions from four- and five-photon ionization of Mg in the vicinity of the 4-photon excited $3p^2 \ ^1S_0$ state	180
PO-103	G. Duxbury	Renner-Teller Coupling In H_2S^+ : Partitioning The Rovibronic And Spinorbit Coupling Hamiltonian	181
PO-104	M. Eklund	Strong-field photodetachment of C_2^-	182

PO-105	A.G. Galstyan	Non-dipole effects in $(\gamma, 2e)$ processes caused by photon momentum	183
PO-106	A.G. Galstyan	2D momentum distribution of electron in transfer ionization of helium atom by fast proton	184
PO-107	N. D. Gibson	Inner-shell photodetachment from O^-	185
PO-108	G. F. Gribakin	Measuring positron-atom binding energies through laser-assisted photorecombination	186
PO-109	A. N. Grum-Grzhimailo	Two- and Three-Photon Atomic Double Ionization by Intense FEL Pulses	187
PO-110	O. Isaksson	Levitation and manipulation of aerosol particles by radiation pressure	188
PO-111	G. Kashenock	Suppression of endohedral cerium $4d \rightarrow 4f$ resonance in photoabsorption of $Ce@C_{82}^+$	189
PO-112	G. Kashenock	Photoionization from the deepest valence-band σ -shells of fullerenes C_{60} and C_{20} : δ -potential approach	190
PO-113	A. O. Lindahl	Resonances and thresholds in negative ion photodetachment	191
PO-114	F. Menas	The second Born approximation for the ionization of atoms	192
PO-115	A. V. Loboda	Electron collisional spectroscopy of neutral atoms and multicharged ions in plasma within combined energy and Debye shielding approach	193
PO-116	M. Pawlak	Resonance states of atomic hydrogen in combined ac and dc fields	194
PO-117	P. Andersson	Spectroscopic analysis of the blue light emitted from Middleton type Cesium sputter negative ion sources.	195
PO-118	T. Tanabe	Variation of photodissociation spectra of molecular anions with storage time in an electrostatic storage ring	196
PO-119	R. Tymchyk	Autoionizing states of Ca in the problem of ionization of calcium atom by the electrons	197
PO-120	C. W. Walter	Observation of bound-bound transitions in the negative ion of lanthanum	198

PO-121	A.S. Zlatov	Spectral properties of fluorescence labels based on different sizes nanodimension-size structures	199
PO: Quantum Optics			201
PO-122	H.K. Avetissian	Harmonic generation on highly charged hydrogen-like ions at the multiphoton resonant interaction with x-ray laser	202
PO-123	E. Gazazyan	All-Optical Toffoli gate in the solid	203
PO-124	A.-V. Glushkov	Relativistic energy approach to atoms, ions and nuclei in a super strong laser field	204
PO-125	T. Kirova	Manifestation of dark state formation in Na hyperfine level system	205
PO-126	V. Meshkov	First principle calculation on thermophysical and transport properties of alkali-rare gas systems	206
PO-127	J.S. Dehesa	Entanglement in Helium	207
PO-128	J. Pedregosa-Gutierrez	An Ion Trap for Very Large Clouds	208
PO-129	I. Tóth	($e, 2e$) ionization of molecular hydrogen	209
PO-130	N. V. Vitanov	High-fidelity quantum information processing by composite pulses	210
PO-131	S. Nikolic	Electromagnetically induced transparency due to Zeeman coherence in buffer-gas cell - effects of laser radial profile and intensity . . .	211
PO: Teaching Quantum Physics			213
PO-132	P.A. Bouvrie	Quantum entanglement in exactly soluble atomic models: the Moshinsky model with three electrons, and with two electrons in a uniform magnetic field	214
PO-133	A. Rosén	Undergraduate research: Laboratory experiments with many variables	215
PO-134	A.-S. Martensson	Extended Cat Television Diagram (ECTD) for Quantum Physics in High School.	216

PO: Ultrafast processes	217
PO-135 C. L. Arnold	
Attoscience in Lund	218
PO-136 B. Bergues	
Attosecond Tracing of Non-Sequential Double Ionization in a Single Laser Cycle	219
PO-137 S. Borbély	
Ionization of H by few-cycle XUV laser pulses: Spatial and temporal interference effects	220
PO-138 S. Borbély	
Iterative solution of the time-dependent Schrödinger equation . . .	221
PO-139 A. C. Brown	
Harmonic Generation in Time Dependent <i>R</i> -Matrix Theory	222
PO-140 E. Lorek	
High Harmonic Generation at 200 kHz repetition rate	223
PO-141 M. Yu. Emelin	
Role of magnetic field in strong-field atomic stabilization	224
PO-142 M. Yu. Emelin	
Formation of extremely short pulses from resonant radiation in hydrogen-like medium: three-level model versus time-dependent Schrödinger equation	225
PO-143 A.-V. Glushkov	
Cooperative muon-gamma-nuclear spectroscopy of atomic systems	226
PO-144 K. Hansen	
Resonant and non-resonant ionizations of xenon with 388 nm femtosecond laser pulses	227
PO-145 C. M. Heyl	
Enhanced High-Order Harmonic Generation using dual gas targets	228
PO-146 A. Jiménez-Galán	
Study of Fano resonances with the Rabitt technique	229
PO-147 M. Khokhlova	
Theory of resonant high-order harmonic generation by low-frequency laser field	230
PO-148 D. Kroon	
Timing measurements of an attosecond pulse train using a stabilized interferometer	231
PO-149 E. Lorek	
High Harmonic Generation at 200 kHz repetition rate	232
PO-150 P. Rudawski	
An intense source of high-order harmonics	233
PO-151 P. Vindel-Zandbergen	
Laser induced dynamics in the Shin-Metiu-Engel model: controlling singlet-triplet transition with the non-resonant Starck effect	234

Index by author

235

Plenary Lectures

Attosecond physics: the first decade

F. Krausz¹

¹*Max-Planck-Institut für Quantenoptik, Garching, Germany, Ludwig-Maximilians-Universität München, München, Germany*

Corresponding Author: krausz@lmu.de

Electron motion and light waves form the basis of life: the microscopic motion of electrons creates light, which supplies our globe with life-giving energy from the sun; electrons transform light into biological energy during photosynthesis and into biological signal endowing us with the capability of seeing the world around us. Upon their motion inside and between atoms, electrons emit light, carry and process information in biological systems and man-made devices; create, destroy, or modify molecules, affecting thereby biological function. Consequently, they are key players in physical, chemical, and life sciences; information, industrial, and medical technologies likewise.

During the past ten years (2001-2011), advances in laser science opened the door to watching and controlling these hitherto inaccessible dynamics: the motion of electrons at the atomic scale and light wave oscillations (being mutually the cause of each other) evolving on attosecond time scales.

Key tools include waveform-controlled few-cycle laser light and attosecond pulses of extreme ultraviolet and soft-X-ray light. They provide a force capable of steering electrons inside and between atoms and a probe for tracking their motion. Insight into and control over microscopic electron motion are likely to be important for developing brilliant sources of X-rays, understanding molecular processes relevant to the curing effects of drugs, the transport of bioinformation, or the damage and repair mechanisms of DNA, at the most fundamental level, where the borders between physics, chemistry and biology disappear. Once implemented in condensed matter, the new technology will be instrumental in advancing electronics and electron-based information technologies to their ultimate speed: from microwave towards lightwave frequencies.

Probing Matter from Within using Ultra-Intense and Ultra-Fast X-Rays from the LCLS Free Electron Laser

N. Berrah¹

¹*Department of Physics, Western Michigan University Kalamazoo, USA*

Corresponding Author: nora.berrah@wmich.edu

Short x-ray pulses from free electron lasers (FEL) open a new regime for all scientific research. The first x-ray FEL, the Linac Coherent Light Source (LCLS) at the SLAC National Laboratory on the Stanford campus, provides intense short pulses that allow the investigation of non-linear and multi-photon processes, including multiple core-holes in atoms, molecules and clusters.

The response of molecular and cluster systems to the ultra-intense, femtosecond x-ray radiation was investigated. Sequential multiphoton ionization, non-linear processes, frustrated absorption [1] and double core hole production mechanisms [2,3] in molecules and clusters will be presented.

This work was done in collaboration with L. Fang, T. Osipov, B. Murphy, M. Hoener, E. Kukk, E. Kanter, S. T. Pratt, O. Kornilov, O. Gessner, M. Gueher, P. Bucksbaum, C. Buth, M. Chen, F. Tarantelli, K. Ueda, R. Feifel, P. van der Meulen, P. Salen, H. Schmidt, R. Thomas, M. Larsson, R. Richter, K. C. Prince, J. D. Bozek, C. Bostedt, S. Wada, M. Piancastelli, M. Tashiro, and M. Ehara.

References

- [1] M. Hoener et al., Phys. Rev. Lett. 104, 253002 (2010)
- [2] L. Fang et al., Phys. Rev. Lett 105, 083005 (2010)
- [3] N. Berrah et al., Proc. Natl. Acad. Sci. (PNAS), 108, issue 41, 16912 (2011).

Rydberg Fingerprint Spectroscopy: Probing the Excited States and Ionisation Dynamics of Fullerenes

E.E.B. Campbell¹

¹*EaStCHEM, School of Chemistry, University of Edinburgh, Edinburgh EH9 3JJ, Scotland*

Corresponding Author: eleanor.campbell@ed.ac.uk

The interaction of fullerene beams with intense laser pulses has been studied since the first observation of fullerenes in time-of-flight mass spectrometry in the mid-eighties. Fullerenes are interesting species to study since they are relatively large molecules but they are straightforward to introduce into the gas phase and have the additional advantages of consisting of only one element (carbon) and having a high symmetry (Ih) that simplifies theoretical treatment. Because of the relatively unusual relationship between C-C bond energy (high) and ionisation potential (low), fullerenes have been shown to be good model systems for studying the competition between different thermal decay mechanisms such as thermionic emission, radiative cooling and fragmentation. In recent years, focus has been placed on studying photon-fullerene interactions leading to electron emissions at timescales before full energy equilibration can take place. When ionising with fs lasers, fullerenes, and other conjugated molecules, show well-resolved peak structure in their photoelectron spectra that can be attributed to single photon ionisation of a large range of excited states thus providing a fingerprint of the molecule [1]. The range of excited states that is produced in the interaction with the fs laser pulses is independent of the laser wavelength. For fullerenes, strong peaks are observed that are attributed to the excitation of SAMO states (super-atom molecular orbitals), these are very simple hydrogenic-type orbitals that are centred on the fullerene core rather than on the carbon atoms. They are a consequence of the hollow nature of the molecule [2]. New studies that combine fs Rydberg fingerprint spectroscopy with angular-resolved photoelectron spectra obtained using velocity map imaging and time-dependent density functional theory [3] are shedding new light on the population of these states and the reasons for their prominence in the photoelectron spectra. Techniques are also being developed that can provide information on the timescale of electron emission [4] and a probe of the onset and origin of thermal electron emission. In this talk an overview of the recent fullerene photoionisation studies and their relevance for understanding the ionisation dynamics and mechanisms of large molecules will be given.

References

- [1] C. Schick and P. Weber, *J. Phys. Chem. A* **105** (2001) 3735; M. Boyle *et al.*, *Phys. Rev. Lett.* **87** (2001) 273401
- [2] M. Feng, J. Zhao, and H. Petek, *Science* **320** (2008) 359-362
- [3] J. O. Johansson *et al.*, *Phys. Rev. Lett.* **108** (2012) 173401
- [4] J. O. Johansson *et al.*, *J. Chem. Phys.* **136** (2012) 164301

Taming molecular beams

G. Meijer¹

¹*Fritz-Haber-Institut der Max-Planck-Gesellschaft, Faradayweg 4-6, 14195 Berlin, Germany*

Corresponding Author: meijer@fhi-berlin.mpg.de

Getting ever better control over gas-phase molecules is an important research theme and drives progress in the field of molecular physics. The motion of polar molecules in a beam can be manipulated with inhomogeneous electric and magnetic fields. Static fields can be used to deflect or focus molecules, whereas time-varying fields can be used to decelerate or accelerate beams of molecules to any desired velocity. I will give an overview of the fascinating new possibilities that this molecular beam technology presently offers, ranging from novel scattering experiments and lifetime measurements on trapped molecules to the preparation of pure samples of selected structural isomers [1]. The miniaturization of electric field structures enables the manipulation of polar molecules at close distance from a surface, and I will report on the progress in creating a molecular laboratory on a chip [2]. Time permitting, I will also report on the recent experimental realization of a microwave decelerator for neutral polar molecules, suitable to decelerate and focus a beam of molecules in high-field-seeking states [3].

References

- [1] S. Y. T. van de Meerakker, H. L. Bethlem, and G. Meijer, *Nature Physics* **4**, 595–602 (2008)
- [2] S. A. Meek, H. Conrad, and G. Meijer, *Science* **324**, 1699–1702 (2009)
- [3] S. Merz *et al.*, arXiv:1204:4019

Dynamic behavior of ultra cold atomic gases

S. Stringari¹

¹*Department of Physics, University of Trento, Italy*

Corresponding Author: stringar@science.unitn.it

I will present an overview of recent advances in the study of the collective dynamics in harmonically trapped, ultra cold atomic gases. I will discuss in particular the behavior of the collective oscillations of strongly interacting Fermi gases at both zero and finite temperature and recent achievements on the center of mass oscillation in spin orbit coupled Bose-Einstein condensates. Both theoretical and experimental results will be discussed.

New frontiers in ultracold quantum gases

R. Grimm¹

¹*Institut für Experimentalphysik, Universität Innsbruck, 6020 Innsbruck, Austria, and
Institute für Quantenoptik und Quanteninformation (IQOQI), Austrian Academy of Sciences,
6020 Innsbruck, Austria*

Corresponding Author: rudolf.grimm@uibk.ac.at

Ultracold quantum gases at nanokelvin temperatures in the degenerate regime offer a rich playground for studying the fundamental behavior of interacting quantum matter, based on the exquisite control of experimental parameters and the possibility to tune the interparticle interactions. The results show novel phenomena and challenge theoretical descriptions of many-body quantum physics [1].

After introducing into the general ideas of the field, I will present examples from ongoing experimental research in Innsbruck. First, as an example related to condensed-matter physics, I will present the observation of quasiparticles in a degenerate Fermi gas, including the observations of “repulsive polarons” [2]. Second, as an example connecting to nuclear physics, I will discuss the observation of “Efimov states” [3]. Finally, as a most recent development, I will present the Bose-Einstein condensation of a new atomic species, atomic erbium featuring strongly anisotropic, dipolar interactions [4].

References

- [1] I. Bloch, J. Dalibard, and W. Zwerger, *Rev. Mod. Phys.* **80**, 885 (2010)
- [2] C. Kohstall *et al.*, *Nature* **485**, 615 (2012)
- [3] F. Ferlaino and R. Grimm, *Physics* **3**, 9 (2010)
- [4] K. Aikawa *et al.*, *Phys. Rev. Lett.* **108**, 210401 (2012)

Molecular line lists for the opacity of exoplanets and other atmospheres

Jonathan Tennyson¹

¹*Department of Physics and Astronomy, University College London, London WC1E 6BT, UK*
Corresponding Author: j.tennyson@ucl.ac.uk

At elevated temperatures the spectra of polyatomic molecules become extremely complicated with millions, or even billions, of transitions potentially playing an important role. The atmospheres of cool stars and "hot Jupiter" extrasolar planets are rich with molecules in the temperature range 1000 to 3000 K and their properties are strongly influenced by the infrared and visible spectra of these molecules. Access to extensive lists of transitions is essential for interpreting even the rather simple spectra that can be obtained from exoplanets [1]. So far there are extensive, reliable lists of spectral lines for a number of species including some stable diatomics, water, ammonia. Data is almost completely lacking for many key species such as methane.

The ExoMol project [2] aims to construct line lists of molecular transitions suitable for spectroscopic and atmospheric modelling of cool stars and exoplanets [3]. As at elevated temperatures it is necessary to consider huge numbers of lines even for a single species, direct determination of these line lists by laboratory measurements is problematic. Line lists therefore are best computed on the basis of robust theoretical models tested against available laboratory data rather than constructed experimentally. Illustrative examples will be discussed along with their application to a wide variety of astronomical and terrestrial problems. The progress in generating the full set of molecular data will be given.

References

- [1] G Tinetti *et al.*, *Nature*, **448**, 169-171 (2007).
- [2] www.exomol.com
- [3] J. Tennyson and S. N. Yurchenko, *Mon. Not. R. astr. Soc.* (in press); arXiv:1204.0124

Confessions of a converted lecturer.

E. Mazur¹

¹*Harvard University, 29 Oxford Street, 02138 Cambridge Massachusetts, USA*

Corresponding Author: mazur@physics.harvard.edu

I thought I was a good teacher until I discovered my students were just memorizing information rather than learning to understand the material. Who was to blame? The students? The material? I will explain how I came to the agonizing conclusion that the culprit was neither of these. It was my teaching that caused students to fail! I will show how I have adjusted my approach to teaching and how it has improved my students' performance significantly.

Is Vacuum Really Empty?

P. Delsing¹

¹*Chalmers University of Technology, Microtechnology and nanoscience, Kemivägen 9, 41296 Gteborg, Sweden*

Corresponding Author: per.delsing@chalmers.se

We have recently been able to create light from vacuum using superconducting circuits. At the heart of the experiment is one of the weirdest, and most important, tenets of quantum mechanics: the principle that empty space is anything but empty. Quantum theory predicts that a vacuum is actually a writhing foam of particles fitting in and out of existence, s o called virtual particles. If a mirror is moved through the vacuum at a speed close to the speed of light, these virtual particles can be forced into reality and in that way light can be created from vacuum.

The ALPHA Experiment at CERN: Physics with Trapped Antihydrogen

J. Hangst¹

¹*Physics and Astronomy, Aarhus University, Ny Munkegade, DK-800, Aarhus, Denmark*

Corresponding Author: Jeffrey.hangst@cern.ch

The ALPHA team can keep the antihydrogen atoms trapped for 1000 seconds. This is long enough to begin to study them - and conduct the precision measurements necessary to investigate a symmetry known as CPT. According to CPT symmetry a particle moving forward through time in our universe should be indistinguishable from an antiparticle moving backwards through time in a mirror universe, and it is thought to be perfectly respected by nature. CPT symmetry requires that hydrogen and antihydrogen have identical spectra. "Any hint of CPT symmetry breaking would require a serious rethink of our understanding of nature. But half of the universe has gone missing, so some kind of rethink is apparently on the agenda."

Progress Reports

Photoelectron diffraction imaging of molecular dynamics

P. Johnsson¹, A. Rouzée², A. Hundertmark², L. Rading¹, S. Düsterer³, F. Tavella³,
N. Stojanovic³, A. Al-Shemmary³, M. Gensch⁴, Ph. Wernet⁵, T. Leitner⁵, and
M. J. J. Vrakking²

¹Lund University, P.O. Box 118, SE-22100 Lund, Sweden

²Max-Born-Institut, Max-Born Strasse 2A, D-12489 Berlin, Germany

³HASYLAB at DESY, Notkestrasse 85, D-22603 Hamburg, Germany

⁴Helmholtz-Zentrum Dresden-Rossendorf, Bautzner Landstr. 400, D-01328 Dresden, Germany

⁵Helmholtz-Zentrum Berlin, Albert-Einstein-Strasse 15, D-12489 Berlin, Germany

Corresponding Author: per.johnsson@fysik.lth.se

We will report on experiments performed at FLASH, aiming to follow molecular dynamics in time by studying photoelectrons emitted through single-photon ionization by the XUV/soft X-ray FEL pulses. Our approach exploits the fact that electrons leaving the molecule may scatter off one of the other nuclei, or interfere with electrons emitted from equivalent sites in the molecule [1]. These processes encode diffractive information in the photoelectron angular distribution that can be used as a detailed probe of molecular structure when the photoelectron angular distribution is measured in the molecular frame, i.e. in a coordinate system that is fixed with respect to the molecular axis. We use laser-induced alignment to manipulate the angular distribution of molecular samples in combination with the use of a velocity map imaging spectrometer [2], which permits molecular frame measurements of kinetic and angular distributions of electrons or ions with high count rates. In order to perform these experiments a pump-pump-probe arrangement has been developed, where a first optical pump laser pulse is used to initiate the alignment dynamics, a second pump laser pulse initiates dynamics in the molecules under investigation, and the role of the probe laser is played by the FLASH FEL, at a variable time delay with respect to the other two lasers. The first realization of field-free molecular alignment at FLASH, making use of CO₂ molecules [3], will be presented, as well as our attempts to observe time-dependencies in the molecular frame photoelectron distribution of dissociating Br₂ molecules [4] (see Fig. 1), including the results from our latest beamtime in May 2011.

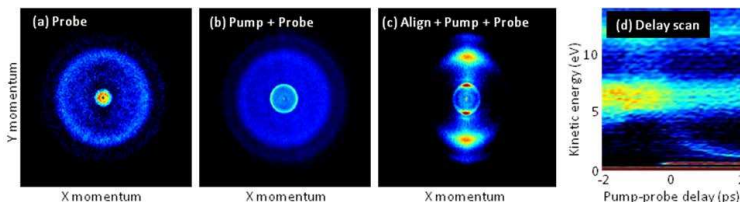


Figure 1: Br₂⁺ ions resulting from dissociation of Br₂ by 13 nm light from FLASH. Momentum distributions for ionization by (a), the FEL pulse alone, (b), the FEL pulse preceded by a 400 nm dissociation pulse and (c), with an IR alignment pulse. Panel (d) shows the kinetic energy distribution as a function of delay between the 400 nm dissociation pulse and the FEL pulse. A sharp time-dependent contribution is observed due to an additional kinetic energy from Coulomb repulsion being imparted to the dissociating atoms when they are ionized at short inter-nuclear distances.

References

- [1] A. Landers *et al.*, Phys. Rev. Lett. **87**, 013002 (2001)
- [2] P. Johnsson *et al.*, J. Mod. Opt. **55**, 2693 (2008)
- [3] P. Johnsson *et al.*, J. Phys B **42**, 134017 (2009)
- [4] N. Berrah *et al.*, J. Mod Opt. **57**, 1015 (2010)

50 years of ^3He optical pumping: “When only the best will do”

G. Tastevin

Laboratoire Kastler Brossel, ENS - CNRS - UPMC, 24 rue Lhomond, 75005 Paris, France

Corresponding Author: tastevin@lkb.ens.fr

In the early 1960’s two indirect optical pumping (OP) techniques for polarising the nuclear spin of the ^3He isotope have been proposed: spin-exchange (SE) with optically pumped alkali atoms [1, 2] and metastability exchange (ME) with optically pumped metastable helium atoms [3, 4, 5]. The efficiency of SEOP was poor but MEOP found immediate application for reactions with particle beams, then opened the way to many novel studies involving the dilute and dense fluid phases of ^3He at low temperature. Hyperpolarised ^3He gas has since been used in a variety of research fields including nuclear and particle physics (polarised target for scattering experiments, production of polarised ^3He ions), tests of fundamental symmetries (spin-1/2 maser or free-precession probe for precision magnetometry), neutron science (broadband spin polariser or analyser), material science and biomedical MRI (exogeneous NMR tracer for relaxometry and functional imaging).

Recent years have seen remarkable advances in the decades-long struggle to develop the two OP techniques, driven by the demand and the success of ^3He -based neutron spin filters and lung MRI. Thanks to technical breakthroughs, better optical diagnostic tools, and improved physical insight, very high production rates (0.5 bar·L/h for SEOP and 1–5 bar·L/h for MEOP) and nuclear polarisations (slightly below 70% for SEOP and 80% for MEOP) are now achieved under optimal conditions. However these values are still below expectations and correspondingly many efforts are underway to understand the origin of current limitations for both techniques.

The processes involved in OP, exchange, and relaxation will be reviewed. The outcomes and puzzling results of various systematic experimental investigations carried out using the two OP techniques will be briefly reported and discussed on the basis of the scrutinised rate equations and angular momentum budgets (hybrid SEOP, impact of temperature, pressure-broadening collisions, OP light, alkali density, or cell walls on polarisation loss and photon demand; plasma conditions, photon efficiency, and laser-induced relaxation for MEOP operated at high laser power, high magnetic field, or high gas pressure). Perspectives for further improvement of the quantity and polarisation of ^3He gas will be presented.

References

- [1] M.A. Bouchiat, T.R. Carver, and C.M. Varnum, *Phys. Rev. Lett.* **5**, 373–375 (1960)
- [2] T.G. Walker and W. Happer, *Rev. Mod. Phys.* **69**, 629–642 (1997)
- [3] G.K. Walters, F.D. Colegrove, and L.D. Schearer, *Phys. Rev. Lett.* **8**, 439–442 (1962)
- [4] F.D. Colegrove, L.D. Schearer, and G.K. Walters, *Phys. Rev.* **132**, 2561–2571 (1963)
- [5] M. Batz, P.-J. Nacher, and G. Tastevin, *J. Phys.: Conf. Ser.* **294**, 012002 (2011) - 21 p.

Towards laser cooling of atomic anions

Alban Kellerbauer¹

¹Max Planck Institute for Nuclear Physics, Saupfercheckweg 1, 69117 Heidelberg, Germany

Corresponding Author: a.kellerbauer@cern.ch

Atomic anions are generally not amenable to optical spectroscopy because they are loosely bound systems and rarely have bound excited states. Until now, there are only very few negative ions with strong bound-bound electronic transitions. [1,2]. These electric-dipole transitions may provide unique insight into the structure of atomic anions. In addition, they may enable the preparation of ultracold ensembles of negative ions. Currently available cooling techniques for negatively charged particles allow cooling only to the temperature of the surrounding cryogenic environment, typically at 4 K if the apparatus itself is cooled with liquid helium. At these temperatures, the achievable precision of spectroscopic measurements is often limited by inhomogeneous broadening due to thermal motion.

Laser excitation of the electric-dipole transition in atomic anions could be used to laser-cool them to microkelvin temperatures [3]. If demonstrated to be successful, the technique would allow the cooling of any species of negatively charged particles – from subatomic particles to molecular ions – to ultracold temperatures by sympathetic cooling. We have been investigating the bound-bound electric-dipole transition in Os^- by high-resolution laser spectroscopy to ascertain its suitability for laser cooling [4–6]. The principle of the method, its potential applications, as well as experimental results will be presented.

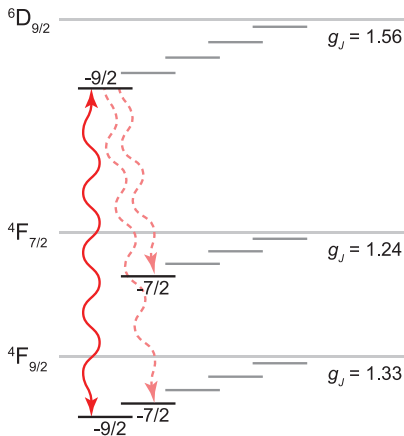


Figure 1: Partial energy level diagram of Os^- in a magnetic field. The potential laser cooling transition is indicated by a solid arrow, the decay to ‘dark’ states by dashed arrows.

References

- [1] R. C. Bilodeau and H. K. Haugen, Phys. Rev. Lett. **85** (2000) 534
- [2] C. W. Walter *et al.*, Phys. Rev. A **84** (2011) 032514
- [3] A. Kellerbauer and J. Walz, New J. Phys. **8** (2006) 45
- [4] U. Warring *et al.*, Phys. Rev. Lett. **102** (2009) 043001
- [5] A. Fischer *et al.*, Phys. Rev. Lett. **104** (2010) 073004
- [6] A. Kellerbauer *et al.*, Phys. Rev. A **84** (2011) 062510

Deterministic few-fermion quantum systems

Gerhard Zürn^{1,2}, Thomas Lompe^{1,2,3}, Andre Wenz^{1,2}, Martin Ries^{1,2},
Vincent Klinkhamer^{1,2}, Andrea Bergschneider^{1,2}, Simon Murmann^{1,2}, and
Selim Jochim^{1,2,3}

¹*Physikalisches Institut, Ruprecht-Karls-Universität Heidelberg, Germany*

²*Max-Planck-Institut für Kernphysik, Heidelberg, Germany*

³*ExtreMe Matter Institute EMMI, GSI Helmholtzzentrum für Schwerionenforschung,
Darmstadt, Germany*

Corresponding Author: jochim@uni-heidelberg.de

Few-particle Fermi systems are the basic building blocks of all matter which have been studied extensively in atomic, nuclear and condensed matter physics. In our experiments, we have realized few-fermion systems consisting of 1-10 atoms in a tightly confining optical trap in which the interaction and all quantum mechanical degrees of freedom can be controlled [1]. These deterministic ensembles are ideally suited for the quantum simulation of few-body systems.

To establish an experimental toolbox we first studied the two-particle system. By comparing a noninteracting spin polarized system with an interacting system containing two different spin states we could demonstrate fermionization of the two distinguishable particles for diverging repulsive coupling strength by showing that the square modulus of the wave function of the two systems is the same in our quasi 1-D configuration [2].

We have extended our study to up to six particles with both attractive and repulsive interactions. In the first case we observe a strong odd-even effect in the interaction energy and correlated pair tunneling out of a tilted trap. For strong repulsive interactions we observe ferromagnetic correlations, when the repulsion between distinguishable particles becomes stronger than the Fermi energy.

References

- [1] F. Serwane, G. Zürn, T. Lompe, T.B. Ottenstein, A.N. Wenz, and S. Jochim, *Science* **332**, 6027 (2011)
- [2] G. Zürn, F. Serwane, T. Lompe, A. N. Wenz, M. G. Ries, J. E. Bohn, and S. Jochim, *PRL* **108**, 075303 (2012)

Atom Trap, Krypton-81, and Global Groundwater

Z.T. Lu¹

¹*Oak Ridge National Laboratory*

Corresponding Author: liuy@ornl.gov

The long-lived noble-gas isotope ^{81}Kr is the ideal tracer for old water and ice in the age range of 10^5 – 10^6 years, a range beyond the reach of ^{14}C . ^{81}Kr -dating, a concept pursued in the past four decades by numerous laboratories employing a variety of techniques, is now available for the first time to the earth science community at large. This is made possible by the development of an atom counter based on the Atom Trap Trace Analysis (ATTA) method, in which individual atoms of the desired isotope are selectively captured and detected with a laser-based atom trap. ATTA possesses superior selectivity, and is thus far used to analyze the environmental radioactive isotopes ^{81}Kr , ^{85}Kr , and ^{39}Ar . These three isotopes have extremely low isotopic abundances in the range of 10^{-16} to 10^{-11} , and cover a wide range of ages and applications. In collaboration with earth scientists, we are dating groundwater and mapping its flow in some major aquifers around the world.

This work is supported by DOE, Office of Nuclear Physics, under contract DE-AC02-06CH11357; and by NSF, Division of Earth Sciences, under award EAR-0651161.

Two- and Three-Photon Atomic Double Ionization by Intense FEL Pulses

A. N. Grum-Grzhimailo¹, E. V. Gryzlova¹, S. Fritzsche², and N. M. Kabachnik^{1,3}

¹*Skobeltsyn Institute of Nuclear Physics, Lomonosov Moscow State University, 119991 Moscow, Russian Federation*

²*GSI Helmholtzzentrum für Schwerionenforschung, D-64291 Darmstadt, Germany and Department of Physics, University of Oulu, PO Box 3000, Fin-90014, Finland*

³*European XFEL GmbH, Albert-Einstein-Ring 19, D-22607 Hamburg, Germany*

Corresponding Author: algrgr1492@yahoo.com

With the advent of Free-Electron Lasers (FELs) operating in the short-wavelength regime and generating extremely intense femtosecond pulses, nonlinear processes in the XUV and X-ray wavelength range are now accessible experimentally [1,2]. In this range, the energy of a single photon is already enough to ionize the target. When the photon energy is higher than the ionization threshold of the ion, it appears that sequential two-photon double ionization (2PDI) dominates in which the first photon produces an ion which is subsequently ionized by the second photon from the same pulse. For the photon energies between the atomic and ionic ionization thresholds, the second-step ionization proceeds via two-photon absorption, leading to three-photon double ionization (3PDI). In sequential 2PDI and 3PDI, the individual energy of each of the two emitted electrons is fixed by energy conservation. Studies of 2PDI and 3PDI, the simplest nonlinear reactions in the XUV, are at their beginning. They can provide a wealth of new information on photoionization amplitudes, cross-sections and transition probabilities in ions, allocate ionic autoionizing states, reveal dynamic correlations between two sequentially emitted photoelectrons, etc. The talk overviews developments in this new field. The following points are addressed: angular distributions and correlations of photoelectrons in sequential 2PDI and 3PDI [3–6], effects of alignment and coherency of the intermediate ionic states [6], resonant [7] and doubly resonant [8] sequential 3PDI. Theoretical predictions, based on statistical tensor approach combined with multi-configurational Hartree-Fock and Dirac-Fock calculations, are illustrated by first experimental data [1,7–9].

It is known that already at photon energies of a few hundreds eV, the photoelectron angular distribution in atomic single-photon ionization can be affected significantly by interferences between the electric dipole (E1) and electric quadrupole (E2) photoionization amplitudes. Thus, nondipole effects should show up also in the XUV/X-ray nonlinear atomic processes, first of all presumably in the angular distributions of emitted electrons. The nondipole effects in nonlinear photoprocesses in XUV is so far an opened field. First theoretical predictions will be presented of nondipole effects in the 2PDI.

This research is partly supported by the Russian President grant MK-6509.2012.2

References

- [1] M. Braune *et al.*, *XXV Int. Conf. on Photonic, Electronic and Atomic Collisions* (Freiburg, Germany, 2007), Abstracts, Fr034 and private communications
- [2] A. Rudenko *et al.*, *J. Phys. B* **43**, 194004 (2010)
- [3] A.S. Kheifets, *J. Phys. B* **40**, F313 (2007)
- [4] S. Fritzsche *et al.*, *J. Phys. B* **41**, 165601 (2008); *ibid* **42**, 145602 (2009); *ibid* **44**, 175602 (2011)
- [5] A.N. Grum-Grzhimailo *et al.*, *J. Phys. Conf. Ser.* **194**, 012004 (2009)
- [6] E.V. Gryzlova *et al.*, *J. Phys. B* **43**, 225602 (2010)
- [7] H. Fukuzawa *et al.*, *J. Phys. B* **43**, 111001 (2010)
- [8] E.V. Gryzlova *et al.*, *Phys. Rev. A* **84**, 063405 (2011)
- [9] M. Kurka *et al.*, *J. Phys. B* **42**, 141002 (2009)

Remembering Miss Meitner: History, Memory, and the Future of Physics

R.M. Friedman¹

¹ *University of Oslo, Norway*

Corresponding Author: robert.friedman@iakh.uio.no

As a historian of science who had dramatised his PhD thesis for television, I eagerly participated in discussions on science related theatre prompted by the spectacular success of Michael Frayn's 'Copenhagen'. At two symposia on the relations between science, drama, and history organised by the Niels Bohr Archive in Copenhagen, I asked, as others have asked: can drama provide insight into the scientific enterprise? can theatre be used for exploring the history of science? My reflections on juggling the demands of scholarship with those of art as well as my tentative outlines for history of science based plays seemed safe enough in an academic auditorium, but subsequently I was invited to write one such play for theatrical production. In moving from idea to script to performance, I gained further respect for the difficulties of harmonising history and drama. To dramatised history of science is a risky endeavour, but one worth the effort

Why do recognized textbooks in physics represent a quasi-history of Planck's, Einstein's and Bohr's development of quantum physics?

R. Renström¹

¹*Universitetet i Agder, Fåmyråsen 56, 4640 Søgne, Norway*

Corresponding Author: reidun.renstrom@uia.no

In my unpublished thesis, "The Development of Quantum Physics, in Historic Accounts, Textbooks and Classrooms", I investigated representations of the development of quantum physics in well-established, recent textbooks which are widely used at universities today. The conclusion of my investigation is that the myths identified by historians of science are still very much alive in the textbooks. In my thesis I claim that the way these textbooks represent Bohr's development of a model of the atom and the theory of the hydrogen atom are indeed also a quasi-history. The myths my thesis refer to are: In 1911 Rutherford proposed a planet model of the atom that answered many questions, and was generally accepted by physicists. There was however one big problem with the model; according to classical theory Rutherfords atom was unstable and would collapse. One of many physicists losing sleep over this problem was Bohr, who soon recognized that the emission line spectra indicate that atoms emit photons with specific frequencies and energy. Therefore said Bohr, each atom must be able to exist with only certain specific values of internal energy. The textbook story of the development of quantum physics is framed historically but it seems no attempt has been made to convey history truthfully. The real history is distorted in a systematic way to support the view that the main factors in the progress of physics knowledge are always shocking contradictions between theoretical expectations on the one hand, and observable facts or even common sense on the other. As a matter of fact, there were no crises brought about by conflicts between classical theories and experimental results that could motivate Planck in 1900, Einstein in 1905 or Bohr in 1913 to develop their quantum theories. Quantum physics does not owe its origins to any failure in classical physics.

Is the electron round?

J. J. Hudson¹, D. M. Kara¹, I. J. Smallman¹, B. E. Sauer¹, M. R. Tarbutt¹, and E. A. Hinds¹

¹Centre for Cold Matter, Blackett Laboratory, Imperial College London, Prince Consort Road, London SW7 2AZ, UK.

Corresponding Author: m.tarbutt@imperial.ac.uk

The electric dipole moment (EDM, d_e) of the electron is a measure of the electron's shape, a non-zero value implying that the electron is not spherical. A non-zero EDM violates time-reversal symmetry which, in most models of physics, is equivalent to the symmetry between matter and antimatter (CP symmetry). The Standard Model of particle physics predicts a non-zero value for the electron EDM, but one which is exceedingly small [1]. Extensions to the Standard Model, such as supersymmetric extensions, predict that the EDM should be much larger [2] and within the range of current experiments. This makes the search for the electron EDM a powerful way to search for new physics and constrain the possible extensions. The size of the electron EDM is also intimately related to the puzzling question of why the Universe contains so little antimatter [3].

Certain heavy, polar molecules are exceptionally sensitive to the electron EDM. Exploiting this sensitivity, we have made the most precise measurement to date of d_e by measuring how the spin-precession rate of YbF molecules changes in an applied electric field. We obtain a result consistent with zero and set an upper limit of $|d_e| < 10.5 \times 10^{-28} e\text{cm}$ at the 90% confidence level [4]. This measurement of atto-electronvolt energy shifts in a molecule probes new physics at the tera-electronvolt energy scale. Indeed, it is difficult to reconcile our result with the popular idea that new supersymmetric particles may exist at masses of a few hundred GeV [1]. New measurements, with improved sensitivity, are now underway in our laboratory and future improvements, including the use of a cryogenically-cooled source of YbF molecules and laser cooling of the molecules, hold the promise of further very large improvements in sensitivity.

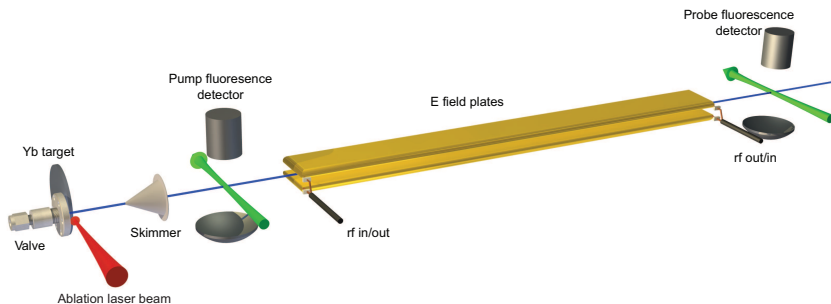


Figure 1: Schematic diagram of the experiment. The apparatus measures how the spin precession rate of YbF molecules changes in an applied electric field, and this determines the electron EDM.

References

- [1] M. Pospelov and A. Ritz, *Ann. Phys.* **318**, 119-169 (2005)
- [2] W. Bernreuther and M. Suzuki, *Rev. Mod. Phys.* **63**, 313-340 (1991)
- [3] A. D. Sakharov, *Pis'ma ZhETF* **5**, 32-35 (1967); *Sov. Phys. JETP Lett.* **5**, 24-27 (1967)
- [4] J. J. Hudson *et al.*, *Nature* **473**, 493-497 (2011)

High-harmonic spectroscopy of electronic dynamics in molecules

P. M. Kraus¹, A. Rupenyan¹, J. Schneider¹, and H. J. Wörner¹

¹Laboratory for physical chemistry, ETH Zürich, Wolfgang-Pauli-Strasse 10, 8093 Zürich, Switzerland

Corresponding Author: woerner@phys.chem.ethz.ch

Recent progress in applying high-harmonic generation (HHG) to study electronic structure and dynamics in molecules will be presented. High-harmonic generation occurs when an intense femtosecond laser pulse interacts with a molecule. An electron is removed through strong-field ionization, accelerated by the laser field and allowed to recombine with the parent ion. The short de-Broglie wavelength of the electron and the precise timing of the recollision process enable the characterization of electronic structure and dynamics with atomic spatial resolution and attosecond temporal resolution.

The sensitivity of the HHG process to electronic structure is now well established. We have investigated the relative roles played by multielectron effects, the geometric and the electronic structure in high-harmonic spectra of molecules. We study the isoelectronic molecules CO₂ and N₂O that have a nearly identical overall length. In N₂O we find a gradual decrease of ionization from lower orbitals with increasing wavelength of the generating field, similar to previous observations in CO₂. We then isolate purely structural signatures in the spectra of both molecules and show that they reflect subtle differences in the electronic structure of the molecules.

Building on recent progress in field-free orientation of molecules, we study high-harmonic generation from oriented OCS molecules. The broken inversion symmetry of the medium leads to the generation of even harmonics. The analysis of these spectra and their comparison with *ab initio* quantum scattering calculations enables the characterization of the non-centrosymmetric electronic structure of OCS. We extend these measurements to small polyatomic molecules with substituents of very different ionization potentials which are expected to give rise to charge migration on the attosecond time scale.

The application of HHG to probing purely electronic dynamics in neutral molecules has been long anticipated and studied theoretically, but it has never been observed experimentally. We report the observation and characterization of an electronic wave packet in the neutral NO molecule, generated by a femtosecond pump pulse and probed through polarization-sensitive measurements of the emitted high harmonics.

The scientific approach to teaching: Research as a basis for course design.

E. Mazur¹

¹*Harvard University, 29 Oxford Street, 02138 Cambridge Massachusetts, USA*

Corresponding Author: mazur@physics.harvard.edu

Discussions of teaching – even some publications – abound with anecdotal evidence. Our intuition often supplants a systematic, scientific approach to finding out what works and what doesn't work. Yet, research is increasingly demonstrating that our gut feelings about teaching are often wrong. In this talk I will discuss some research my group has done on gender issues in science courses and on the effectiveness of classroom demonstrations.

Electromagnetically Induced Transparency via Cooperative Emission in a Cavity

R. Röhlsberger¹, H. C. Wille¹, K. Schlage¹, and B. Sahoo¹

¹Deutsches Elektronen Synchrotron DESY, Notkestr. 85, 22607 Hamburg, Germany

Corresponding Author: ralf.roehlsberger@desy.de

A planar cavity can be employed to prepare superradiant states of excited atoms that are coupled to the standing wavefield in a cavity mode. This principle has been applied recently to observe the collective Lamb shift L_N in single-photon superradiance from resonant ^{57}Fe nuclei that have been excited by pulses of 14.4 keV synchrotron radiation [1]. The ^{57}Fe atoms have been embedded in a single 1 nm thick layer in the center of a cavity consisting of a carbon guiding layer sandwiched between two Pt layers acting as mirrors [2], see Fig. 1a.

A qualitatively new situation is encountered when two resonant ^{57}Fe layers instead of one are placed in a cavity, as sketched in Fig. 1b. right. A pronounced dip in the cavity reflectivity is observed when one of the ^{57}Fe layers is located in a node, the other one in an antinode of the standing wave in the cavity. We have shown that this is a signature of electromagnetically induced transparency (EIT) [3]. Cooperative emission plays a crucial role for EIT in this system: While the layer in the antinode exhibits strong superradiant enhancement of its decay width, the layer located in the antinode remains subradiant and thus corresponds to the metastable state in the three-level scheme of an EIT system, as illustrated in Fig. 1c. The radiation field in the cavity mixes these two levels and the resulting quantum interference eventually leads to a pronounced transparency at the resonance energy ($\Delta = 0$) of the nuclei where the system is completely opaque otherwise, see Fig. 1d, as demonstrated recently at the synchrotron radiation source PETRA III at DESY [3]. We expect that this technique, based on coherent light scattering, can be generally applied to any ensembles of resonant emitters (atoms, ions, quantum dots) properly placed in optical cavities.

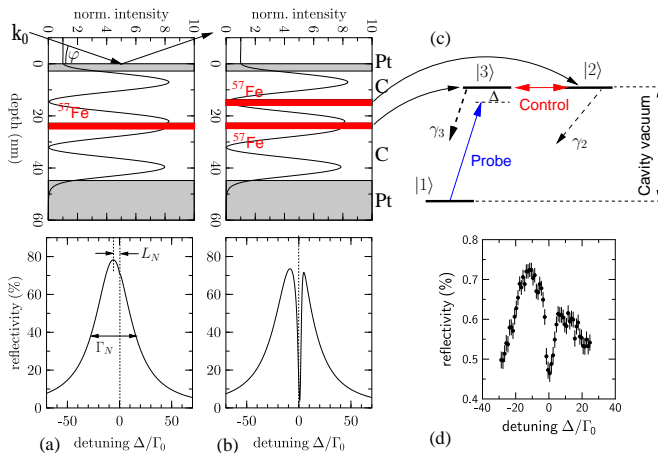


Figure 1: Cooperative emission from ^{57}Fe nuclei in a cavity leads to EIT.

References

- [1] R. Röhlsberger, K. Schlage, B. Sahoo, S. Couet, and R. Rüffer, *Science* **328**, 1248–1251 (2010)
- [2] R. Röhlsberger, *J. Mod. Opt.* **57**, 1979–1992 (2010)
- [3] R. Röhlsberger, H. C. Wille, K. Schlage, and B. Sahoo, *Nature* **482**, 199–203 (2012)

Direct Observation of Spin Flips with a Single Isolated Proton

A. Mooser^{1,2,3}, K. Blaum^{4,5}, H. Kracke^{1,2,3}, C. Leiteritz², W. Quint^{3,5},
C. Rodegheri^{2,4}, S. Ulmer⁶, and J. Walz^{1,2}

¹Helmholtz Institut Mainz, Johannes Gutenberg-Universität Mainz, 55099 Mainz, Germany

²Institut für Physik, Johannes Gutenberg-Universität Mainz, 55099 Mainz, Germany

³GSI Helmholtzzentrum für Schwerionenforschung, 64291 Darmstadt, Germany

⁴Max-Planck-Institut für Kernphysik, 69117 Heidelberg, Germany

⁵Ruprecht-Karls-Universität, 69047 Heidelberg, Germany

⁶RIKEN Advanced Science Institute, Hirosawa, Wako, Saitama 351-0198, Japan

Corresponding Author: mooser@uni-mainz.de

Applying the continuous Stern-Gerlach effect, spin flips with a single isolated proton were observed for the first time. This is the most important step towards a high precision measurement of the particle's g -factor and a million-fold improved test of the matter-antimatter-symmetry. A number of precision experiments measured the g -factor of the proton with various methods, but up to now the g -factor has never been measured directly. The most precise value for the g -factor results from measurements by Winkler *et al.* [1]. In this experiment the magnetic moment of the proton bound in atomic hydrogen has been determined with a relative precision of 10^{-8} by spectroscopy of the Zeeman effect on the hyperfine splitting. The free proton g -factor has been deduced from this measurement by subtracting theoretical bound state contributions. Our experiment, in contrast, aims for the first direct measurement of the g -factor of a single isolated proton stored in a Penning trap at a relative precision of 10^{-9} or better [2]. The measuring process and the experimental setup can be applied for protons as well as for antiprotons, whose g -factor is currently known to a relative precision of 10^{-3} , only [3]. Thus an improvement of six orders of magnitude is feasible. The measurement and comparison of the magnetic moment of the proton and antiproton will provide a stringent experimental test of the CPT-theorem [4]. The single proton is stored in a double Penning trap setup. This allows for the spatial separated measurement of the cyclotron frequency ν_c of the proton and the detection of its spin state for the determination of the Larmor frequency ν_L . The g -factor can then be calculated as $g = 2\nu_L/\nu_c$. The simultaneous measurement of these frequencies allow for a magnetic field independent measurement of the g -factor. The cyclotron frequency is determined in a homogeneous magnetic field in the so-called precision trap by measuring the three eigenmotions of the ion in the Penning trap, demonstrated in [5], and applying the invariance theorem [6]. The Larmor frequency can be determined from the proton spin flip resonance curve, obtained by scanning an external excitation field over the Larmor frequency. To this end the spin state of the ion has to be detected. This detection is based on a coupling of the particle's magnetic moment μ to its axial oscillation frequency ν_z . The coupling is achieved by an inhomogeneous magnetic field component B_2 , the magnetic bottle, in the so-called analysis trap and results in an axial frequency shift according to the spin orientation [7]. We recently demonstrated the first successful induction of spin flips by measuring the Larmor resonance curve in the analysis trap [8].

References

- [1] P. F. Winkler *et al.*, Phys. Rev. A **5**, 83 (1972)
- [2] C. C. Rodegheri *et al.*, Hyperfine Interact. **194**, 93 (2009)
- [3] T. Pask *et al.*, Phys. Lett. B **678**, 55 (2009)
- [4] R. Bluhm *et al.*, Phys. Rev. Lett. **79**, 1432 (1997)
- [5] S. Ulmer. Phys. Rev. Lett., **107**, 103002 (2011)
- [6] L. Brown and G. Gabrielse, Phys. Rev. A **25**, 2423 (1982)
- [7] W. Quint *et al.*, Nucl. Inst. Meth. Phys. Res. B **214**, 207 (2004)
- [8] S. Ulmer. Phys. Rev. Lett., **106**, 253001 (2011)

Exploring the knowledge structure of introductory quantum mechanics

C. Lindstrøm

Faculty of Teacher Education, Oslo and Akershus University College, Oslo, Norway

Corresponding Author: Christine.Lindstrom@hioa.no

Quantum Mechanics is a challenging and non-intuitive core area of physics. In my talk I will present a successful teaching intervention that included the topics of Quantum Mechanics and Mechanics in first year university physics. I will discuss a theoretical framework that focuses on the knowledge taught: how it can shed light on the positive results of the teaching intervention, how it can help us, as physics educators, increase our understanding of the content we teach, and how we can make physics more accessible to and enjoyable for our students.

In 2007, a successful year-long teaching intervention in first year physics involving 698 students was carried out at the University of Sydney, Australia. Students were randomly allocated into two different tutorial groups: inquiry-based Workshop Tutorials, run since 1995, or the more strongly scaffolding newly developed Map Meetings. The former consisted of 50 minutes of collaborative problem solving; in the latter, such collaborative work was reduced to 25 minutes, sandwiched between a 15-minute summary lecture and a 10-minute concluding plenary session, both led by the tutorial supervisor. The main result was that in the course for students without any prior formal physics instruction, Map Meetings had 50% fewer students at risk of failing compared to Workshop Tutorials [1].

The focus of Map Meetings was the Link Map, an A4-sheet with a non-linear summary of the weekly topic, around which both the summary lecture and the problem sheet centred. The Link Maps and summary lectures were overwhelmingly the focus of students positive feedback on Map Meetings and were seen as the main reason for their success [2].

After the conclusion of the experiment, the collection of Link Maps were analysed to gain insight into why they were so successful. Bloom's taxonomy, Bernstein's idea of knowledge structures and some of Maton's Legitimation Code Theory (the latter two both Sociologists of Education) were particularly useful frameworks to understand how the physics topics had been presented on the Link Maps and why this appeared to be particularly useful to the students.

Bernstein described hierarchical knowledge structures as "a coherent, explicit and systematically principled structure, hierarchically organized [that] ... attempts to create very general propositions and theories, which integrate knowledge at lower levels, and in this way shows underlying uniformities across an expanding range of apparently different phenomena" [3]. He frequently used physics as an example of a discipline with such a knowledge structure, but he never provided any specific analyses of the subject.

The analyses I will present support the perception that physics is a hierarchical field. However, although the discipline itself is hierarchical, the subset of the discipline taught to students is not always hierarchical. The reason for this is the limited amount of knowledge that students can construct in a semester. This brings to the fore the importance of the teacher or lecturer in sequencing and pacing the delivery of the material to facilitate cumulative knowledge-building in a hierarchically structured discipline, such as physics.

References

- [1] L. Lindstrøm and M. D. Sharma, Link maps and map meetings: Scaffolding student learning Physical Review Special Topics – Physics Education Researchl **5**, 010102 (2009)
- [2] C. Lindstrøm, *Link Maps and Map Meetings: A theoretical and experimental case for stronger scaffolding in first year university physics education* (Unpublished PhD thesis, University of Sydney, Sydney, Australia, 2010)
- [3] B. Bernstein, *Pedagogy, symbolic control, and identity: Theory, research, critique* (Taylor & Francis, London, Washington, D.C., 1996, p. 172)

Particle Traps in Modern Physics Education

K.D.A. Wendt¹, T. Leopold¹, and A. Schmitt¹

¹*Institut für Physik, Johannes Gutenberg Universität Mainz, D-55099 MAINZ, Germany*

Corresponding Author: klaus.wendt@uni-mainz.de

Numerous techniques to trap and localise charged and neutral particles, i.e. ions and atoms, have been developed and were permanently refined during the last 40 years. They can be regarded as essential basis for most of the developments and the tremendous progress observed in visualizing, understanding and today even applying quantum physics effects. Charged particles are most easily confined by overlaying ac and dc electric fields in "Paul Traps" or in combined dc electric and magnetic fields in "Penning Traps". Neutral particles can be cooled and decelerated by laser light fields for final storage in "Magneto-Optical Traps (MOTs)" or purely magnetic dipole field traps. For the purpose of visualisation, education and exhibition all these techniques can be demonstrated most impressively on macroscopic particles [1-3]. Some of them rely on simple and low-cost experimental equipment, which can be constructed and applied in class room [4].

Stimulating tutorials on various aspects of modern physics, including introductions to most recent investigations in quantum optics, the physics of accelerator physics and storage rings or the handling of antimatter (read also the best seller *Illuminati* by Dan Brown) can be based around simple macro-particle traps for charged particles, similarly useful in scientific education and motivation for students in high school or university level. Investigation of the trapping behaviour and orbiting motion of charged lycopodium seeds in a Paul trap (Fig.1) and their visualisation by scattered light from simple laser pointers or via CCD-camera observation opens the way to and enriches the presentation of state-of-the-art experiments involving quantum phenomena. These include the principle of strong focussing, coupling of microscopic and macroscopic degrees of freedom, entanglement, Bose-Einstein condensation as well as their applications, e.g. in ion trap clocks, quantum information processing and quantum computers. Due to the simplicity of the corresponding demonstration experiments this can even be presented as hands-on experiments in school or university classes. Here we present educational versions of Paul Traps with different longitudinal and circular geometries, which can both be constructed with low costs and commercially available parts, as well as demonstration models of particle accelerators or the antimatter trap from the permanent exhibition "Univers de particules" at CERN [5].

References

- [1] H. Winter and H. W. Ortjohann, *Am. J. Phys.*, **59** (9), 807-813 (1991).
- [2] A. Ashkin, *Science* **210**, 1081 (1980).
- [3] R. Tuckermann, S. Bauerecker and B. Neidhart, *Angew. Phys.*, **32**, 2 (2001).
- [4] A. Schmitt, *Praxis der Naturwissenschaften*, **51**, 34 (2002).
- [5] <http://cdsweb.cern.ch/record/1271472/>

Not what it seems? Teaching and learning introductory quantum physics.

J. Hardy¹

¹ *The University of Edinburgh School of Physics and Astronomy, Mayfield Road, EH9 3JZ
Edinburgh, United Kingdom*

Corresponding Author: j.hardy@ed.ac.uk

Quantum mechanics is widely regarded as one of the most challenging topics in the undergraduate curriculum. It abounds with abstract and often counter-intuitive findings and paradoxes and poses real conceptual challenges to students. Furthermore, as quantum mechanics is the corner stone of modern physics it is crucial for students to understand the subject in order to progress. In recent years there have been significant advances in understanding and addressing the problems and misconceptions that face students when they first encounter quantum mechanics. Much of this research has stemmed from the extensive literature on the enhancement of conceptual understanding in classical mechanics teaching, which includes detailed studies into the concepts students have most problems with, and how best to teach these. One way of discovering common misconceptions is with the use of diagnostic tests, and a number of such tests are now available to measure conceptual understanding in quantum mechanics. Similarly, a range of instructional strategies and resources have been developed to encourage student interaction and participation, especially in large early years classes.

Many of these have been adapted and adopted for use in introductory physics courses, including quantum mechanics, at the University of Edinburgh. In this talk I will describe how these, together with other instructional developments, have brought about a real change in the way the students are challenged to engage with the material that they encounter in their studies.

Contributed Talks

Multi-electron dynamics in time-dependent R-matrix theory

H.W. van der Hart¹, S. Hutchinson^{1,2}, and M.A. Lysaght^{1,3}

¹*Centre for Theoretical Atomic, Molecular and Optical Physics, Queen's University Belfast, Belfast BT7 1NN, United Kingdom*

²*Department of Physics and Astronomy, University College London, Gower Street, London WC1E 6 BT, United Kingdom*

³*ICHEC, Tower Building, Trinity Technology and Enterprise Campus, Grand Canal Quay, Dublin 2, Ireland*

Corresponding Author: h.vanderhart@qub.ac.uk

Over the last 10 years, great progress has been made in developing laser systems capable of generating pulses with sub-femtosecond duration [1,2]. This progress has enabled experiment to observe atomic and molecular dynamics in the sub-femtosecond regime. Examples of this dynamics include dynamics of shake-up states in Ne^+ following high-frequency ionization of Ne [3], and time delay between the emission of 2s and 2p electrons in Ne [4].

New theoretical techniques are needed to describe the response of matter to ultra-short light pulses. The ultra-short duration of the light pulse leads to the requirement for solving the time-dependent Schrödinger equation. The high photon energies associated with ultra-short light pulses, on the other hand, allow multi-electron excitation and de-excitation during the pulse. The accurate description of the atomic response must therefore be able to account for a multi-electron response to the light pulse.

To accurately solve the time-dependent Schrödinger equation, with the inclusion of multi-electron excitation, we have developed time-dependent R-matrix theory over the last few years [5]. In this theory, the standard R-matrix approximation is maintained: close to the nucleus, in the inner region, all interactions between all electrons are accounted for, whereas in the outer electron, one electron is allowed to escape from the residual ion, and this electron only experiences long-range interactions with the residual ion. Within each time-step $t_q \rightarrow t_{q+1}$, we solve the following equation:

$$(H_{q+1/2} - E)\Psi_{q+1} = -(H_{q+1/2} + E)\Psi_q, \quad (1)$$

where $H_{q+1/2}$ is the Hamiltonian at the mid-point of the time interval, Ψ is the wavefunction, and $E \equiv 2i/\Delta t$ is an imaginary energy related to the time-step. The calculation proceeds by determining the R -matrix and an inhomogeneous T -vector at the inner-region boundary. These are propagated through the outer region. At a sufficiently large distance, the wavefunction-vector F can be set to 0. This vector is then propagated inwards to the inner-region boundary. Once the R -matrix, T -vector and F -vector are obtained, the new wavefunction can be constructed.

As a demonstration of time-dependent R-matrix theory, we have investigated ultra-fast dynamics in the $2s2p^2$ configuration of C^+ [6,7]. An initial short pulse excites this configuration from the $2s^22p$ ground state. A second delayed pulse then ionizes the system. By varying the time delay between the pulses, we can then investigate the dynamics occurring within this configuration. Small changes to the initial state cause significant difference to the dynamics. When the initial state has magnetic quantum number $M = 0$, the dynamics in the $2s2p^2$ configuration is spatial dynamics. On the other hand, when $M = 1$, spin dynamics occurs.

References

- [1] P. B. Corkum and F. Krausz, *Nature Physics* **3**, 381 (2007)
- [2] G. Sansone *et al.*, *Science* **314**, 443 (2006)
- [3] M. Uiberacker *et al.*, *Nature* **446**, 627 (2007)
- [4] M. Schultze *et al.*, *Science* **328**, 1658 (2010)
- [4] M. A. Lysaght *et al.*, *Phys. Rev. A* **79**, 053411 (2009)
- [4] M. A. Lysaght *et al.*, *Phys. Rev. Lett.* **102**, 193001 (2009)
- [7] S. Hutchinson *et al.*, *J. Phys. B* **44**, 215602 (2011)

Visualization of electronic motion in carbon atoms

H. Hultgren^{1,2}, M. Eklund^{1,2}, D. Hanstorp², and I. Yu. Kiyani^{1,3}

¹*Physikalisches Institut, Albert-Ludwigs-Universität, D-79104 Freiburg, Germany*

²*Department of Physics, University of Gothenburg, SE-412 96 Gothenburg, Sweden*

³*Helmholtz-Zentrum für Materialien und Energie, 12489 Berlin, Germany*

Corresponding Author: hannes.hultgren@physik.uni-freiburg.de

We present direct observations of electron dynamics in the ground state of an atom. An electronic wave packet is created by coherently populating the three fine structure levels in the ground state of carbon through a strong field photodetachment process of the negative carbon ion. Subsequently, the wave packet is probed by strong field ionization using a femtosecond IR laser pulse. The detached electrons are detected in an electron imaging spectrometer operated in the velocity mapping regime[1]. Fig.1 A-C shows the energy and angular distribution of the emitted electrons at three different pump-probe delay times. The laser polarization is vertical in the images, and the distance from the centre represents the momentum of the electrons. The probe step projects the atom's electron density along the laser polarization directly on to our detector, seen as vertically aligned jets. The yield of the most energetic electrons detected in this experiment corresponds to the absorption of more than 40 photons. Fig.1 D shows the yield of electrons detected within the white rectangles in Fig.1 A-C, as a function of the time delay between the pump and the probe pulses. We interpret the strong modulation of high energy electrons as a spatial rearrangement of the electron cloud in the atom. This is the first direct visualization of a wave packet oscillation in the ground state of an atom.

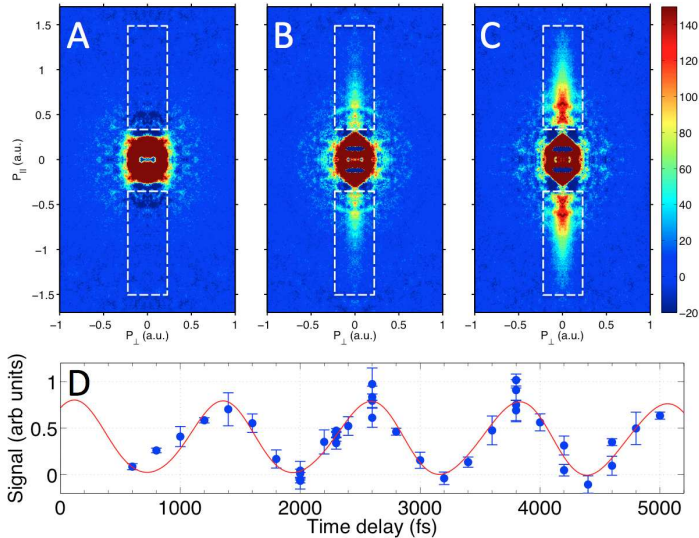


Figure 1: *A, B and C: Angular resolved electron spectra at delay times of 2000fs, 2300fs and 2600fs with the probe laser vertically aligned. D: The integrated yield of high energy electrons emitted along the laser polarization, plotted as a function of the delay time between the pump and probe laser pulses.*

References

[1] Boris Bergues et al. Phys. Rev. A **75**, 063415 (2007)

Photoionization time-delay measurements and calculations in various gases

D. Guénot¹, K. Klünder¹, C. L. Arnold¹, M. Gisselbrecht¹, T. Fordell¹, M. Miranda¹, D. Kroon¹, P. Johnsson¹, J. Mauritsson¹, J. M. Dahlström², E. Lindroth², A. Maquet³, R. Taïeb³, and A. S. Kheifets⁴

¹Department of Physics, Lund University, SE-221 00 Lund, Sweden

²Department of Physics, Stockholm University, Sweden

³Laboratoire de Chimie Physique-Matière et Rayonnement, Université Pierre et Marie Curie, 11, Rue Pierre et Marie Curie, 75231 Paris Cedex, 05, France

⁴Research School of Physical Sciences, The Australian National University, Canberra ACT 0200, Australia

Corresponding Author: diego.guenot@fysik.lu.se

The development of ultrashort light pulses in the attosecond range allows scientists to tackle temporal aspects of electron transitions in atoms, molecules and more complex systems. In this work, we present experimental measurements and theoretical calculations of the photoemission time delays [1] difference between the 3s and 3p shells in Argon [2] as well as between Argon and other valence shells from noble gases (Krypton, Neon, Xenon). The experimental measurements are performed using the RABITT technique (Reconstruction of Attosecond Bursts by Interference of Two-photon Transition). An active stabilization between the two arms of the Mach-Zender interferometer needed for the RABITT scans allow us to extract the relative photoemission time delays between two gases by performing consecutive scans in the two gases. The measured delays spans between 10 and 100 attosecond depending on the gas and the electron energy. The theoretical approach includes intershell correlation effects between the valence and the inner shells within the framework of the random phase approximation with exchange (RPAE).

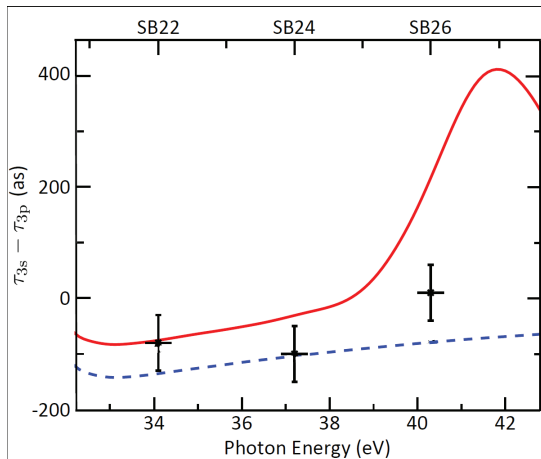


Figure 1: Comparison between our theoretical calculations (dashed blue line, HF, red line, RPAE) and experiments

References

[1] M. Schultze *et al.*, Science 328, **1658** (2010). [2] K. Klünder *et al.*, Phys. Rev. Lett. **106**, 143002 (2011). [3] P. M. Paul *et al.*, Science **292**, 1689 (2001).

Theory of attosecond delays in laser-assisted photoionization: Including electron–hole interactions

J. M. Dahlström¹, T. Carette¹, E. Lindroth¹, D. Guénot², K. Klünder², M. Gisselbrecht², J. Mauritsson², A. L’Huillier², A. Maquet^{3,4}, and R. Taïeb^{3,4}

¹Department of Physics, Stockholm University, SE-106 91 Stockholm, Sweden

²Lund University, SE-221 00 Lund, Sweden

³Université Pierre et Marie Curie (UPMC), 75231 Paris, France

⁴CNRS, UMR 7614, LCPMR, Paris, France

Corresponding Author: Marcus.Dahlstrom@fysik.su.se

We study the temporal aspects of laser-assisted extreme ultraviolet (XUV) photoionization using attosecond pulses of harmonic radiation [1]. Our aim is to derive the general form of the *phase* of the relevant transition amplitudes: (d), (a) and (e), corresponding to the photon-processes sketched in Fig. 1. Furthermore, we make the connection between these phases and the attosecond time-delays that have been recently measured in experiments [2,3]. We find that the overall phase contains two distinct types of contributions: one is expressed in terms of the phase-shifts of the photoelectron continuum wavefunction while the other is linked to continuum–continuum transitions induced by the infrared (IR) laser probe. Going beyond the single-active electron approximation, allows for interesting electron–hole interactions, where the photoelectron can induce transitions in the remaining ion. We perform *ab initio* calculations and study electron–hole correlation effects in attosecond photoionization processes of noble-gas atoms, such as Neon and Argon, using exterior-complex scaling and many-body perturbation theory (RPA).

References

[1] J.M. Dahlström *et al.*, Chem. Phys. [in print] (2012)

<http://dx.doi.org/10.1016/j.chemphys.2012.01.017>

<http://arxiv.org/abs/1112.4144>

[2] K. Klünder, J.M. Dahlström *et al.*, Phys. Rev. Lett. **106**, 143002 (2011)

[3] M. Schultze *et al.*, Science **328**, 1658 (2010).

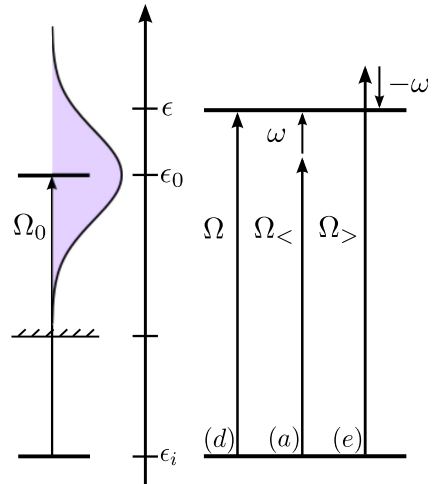


Figure 1: (d) Photoionization by an attosecond pulse with XUV frequency, Ω . Laser-assisted photoionization by absorption (a) or emission (e) of an IR-probe photon, ω , yields attosecond temporal information about the single-photon ionization process.

Spin dynamics of electrons in strong fields studied via bremsstrahlung from a polarized electron beam

S. Tashenov¹, T. Bäck², B. Cederwall², A. Khaplanov², K.-U. Schässburger², R. Barday³, J. Enders³, Yu. Poltoratska³, A. Surzhykov^{1,4}, V. Yerokhin^{1,4,5}, and D. Jakubassa-Amundsen⁶

¹*Physikalisches Institut der Universität Heidelberg, 69120 Heidelberg, Germany*

²*Royal Institute of Technology, SE-10691 Stockholm, Sweden*

³*Institut für Kernphysik, Technische Universität Darmstadt, 64289 Darmstadt, Germany*

⁴*GI Helmholtzzentrum für Schwerionenforschung GmbH, 64291 Darmstadt, Germany*

⁵*Center for Advanced Studies, St. Petersburg State Polytechnical University,*

Polytekhmicheskaya 29, St. Petersburg 195251, Russia

⁶*Mathematics Institute, University of Munich, Theresienstrasse 39, 80333 Munich, Germany*

Corresponding Author: tashenov@physi.uni-heidelberg.de

Radiation spectra in relativistic electron-atom collisions are dominated by bremsstrahlung. It is one of the fundamental ways the electromagnetic field interacts with matter: it occurs for every charged particle moving through matter and most of its properties are understood classically. For this reason bremsstrahlung can be used to study dynamics of colliding particles. One takes a particular interest in the dynamics because of the strong electric fields experienced by the electron in the scattering process. In these fields and in the regime of hard x-rays the dynamics is dominated by effects which do not exist at low energies. Here the electron spin and relativity play a key role.

Bremsstrahlung has long been considered to be sensitive to the spin of the electron. It was predicted that linear polarization of the emitted photons should rotate out of the reaction plane when spin-polarized electrons collide with heavy atoms [1-3]. However it was not until recently that experiments in this direction became possible [4]. We have optimized the technique of photon polarimetry by means of Compton and Rayleigh scattering, applied to a segmented germanium detector, and significantly improved its efficiency and resolution. The angular resolution of $\sigma = 0.3^\circ$ is an achievement of Compton polarimetry. With this accuracy we for the first time became sensitive to these effects.

Linear polarization of hard x-rays emitted in the process of the atomic field electron bremsstrahlung was measured with a polarized electron beam. The correlation between the initial orientation of the electron spin and the angle of photon polarization was systematically studied. The results are in a good agreement with the fully-relativistic calculations. They are also explained classically and in a unique way manifest that due to the spin-orbital interaction the electron scattering trajectory is not confined to a single scattering plane. Such an observation is typically not possible in scattering experiments.

The developed photon polarimetry technique with a passive scatterer, due to its efficiency and accuracy, allows for novel applications. Bremsstrahlung polarization correlations lead to a new method of polarimetry of electron beams. Such a method is sensitive to all three components of the electron spin, and it can be applied in a broad range of the electron beam energies from ≈ 100 keV up to a few 10 MeV.

In a similar way the experiment confirms the theoretical predictions for the polarization correlations in radiative recombination. These correlations lead to the unique method of polarimetry of heavy ion beams [5].

References

- [1] H.K. Tseng and R.H. Pratt, *Physical Review A* **7**, 1502 (1973)
- [2] D.H. Jakubassa-Amundsen, *Physical Review A* **82**, 042714 (2010)
- [3] V.A. Yerokhin and A. Surzhykov, *Physical Review A* **82**, 062702 (2010)
- [4] S. Tashenov *et al.*, *Physical Review Letters* **107**, 173201 (2011)
- [5] A. Surzhykov *et al.*, *Physical Review Letters* **94**, 203202 (2005).

Alkali atoms on superfluid helium droplets - laser excitation of an exotic Rydberg complex

Florian Lackner¹, Günter Krois¹, Markus Koch¹, and Wolfgang E. Ernst¹

¹*Institute of Experimental Physics, Graz University of Technology, Petersgasse 16, A-8010 Graz, Austria*

Corresponding Author: wolfgang.ernst@tugraz.at

CT

Superfluid helium droplets (He_N) have attracted strong interest as cold hosts for the investigation of weakly bound molecules. Whereas the host-dopant interaction is weak for neutral atoms or molecules, ion impurities may be surrounded by frozen shells of polarized helium atoms. An extreme example of the different behavior is given by alkali metal impurities that stay at the surface of the droplet but immerse into the droplet as cations releasing a considerable amount of binding energy [1]. In highly excited states near the ionization threshold of the alkali atom, the transition from surface to interior location can be followed [2]. Here, nanodroplets of several thousand helium atoms are doped with single rubidium (Rb) atoms. While on the droplet, the Rb valence electron is excited in two steps through an intermediate state into nS , nP , nD , and nF Rydberg states. Excited states are ionized by a third laser photon and the resulting Rb^+-He_m ions are monitored by a time-of-flight mass spectrometer. Complete excitation spectra from the Rb 5D state manifold to the ionization threshold are presented for various droplet sizes. On-droplet Rydberg excitations are resolved up to about $n = 20$. The energies are compared with those of free Rb atom Rydberg states and quantum defects as well as the on-droplet ionization threshold are derived. Both the ionization threshold and the quantum defects turn out to be droplet size dependent [3]. Our findings support a qualitative picture in which the helium nanodroplet forms a dielectric around the Rb^+ reducing the electric field and the interaction of the outer electron with the Rb^+ core orbitals, thus resulting in a lower ionization potential and a smaller quantum defect. This research has been supported by the Austrian Science Fund (FWF) under Grant FWF-E-P19759 and the EFRE Program of the European Union and the Region of Styria.

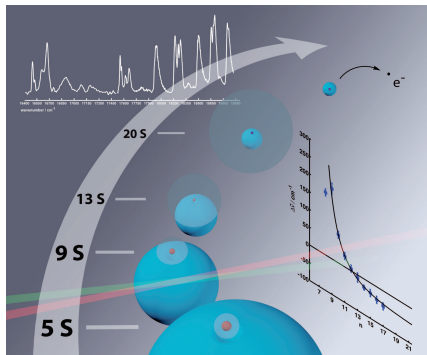


Figure 1: Schematic of an alkali atom on a helium droplet excited into high- n states while the ionic core submerges from the surface into the droplet.

References

- [1] M. Theisen, F. Lackner, G. Krois, and W. E. Ernst, *J. Phys. Chem. Lett.* **2**, 2778 (2011)
- [2] F. Lackner, G. Krois, M. Theisen, M. Koch, and W. E. Ernst, *PCCP* **13**, 18781 (2011)
- [3] F. Lackner, G. Krois, M. Koch, and W. E. Ernst, submitted to *J. Phys. Chem. Lett.*

Decay Of Rydberg Hydrogen Atoms And Molecules After Rydberg-Stark Deceleration And Off-Axis Trapping

Ch. Seiler¹, S. D. Hogan¹, and F. Merkt¹

¹Laboratory of Physical Chemistry, ETH Zurich, CH-8093 Zurich, Switzerland

Corresponding Author: christian.seiler@phys.chem.ethz.ch

The development of methods to decelerate and manipulate the translational motion of Rydberg atoms and molecules in the gas phase using static and time-varying inhomogeneous electric fields [1] has led to the experimental realization of Rydberg atom optics elements including a lens [2], a mirror [3] and two- and three-dimensional traps [4, 5]. These experiments make use of the very large electric dipole moments associated with Rydberg Stark states. These methods were also applied to Rydberg states of molecular hydrogen [6, 7]. Recently, we have also demonstrated the deceleration of a seeded, pulsed, supersonic beam of hydrogen atoms with an initial velocity of 600 m/s followed by a rapid, adiabatic 90° deflection and subsequent electrostatic trapping within approximately 25 μ s using pulsed electric fields of a few kV/cm [8].

In experiments in which the Rydberg atoms and molecules are trapped, trap losses can arise from transitions induced by blackbody radiation, from collisions between the trapped Rydberg atoms or molecules and collisions with the background gas. In molecular Rydberg states, predissociation also contributes to the trap losses, and the ability to trap the Rydberg molecules enables one to study slow predissociation over several milliseconds. We have shown that the dominant trap loss mechanism in hydrogen atom trapping experiments is blackbody-radiation-induced ionization at room temperature and at $T \approx 125$ K [8]. To quantify trap loss processes other than blackbody-radiation-induced transitions, an experimental setup which can be operated at 11 K has been developed. At these temperatures, the fluorescence lifetime of H Rydberg atoms and the slow predissociation of H₂ Rydberg molecules were experimentally determined.

References

- [1] S. R. Procter et al, Chem. Phys. Lett. **374**, 667–675 (2003)
- [2] E. Vliegen, P. Limacher, and F. Merkt, Eur. Phys. J. D **40**, 73–80 (2006)
- [3] E. Vliegen, and F. Merkt, Phys. Rev. Lett. **97**, 033002 (2006)
- [4] E. Vliegen, S. D. Hogan, H. Schmutz, and F. Merkt, Phys. Rev. A **76**, 023405 (2007)
- [5] S. D. Hogan, and F. Merkt, Phys. Rev. Lett. **100**, 043001 (2008)
- [6] S. D. Hogan, Ch. Seiler, and F. Merkt, Phys. Rev. Lett. **103**, 123001 (2009)
- [7] Ch. Seiler, S. D. Hogan, and F. Merkt, Phys. Chem. Chem. Phys. **13**, 19000–19012 (2011)
- [8] Ch. Seiler et al, Phys. Rev. Lett. **106**, 073003 (2011)

Optical transitions in highly charged ions for atomic clocks with enhanced sensitivity to variation of fundamental constants

J.C. Berengut¹, V.A. Dzuba¹, V.V. Flambaum¹, and A. Ong¹

¹*School of Physics, University of New South Wales, Sydney 2052, Australia*

Corresponding Author: jcb@phys.unsw.edu.au

CT

Optical transitions can occur in some highly charged ions when the ion stage and nuclear charge are tuned such that orbitals with different principal quantum number and angular momentum are nearly degenerate. In such cases the transition energy may be within laser range even though the ionisation energy is large (of order several hundred eV). We have identified several such systems and shown that they have a number of properties that could make them suitable for atomic clocks with high accuracy. Strong E1 transitions provide options for laser cooling and trapping, while narrow transitions can be used for high-precision spectroscopy and tests of fundamental physics. In particular we found transitions that would have the highest sensitivity to variation of the fine-structure constant ever seen in atomic systems.

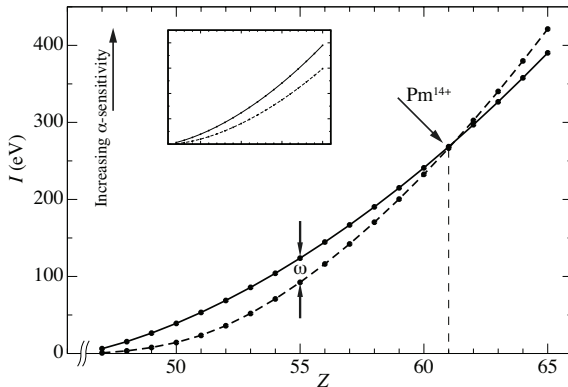


Figure 1: *Dirac-Fock ionisation energies of 5s (solid) and 4f_{7/2} (dashed) levels for the Ag isoelectronic sequence. At the crossing point it is possible to find optical transitions between the levels where over 99% of the ionisation energy cancels and the difference is within the range of lasers (a few eV).*

Inset — a typical example with no level crossing: 5s and 5d_{5/2} levels in the same isoelectronic sequence.

References

- [1] J. C. Berengut, V. A. Dzuba, V. V. Flambaum, *Phys. Rev. Lett.* **105**, 120801 (2010)
- [2] J. C. Berengut *et al.*, *Phys. Rev. Lett.* **106**, 210802 (2011)

Sisyphus Cooling of Polyatomic Molecules

R. Glöckner¹, B.G.U. Englert¹, A. Prehn¹, M. Zeppenfeld¹, and G. Rempe¹

¹Max-Planck-Institut für Quantenoptik, Hans-Kopfermann-Str. 1, 85748 Garching, Germany
Corresponding Author: rosa.gloeckner@mpq.mpg.de

Developing methods to prepare cold and ultracold molecular ensembles would enable fundamental studies, ranging from many-body physics and quantum information to quantum controlled collisions and chemistry. However, a cooling mechanism for polyatomic molecules with the capability to cool to the ultracold regime has up to now seemed infeasible. Here we present the first experimental realisation of opto-electrical cooling [1] using trapped CH_3F [2]. In this general Sisyphus-type cooling scheme the strong interaction of polar molecules with electric fields is exploited to remove a large fraction of the kinetic energy in each step of the cooling cycle. For dissipation, vibrational and rotational molecular states are driven using infrared and microwave fields, with homogeneous electric fields in the trap allowing selective addressing of rotational M-sublevels. We demonstrate the potential of the scheme by reducing the temperature by more than a factor of 4, with the phase-space density increased by a factor of 7. With an improved trap design we expect cooling to the μK regime.

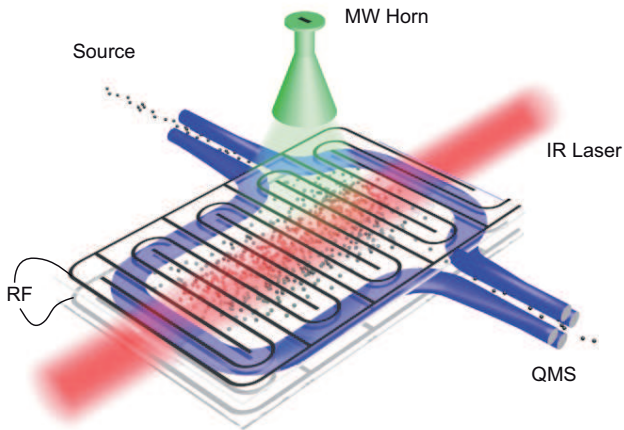


Figure 1: *Experimental setup: a microstructured electric trap confines the molecules with radiation fields for cooling applied as indicated.*

References

- [1] M. Zeppenfeld *et al.*, Phys. Rev. A **80**, 041401(R) (2009).
- [2] B.G.U. Englert *et al.*, Phys. Rev. Lett **107**, 263003, (2011).

A compact laser-cooling strontium source for a transportable optical lattice clock

M. Schioppo¹, N. Poli¹, G. M. Tino¹, and the SOC team^{1,2,3,4,5}

¹*Dipartimento di Fisica e Astronomia and LENS, Università di Firenze and INFN Sezione di Firenze, Via Sansone 1, 50019 Sesto Fiorentino, Italy*

²*Heinrich-Heine-Universität Dsseldorf, Düsseldorf, Germany*

³*Observatoire de Paris, Paris, France*

⁴*Physikalisch-Technische Bundesanstalt, Braunschweig, Germany*

⁵*Ecole Normale Supérieure, Paris, France*

Corresponding Author: Marco.Schioppo@fi.infn.it

Here we report on the status of a compact system for the production of laser-cooled strontium atomic samples. This system has been realized in the framework of the project “Space Optical Clocks” (SOC) funded by the European Space Agency (ESA) [1] for developing demonstrators of transportable lattice clocks for applications on earth and in space. Novel design solutions allowed us to reduce size, weight and power consumption with respect to traditional apparatus for laser cooling [2,3]. At the same time a high degree of operation reliability has been ensured by a modular architecture. The main modules are: diode lasers, fiber distribution systems and vacuum apparatus. The system routinely produces an atomic sample of about 1×10^6 ^{88}Sr atoms at the μK temperature by means of a two-stages magneto optical trap operating on the $^1\text{S}_0 - ^1\text{P}_1$ and $^1\text{S}_0 - ^3\text{P}_1$ transition, respectively at 461 nm and 689 nm. The atomic sample is efficiently loaded into a vertical optical lattice at the magic wavelength 813 nm for the strontium clock transition $^1\text{S}_0 - ^3\text{P}_0$ at 698 nm. By employing the compact strontium source and the stationary clock laser at LENS [4] a preliminary spectroscopy of the clock transition was performed (see Fig. 1). Within the project “Towards Neutral-atom Space Optical Clocks” funded by the EU 7th framework programme [5] the laser-cooling atomic source here presented will be integrated with compact subsystems to realize a transportable strontium lattice clock.

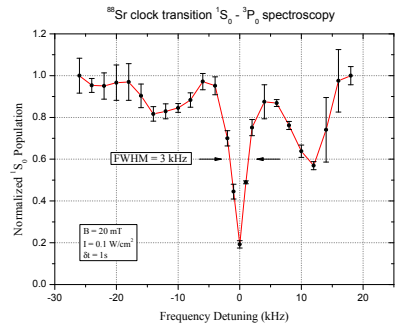
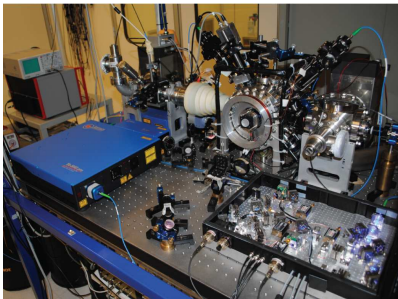


Figure 1: *Left: the compact laser-cooling strontium source assembled on a breadboard 90 cm \times 120 cm. Right: preliminary spectroscopy of the strontium clock transition $^1\text{S}_0 - ^3\text{P}_0$.*

References

- [1] G. M. Tino *et al.*, Nuclear Physics B Proceedings Supplements **166**, 159 (2007)
- [2] M. Schioppo *et al.*, Proceedings of EFTF 2010, http://www.congrex.nl/EFTF_Proceedings/
- [3] M. Schioppo Ph.D. thesis, Università degli Studi di Firenze (2011), <http://coldatoms.lens.unifi.it/optical-atomic-clock/documents.html>
- [4] M. G. Tarallo *et al.*, Appl. Phys. B **103**, 17–25 (2010)
- [5] http://www.exphy.uni-duesseldorf.de/optical_clock/soc2/index.php/

Theoretical and experimental studies of In I, Sn II, Sb III, and Te IV atomic properties

A. Petryla¹, S. Verdebout², J. Grumer³, H. Hartman⁴, G. Gaigalas¹, and P. Jönsson⁴

¹*Vilnius University, Institute of Theoretical Physics and Astronomy, A. Goštauto 12, LT-01108 Vilnius, Lithuania*

²*Chimie Quantique et Photophysique, CP160/09, Université Libre de Bruxelles, , Av. F.D. Roosevelt 50, B-1050 Brussels, Belgium*

³*Department of Physics, Lund University, Sweden*

⁴*Group for Materials Science and Applied Mathematics, School of Technology, Malmö University, 205 06 Malmö, Sweden*

Corresponding Author: Jon.Grumer@teorfys.lu.se

We use relativistic multiconfiguration Dirac-Hartree-Fock and configuration interaction calculations to study $5s^2nl$ and $5s5p^2$ configurations of In I, Sn II, Sb III, and Te IV [1]. Energies, transition amplitudes, Landé gJ -factors, and hyperfine constants are calculated using a correlation model that accounts for valence and core-valence correlation. Also spin- and orbital polarization effects are accounted for by single excitations from all core-shells to an increasing set of active orbitals. Transformed to the LSJ-coupling scheme, using the new features of the GRASP2K program [2,3], the calculated wave functions shed light on the difficulties in labeling some states due to the extensive $5s^25d$ and $5s5p^2$ configuration interaction.

Our results are compared with experimental values and values from relativistic many-body perturbation theory (RMBPT) and all-order single-double (SD) calculations [4,5]. The theoretical work is complemented with experiment, and new hyperfine interaction constants are derived for several states in In I from high resolution Fourier Transform Spectra [6].

References

- [1] A. Petryla, S. Verdebout, J. Grumer, H. Hartman, and P. Jönsson work in progress (2012).
- [2] G. Gaigalas, T. Žalandauskas, and Z. Rudzikas, *At. Data and Nucl. Data Tables*, 84 (2003) 99.
- [3] P. Jönsson, G. Gaigalas, J. Bieroń, C. Froese Fischer, and I.P. Grant, *Comput. Phys. Commun.* to be submitted (2012).
- [4] U. I. Safronova, M. S. Safronova, and M. G. Kozlov *Phys. Rev. A* 76 (2007) 022501.
- [5] V. A. Dzuba and V. V. Flambaum, *Phys. Rev. A* 71(2005) 052509.
- [6] H. Hartman work in progress (2012).

Confinement-induced collapse of a dipolar Bose-Einstein condensate in an optical lattice

J. Billy¹, E. Henn¹, S. Müller¹, T. Maier¹, H. Kadau¹, M. Schmitt¹, M. Jona-Lasinio²,
L. Santos², A. Griesmaier¹, and T. Pfau¹

¹*5. Physikalisches Institut, Universität Stuttgart, Pfaffenwaldring 57, D-70569 Stuttgart, Germany*

²*Institut für Theoretische Physik, Leibniz Universität Hannover, D-30167 Hannover, Germany*

Corresponding Author: j.billy@physik.uni-stuttgart.de

We experimentally investigate the instability and collapse dynamics of a dipolar Bose-Einstein condensate (dBEC) in a 1D optical lattice. In contrast to the usual method relying on a change in the contact interaction energy, the instability is here induced by a change in the confining potential, while keeping the interaction strength constant. Only a dBEC offers this possibility, since its stability threshold strongly depends on the lattice depth due to the anisotropic character of the dipolar interaction [1]. The system considered here consists of a ⁵²Cr BEC with reduced scattering length, initially confined in the trap created by a shallow optical lattice superimposed to a crossed optical dipole trap. We show that such a system can exhibit two types of collapse: the system can either be driven to instability in-trap by changing the lattice depth only, the subsequent collapse dynamics showing in this case strong in-trap atom losses. In contrast, in the extreme case where the trapping potential is completely switched off, the dBEC may also become unstable and collapse in time-of-flight, which is also a unique feature of dipolar systems.

References

[1] S. Müller *et al.*, Phys. Rev. A **84**, 053601 (2011)

The anisotropic excitation spectrum of a dipolar Bose-Einstein Condensate

G. Bismut¹, B. Pasquiou¹, L. Vernac¹, E. Marechal¹, P. Pedri¹, B. Laburthe-Tolra¹,
and O. Gorceix¹

¹*Laboratoire de Physique des Lasers, Université Paris 13 and CNRS, UMR7538, F-93430, Villetaneuse, France*

Corresponding Author: olivier.gorceix@univ-paris13.fr

We use Raman-Bragg spectroscopy to measure the excitation spectrum of a trapped spin-polarized degenerate quantum gas made of highly magnetic chromium atoms. Spectra are recorded for orthogonal orientations of the spin (equivalently of the magnetic field) with respect to the trap axes. Our outcomes for long-wavelength excitations demonstrate how the strong long-range and anisotropic interaction between the magnetic dipoles of the atoms converts into an anisotropy of the sound velocity inside the BEC. As we span the frequency domain from the phonon range up to the single-particle limit, the excitation energy is clearly different for parallel and perpendicular orientations of the excitation wave-vector with respect to the spin polarization axis. In the phonon range, relative shifts in the excitation energy up to 0.15 were demonstrated when flipping the spin polarization axis. Despite a lower relative impact, the anisotropy shows up as well in the high-energy limit. The analysis of our data shows that the shifts induced by the dipolar mean field are in good agreement with theoretical predictions throughout the whole spectrum. This work complements previously published studies of the collective excitations of the chromium BEC when an analogous anisotropy was demonstrated by parametric excitation of the low-energy modes of the system [1]. We provide an experimental demonstration of a new dipolar effect in a dilute quantum fluid. We plan to use the Bragg spectroscopy scheme to deepen our understanding of the magnetization processes in the multicomponent spin-3 chromium condensate with special interest for 2D and 1D systems [2,3].

References

- [1] G. Bismut et al, Phys. Rev. Lett. **105**, 040404 (2010)
- [2] B. Pasquiou et al, Phys. Rev. Lett. **106**, 255303 (2011)
- [3] B. Pasquiou et al, Phys. Rev. Lett. **108**, 045307 (2012)

Are relativistic corrections needed to describe the adiabatic passage of matter waves?

A. Benseny¹, J. Bagudà¹, X. Oriols², and J. Mompart¹

¹*Departament de Física, Universitat Autònoma de Barcelona, E-08193, Bellaterra, Spain*

²*Departament d'Enginyeria Electrònica, Universitat Autònoma de Barcelona, E-08193, Bellaterra, Spain*

Corresponding Author: albert.benseny@uab.cat

The detailed analysis of quantum and relativistic phenomena that defy our ‘limited’ classical intuition, such as the Einstein–Podolsky–Rosen or the twin paradoxes, has allowed physicists to achieve a deeper understanding of quantum mechanics and relativity. In this work, we have numerically investigated the coherent transport of a Bose–Einstein condensate (BEC) or a single atom by means of the spatial adiabatic passage (SAP) technique [1,2], that exhibits a paradoxical behaviour when the process is slowed down. This technique consists in transporting a BEC from the left to the right trap of a triple-well potential, see Fig. 1(a), by modifying the time-dependent heights of the barriers that define the three traps, in such a way that the state of the system follows adiabatically an energy eigenstate of the system, the spatial dark state, from the left to the right trap. Since the spatial dark state only populates the vibrational ground states of the two extreme wells and presents at all times a node in the central region, the SAP technique implies matter wave transport between two distant regions separated by a non-populated area, see Fig. 1(b). Furthermore, by slowing down the process, the population in the central region can be made arbitrarily small [2], and one could naively conclude that an instantaneous atomic transport from the left to the right trap can appear in the limit of perfect adiabaticity.

Unraveling the time-dependent Gross–Pitaevskii or Schrödinger equations in terms of quantum Bohmian trajectories [3], see Fig. 1(c), we show that as the process is slowed down, the vanishing central region occupation leads to an increase of the Bohmian velocities in that region, see Fig. 1(d). This growth has no apparent limit and would eventually imply trajectories faster than the speed of light, even though the average velocities are extremely smaller. Since a correct relativistic treatment of Bohmian trajectories does not allow superluminal velocities [4], in the regime of almost perfect adiabaticity, the non-relativistic TDSE does not correctly describe the spatial adiabatic transport of cold atoms, and relativistic corrections should be taken into account.

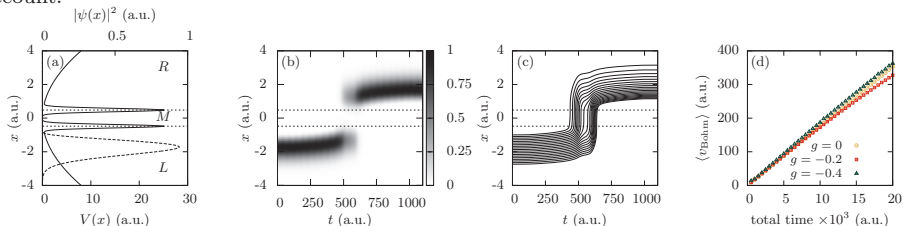


Figure 1: (a) Initial probability density of the BEC and potential barriers defining the triple-well potential. Time evolution of (b) the BEC probability density and (c) the Bohmian trajectories associated to the evolution. (d) Linear growth of the mean Bohmian velocity at the node with the total duration of the process, for different BEC interaction strengths.

References

- [1] K. Eckert *et al.*, Phys. Rev. A **70**, 023606 (2004).
- [2] M. Rab *et al.*, Phys. Rev. A **77**, 061602R (2008).
- [3] D. Bohm, Phys. Rev. **85**, 166 (1952).
- [4] C. R. Leavens and R. Sala Mayato, Ann. Phys. **7**, 662 (1998).

Optical manipulation of microparticles in vacuum

Y. Arita¹, M. Mazilu¹, and K. Dholakia¹

¹*SUPA, School of Physics and Astronomy, University of St Andrews, North Haugh, St Andrews, KY16 9SS, United Kingdom*

Corresponding Author: ya10@st-and.ac.uk

The generation and manipulation of measurable quantum entanglement is one of the grand challenges of modern physics, and provides the basis of applications such as quantum computing, quantum communications and high-precision spectroscopy [1]. Suitable systems include trapped ions that are laser cooled to just a few microkelvin and atoms stored in extremely small cavities [2]. Recently, international consensus shows the emergence of quantum state preparation using macroscopic objects [3]. To reach this regime, the coupling between particles and their thermal environments must be minimized. In this context, an optically trapped particle in vacuum is an ideal system for investigating quantum effects in a mechanical system, due to its near-perfect isolation from the thermal environment, and could even allow cooling the mechanical motion of a trapped particle from room temperature down to the quantum ground state where its dynamics are dominated by quantum mechanics [4]. Towards this goal, we develop a system to controllably levitate and optically trap microparticles in both air and vacuum environments, and investigate the intricate dynamics of such trapped microparticles when they are both optically trapped and rotated. Previously, we presented a technique to measure the viscosity of sub-picoliter volumes of gaseous medium using rotating microparticles [5]. The rotation of microparticles is achieved by trapping a birefringent spherical vaterite crystal with a circularly polarized light. Transfer of angular momentum from the circularly polarised beam to the particle results in a torque on the trapped object. The transmitted light is analysed to determine the applied torque to the particle and its rotation rate. We demonstrate controlled rotation of trapped microparticles with different particle sizes and optical powers in vacuum and explore how the recorded viscosity varies as a function of background pressure. Furthermore, we see evidence of coupling between the rotational and translational degrees of freedom of the trapped object offering new perspectives on particle dynamics.

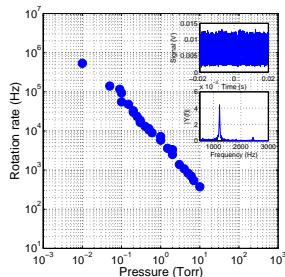


Figure 1: Rotation rate of an optically trapped birefringent microparticle ($4.4\mu\text{m}$ in diameter) in vacuum. Insets show the detector signal of a rotating particle and its power spectrum showing a rotation rate of 1.2 kHz.

References

- [1] B. Julsgaard, A. Kozhkin, and E. S. Polzik, *Nature* **413**, 400–403 (2001)
- [2] D. E. Chang *et al.*, *P Natl Acad Sci USA* **107**, 1005–1010 (2010)
- [3] S. Singh *et al.*, *Phys Rev Lett* **105**, 213602(1)–213602(4) (2010)
- [4] M. G. Raizen, T. C. Li, and S. Kheifets, *Nat Phys* **7**, 527–530 (2011)
- [5] Y. Arita *et al.*, *Anal Chem* **83**, 8855–8858 (2011)

A universal matter-wave interferometer in the time-domain

J. Rodewald¹, P. Haslinger¹, N. Dörre¹, P. Geyer¹, S. Nimmrichter¹, and M. Arndt¹

¹*University of Vienna, Vienna Center for Quantum Science and Technology VCQ, Faculty of Physics, Boltzmannngasse 5, A-1090 Vienna*

Corresponding Author: jonas.rodewald@univie.ac.at

We present a novel matter-wave interferometer of the Talbot Lau type which utilizes three pulsed ionization gratings [1][2]. These optical structures are realized by standing laser waves in which the photoionization probability depends periodically on the distance from the reflecting mirror. In combination with an external field for ion removal such gratings act as pulsed absorptive masks [3] and allow us to operate the interferometer in the time-domain [4]. This brings a decisive gain in count rate, visibility and measuring precision. Since optical gratings interact in a non-dispersive way with the passing particles, the experiment will be a powerful tool to probe quantum theory on an increasingly large mass scale and to search for new decoherence effects, such as continuous spontaneous localization [5][6]. We emphasize the universality of this interferometer: the suitability of a nanoparticle for the experiment is merely limited by its single photon ionization cross section at the lasers wavelength ($\lambda = 157$ nm). Possible candidates are thus many metallic and organic molecular clusters as well as some atomic species.

References

- [1] E. Reiger, L. Hackermüller, M. Berninger, and M. Arndt, *Opt. Comm.* **264**, 326 (2006)
- [2] K. Hornberger, S. Gerlich, P. Haslinger, S. Nimmrichter, and M. Arndt, *Rev. Mod. Phys.* **84**, 157 (2012)
- [3] S. Nimmrichter, P. Haslinger, K. Hornberger, and M. Arndt, *New. J. Phys.* **13**, 075002 (2011)
- [4] S. B. Cahn, A. Kumarakrishnan, U. Shim, T. Sleator, P. R. Berman, and B. Dubetsky, *Phys. Rev. Lett.* **79**, 784 (1997)
- [5] S. L. Adler and A. Bassi, *Science* **325**, 275 (2009)
- [6] S. Nimmrichter, K. Hornberger, P. Haslinger, and M. Arndt, *Phys. Rev. A* **83**, 043621 (2011)

Renner-Teller Coupling In H_2S^+ : A Comparison Of Theory With Optical Spectra And Recent Pfi And Mati Experimental Results

G. Duxbury¹, Ch. Jungen², A. Alijah³, J.-P. Maier⁴, R. Kuhn⁴, and D. Klapstein⁴

¹*Department of Physics, SUPA, John Anderson Building, University of Strathclyde, 107 Rottenrow, Glasgow G4 0NG, Scotland, UK*

²*LAC, 1Laboratoire Aim Cotton du CNRS, Université de Paris-Sud, 91405 Orsay, France*

³*GSMA, UMR CNRS 6089, Université de Reims Champagne-Ardenne, B.P. 1039, 51687 Reims Cedex 2, France*

⁴*Departement Chemie, Universität Basel, Klingelbergstrasse 80, CH-4056 Basel, Switzerland*
Corresponding Author: g.duxbury@strath.ac.uk

Most of the early studies of H_2S^+ focussed on the comparison between the medium resolution photoelectron spectra of hydrogen sulphide [1],[2], and the high resolution emission spectrum of the $\text{A}^2\text{A}_1\text{-X}^2\text{B}_1$ transition of the ion [1],[3],[4]. After a gap of ten years, higher resolution valence photoelectron spectra were published by Balzer et al.[5], which made use of the experimental and theoretical work of the earlier studies, particularly [4], to assign the vibronic structure of the photoelectron spectrum.

Recently, with the advent of improved photoelectron [5] and pulsed field ionisation spectrometers [6], and also a mass-analysed threshold ionisation approach [7], there has been a renewal of interest in the spectroscopy and dynamics of the formation and the fragmentation of the hydrogen sulphide ion. In their analysis of the pulsed field ionisation spectrum of H_2S Hochlaf et al. suggested that the band origin of the A^2A_1 state of H_2S^+ should be changed. By making use of some unpublished emission spectra of H_2S^+ and D_2S^+ recorded by Maier, Kuhn and Klapstein we have confirmed that the original band origins given in [1], [3] and [4] are correct. We also noted that the numbering of the K-structure of the vibronic bands close to the barrier to linearity is also in error, as may be seen from the spectra analysed in [4] and [5].

In this contribution we compare the results derived from these new experiments with the analysis of the original emission spectra. The results are also compared with the predictions made using the stretch-bender approach to the calculation of the effects on the Renner-Teller coupling of large amplitude vibrational motion [8]. One of the most interesting results of this approach is the comparison between the rotationally resolved spectra of the $\text{A}^2\text{A}_1\text{-X}^2\text{B}_1$ transition of H_2S^+ recorded by Han, Kang and Kim [7] and the emission spectra of Duxbury, Jungen and Rostas [3]. As Han et al. [7] followed the renumbering of Hochlaf et al. [6] we have reduced their values of ν_2' by 1. Their measured frequencies for $\text{K}'=0$ transitions of $\nu_2'=8$ match those we measured for $\text{K}'=0$ transitions of $\nu_2'=7$. Similarly those of $\text{K}'=1$ transitions of $\nu_2'=7$ match those which we recorded for $\nu_2'=6$. However the higher energy transitions recorded by Han et al. are absent in our emission spectra. Our spectra break off once the predissociation is more rapid than the emission probability, whereas in the MATI spectra of Han et al. these ro-vibronic spectra may still be recorded as they do not depend upon the measurement of an emission spectrum.

References

- [1] R. N. Dixon, G. Duxbury, M. Horani and J. Rostas, *Molec. Phys.* 22, 977 (1971)
- [2] L. Karlsson, *et al.*, *Physica Scripta* 13, 229 (1976)
- [3] G. Duxbury, M. Horani and J. Rostas, *Proc. R. Soc. A.* 331, 109 (1972)
- [4] G. Duxbury, Ch. Jungen and J. Rostas, *Molec. Phys.* 48, 719 (1983)
- [5] P. Balzer *et al.*, *Chem. Phys.* 195, 403 (1995)
- [6] M. Hochlaf, K.-M. Weitzel and C. Y. Ng, *J. Chem. Phys.* 120, 6994 (2004)
- [7] S. Han, T. Y. Kang, and S. K. Kim, *J. Chem. Phys.* 132, 124304 (2010)
- [8] A. Alijah and G. Duxbury *J. Mol. Spectrosc.* 211, 7 (2002)

Multi-electron dissociative ionization of clusters under ps and fs laser irradiation: the case of alkyl-halide clusters

G. Karras¹, C. Kosmidis¹

¹Department of Physics, University of Ioannina, 45110 Ioannina, Greece

Corresponding Author: gabriel.karras@gmail.com

The Multi-electron dissociative ionization (MEDI) of alkyl-halide clusters induced by 35 ps (at 266, 532 and 1064 nm) and 20 fs (at 400 and 800 nm) laser pulses is reported. In most cases the MEDI of clusters, is observed at substantially lower laser intensities than those reported for the monomer molecules, while the fragment ions are released with higher kinetic energies Figure 1. For ps laser pulses, single cluster ionization is achieved through multi-photon absorption process. At $\lambda=266$ nm the dominant dissociation mechanism found to be the AID mechanism, while at 532 and 1064 nm clusters disintegrate due to Coulomb explosion process. In the latter case the combined action of the laser and the internal electric field results to the formation of multiply charged ions at laser intensities far below than those expected from theory and with high kinetic energies. In the fs regime the MEDI of neutral clusters was confirmed for both 400 and 800 nm. As it was expected multi-photon absorption processes found to be favored for 400 nm while field ionization processes mediated the interaction at 800 nm. For $\lambda=800$ nm field ionization processes resulted in the formation of ions from different fragmentation channels, which also exhibited different angular distributions. Ions with high kinetic energies, originating from the combined action of the laser and the internal electric field exhibit isotropic angular distribution, while those originating from the screening of the internal electric field, due to the collective oscillation of the electron cloud inside the cluster environment, found to possess anisotropic angular distribution perpendicular to the laser polarization vector. On the contrary, ions with low kinetic energies, originating from an electron impact ionization process, are ejected anisotropically, with maximum of their distribution parallel to the laser polarization vector. The comparative study between ps and fs laser pulses revealed that in both cases and for all wavelengths applied, single cluster ionization is achieved through multi-photon absorption process. Furthermore, for fs laser irradiation the cluster geometry remains almost unchanged during the interaction because of the ultra-short duration of the pulse. Due to this, the suppression of the intracluster potential barriers are lower than in the case of ps laser pulses and so the appearance of the same multiply charged fragments at laser intensities two orders of magnitude higher in the case of fs laser pulses is conceivable. Also, the higher charge multiplicities that were recorded for ps laser pulses are interpreted on the same grounds. Finally, it seems that the cluster density is a critical parameter and responsible for the increase of the appearance intensity thresholds as the molecular chain length increases when lighter halogen atoms are participating in the molecular skeleton [1].

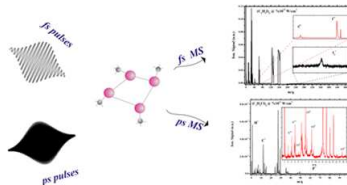


Figure 1: Comparative study of the interaction ethyl-iodide and ethyl-chloride clusters in the ps and fs time domain.

References

[1] G. Karras, and C. Kosmidis, submitted for publication

Photo-double ionization on the attosecond time scale

E. P. Månsson¹, C. L. Arnold², D Guénot², D. Kroon², A. L'Huillier²,
S. Ristinmaa Sörensen¹, and M. Gisselbrecht^{1,2}

¹*Division of Synchrotron Radiation Research, Lund University, SE-221 00 Lund, Sweden*

²*Division of Atomic Physics, Lund University, SE-221 00 Lund, Sweden*

Corresponding Author: erik.mansson@sljus.lu.se

Double ionization by absorption of a single photon represents one of the most fundamental processes that can only be understood by considering Coulomb interaction between the electrons. This has stimulated experimental development to characterize the electron pair as well as theoretical work to understand the physical processes behind the emission of two electrons [1].

Recently, attosecond pump-probe experiments have gained access to single ionization dynamics at its natural time scale [2]. Here we present the first attosecond dynamics experiment on double ionization of xenon with the electrons detected in coincidence. Access to electron pair dynamics is important for the advance of nonlinear theories based on the time dependent Schrödinger equation. Previous studies on double ionization of xenon have focused on the complex one-photon double ionization dynamics [3] and the exploration of two-color two-photon double ionization with a single harmonic [4]. The latter revealed that the sequential absorption process dominates, suggesting that non-sequential absorption requires shorter light pulses.

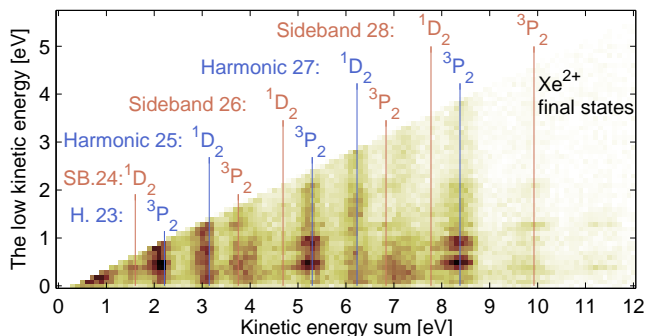


Figure 1: Electron energy sharing intensity (pair count rate), integrated across all delays.

In our experiment, we photo-double ionize xenon with attosecond pulse trains (APTs). An IR pulse is used as a dressing field in the perturbative regime to manipulate the ionization dynamics. Coincident electron detection distinguishes double from single ionization and provides access to the dynamics of the correlated electron pair. Figure 1 shows the sharing of excess energy between the electrons, which allows us to identify the electronic states involved. We study the intensity as function of the delay between the APT and the IR pulse, for selections of kinetic energy sum and energy sharing. We find that several regions show intensity oscillations on the attosecond time scale, which can be attributed to non-sequential two-photon absorption. This opens up exciting possibilities to investigate time-delays between different energy sharings, as an extension of what was done for single ionization [2].

References

- [1] J. S. Briggs and V. Schmidt, *J. Phys. B*, **33**, R1–R48 (2000)
- [2] K. Klünder *et al.*, *Phys. Rev. Lett.* **106**, 143002 (2011)
- [3] J. H. D. Eland *et al.*, *Phys. Rev. Lett.* **90**, 053003 (2003)
- [4] O. Guyétand *et al.*, *J. Phys. B*, **41**, 065601 (2008)

Double photoionization of Kr and Ar

P. Linusson¹, S. Fritzsche^{2,3}, M. Mucke⁴, J.H.D. Eland^{4,5}, L. Hedin⁴, and R. Feifel⁴

¹Department of Physics, Stockholm University, SE-106 91 Stockholm, Sweden

²Department of Physics, P.O. Box 3000, Fin-3004 University of Oulu, Finland

³GSI Helmholtzzentrum für Schwerionenforschung D-64291 Darmstadt, Germany

⁴Department of Physics and Astronomy, Uppsala University, Box 516, SE-751 20 Uppsala, Sweden

⁵Department of Chemistry, Physical and Theoretical Chemistry Laboratory, Oxford University, South Parks Road, Oxford OX1 3QZ, United Kingdom

Corresponding Author: Per.Linusson@fysik.su.se

The simultaneous emission of two electrons from a free atom by impact of a single photon, called double photoionization (DPI), has attracted considerable attention during recent years. In a one-particle picture such a process cannot occur at all. In order to describe it properly, electron-electron interaction must be taken into account. The relevance of DPI to our understanding of electron correlation has been an important factor in attracting the interest of researchers. Most of the work on DPI, especially the theoretical, has been done on helium, for which the literature is quite comprehensive. More complicated systems, however, are by far less explored [1, 2].

From an experimental point of view, the study of DPI has been greatly facilitated by several different coincidence techniques developed over the last two decades. In our work presented here, we have used the so-called Time-Of-Flight PhotoElectron-PhotoElectron (TOF-PEPECO) COincidence technique based on a magnetic bottle, as originally introduced by Eland *et al.*[3], for the study of DPI processes in krypton and argon.

We will present our recent results on core-valence ($3d^{-1}4p^{-1}$) ionization of krypton, and the creation of double core vacancies ($2p^{-2}$) of argon upon single-photon absorption. The experimental results are compared with theory based on a new computational scheme within the Multi-Configurational Dirac-Fock method.

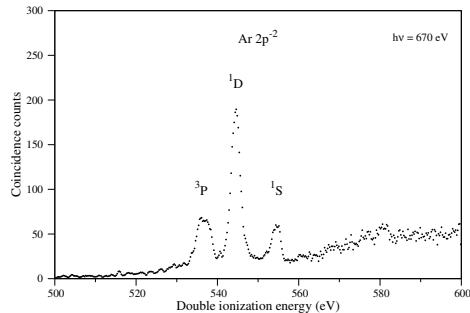


Figure 1: Experimental spectrum of the $Ar\ 2p^{-2}$ doubly-core-ionized states created by single-photon absorption.

References

- [1] P. Bolognesi, G. C. King, L. Avaldi, Rad. Phys. Chem. **70**, 207 (2007)
- [2] J.H.D. Eland, Adv. Chem. Phys. **141**, 103 (2009)
- [3] J.H.D. Eland *et al.*, Phys. Rev. Lett. **90**, 053003 (2003)

The MAGIA experiment: status and prospects

Q. Bodart¹, Y.-H. Lien¹, G. Rosi¹, F. Sorrentino¹, G. M. Tino¹, L. Cacciapuoti², and M. Prevedelli³

¹*Dipartimento di Fisica e Astronomia & INFN, Università di Firenze, via Sansone 1 50019 Sesto Fiorentino (FI), Italy*

²*European Space Research and Technology Centre, Keplerlaan 1, 2201 AZ Noordwijk, The Netherlands*

³*Dipartimento di Fisica dell'Università di Bologna, via Irnerio 46, 40126 Bologna, Italy*

Corresponding Author: sorrentino@fi.infn.it

We will report on the status of the MAGIA experiment for the accurate measurement of the gravitational constant G . The experiment is based on a light-pulse atom interferometry gravity gradiometer detecting the gravitational field generated by a well characterized set of source masses (fig. 1).

⁸⁷Rb atoms, trapped and cooled in a magneto-optical trap (MOT), are launched upwards in a vertical vacuum tube with a moving optical molasses scheme, producing an atomic fountain. Near the apogees of the atomic trajectories, a measurement of their vertical acceleration is performed by a Raman interferometry scheme. External source masses are positioned in two different configurations (C_1 and C_2) and the induced phase shift is measured as a function of masses positions.

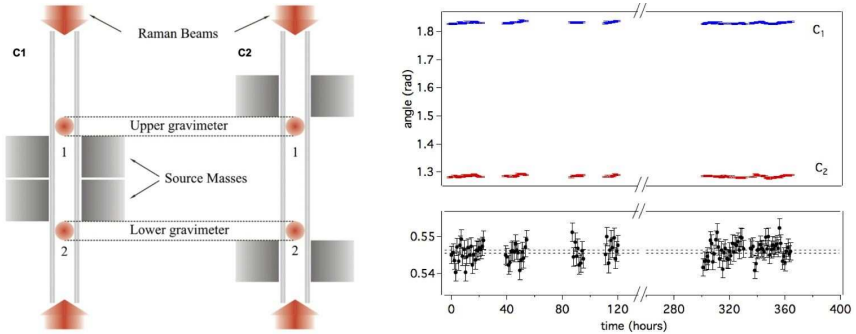


Figure 1: Left: scheme of the MAGIA experiment. Right: (top) Modulation of the differential interferometric phase measured by the atomic gravity gradiometer when the distribution of the source masses is alternated between configuration C_1 (upper points) and C_2 (lower points); (down) resulting values of the angle of rotation.

Goal of the experiment is to measure G with 100 ppm accuracy. After a preliminary measurement with $\sim 0.1\%$ precision [1], we recently operated several upgrades to apparatus [2]. In particular, we improved the SNR and long term stability/reproducibility; we also improved the control on sources of systematic error through a careful calibration of detection efficiencies, atomic trajectories and source masses positions. Fig. 1 shows a typical long-run measurement of the gravity gradient change.

References

[1] G. Lamporesi et al., *Determination of the Newtonian Gravitational Constant Using Atom Interferometry*, Phys. Rev. Lett. **100** 050801 (2008).

[2] F. Sorrentino et al., *Sensitive gravity-gradiometry with atom interferometry: progress towards an improved determination of the gravitational constant*, New. J. Phys. **12** 095009 (2010).

Frequency metrology in quantum degenerate helium

Rob van Rooij¹, Joe Borbely¹, Juliette Simonet², Maarten Hoogerland³,
Kjeld Eikema¹, Roel Rozendaal¹, and Wim Vassen¹

¹LaserLaB VU University, Department of Physics, Amsterdam, the Netherlands

²ENS, LKB, Paris, France

³Department of Physics, University of Auckland, Auckland, New Zealand

Corresponding Author: w.vassen@vu.nl

We have measured the absolute frequency of the 1557-nm doubly forbidden transition between the two metastable states of helium, 2^3S_1 (lifetime 8000 s) and 2^1S_0 (lifetime 20 ms), with 1 kHz precision [1]. With an Einstein coefficient of 10^{-7} s^{-1} this is one of weakest optical transitions ever measured. The measurement was performed in a Bose-Einstein condensate of $^4\text{He}^*$ as well as in a Degenerate Fermi Gas of $^3\text{He}^*$, trapped in a crossed dipole trap (see Fig. 1). From the isotope shift we deduced the nuclear charge radius difference between the α -particle and the helion. Our value differs by 4σ with a very recent result obtained on the $2^3S - 2^3P$ transition [2].

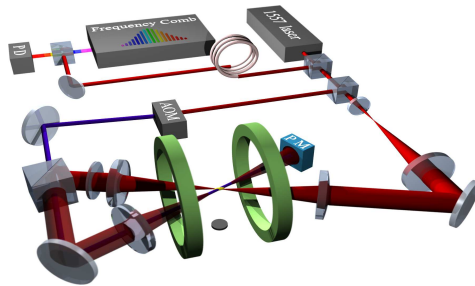


Figure 1: *Experimental setup. A small fraction of the 1557-nm laser light is split off and coupled via a fiber-optic link to be referenced to a fiber-based frequency comb. A heterodyne signal is monitored on a fast photodiode (PD) to determine the absolute frequency of the 1557-nm laser. The remaining light is divided into the trap beam and the spectroscopy beam. A crossed-beam dipole trap configuration is realized by focusing both the incident and returning trap beam (with orthogonal linear polarizations) at the center of the magnetic trap (represented by the green coils). The spectroscopy beam is frequency shifted by a 40-MHz acousto-optic modulator (AOM), overlapped with the returning trap beam and absorbed by a thermopile power meter (PM). A microchannel plate detector is positioned underneath the trap for temperature and atom number determination (from Science).*

References

- [1] R. van Rooij *et al.*, Science **333**, 196–198 (2011)
- [2] P. Cancio Pastor *et al.*, arXiv:1201.1362 (2012)

Determination of nuclear parameters and fundamental constants by frequency metrology in low-lying triplet states of He

L. Consolino^{1,2}, P. Cancio Pastor^{1,2}, G. Gisufredi^{1,2}, P. De Natale^{1,2}, M. Inguscio¹, V. Yerokhin², and K. Pachucki³

⁴*Istituto Nazionale di Ottica-CNR (INO-CNR), Via Nello Carrara 1, I-50019 Sesto Fiorentino, Italy*

¹*European Laboratory for Non-Linear Spectroscopy (LENS) and Dipartimento di Fisica, Università di Firenze, Via N. Carrara 1, I-50019 Sesto Fiorentino, Italy*

²*St. Petersburg State Polytechnical University, Polytekhnicheskaya 29, St. Petersburg 195251, Russia*

³*Faculty of Physics, University of Warsaw, Hoza 69, 00-681 Warsaw, Poland*

Corresponding Author: pablo.cancio pastor@ino.it

Spectacular progress of experimental techniques and ab initio quantum electrodynamics (QED) calculations, achieved in the last decades, has made precision spectroscopy of light atoms a unique tool for the determination of fundamental constants and properties of atomic nuclei. In helium, recent optical frequency comb assisted metrology of optical transitions in both stable He isotopes [1-3] has achieved a relative precision of about 10^{-11} , and thus become sensitive to the uncertainties of the Rydberg constant and of the nuclear charge radius. While the present theory is not accurate enough to provide the nuclear charge radii of ^3He and ^4He separately, it can provide their difference δr^2 , as the isotope shift is considerably simpler to calculate than the energy levels. Significant discrepancies in δr^2 determined from 2^3S-2^1S [2] and 2^3S-2^3P [1,3,4] isotope shift measurements, all performed consistently within the same theory [3,5], can prospect possible additional effects beyond the standard QED as already discussed in the literature with regard to the quoted discrepancy for the proton charge radius [6].

A recent determination of the fine structure constant [7], made by comparison of the theoretical prediction and the experimental results for the ^4He fine structure in 2^3P states, is another example of improvement of fundamental physics knowledge from precise He spectroscopy. We have recently improved the nonrelativistic QED calculation of the combined fine and hyperfine structure of the 2^3P levels of ^3He with the complete treatment of the $m\alpha^6$ corrections [5]. The achieved uncertainty of such calculation take to a determination of α from ^3He measurements with an accuracy at least equal to that of other He isotope if the frequency of 2^3P hyperfine transitions will be measured with a precision comparable to those of the 2^3P fine transitions in ^4He .

Here we present a summary of our recent research focused on frequency metrology of low-lying triplet levels of stable He isotopes and their fundamental physics implications. In addition, a possible determination of the helion magnetic moment by using spectroscopic measurements and QED calculations of the combined 2^3P fine and hyperfine structure is discussed.

References

- [1] P. Cancio Pastor *et al.*, Phys. Rev. Lett. **92**, 023001 (2004), [(E) *ibid* **97**, 139903 (2006)].
- [2] R. van Rooij, *et al.*, Science **333**, 196 (2011).
- [3] P. Cancio Pastor, L. Consolino, G. Gisufredi, P. D. Natale, M. Inguscio, V. A. Yerokhin, and K. Pachucki, Phys. Rev. Lett. , in print (2012).
- [4] D. Shiner, R. Dixon, and V. Vedantham, Phys. Rev. Lett. **74**, 3553 (1995).
- [5] K. Pachucki, V. A. Yerokhin and P. Cancio Pastor, submitted to Phys. Rev. A (2012)
- [6] R. Pohl *et al.*, Nature (London) **466**, 213 (2010).
- [7] K. Pachucki and V. A. Yerokhin, Phys. Rev. Lett. **104**, 070403 (2010).

Resonant high-order harmonic generation: beyond the three-step model

V. Strelkov¹, M. Khokhlova^{1,2}, A. Gonoskov³, I. Gonoskov³, and M. Yu. Ryabikin³

¹*A.M.Prokhorov General Physics Institute of the Russian Academy of Sciences, , 38 Vavilova st., Moscow 119991, Russia*

²*Faculty of Physics, Lomonosov Moscow State University, Vorob'evy Gory, Moscow 119991, Russia*

³*Institute of Applied Physics of the Russian Academy of Sciences, , 46 Ulyanov st., Nizhny Novgorod 603950, Russia*

Corresponding Author: v-strelkov@fpl.gpi.ru

High harmonic generation (HHG) via interaction of intense laser radiation with matter provides a unique source of coherent collimated xuv femto- and attosecond pulses. Simple, but very fruitful three-step model [1,2] of the HHG describes it as result of tunneling ionization, classical free electronic motion in the laser field, and recombination accompanied by the XUV emission upon the return to the parent ion. In this paper we consider two cases where the HHG study assumes essential development of this model.

We present a four-step HHG model describing generation of the harmonic resonant with the transition between the ground and an autoionizing state of the generating atom or ion [3]. The first two steps are the same as in the three-step model, but instead of the last step (radiative recombination from continuum to the ground state) the free electron is trapped by the parent ion, so that the system (parent ion + electron) lands in the autoionizing state, and then it relaxes to the ground state emitting XUV. The results of the numerical and analytical calculations based on this model are in good quantitative agreement with the experiments showing HHG enhancement up to two orders of magnitude when the harmonic is resonant with the transition frequency (recent experimental results are presented in review [4] and references therein). Moreover, our simulations predict the phase-locking of the resonantly-enhanced harmonics. This allows production of an attosecond pulse train using such harmonics.

The second example deals with polarization properties of the HH generated from atoms and molecules. The harmonics generated by atoms in elliptically-polarized laser field are elliptically polarized, and the polarization ellipse of the harmonic is rotated by a certain angle with respect to that of the fundamental. This rotation can be well described with the three-step model considering a CLASSICAL electronic motion after the photoionization. The harmonic ellipticity itself, however, can be hardly understood taking into account only classical motion properties. We show [5] that this ellipticity originates from quantum-mechanical uncertainty of the electron motion. The analytical theory is verified with the exact numerical TDSE solution. The results reasonably agree with experimentally measured polarization properties of harmonics both in case of atomic and molecular HHG. The outlook of this work is study of the polarization properties of resonant HH.

References

- [1] P. B. Corkum, Phys. Rev. Lett., **71**, 1994 (1993)
- [2] K. J. Schafer *et al.*, Phys. Rev. Lett., **70**, 1599 (1993)
- [3] V. V. Strelkov, Phys. Rev. Lett., **104**, 123901 (2010)
- [4] R. A. Ganeev, Journal of Modern Optics, **59**, 409 (2012)
- [5] V.V. Strelkov *et al.*, Phys. Rev. Lett., **107**, 043902 (2011)

Analytic Description of High-Order Harmonic Generation by an Intense Few-Cycle Laser Pulse

M. V. Frolov¹, N. L. Manakov¹, A. M. Popov², O. V. Tikhonova², E. A. Volkova²,
A. A. Silaev³, N. V. Vvedenskii³, and Anthony F. Starace⁴

¹Department of Physics, Voronezh State University, Voronezh 394006, Russia

²D.V. Skobeltsyn Institute of Nuclear Physics, M.V. Lomonosov Moscow State University, Moscow 199991, Russia

³Institute of Applied Physics, Russian Academy of Sciences, Nizhny Novgorod 603950, Russia

⁴Department of Physics and Astronomy, The University of Nebraska, Lincoln NE 68588-0299, USA

Corresponding Author: astarace1@unl.edu

Based on a theoretical model for describing the interaction of an electron, weakly bound in a short-range potential, with an intense, few-cycle laser pulse, we have derived detailed analytic expressions for the spectral density of high-order harmonic generation (HHG) in terms of the key parameters of the laser pulse, including the number, N , of optical cycles and the carrier-envelope phase (CEP) [1]. In the tunneling approximation, closed-form formulas are obtained. These were used in [2] to describe key features of HHG by both H and Xe atom targets in an intense, few-cycle laser pulse. We provide here a complete analysis of the dependence of the HHG spectrum on both N and the CEP ϕ of an N -cycle laser pulse. Most importantly, we show analytically that the structure of the HHG spectrum stems from interference between electron wave packets originating from electron ionization from neighboring half-cycles near the peak of the intensity envelope of the few-cycle laser pulse. Such interference is shown to be very sensitive to the CEP. The usual HHG spectrum for a monochromatic driving laser field (comprising harmonic peaks at odd multiples of the carrier frequency and spaced by twice the carrier frequency) is shown analytically to occur only in the limit of very large N , and begins to form, as N increases, in the energy region beyond the HHG plateau cutoff, as shown in Fig. 1.

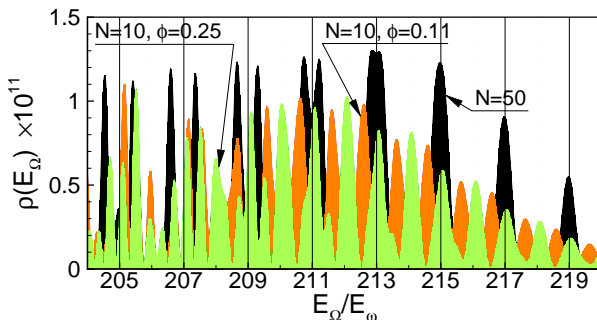


Figure 1: Spectral density distribution $\rho(E_\Omega, \phi)$ vs. E_Ω/E_ω ($E_\omega = \hbar\omega$) in the plateau cutoff region for a Gaussian pulse with peak intensity $I = 2 \times 10^{14}$ W/cm², carrier wavelength $\lambda = 1.6$ μ m, N optical cycles (FWHM), and CEP ϕ . Green (light grey) curve: $N = 10$, $\phi = 0.25$; orange (dark grey) curve: $N = 10$, $\phi = 0.11$; black curve: $N = 50$ (no dependence on ϕ).

References

- [1] M.V. Frolov *et al.*, Phys. Rev. A **85**, 033416 (2012)
- [2] M.V. Frolov *et al.*, Phys. Rev. A **83**, 021405(R) (2011)

Photodetachment dynamics of H^- by few-cycle laser pulses

S. F. C. Shearer¹, C. R. J. Addis²

¹*Centre for Theoretical Atomic, Molecular and Optical Physics, Queen's University Belfast, Belfast BT7 1NN, N.Ireland*

²*School of Engineering and Physical Sciences, Heriot-Watt University, Edinburgh, EH14 4AS Scotland*

Corresponding Author: f.shearer@qub.ac.uk

The recent adiabatic saddle-point method of Shearer et al [1] is applied to study strong field photodetachment of H^- by few-cycle linearly polarized laser pulses, of frequencies near the two-photon detachment threshold. In our work we assume an ir laser with frequency ω , polarized along the \hat{z} axis, whose time-dependent vector potential is given by,

$$\mathbf{A}(t) = A(t)\hat{z} = A_0 \left[\sin^2 \left(\frac{\omega t}{2N} \right) \sin(\omega t + \alpha) \right] \hat{z}. \quad (1)$$

Here N is the number of optical cycles in the pulse and α is the CEP. The peak value A_0 of the vector potential $A(t)$ is related to the peak laser intensity I_0 by $A_0 = \sqrt{I_0/I_{a.u.}}/\omega = F_0/\omega$ where $I_{a.u.} = 3.515 \times 10^{16}$ W/cm² and F_0 is the peak value of the electric field strength.

The behaviour of the saddle points in the complex time plane for a range of laser parameters is explored. A detailed analysis of the influence of laser intensities (2×10^{11} - 6.5×10^{11} W/cm²), mid-infrared laser wavelengths (1800 -2700 nm) and various carrier envelope phases on (i) photo angular distributions (PADs), (ii) energy spectra and (iii) momentum distributions are presented.

Examination of the PADs reveal main lobes and jet-like structures. Bifurcation phenomena in the PADs are also observed as the wavelength and intensity increases. Our simulations show that the (i) PADs and (ii) energy spectra are extremely sensitive to the CEP and thus measuring such distributions provide a useful tool for determining this phase.

The symmetrical properties of the electron momentum distributions are also found to be highly correlated with the CEP and this provides an additional robust method for measuring the CEP of a laser pulse.

We also show that the momentum distributions contain signatures of the dominant frequency modes operating at our chosen range of laser parameters in the mid -infrared region near the two-photon threshold. The frequency modes arise from equation (1) above, which may be re-cast in the form,

$$A(t) = \frac{A_0}{4} (2 \sin(\omega_1 t + \alpha) - \sin(\omega_2 t + \alpha) - \sin(\omega_3 t + \alpha)), \quad (2)$$

where $\omega_1 = \omega$, $\omega_2 = \omega \left(1 + \frac{1}{N}\right)$ and $\omega_3 = \omega \left(1 - \frac{1}{N}\right)$. Our work indicates that the 2D momentum distributions may serve as a useful probe in identifying all combinations of allowable frequency components that lead to photodetachment near the two-photon threshold.

Our calculations further show that for a 3-cycle pulse inclusion of all 8 saddle points are required in the evaluation of transition amplitude to yield an accurate description of the photodetachment process. This is in contrast to recent results for a 5-cycle pulse [1].

Finally our calculations are compared with available S-matrix theory [2], the generalised phased Bessel function treatment [3], Floquet calculations [4] and experimental data [5].

References

- [1] S. F. C. Shearer, M. C. Smyth and G. F. Gribakin, *Phys. Rev. A*, **84**, 033409, (2011).
- [2] L. -Y. Peng, Q. Gong and A. F. Starace, *Phys. Rev. A* **77**, 065403, (2008).
- [3] L. Bai, J. Zhang, X. Zhang and Z. Xu, *Phys. Rev. A* **74**, 025402 (2006).
- [4] D. A. Telnov and Shih- I. Chu, *Phys. Rev. A* **66**, 063409, (2002).
- [5] R. Reichle, H. Helm, and I. Yu. Kiyan, *Phys. Rev. Lett.* **87**, 243001 (2001); *Phys. Rev. A* **68** 063404, (2003).

Teaching Quantum Mechanics using Nanoscience

D. Hessman¹, G. Ohlén²

¹*Solid State Physics, Lund University, SE-221 00 Lund, Sweden*

²*Mathematical Physics, Lund University, SE-221 00 Lund, Sweden*

Corresponding Author: Gunnar.Ohlen@matfys.lth.se

At Lund Institute of Technology we give a course in quantum mechanics (QM) already in the first year for the students of Engineering Physics. This course is given as a collaboration between Mathematical Physics and Solid State Physics.

The aim is to introduce students to QM in an engineering context using examples from nanoelectronics. Such systems can often be accurately modeled by piecewise constant potentials. Using only elementary mathematics and these simple models we are able to discuss several interesting physical phenomena such as transport theory, tunnel effect and bound states in quantum billiards of different dimensions.

For the laboratory work we have developed a teaching strategy that involves the students in the planning of the experiments. This is achieved by giving the students open questions that they solve in group discussions prior to their experimental work.

Conclusions:

- By keeping mathematics simple - avoiding spherical coordinates - we can focus on the fundamental physical concepts of QM.
- By doing experiments with nanodevices the students can simultaneously study the systems both experimentally and theoretically.
- The simplicity of these systems make it possible for the students to write their own computer code, both to solve problems and to make more advanced simulations.
- Our experience is that the students learn concepts better by discussing open problems and testing their ideas on real physical systems.

Photomixing for Precision Measurements in the Terahertz Regime

Florin Lucian Constantin¹

¹*Laboratoire PhLAM, CNRS UMR 8523, 59655 Villeneuve d'Ascq, France*

Corresponding Author: FL.Constantin@univ-lille1.fr

The optical heterodyne conversion (photomixing) is a well-established technique for terahertz continuous-wave generation and detection [1]. The standard photomixer design relies on a LTG-GaAs epitaxial photoconductor coupled with a planar antenna which has a response time in the sub-ps range. Two cw lasers emitting around 825 nm are detuned by a THz frequency gap, spatially overlapped and modulate the conductance of the device. Upon the photomixer is biased, the photocurrent oscillating at the difference-frequency drives the antenna that radiates a monofrequency THz-wave which can be tuned over a broad frequency span. The frequency stabilisation of the lasers against a passive frequency standard allowed the application of the photomixing to the molecular spectroscopy [2].

This contribution points out the potentialities of the optical and electrical response of the photomixer for addressing its entire frequency bandwidth. The application to the ultrafast modulation of the THz radiation is discussed. Laser modulation is provided by frequency shifting the laser frequency with an acousto-optical modulator driven by a radiofrequency synthesizer with modulation capabilities. Quadratic response of the photomixer to the optical fields allows transferring the modulation of the optical beat to the terahertz domain. Alternatively, direct-current modulation of the photomixer emission is demonstrated by coupling microwaves to the antenna through a transmission line. Conversely, THz-wave detection with the photomixer is demonstrated by exploiting its intrinsic non-linear electrical response [3]. Rectification of the electric field induced in the antenna by a THz beam from an independent source leads to a dc signal. In addition, the mixing between the THz source and the optical beat allows implementing with the photomixer a phase-coherent heterodyne detection scheme. This device offers new opportunities for multi-frequency emission and detection in the THz regime.

References

- [1] S. Verghese *et al.*, J. Appl. Phys. **73**, 3824–3826 (1998)
- [2] L. Aballea, and L.F. Constantin, European Phys. J. Appl. Phys. **45**, 21201-1–21201-2 (2009)
- [3] Florin Lucian Constantin, IEEE J. Quantum Electron. **47**, 1458–1462 (2011)

Schemes for high-precision measurements of the ionization and dissociation energies of molecular hydrogen

D. Sprecher¹, F. Merkt¹

¹Laboratory of Physical Chemistry, ETH Zurich, 8093 Zurich, Switzerland

Corresponding Author: sprecher@phys.chem.ethz.ch

Molecular hydrogen is the most important system for testing quantum mechanics and quantum electrodynamics in molecules. The comparison of experimental and theoretical values of the dissociation energies of H₂, HD, and D₂ has a long history and led to a quantitative understanding of chemical binding. The most precise determination of the dissociation energies was carried out recently by measuring three intervals independently: the $1s\sigma X \rightarrow 2s\sigma EF$ interval [1], the $2s\sigma EF \rightarrow np$ ($n \approx 60$) interval [2-4], and the electron binding energy of the np Rydberg states [3-6]. All values are in agreement with the results of the latest *ab initio* calculations [7,8] within the uncertainty limit of 30 MHz (0.001 cm^{-1}). New measurements with an improved accuracy will allow for a more stringent test of future *ab initio* calculations. We will discuss several schemes of an experiment aiming at sub-MHz accuracy and present the results of preliminary measurements.

References

- [1] S. Hannemann *et al.*, Phys. Rev. A **74**, 062514 (2006)
- [2] J. Liu *et al.*, J. Chem. Phys. **130**, 174306 (2009)
- [3] J. Liu *et al.*, J. Chem. Phys. **132**, 154301 (2010)
- [4] D. Sprecher *et al.*, J. Chem. Phys. **133**, 111102 (2010)
- [5] A. Osterwalder *et al.*, J. Chem. Phys. **121**, 11810 (2004)
- [6] D. Sprecher *et al.*, Faraday Discuss. **150**, 51 (2011)
- [7] K. Piszczatowski *et al.*, J. Chem. Theory Comput. **5**, 3039 (2010)
- [8] K. Pachucki and J. Komasa, Phys. Chem. Chem. Phys. **12**, 9188 (2010)

Polarization effects on multilevel rubidium atoms induced by optical frequency comb

N. Vujicic¹

¹*Institute of Physics, HR-10 000 Zagreb, Croatia*

Corresponding Author: natasav@ifs.hr

The subject of this study are polarization effects induced by resonant interaction of rubidium atoms with optical frequency comb. Such polarizations effects, induced by interaction of atoms with optical frequency comb are, as far as we know, for the first time experimentally studied. Ultrashort, mode-locked, phase-stabilized femtosecond (fs) laser with high repetition rates produces stabilized wide-bandwidth optical frequency comb (a spectrum consisting of a series of evenly spaced sharp lines) [1]. In the previous papers [2,3,4] a modified direct frequency comb spectroscopy (modified DFCS), which utilizes a fixed frequency comb spectrum and an additional continuous-wave (cw) scanning probe laser, was presented. It was shown that resonant excitation of room-temperature rubidium and cesium atoms by discrete frequency comb optical spectrum results in the comblike velocity distribution of the excited-state hyperfine level populations and velocity selective population transfer between the atomic ground-state hyperfine levels. Detailed theoretical investigation of the fs pulse train interaction with multilevel atom was performed, provided not only qualitative but also quantitative description of the interacting atom-laser system, as was illustrated by the excellent agreement with the experimental results. The effect of velocity selective optical pumping (VSOP), induced by frequency comb excitation, gave us novel information about the frequency comb excitation in Doppler-broadened atomic systems.

Here, we present the experimental study of Zeeman components optical pumping effects, induced by resonant interaction with circularly polarized fs laser pump laser in external static magnetic field resulting in induced anisotropy of medium [5]. If such, optically prepared, medium is examined by resonant linearly polarized cw probe laser at 795 nm, the effects of rotation of polarization of probe beam can be observed. The phenomenon of polarization rotation of linearly polarized cw probe optical field in room-temperature rubidium vapor have been investigated for different polarizations of the fs pump laser (σ^+ i σ^-), in dependence on fs pump laser power as well as on external magnetic field strength. Semi-classical model of probe beam propagation through anisotropic medium [5,6] gives good description of system and is in accordance with observed experimental results.

References

- [1] T. Udem, R. Holzwarth, and T. Hänsch, *Nature* **416**, 233 (2002)
- [2] D. Aumiler, T. Ban, H. Skenderovi and G. Pichler, *Phys. Rev. Lett.* **95**, 233001 (2005)
- [3] T. Ban, D. Aumiler, H. Skenderovi and G. Pichler, *Phys. Rev. A* **73**, 043407 (2006)
- [4] N. Vujicic, S. Vdovic, D. Aumiler, T. Ban, H. Skenderovi and G. Pichler, *Eur. Phys. J. D* **41**, 447 (2007)
- [5] M. L. Harris, C. S. Adams, S. L. Cornish, I. C. McLeod, E. Tarleton, and I. G. Hughes, *Phys. Rev. A* **73**, 063509 (2006)
- [6] S. Li, B. Wang, X. Yang, Y. Han, H. Wang, M. Xiao, and K. Peng, *Phys. Rev. A* **74**, 033821 (2006)

Energy dependence of photoelectron angular distributions from two-photon ionization of Strontium in the proximity of the $5p^2\ ^1S_0$ doubly excited state

A. Dimitriou¹, S. Cohen¹, and A. Lyras¹

¹*Department of Physics, University of Ioannina, 45110 Ioannina, Greece*

Corresponding Author: adimitr@cc.uoi.gr

Electron Energy Analysis and Photoelectron Angular Distributions (PADs) from multiphoton ionization of Alkalibe Earth atoms can reveal important information concerning the properties of doubly excited and highly correlated states lying above the first ionization threshold. That was recently demonstrated for the case of two-photon excitation of the fairly well isolated $3p^2\ ^1S_0$ state of Mg^1 , where experimental measurements confirm, to a large extend, earlier theoretical results ^{2,3,4}. The present study extends this investigation to the heavier and more complex Sr atom and, particularly, to the energy range comprising the $5p^2\ ^1S_0$ doubly excited state. (Fig. 1) (a) displays a simplified energy level diagram and the excitation scheme. Our experimental apparatus is capable of detecting both positive ions and electrons¹. The laser wavelength dependence of Sr^+ , given in (Fig. 1) (b) , reveals several resonances. The broad one at $\sim 367\text{nm}$ is due to the $5p^2\ ^1S_0$ state while the sharp ones are assigned to the nearby autoionizing $4d6d\ J = 0, 2$ manifold⁵. Recorded PADs from two photon ionization are fitted to Eq. (1):

$$S(\omega, \theta) = \beta_0 + \beta_2 P_2(\cos\theta) + \beta_4 P_4(\cos\theta), \quad \beta_0 = 1 \quad (1)$$

which is appropriate for linearly polarized light and where $P_{2k}(\cos\theta)$, $k = 1, 2$ are the Legendre polynomials. The laser wavelength dependence of the parameters β_4 and β_2 are given in (Fig. 1) (c) and (d) respectively. The considerable variation of both parameters around the $5p^2\ ^1S_0$ resonance is evident. Also noticeable is the fact that on the $4d6d\ ^1S_0$ resonance both parameters are practically zero, the electron distribution is isotropic and above threshold ionization (ATI) is observed. These data, along with PAD recordings on ATI electron energy peaks, are to be presented in the conference.

Acknowledgements: This research has been co-financed by the European Union (European Social Fund ESF) and Greek national funds through the Operational Program "Education and Lifelong Learning" of the National Strategic Reference Framework (NSRF) - Research Funding Program: Heracleitus II. Investing in knowledge society through the European Social Fund.

References

- [1] A. Dimitriou, S. Cohen, and A. Lyras, *J. Phys B: At. Mol. Opt. Phys* **44**, 135001 (2011)
- [2] R. Moccia and P. Spizzo, *J. Phys. B* **21**, 1133-1143 (1988)
- [3] E. Luc-Koenig, A. Lyras, J-M. Lecomte, M. Aymar. *J. Phys B: At. Mol. Opt. Phys* **30**, 5213 (1997)
- [4] L. L. Nikolopoulos, *Phys. Rev. A* **71**, 033409-1 (2005)
- [5] M. Kompitsas, S. Goutis, M. Aymar and P. Camus. *J.PhysB: At.Mol. Opt. Phys* **24**, 1557 (1991)

Interference effects for electron transfer in ion-molecule keV.u⁻¹ collisions

Hicham Agueny^{1,2}, Abdelkader Makhoute¹, and Alain Dubois²

¹Laboratoire de Physique du Rayonnement et des Interactions Laser-Matière (LPRILM),
Université Moulay Ismaïl, MA-50003 Meknes, Maroc

²Laboratoire de Chimie Physique - Matière et Rayonnement (UMR 7614), Université Pierre et Marie Curie - CNRS, F-75005 Paris, France

Corresponding Author: h.agueny@gmail.com

In recent years, Young-type interference effects have been observed experimentally and studied theoretically for capture and transfer-excitation in collisions between low-charge ion and dihydrogen molecule. For instance, Schmidt *et al.* [1] have reported the direct experimental evidence of two-center interferences for single capture electron in H²⁺-H₂ collisions while same phenomenon was observed by Misra *et al.* [2] for double capture in the same system. On the other hand Støchkel *et al.* [3] demonstrated two-center interferences for transfer-excitation in H⁺-H₂ fast collisions. It is worth noting that these previous studies focus in the high energy range (0.3-1.3 MeV.u⁻¹) and discuss differential cross sections as a function of the angle between the molecular axis and the projectile direction. No theoretical nor experimental studies of interference effects have been performed at low and intermediate energies.

In the conference we shall present a study of such effects in H⁺-H₂⁺ collisions for energies ranging from 0.25 to 100 keV.u⁻¹ (v= 0.1 - 2 a.u.). The results stem from a semiclassical close-coupling (SCCC) approach to solve the time-dependent Schrödinger equation. The differential cross sections were calculated by using the Eikonal method [4,5] in which the probability amplitudes from the SCCC calculations were augmented by proper asymptotic Coulombic (internuclear and electron-nucleus) phases. From the differential cross sections for electron capture interference effects will be discussed as functions of (i) the scattering angle (cf. Fig. 1) and (ii) the angle θ_m between the molecular axis and the projectile velocity.

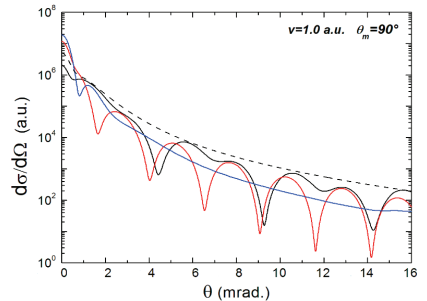


Figure 1: Differential cross sections (DCS) of electron capture as a function of the scattering angle in 25 keV.u⁻¹ H⁺-H₂⁺ collisions. The molecular target is aligned perpendicular to the projectile velocity. Black line : DCS; red line : same but with only internuclear Coulombic phase ; blue line : DCS with only electron-nucleus phase ; dashed line : DCS for H⁺-H collisions.

References

- [1] H.T. Schmidt *et al.*, Phys. Rev. Lett. **101**, 083201 (2008)
- [2] D. Misra *et al.*, Phys.Rev. Lett. **102**, 153201 (2009)
- [3] K. Støchkel *et al.*, Phys. Rev. A **72**, 050703(R) (2005)
- [4] B.H. Bransden and M.R.C. McDowell, *Charge exchange and the theory of ion-atom collisions* (Clarendon Press, Oxford, 1992)
- [5] A. Dubois, S.E. Nielsen and J.P. Hansen, J. Phys. B **26**, 705 (1993)

Internal ground state preparation of molecular ions in a cryogenically-cooled ion trap with a combination of rotational laser-cooling and state-selective dissociation

A. D. Gingell¹, K. Hansen¹, M. Schwarz², O. O. Versolato², A. Windberger²,
L. Kłosowski^{1,4}, J. Ullrich^{2,3}, J.R. Crespo López-Urrutia², and M. Drewsen¹

¹*Department of Physics and Astronomy, University of Aarhus, Ny Munkegade 120, DK-8000 Aarhus C, Denmark*

²*Max-Planck-Institut für Kernphysik, Saupfercheckweg 1, 69117 Heidelberg, Germany*

³*Physikalisch-Technische Bundesanstalt, Bundesallee 100, 38116 Braunschweig, Germany*

⁴*Nicolaus Copernicus University, Institute of Physics, Grudziadzka 5/7, 87-100 Toruń, Poland*

Corresponding Author: drewsen@phys.au.dk

Owing to their unique properties, cold molecular ions have great potential for a range of novel scientific and technological innovations: ultra-precise spectroscopic measurements, new time and frequency standards, ultra-sensitive mass spectrometers, precise control of chemical processes on the quantum level with single-molecule sensitivity.

Working with MgH^+ molecular ions in a linear Paul trap, we have routinely performed simultaneous cooling of both translational and rotational degrees of freedom (vibrational excitation is frozen out at room temperature), via sympathetic-cooling mediated by co-trapped Doppler laser-cooled Mg^+ atomic ions [1] and blackbody-mediated laser-cooling, respectively [2]. Recent experiments have demonstrated a rotational ground-state population of 36.7 ± 1.2 %, equivalent to that of a thermal distribution at about 20 K [1].

We present here extensions to this work that employ a new cryogenically-cooled ion trapping environment at 4 K. Ions are completely shielded from room-temperature blackbody radiation except over a solid angle of about 1 %, which corresponds to apertures present for ion imaging and for admission of laser beams. Steady-state ground state population fractions approaching 70 % can be routinely maintained in conjunction with the same continuous rotational laser-cooling as applied in Ref. [1]. Furthermore, molecular ion ensembles with a rotational ground state fraction approaching 95 % have been obtained through state-selective Resonance Enhanced Multi-photon Dissociation (REMPD) of molecules in higher lying states. This latter ground state purification technique can also be used in a probabilistic sense to prepare a single ion in the rovibrational ground state with a similarly high degree of probability.

The presented rovibrational ground state preparation scheme should be generalizable to any diatomic polar molecular ion, given appropriate mid-infrared laser sources for rotational cooling and laser sources for state-selective dissociation.

References

- [1] K. Mølhave, and M. Drewsen, *Phys. Rev. A* **62**, 011401 (2000)
- [2] P. F. Staunum *et al.*, *Nat. Phys.* **6**, 271 (2010)

Chaos-induced enhancement of resonant multi-electron recombination in highly charged ions: Statistical theory

V.A. Dzuba¹, V.V. Flambaum¹, C. Harabati¹, and G. F. Gribakin²

¹*School of Physics, University of New South Wales, Sydney 2052, Australia*

²*Department of Applied Mathematics and Theoretical Physics, Queen's University, Belfast BT7 1NN, Northern Ireland, UK*

Corresponding Author: v.flambaum@unsw.edu.au

We developed a statistical theory for the resonant multi-electron recombination based on properties of chaotic eigenstates. Level density of many-body states exponentially increases with the number of excited electrons. When the residual electron-electron interaction exceeds the interval between these levels, the eigenstates (called compound states or compound resonances if these states are in continuum) become "chaotic" superposition of a large number of Hartree-Fock determinant basis states. This situation takes place in some rare-earth atoms and majority of multiply-charged ions excited by the electron recombination. We developed a theory of the resonant multi-electron recombination via di-electron doorway states leading to such compound resonances [1,2].

The result gives the radiative capture cross-section averaged over small energy interval containing several compound resonances. The experiment does not resolve particular compound resonances (since the interval between them ≤ 1 meV), therefore, our theory correctly describe experimental data [3]. Recently the rate coefficient was measured for W^{20+} ion where it exceeds the direct radiative recombination coefficient by three order of magnitude [4]. We performed numerical calculations for the electron recombination with tungsten ions W^{q+} , $q = 17 - 24$. We derived the formula for the resonance capture cross-section

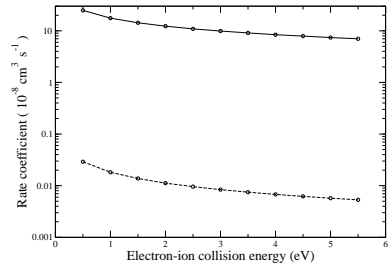


Figure 1: Calculated rate coefficient for electron-ion recombination of W^{20+} ion versus relative collision energy. The dashed curve is the direct radiative recombination rate coefficient.

$$\bar{\sigma}_{cap} = \frac{\pi^2}{2k^2} \sum_{abh,lj} \frac{\Gamma_{spr} |\langle a, b | \hat{v} | h, \varepsilon_c l j \rangle - \langle a, b | \hat{v} | \varepsilon_c l j, h \rangle|^2}{(\varepsilon_c - \varepsilon_a - \varepsilon_b + \varepsilon_h)^2 + \Gamma_{spr}^2/4} \langle \hat{n}_h \hat{n}_c (1 - \hat{n}_a)(1 - \hat{n}_b) \rangle, \quad (1)$$

where $\langle a, b | \hat{v} | h, \varepsilon_c l j \rangle$ and $\langle a, b | \hat{v} | \varepsilon_c l j, h \rangle$ are the Coulomb direct and exchange matrix elements, respectively, $\Gamma_{spr} \approx 10$ eV is the spreading width and n_a, n_b, n_h, n_c are the orbital occupation numbers in the initial state for the associated orbitals. The numerical results for the rate coefficients $\alpha = v\bar{\sigma}_{cap}$ presented by a solid line in Fig. (1) is three order of magnitude over the direct radiative rate coefficient (the dashed line in the figure). Thus it is in good agreement with the experiment [4].

References

- [1] G. F. Gribakin, A. A. Gribakina, and V. V. Flambaum, *Aust. J. Phys.* **52**, 443–457 (1999).
- [2] V. V. Flambaum *et al.*, *Phys. Rev. A* **60**, 012713-7 (2002)
- [3] W. R. Hoffknecht *et al.*, *J. Phys. B* **31**, 2415–2428 (1998)
- [4] S. Schippers *et al.*, *Phys. Rev. A* **83**, 012711-6 (2011)

Investigation of (quasi) symmetric slow collisions between highly charged ions and free atoms

E. Lamour¹, J. Mérot¹, F. Mezdari¹, C. Prigent¹, R. Reuschl¹, J.-P. Rozet¹, S. Steydli¹, M. Trassinelli¹, and D. Vernhet¹

¹ CNRS and Université Pierre et Marie Curie, INSP, UMR7588, 4 Place Jussieu, F-75005 Paris, France

Corresponding Author: martino.trassinelli@insp.jussieu.fr

Collision between slow ions with atoms is one of the basic interactions involved in important phenomena such as those from solar wind colliding with comets. These interactions have been extensively investigated in laboratory environment in the past decades providing valuable informations for the interpretation of astronomical X-ray spectra [1]. Today, there is still a lack of data for symmetric collisions, i.e. highly charged ions colliding on heavy targets, for which contribution from multi-electron exchange processes is important. We present here a new experiment on (quasi) symmetric collision between slow highly-charged ions, namely Ar^{17+} ($v = 0.53$ a.u.), on gaseous Ar and N_2 targets [2]. The investigation has been carried out using low- and high-resolution X-ray spectroscopy. Thanks to an accurate efficiency calibration of our spectrometers and the complete determination of the ion beam - gas jet target overlap, we extract absolute X-ray emission cross sections. These values are in agreement with the unique previous values from Tawara *et al* [3], with an improvement by a factor of two in the accuracy. Resolving the whole He-like Ar^{16+} Lyman series from $n = 2$ to 10 with our crystal spectrometer (see Figure 1) enables to determine precisely the distribution $\{\mathcal{P}_n\}$ of the electron capture probability and the preferential n_{pref} level of the selective single-electron capture. Evaluation of cross sections for this process as well as for the contribution of multiple-capture is carried out. Their sensitivity to the ℓ -distribution of n levels populated by single-electron capture is clearly demonstrated, providing a stringent benchmark for theories. In addition, the hardness ratio \mathcal{H} , commonly used to determine abundance of elements when interpreting astrophysical X-ray spectra, is extracted. Due to the influence of the decay of the metastable $1s2s\ ^3S_1$ state on this ratio, transposition of \mathcal{H} value from 'laboratory ion-collision' towards interpretation of spectra from comets and solar wind should be made with caution. For the first time, from the analysis of our high-resolution spectra, such influence is studied.

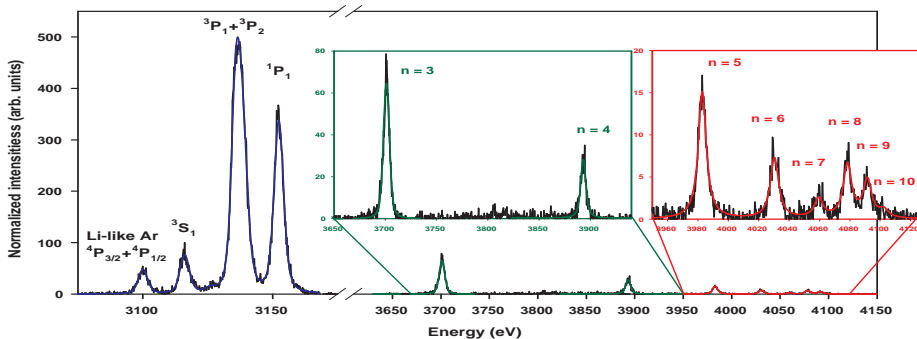


Figure 1: High resolution spectra of Ar^{16+} X-ray transitions observed with an argon target.

References

- [1] T.E. Cravens Science **296**, 1042-1045 (2002)
- [2] M. Trassinelli, C. Prigent, E. Lamour, F. Mezdari, J. Mérot, R. Reuschl J.-P. Rozet, S. Steydli and D. Vernhet, J. Phys. B **45**, 085202 (2012)
- [3] H. Tawara, P. Richard, U.I. Safronova and P.C. Stancil, Phys. Rev. A **64**, 042712 (2001)

A trapped atom interferometer for the measurement of short range forces

, A. Hilico, B. Pelle, Q. Beaufils, G. Tackmann, S. Pélisson, M.-C. Angonin, P. Wolf, and F. Pereira Dos Santos

LNE-SYRTE, Observatoire de Paris, LNE, CNRS, UPMC, 61 avenue de l'Observatoire, 75014 Paris, FRANCE

Corresponding Author: adele.hilico@obspm.fr

I will present the status of an experiment, which aims at performing precise measurements of the interaction forces between atoms and a macroscopic surface, for surface separations from $0.2 \mu\text{m}$ to $10 \mu\text{m}$, where QED effects are predominant [1].

In our experimental apparatus, we realize a trapped atom interferometer in a vertical optical lattice. More precisely, ^{87}Rb atoms are trapped in a bichromatic optical trap. Shallow wells are created by a standing wave of a blue detuned laser at 532 nm and the atoms are transversally confined by a red detuned fiber laser at 1064 nm . Stimulated Raman transitions are used to induce tunnelling into adjacent wells [2], allowing us to perform spectroscopy of Wannier-Stark states [3] or to create thanks to a sequence of two such pulses a Ramsey-type interferometer (cf. Figure 1).

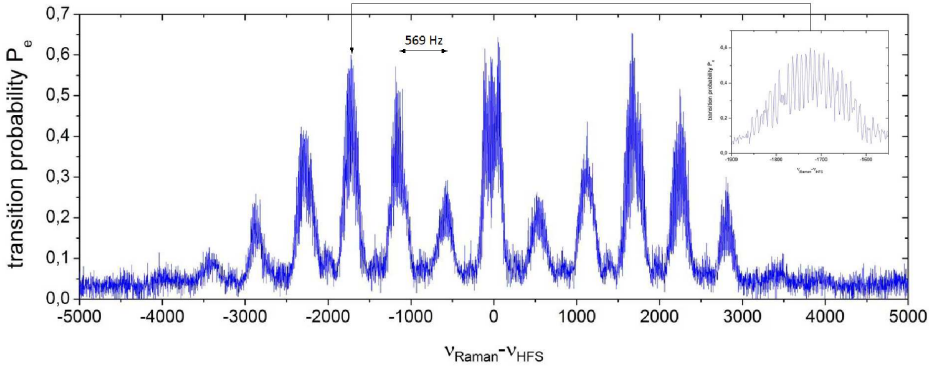


Figure 1: Ramsey-Raman interferometer pattern. Sets of Ramsey fringes are obtained in each of the Rabi pedestals that correspond to transitions between distinct neighbouring Wannier-Stark states.

Currently, our experiment is performed far from the surface of interest, which is set by the retroreflecting mirror of the standing wave. In that case, our interferometer is sensitive to differences in gravitational energies, allowing for the measurement of g with a relative sensitivity of 10^{-5} at 1 s . In this configuration we study the limitations to the sensibility in the measurement and investigate systematic effects related to the trapping and Raman laser beams.

We gratefully acknowledge support by European Commission (iSense project, FET-Open grant number: 250072), Ville de Paris ("Emergence(s)" program) and IFRAF.

References

- [1] P. Wolf *et al.*, Phys. Rev. A **75** 063608 (2007)
- [2] Q. Beaufils *et al.*, Phys. Rev. Lett. **106** 213002 (2011)
- [3] G. Tackmann *et al.*, Phys. Rev. A **84** 063422 (2011)

DESIREE: a unique cryogenic electrostatic storage ring facility for merged ion-beams studies

R. D. Thomas¹, H. T. Schmidt¹, G. Källersjö¹, M. Larsson¹, S. Mannervik¹, P. Reinhed¹, K.-G. Rensfelt¹, S. Rosén¹, H. Zettergren¹, G. Andler¹, H. Danared¹, L. Liljeby¹, M. Björkhage¹, M. Blom¹, L. Brännholm¹, A. Källberg¹, S. Leontein¹, P. Löfgren¹, A. Paál¹, A. Simonsson¹, and H. Cederquist¹

¹*Department of Physics, Stockholm University, SE-106 91 Stockholm, Sweden*

Corresponding Author: rdt@fysik.su.se

I will describe the design of a novel type of storage device currently under construction at Stockholm University, Sweden (detailed here [1], and shown schematically in Fig. 1). This device uses purely electrostatic focussing and deflection elements and allows ion beams of opposite charge to be confined under extreme high vacuum and cryogenic conditions in separate “rings” and then merged over a common straight section. The unique construction of this Double ElectroStatic Ion Ring ExpERiment (DESIREE) apparatus allows for studies of interactions between cations and anions at low and well-defined centre-of-mass energies down to 10 meV.

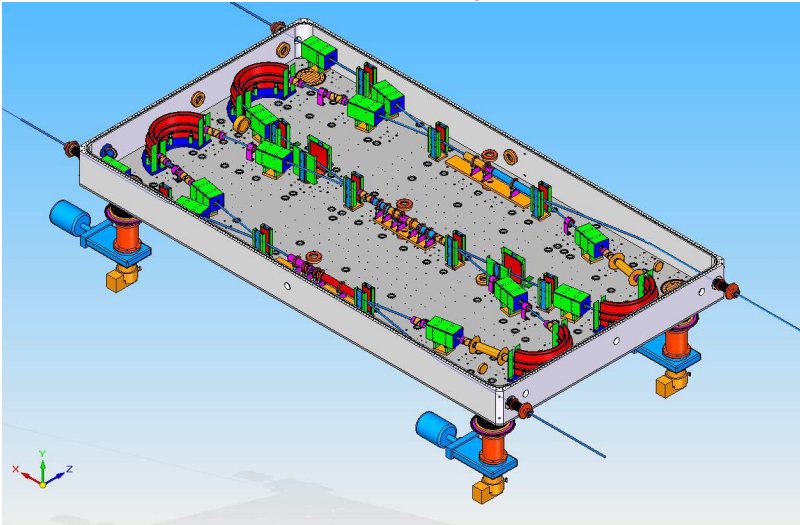


Figure 1: A schematic of DESIREE's heart: the cooled rings and merging region

The technical advantages of using purely electrostatic over magnetic elements are many, but the most relevant are: electrostatic elements are more compact and easier to construct; remanent fields, hysteresis and eddy-currents, highly problematic in magnetic devices, are no longer relevant, and for low energy ion beams (keV vs MeV) electrostatic elements are more efficient to use. I will present the current state of the DESIREE facility, and highlight some of the technical issues that have arisen during its development and construction.

Finally, the advantages of this design are a boon to fundamental experimental studies, not only in atomic and molecular physics but also in the boundaries of these fields with chemistry and biology, and I will discuss several examples of such potential research.

References

- [1] R. D. Thomas *et al.*, Rev. Sci. Instrum. **82**, 065112 (2011)

Drama as part of quantum physics teaching

A.-M. Mårtensson-Pendrill¹

¹*Department of Physics, University of Gothenburg, SE-412 96 Gothenburg, and National Resource Centre for Physics Education, Lund University, SE-221 00 Lund, Sweden*

Corresponding Author: Ann-Marie.Pendrill@fysik.lu.se

Quantum physics teaching can let students encounter physicists as persons. Textbooks and teachers can choose to mention the names of physicists involved and move on to definitions, concepts and equations, followed by wave functions for potential steps and wells of different heights and shapes. Students are expected to learn a set of unfamiliar rules for the mathematical treatment - which has, indeed, been shown to be a powerful tool to describe Nature. The wave-particle duality may be avoided completely or presented as the counter-intuitive rule of "travel as a wave, absorbed / emitted as a particle".

However, when students struggle to make sense of the quantum mysteries told, it may help them to discover that also the iconic physicists in the textbooks struggled with these ideas. A teacher can stop for a while in the strange world of Schrödinger's cat, rather than circumvent the discussions of the implications of quantum physics. Role play can be one way to bring students closer to physicists as persons. Some popular science books can be used as a rough manuscript and students are required to read more about "their" physicist's life and work, as part of the preparation. The "Mad scientist dinner party" in "Uncle Albert and the Quantum Quest" [1] works very well. "Alice in Quantumland" [2] has several chapters suitable for role play, including "The Copenhagen school", which is inhabited by creatures from HC Andersen's fairy tales. In this way, students learn not only about quantum physics, but also of the work of physicists and some aspects of how physics develops, including the use of metaphors.

The physics of the 1900s also involve darker sides, with the Manhattan project and the development of the atomic bomb, where many of the well-known names from the quantum physics textbooks were active. Many archive documents from that time are now easily accessible on the www, including Fermi's description, in his own words, of how he dropped small pieces of paper to estimate the power of the first nuclear explosion at Alamogordo. [3] I have found that a simple role play of the events leading up to and following the Manhattan project gives a chance for students to discuss and reflect on ethical dilemmas and the responsibility of physics and physicist, feeling more comfortable discussing these difficult issues by doing it through the voice of someone else. [4]

References

- [1] R. Stannard, *Uncle Albert and the Quantum Quest* (Faber and Faber, 2005)
- [2] R. Gilmore, *Alice in Quantumland: An Allegory of Quantum Physics* (Copernicus, 1995)
- [3] E. Fermi, *Trinity Test, July 16, 1945, Eyewitness Accounts*
<http://www.dannen.com/decision/fermi.html>
- [4] A.-M. Mårtensson-Pendrill, *The Manhattan Project - a Part of Physics History*, Physics Education **41**, 493-501 (2006)

Contributed Posters



AMO at large facilities

Electron Spin Resonance and Molecular Motion of the $CH_3\dot{C}HCONH_2.HCl$ Radical In Gamma Irradiated L-Alanine Hydrochloride Compound

Ş. Osmanoğlu¹, H. Başkan², K. Sütçü², Y. Dicle², B. Zincircioğlu³, Y.E. Osmanoğlu³,
and N. Ipek⁴

¹*Department of Physics, Faculty of Sciences, Dicle University, Diyarbakır, Turkey*

²*Faculty of Education, Dicle University, Diyarbakır, Turkey*

³*Department of Oncology, Faculty of Medicine, Dicle University, Diyarbakır, Turkey*

⁴*Institute of Science, Dicle University, Diyarbakır, Turkey*

Corresponding Author: yesim-dicle@hotmail.com

The aim of the study was to gain more insight into the mechanism of radical formation in amino acid derivative L-alanine amide hydrochloride (LAAHCl). The identification, orientation, and molecular motion of the free radicals produced by gamma irradiation of the LAAHCl investigated. X-Band Electron Spin Resonance (ESR) spectroscopic measurements at mainly room temperature were performed to obtain ESR spectra from the radicals produced on LAAHCl upon gamma-ray irradiated. The long-lived free radicals observed in LAAHCl compound is the type of $CH_3\dot{C}HCONH_2.HCl$. The α and β proton coupling constants of the radical were studied. Approximate equations are given which relate the observed α and β proton coupling constants and spectroscopic splitting factors of the radical investigated. The obtained results in this work are consistent with the literature data of the alanine radicals.

Key Words: EPR, Free Radical, amino acid derivatives, gamma irradiation.

Influence of Ionizing Radiation Effect on 2-Thiouracil: an EPR Study

Ş. Osmanoğlu¹, H. Başkan², K. Sütçü², Y. Dicle², B. Zincircioğlu³, Y.E. Osmanoğlu³,
and N. Ipek⁴

¹*Department of Physics, Faculty of Sciences, Dicle University, Diyarbakır, Turkey*

²*Faculty of Education, Dicle University, Diyarbakır, Turkey*

³*Department of Oncology, Faculty of Medicine, Dicle University, Diyarbakır, Turkey*

⁴*Institute of Science, Dicle University, Diyarbakır, Turkey*

Corresponding Author: yesim-dicle@hotmail.com

In this study we aimed to carried out the gamma radiation-induced effects on anticancer drug 2-Thiouracil by electron Paramagnetic Resonance Study. The behaviours of free radical signals are investigated at room temperature. For first peak of 2TU corresponding $+1/2 \rightarrow -1/2$ transition was analyzed from the recorded EPR spectra, in terms of line width (H), g factor, peak to peak signal intensity (I) and the distance between first and second peak hyperfine interaction constant (a). Numerical simulation of the evolution of the EPR signal versus dose was performed using exponential function. Estimation of the irradiation dose is possible using exponential function. The stability of free radicals produced upon irradiation was studied over a period of 12 months. These radicals could be detected even after a period of more than 12 months.

Key Words: Epr, Ionizing Radiation, anticancer drug.

Mass and field isotope shift parameters for the $2s - 2p$ resonance doublet of lithium-like ions

J. G. Li¹, C. Nazé¹, M. Godefroid¹, S. Fritzsche², G. Gaigalas³, P. Indelicato⁴, and P. Jönsson⁵

¹*Chimie Quantique et Photophysique, Université Libre de Bruxelles, B-1050 Brussels, Belgium*

²*GSI, Helmholtzzentrum für Schwerionenforschung, D-64291 Darmstadt, Germany and , FIAS Frankfurt Institute for Advanced Studies, D-60438 Frankfurt am Main, Germany*

³*Institute of Theoretical Physics and Astronomy, Vilnius University, LT-01108 Vilnius, Lithuania*

⁴*Laboratoire Kastler Brossel, École Normale Supérieure, CNRS, and Université Pierre et Marie Curie-Paris 6, F-75252 Paris CEDEX 05, France*

⁵*School of Technology, Malmö University, S-20506 Malmö, Sweden*

Corresponding Author: mrgodef@ulb.ac.be

Dielectronic recombination measurements have been proven to be a sensitive tool for deducing changes in the nuclear mean-square charge radii of highly-charged lithium-like neodymium [1]. To make use of this method for other elements and isotopes, mass and field isotope shift calculations are required in order to derive information about the nuclear charge distributions. In this work [2], we estimate and discuss the relativistic mass and field isotope shift factors for the two $2s^2S_{1/2} - 2p^2P_{1/2,3/2}^o$ transitions along the lithium isoelectronic sequence. Using the GRASP2K package [3,4] based on the multi-configuration Dirac-Fock method, the electron correlation and the Breit interaction are taken systematically into account in all the calculations.

Adopting the calculated electronic parameters of isotope shifts, we qualitatively analyze the competition between the mass and field shift contributions for the $2s - 2p$ resonance doublet along the isoelectronic sequence, with the assistance of some empirical relations between Z and the nuclear properties. It is found that the mass shifts and the field shifts possess similar orders of magnitude in the $Z < 40$ range, so that one should consider both of them for a relevant analysis of isotope shifts, especially for extracting the nuclear mean-square charge radii. The field shift contribution grows rapidly towards the high- Z region and becomes quickly dominant.

Quantitative discussions are also made for the $2s^2S_{1/2} - 2p^2P_{1/2,3/2}^o$ line isotope shifts in the case of $^{150,142}\text{Nd}^{57+}$ for which experimental values are available. The present results show that the higher-order nuclear moments often neglected in the calculation of the field shift should be considered for very highly charged ions in order to extract the $\delta\langle r^2 \rangle$ values from experiments. The consistency between GRASP2K and MCDF-gme [5] results will be illustrated.

References

- [1] C. Brandau *et al.*, Phys. Rev. Lett. **100**, 073201 (2008).
- [2] J. G. Li *et al.*, Phys. Rev. A to be submitted.
- [3] P. Jönsson, X. He, C. Froese Fischer, I. P. Grant, Comput. Phys. Comm. **177**, 597 (2007).
- [4] E. Gaidamauskas *et al.*, J. Phys. B: At. Mol. Opt. Phys. **44** 175003 (2011).
- [5] P. Indelicato and J.-P. Desclaux, <http://dirac.spectro.jussieu.fr/mcdf>

Effect of partial coherence of the FEL pulses in two-colour multiple ionization of atoms

A. K. Kazansky¹, N. M. Kabachnik²

¹*Departamento de Física de Materiales, UPV/EHU, E-20018 San Sebastian/Donostia, Spain, Donostia International Physics Center (DIPC), E-20018 San Sebastian/Donostia, Spain, IKERBASQUE, Basque Foundation for Science, E-48011 Bilbao, Spain.*

²*Institute of Nuclear Physics, Moscow State University, Moscow 119991, Russia, European XFEL GmbH, Albert-Einstein-Ring 19, D-22761 Hamburg, Germany.*

Corresponding Author: nkabach@gmail.com

The free-electron laser (FEL) provides extremely bright ultraviolet (XUV) and x-ray radiation by means of self-amplified spontaneous emission (SASE) process. The process of FEL pulse generation has stochastic nature which is reflected in a complicated temporal structure of the pulse. It consists of several or many spikes, each of them is coherent but the phase relation between them is fully statistical [1]. Thus the total pulse has only partial longitudinal (temporal) coherence. The coherence properties of the FEL pulses are characterized by the coherence time which is proportional to the average duration of the spikes. Partial temporal coherence of the FEL pulses can substantially influence the results of investigations of short-pulse interaction with any target. In this report we theoretically study the effect of partial coherence on two-colour (XUV+IR) multiple ionization of atoms. It is well known [2] that when the photoionization of an atom by XUV or x-ray photon occurs in the strong field of an IR optical laser, the photoelectron spectrum contains, beside the usual photoline, some additional lines, the so-called sidebands, with the energy separation between them equal to the IR photon energy. The number and intensity of the sidebands depend on the parameters of the laser field, as well as on the durations of both the XUV and the IR pulses [3]. Our calculations show that partial coherence of the XUV pulses leads to the broadening of the sidebands and of the main photoline. If the coherence time of the FEL pulse is short this broadening can become larger than the energy interval between the sidebands, so that they cannot be resolved even with very good energy resolution of a spectrometer.

References

- [1] G. Geloni *et al.*, *New J. Phys.* **12**, 035021 (2010)
- [2] M. Meyer *et al.*, *J. Phys. B* **43**, 194006 (2010)
- [3] A.K. Kazansky, I.P. Sazhina, and N.M. Kabachnik, *Phys. Rev. A* **82**, 033420 (2010)

Angle-resolved photoelectron spectra from two-color XUV+IR photoionization at FLASH

L. Rading¹, P. Johnsson¹, A. Rouzée², A. Hundertmark², M. J. J. Vrakking², M. Meyer³, P. Radcliffe³, A. K. Kazansky⁴, N. M. Kabachnik^{3,5}, and S. Düsterer⁶

¹Lund University, P.O. Box 118, SE-22100 Lund, Sweden

²Max-Born-Institut, Max-Born Strasse 2A, D-12489 Berlin, Germany

³European XFEL GmbH, Albert-Einstein-Ring 19, D-22761 Hamburg, Germany

⁴Departamento de Física de Materiales, UPV/EHU, E-20018 San Sebastian/Donostia, Spain; IKERBASQUE, Basque Foundation for Science, E-48011 Bilbao, Spain; Donostia International Physics Center (DIPC), E-20018 San Sebastian/Donostia, Spain

⁵Institute of Nuclear Physics, Moscow State University, Moscow 119991, Russia; Donostia International Physics Center (DIPC), E-20018 San Sebastian/Donostia, Spain

⁶HASYLAB at DESY, Notkestrasse 85, D-22603 Hamburg, Germany

Corresponding Author: linnea.rading@fysik.lth.se

With the advent of free-electron lasers (FELs) in the extreme ultraviolet (XUV) and x-ray regions, and of new XUV sources based on high-order harmonic generation (HHG), the experiments with synchronized XUV and infrared (IR) pulses from powerful lasers have received a special attention. Studies of the two-color XUV+IR photoionization can provide fundamental information on the properties of the continuum spectrum of atoms and molecules and on the so-called free-free transitions [1]. In the limiting case when the XUV pulse duration is longer than the period of the IR laser field, specific structures at the wings of a photoline, the so-called sidebands, appear. The sidebands consist of a regular sequence of lines with the interval between lines equal to the laser photon energy.

We will present the results from an experiment performed at FLASH in May 2011, where a velocity map imaging spectrometer (VMIS) was used to measure the full energy and angular distribution of photoelectrons emitted through ionization of rare gases using a two-color XUV+IR field. Sidebands up to high orders (~ 10) were observed (see Fig. 1), and their angular distributions were studied as a function of IR intensity, revealing a strong modulation of the photoelectron yield as a function of angle, as previously predicted theoretically [2] and also observed experimentally for Auger electrons [3].

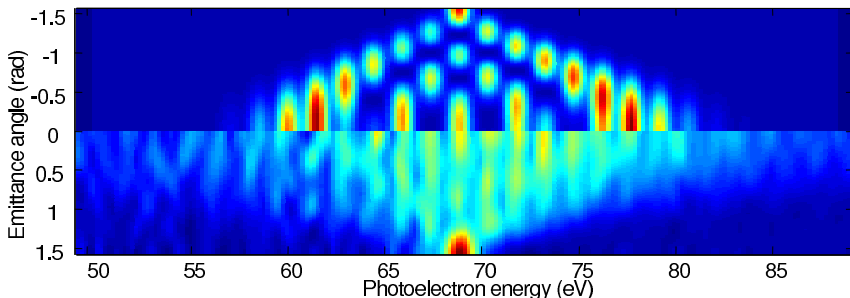


Figure 1: Theoretical (top) and experimental (bottom) angularly-resolved photoelectron spectrum from Neon using a two-color XUV+IR field for an IR intensity of $3 \cdot 10^{12}$ W/cm².

References

- [1] A. Maquet and R. Taïeb, *J. Mod. Opt.* **54**, 1847 (2007)
- [2] A. K. Kazansky, I. P. Sazhina, and N. M. Kabachnik, *Phys. Rev. A* **82**, 033420 (2010)
- [3] M. Meyer, *et al.*, *Phys. Rev. Lett.* **108**, 063007 (2012)

Resonant Inelastic Scattering Spectra of Free Molecules with Vibrational Resolution

J.-E. Rubensson¹, F. Hennies^{1,2}, A. Pietzsch², Y.-P. Sun^{3,4}, B. Kennedy², T. Schmitt⁵, V. N. Strocov⁵, J. Andersson¹, J. Schlappa⁶, A. Föhlisch^{6,7}, and F. Gel'mukhanov³

¹*Department of Physics and Astronomy, Box 516, Uppsala University, SE-751 20 Uppsala, Sweden*

²*MAX-lab, Lund University, Box 118, S-221 00 Lund, Sweden*

³*Department of Theoretical Chemistry and Biology, School of Biotechnology, Royal Institute of Technology, S-106 91 Stockholm, Sweden*

⁴*School of Science, Shandong University of Technology, Zibo, 255049, Shandong, Peoples Republic of China*

⁵*Swiss Light Source, Paul Scherrer Institut, CH-5232 Villigen, Switzerland*

⁶*Institute for Methods and Instrumentation in Synchrotron Radiation Research G-12, Helmholtz-Zentrum Berlin für Materialien und Energie, Albert-Einstein-Str. 15 D-12489 Berlin, Germany*

⁷*Fakultät für Physik und Astronomie, Universität Potsdam, Karl-Liebknecht-Strasse, 24-25 D-14476 Potsdam, Germany*

Corresponding Author: jan-erik.rubensson@fysik.uu.se

Resonant inelastic X-ray scattering (RIXS) reflects fine details in electronic structure and dynamics. The process is site specific on the atomic length scale (sub-nanometer) and time specific on the timescale for nuclear and electronic rearrangements (femto- to attoseconds). Consequently, RIXS spectroscopy has a tremendous potential in atomic and molecular, chemical and condensed matter physics. RIXS techniques have, however, suffered from the lack of adequate radiation sources. In practice this has limited the spectral quality and only a fraction of the inherent advantages have been exploited.

Here RIXS spectra of free molecules (O_2 and CO_2) with an energy resolution ($E/\Delta E \approx 10000$) that allows for separation of individual vibrational excitations [1] are presented. This opens a wealth of new possibilities, provides detailed information about ultrafast dynamics, and facilitates accurate mapping of the final state potential surfaces. We observe spatial quantum beats in the dissociating oxygen molecule [2], establish a new selection rule due to internal spin coupling, and demonstrate hole-electron parity swap during the scattering process [3].

The measurements were made with the SAXES spectrometer [4] at the ADDRESS beamline [5] at the Swiss Light Source of the Paul Scherrer Institut, using a gas/liquid cell with an ultrathin membrane. The data is discussed in terms of ab-initio multimode scattering calculations.

References

- [1] F. Hennies, et al., Phys. Rev. Lett. 104, 193002 (2010).
- [2] A. Pietzsch, et al., Phys. Rev. Lett., 106, 153004 (2011).
- [3] Y.-P. Sun, et al, J. Phys. B 44, 161002 (2011).
- [4] G. Ghiringhelli et al., Rev. Sci. Instrum. 77, 113108 (2006).
- [5] V. N. Strocov et al., J. Synchrotron Radiat. 17, 631 (2010).

Fragmentation of NH_3 investigated using a multi-coincidence ion momentum imaging spectrometer

N. Walsh¹, J. Laksman¹, A. Sankari¹, E. P. Månsson¹, M. Gisselbrecht¹, and S. Ristinmaa Sörensen¹

¹*Department of Synchrotron Radiation Research, Lund University, SE-221 00 Lund, Sweden*
Corresponding Author: noelle.walsh@sljus.lu.se

Resonant core-level excitation allows site-selective (and element-specific) excitation of atoms, molecules and clusters. Investigation of core level excitation processes and characterisation of the electronic structure and nuclear dynamics of core-excited states have been topics of considerable interest during the last two decades and have led to the observation of interesting phenomena such as ultra-fast molecular dissociation [1]. Tunable synchrotron radiation sources have proven invaluable tools in such experiments since they provide radiation of a suitable wavelength to promote the core electron to a higher lying molecular orbital.

In recent years a high resolution multicoincidence momentum imaging ToF mass spectrometer has been developed at Lund University [2] and optimised for use with synchrotron radiation sources. The experimental set-up complete with an 80mm position sensitive detector (Roentdek DLD) provides a kinematically complete description of charged fragments trajectories following a multi-body breakup. The PEPICICO (PhotoElectron-PhotoIon-PhotoIon COincidence) technique employed in the photoexcitation experiments uses the detection of an electron to define the start of a fragmentation process and the time of flight of all ions arriving at the ion detector within a maximum time 'window' are subsequently recorded. With this experimental setup it is therefore not only possible to determine the fragmentation channels in a decay process, but also to investigate the molecular geometry of the core-excited state, as well as to determine the fragment ion linear momenta and the Kinetic Energy Released (KER) in the process.

Here we report PEPICICO results recorded in order to investigate the fragmentation dynamics of gaseous NH_3 molecules following photo-excitation at photon energies ranging from 400eV - 405eV. Resonant core-excitation of NH_3 in this energy region results in electronic transitions from the $\text{N}1s$ to $4a_1$, $2e$, $5a_1$, $6a_1$ and $3e$ molecular states and subsequent de-excitation of these intermediates via Auger decay and dissociation. The experiment was performed at the soft X-ray undulator beamline I 411 at Max-lab, Sweden. The dominant fragment channels observed were H^+/NH_2^+ , H^+/NH^+ and H^+/N^+ . A weak H_2^+/NH^+ channel was also observed following photoexcitation at some photon energies. Assuming that the rotational period of the molecule is longer than the lifetime of the core-excited state, the angular distribution of the ejected fragments allows us to deduce the alignment of the molecule in the intermediate core-excited state (before Auger decay). Furthermore, since the probability of a transition between states depends on the alignment of the molecular symmetry axis relative to the polarisation vector of the radiation, we can also determine if molecular alignment was conserved for each transition. As well as investigating the effect of a particular transition on the geometry of the NH_3 molecule, we also examine the effect of detuning the photon energy to values slightly below or above the resonance energy for a particular transition.

References

- [1] I. Hjelte et al., Chem. Phys. Lett., **334**, 151 (2000)
- [2] J. Laksman, M. Gisselbrecht, E. P. Månsson, D. Céolin and S. L. Sorensen, to be submitted (2012)

Applications of AMO Physics

A generalized relative complexity: application to atomic one-particle densities

P.A. Bouvrie^{1,3}, J.C. Angulo^{1,3}, and J. Antolín^{2,3}

¹*Departamento de Física Atómica, Molecular y Nuclear, Universidad de Granada, 18071-Granada, Spain*

²*Departamento de Física Aplicada, EINA, Universidad de Zaragoza, 50018-Zaragoza, Spain*

³*Instituto Carlos I de Física Teórica y Computacional, Universidad de Granada, 18071-Granada, Spain*

Corresponding Author: angulo@ugr.es

The search of an appropriate measure of relative complexity among density functions is afforded. In doing so, the main properties required for complexity functionals of a given distribution [1], as well as those for discrimination measures among two [2–3] or more [4–5] distributions are considered. A proposal for a generalized relative complexity is provided, enclosing a pioneering definition [6] as a limiting case. A theoretical analysis of the generalized measure for arbitrary distributions is carried out. The applications regard the electron charge densities of neutral atoms, and the results are interpreted on the basis of the main physical properties of the systems considered.

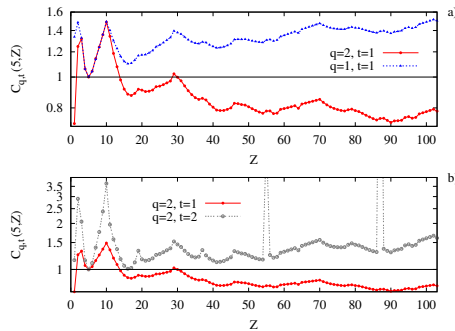


Figure 1: (q,t) -relative complexities among the electron charge density of Boron (nuclear charge $Z' = 5$) and those of all neutral atoms with $Z = 1 - 103$.

References

- [1] R. López-Ruiz, H. L. Mancini, and X. Calbet, *Physics Letters A* **209**, 321–326 (1995)
- [2] R. Carbó-Dorca, J. Arnau, and L. Leyda, *International Journal of Quantum Chemistry* **17**, 1185–1189 (1980)
- [3] A. Nágý, and E. Romera, *International Journal of Quantum Chemistry* **109**, 2490–2494 (2009)
- [4] P. A. Bouvrie, J. Antolín, and J. C. Angulo, *Chemical Physics Letters* **506**, 326–331 (2011)
- [5] J. C. Angulo, J. Antolín, S. López-Rosa, and R. O. Esquivel, *Physica A* **389**, 899–907 (2010)
- [6] A. Borgoo, P. Geerlings, and K. D. Sen, *Physics Letters A* **375**, 3829–3833 (2011)

Primary and secondary kinetic isotope effects on the gas phase reactions $H_2O_2 + X$ ($X=H, Cl$)

H. Bahri¹, Y. Tarchouna¹, S. Marouani¹, H. Koussa¹, and M. Bahri¹

¹Laboratoire de Spectroscopie Atomique Molculaire et Applications, Dpartement de Physique, Facult des Sciences, Universit Tunis-El Manar, le Belvdre 1060 Tunis, Tunisia

Corresponding Author: bahrihajer85@yahoo.com

The kinetic isotope effect (KIE) is the effect of the isotopic substitution on the rate constant of the reaction and it represents a powerful technique for the probing of the reaction mechanisms. In previous works [1, 2, 3] the hydrogen and the OH abstraction paths of the gas phase reaction of the hydrogen peroxide with the H and Cl atoms have been studied. The aim of this work is to study the effect of the primary and secondary isotopic substitutions on the rate constant of the title reactions by studying their effects on the activation energy and on the tunneling contribution. The rate constants were evaluated upon each isotopic substitution over the temperature range from 200 to 2000 K using the ab initio-TST model, by means of the Polyrate 8.0 program. Both H and OH abstraction paths have been considered for the reaction of the hydrogen peroxide with the H atom. However, we limited our study to the H abstraction path for the reaction of the hydrogen peroxide with the Cl atom.

The obtained results show that all the primary H/D substitutions for the different studied reactions produce a normal KIE except that corresponding to the H abstraction path of the $H_2O_2 + D$ reaction for which the KIE seems to be negligible $0.91 \leq KIE \leq 1.01$ (Fig. 1). However, the primary $^{16}O/^{18}O$ and the secondary isotopic substitutions have no effect on the rate constant.

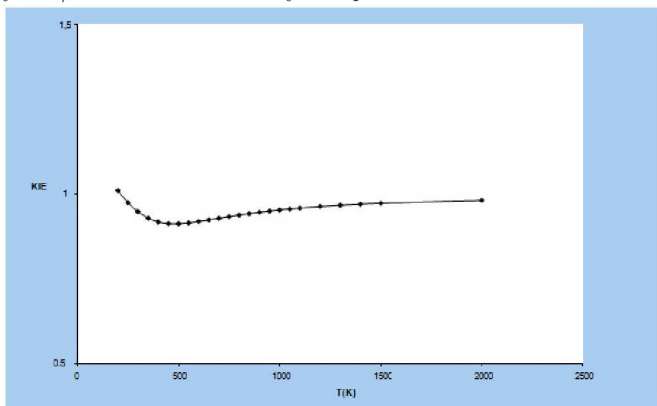


Figure 1: Plot of the TST/ZCT KIE as a function of temperature for the primary substitution corresponding to the H abstraction path of the $H_2O_2 + D$ reaction.

References

- [1] Y. Tarchouna *et al.*, J. Mol. Struct. (THEOCHEM) 758 (2006) 53
- [2] H. Koussa *et al.*, J. Mol. Struct. (THEOCHEM) 770 (2006) 149
- [3] S. Marouani *et al.*, J. Mol. Struct. (THEOCHEM) 905 (2009) 70

Electron-Impact study of AIO using the R-matrix method

M. Bassi¹, S. Kaur², and K.L. Baluja³

¹*Department of Physics, Kalindi College, University of Delhi, Delhi- 110005*

²*Department of Physics, SGTB Khalsa College, University of Delhi, Delhi- 110007*

³*Department of Physics and Astrophysics, University of Delhi, Delhi -110007*

Corresponding Author: drmonikabassi123@yahoo.co.in

A comprehensive study of electron-impact on open shell AIO molecule at low energy (less than 10eV) by using the R-matrix method [1] has been done. In the R-matrix theory the configuration space of the scattering system is divided into an inner and an outer region. Both the regions are treated differently in accordance with the different interactions in each region. In the inner region we use a trial wavefunction where we include all excited states upto 10eV.

The calculation are carried out in two models namely Static Exchange (SE) and many state close coupled (CI) approximation. In the SE calculation no correlation are included except exchange while in the CI calculation polarization and exchange correlation are added due to inclusion of excited states. In the CI calculation we include all single and double excitations. Elastic (integrated and differential), momentum-transfer, excitation and ionization cross sections are calculated. The target states are represented by including correlations via a configuration interaction (CI) technique.

Resonance analysis is carried out to assign the resonance parameters and the parentage by feeding the eigenphase sums to the Breit Wigner profile. The basis set used is 6311G* to represent the atomic orbitals by GTO basis set. The continuum electron is also represented by GTO's and are place at the center of mass of the molecule. We include partial wave upto g wave beyond which Born closure method is employed to obtain cross section.

References

[1] P. G. Burke and K. A. Berrington, *Atomic and Molecular Processes: an R-matrix Approach* (Bristol: Institute of Physics Publishing, UK 1993)

Electron excitation of the $1s2sns(nd)$ LiI^{**} states

H. Bohachov¹, R. Tymchyk¹

¹*Institute of Electron Physics, NAS of Ukraine, 88017 Uzhgorod, Ukraine*

Corresponding Author: bogach_gen@inbox.ru

According to review [1] there are large information about autoionizing states (AIS) of lithium atom, both doublet and quartet. These AIS results from two-electron excitations – one $1s^2$ -core electron and valent electron. Transitions between AIS within quartet and doublet systems separately are known to give many weak spectral lines, mainly founded from beam-foil studies [1]. Three of them (at 371.4, 293.4, and 233.7 nm) were observed when studying Li^+ spectrum, but they were not assigned [2]. Early in [3] using crossed electron and atomic beam techniques the excitation function (EF) of the 293.4 nm line (the $1s2s2p\ ^4P^o - 1s2s3s\ ^4S$ transition) was measured for the first time. Here we present the EF remeasured for this line and describe the results of our attempt to study the EFs for other quartet lines at electron-atom collision.

The experimental setup was in general the same as that used in [3]. In contrast to [3] its data acquisition system was automated using a computer. Due to this we could study a very weak quartet LiI^{**} lines.

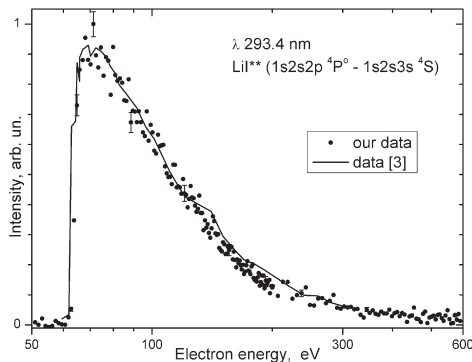


Figure 1: Excitation functions for LiI^{**} quartet line at 293.4 nm.

Fig. 1 shows the EF for strongest quartet line at 293.4 nm obtained. Its comparison with earlier data [3] (see in Fig. 1) demonstrates their clear similarity.

The excitation thresholds of LiI^{**} quartet lines exceed 60 eV [1]. It makes easy to recognize them in spectrum. In the spectra obtained at electron energies of 70-100 eV three lines relating to LiI^{**} quartet system were noticeable. These were the lines at 217.3, 204.0, and 233.7 nm. The first is second member of the $1s2s2p - 1s2sns$ series (with $n=4$), whereas the line at 293.4 nm is its first member. The rest both belong to the $1s2s2p - 1s2snd$ series ($n=4,3$).

These lines were of little intensity comparatively with the line at 293.4 nm and it made difficulties for measuring their EF. In addition the 233.7 nm line lies near to the 233.3 and 234.0 nm lines that belong to principal series LiI . We carried out rough evaluative EF measurements for abovementioned lines. As a whole the EFs obtained were found similar to the EF for the 293.4 nm line despite the fact that initial levels of the lines differ in orbital moment values.

References

- [1] S. Mannervik, *Physica Scripta* **40**, 28–52 (1989)
- [2] G. Herzberg and H. R. Moore, *Can. J. Phys.* **37**, 1293–1313 (1959)
- [3] I. S. Aleksakhin *et al.*, *JETP Lett.* **40**, 1287–1289 (1984)

Excitation cross sections in the collision of protons with He atoms at intermediate and high energies under a three body formalism

R. Fathi¹, F. Shojaei-Akbarabad¹, M. Sadeghi², and M. A. Bolorizadeh^{3,4}

¹*Phys. Dept., Shahid Bahonar University, Kerman, Iran.*

²*Phys. Dept. University of Hormozgan, Bandar Abbas, Iran.*

³*Phys. and Photoincs Dept., Kerman Graduate University of Technology, Kerman, Mahan, Iran.*

⁴*Institute of Photonics, Int. Center for Science, High Technology & the Environmental Sciences, Kerman, Iran.*

Corresponding Author: mabolori@uk.ac.ir

In this work, we have devised a three-body model to calculate the cross sections for the excitation of helium atom by energetic protons. This four-body problem is simplified into a three-body one to implement the Faddeev type formalism, where an electron of helium atom is assumed to be inactive [1]. The ground state, 1^1S , or the excited states, 2^1S and 2^1P , wave function of the active electron is deduced from similar hydrogenic wave functions. In this three-body model, the Faddeev-Watson-Lovelace formalism for excitation channel is used to calculate the transition amplitude [2]. The first order electronic and nuclear interaction is assumed in the collision and the differential cross sections are calculated for 50 KeV up to 1 MeV interaction energies. The results are compared with that of the theoretical and experimental works in the literature [3]. This formalism is advantageous as different terms of the reaction amplitude correspond to the details of the reaction.

References

[1] S. Alston, Phys. Rev. A, **52** 3860-3867 (1995)

[2] R. Fathi, et al, J. Phys. B **42**, 125203-16 (2009)

[3] T. J. Kval, et al, Phys. Rev. A, **32**, 1369-1378 (1985) and F. Martin and A. Salin, J. Phys. B, **28**, 1985-1994 (1995)

Potential scattering devised to calculate the capture cross sections for the collision of proton with methane

F. Shojaei-Akbarabad¹, R. Fathi¹, M. Sadeghi², and M. A. Bolorizadeh^{3,4}

¹*Phys. Dept., Shahid Bahonar University, Kerman, Iran.*

²*Phys. Dept. University of Hormozgan, Bandar Abbas, Iran.*

³*Phys. and Photonics Dept., Kerman Graduate University of Technology, Kerman, Mahan, Iran.*

⁴*Institute of Photonics, Int. Center for Science, High Technology & the Environmental Sciences, Kerman, Iran.*

Corresponding Author: mabolori@uk.ac.ir

In this work, the FWL formalism is extended to the collision of singly charged ion with molecules (methane) [1]. The scattering amplitude and the cross sections are determined by the asymptotic behavior of the stationary scattering wave function [2]. This formalism is advantageous as different terms of the reaction amplitude correspond to the details of the reaction. The calculated capture differential cross sections are compared with the available data in the literature [3] and shown in figure (1).

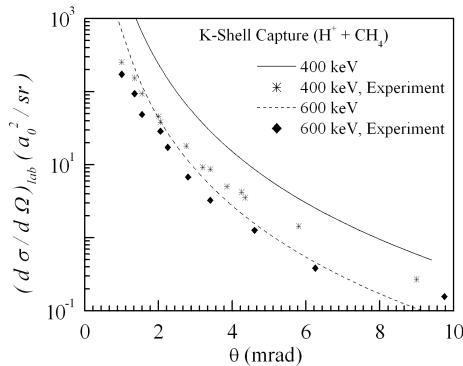


Figure 1

References

- [1] E. Ghanbari Adivi and M.A. Bolorizadeh, J. Phys. B: At. Mol. Opt. Phys. **37** 3321-3338 (2004)
- [2] S. Alston, Phys. Rev. **54**, 2011-2021 (1996)
- [3] B. G. Lindsay, et al, J. Phys. B: At. Mol. Opt. Phys. **38**, 1977-1986 (2005)

Daubechies-3 wavelet basis applied to study the three body proton hydrogen scattering under a Faddeev formalism

M. Sadeghi¹, F. Shojaei-Akbarabad², R. Fathi², and M. A. Bolorizadeh^{3,4}

¹*Phys. Dept. University of Hormozgan, Bandar Abbas, Iran.*

²*Phys. Dept., Shahid Bahonar University, Kerman, Iran.*

³*Phys. and Photoincs Dept., Kerman Graduate University of Technology, Kerman, Mahan, Iran.*

⁴*Institute of Photonics, Int. Center for Science, High Technology & the Environmental Sciences, Kerman, Iran.*

Corresponding Author: mabolori@uk.ac.ir

The Faddeev-Watson-Lovelace formalism is a fully quantum mechanical three-body method to study the charge transfer channel in proton-hydrogen scattering [1]. This formalism is advantageous as different terms of the reaction amplitude correspond to the details of the reaction. The scattering amplitude for the capture channel in the proton-hydrogen collision at high impact energies are written as [2]:

$$A_{FWL} = A_e + A_n \quad (1)$$

where A_e and A_n stands for electron and nucleus interaction amplitudes, respectively. We have developed a mathematical tool to calculate the corresponding integrals employing the Daubechies scalet basis [3]. The results for the cross sections as calculated by:

$$\left(\frac{d\sigma}{d\Omega}\right)_{lab} = (2\pi)^4 M_T^2 \frac{k_f}{k_i} |A_{FWL}|^2 \quad (2)$$

is shown in figure (1), where the results are compared with the exact approximated solutions.

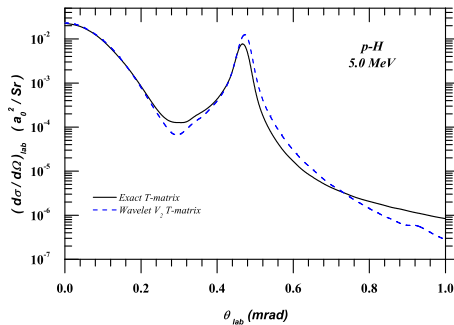


Figure 1

References

- [1] E. Ghanbari Adivi and M.A. Bolorizadeh J. Phys. B: At. Mol. Opt. Phys. **37** 3321-3338 (2004)
- [2] S. Alston, Phys. Rev. **54**, 2011-21 (1996)
- [3] M. Sadeghi, et al, J. Phys. B: At. Mol. Opt. Phys. **43**, 035203 (2010)

Hyperfine structure of laser-dressed atomic states

A. Cininsh¹, V. Kashcheyevs²

¹*Laser Centre, University of Latvia, LV-1002 Riga, Latvia*

²*Faculty of Physics and Math, University of Latvia, LV-1002 Riga, Latvia*

Corresponding Author: arturs.cininsh@lu.lv

Applying a narrow linewidth coherent laser field close to a resonance of a transition in an atomic system results in effect similar to the DC Stark effect. Splitting of initially degenerate levels caused by high frequency fields is called Autler-Townes effect. It has a potential as a tool for achieving quantum state control by using the nonresonant dynamic Stark effect [1] and the selective population of dressed states [2].

Autler-Townes effect is usually described in the dressed state picture, where external field induces mixing between two initially degenerate quantum states. Various types of interactions may complicate the simple two-state picture of the Autler-Townes effect. One of them is interaction between the electronic cloud and the nucleus, which leads to occurrence of hyperfine structure. Due to complexity of mathematical description of such systems effects of hyperfine interactions in Autler-Townes spectra have been studied in particular atomic systems only [3]. The usual approach to address this complexity is numerical simulation of a particular atomic or molecular system. Previous numerical simulations [4] have shown lifting of degeneracies over projections of the total atomic angular momentum F , therefore suggesting novel methods to selectively address hyperfine components of excited atomic and molecular states.

The aim of our work is to develop a general analytical model for the energy spectra of hyperfine splittings of Autler-Townes multiplet components in the limit when the electric dipole coupling with the laser field is much stronger than hyperfine interactions in the system. We consider cases of either linear or circular polarization of the stationary monochromatic laser field. Influence of the hyperfine interactions is evaluated by the means of first order perturbation theory.

The energy shifts of the dressed states caused by the hyperfine interaction depend on the hyperfine structure constants of both ground and excited atomic states. Mixing between dressed states corresponding to different orientations of nuclear spin depends on polarization of the laser field and quantum numbers of the atomic system. There is no mixing between the states if an electronic transition involving change of total electronic angular momentum $\Delta J = \pm 1$ is induced by circularly polarized laser field. Mixing between certain states appears if either a transition involving no change in total electronic angular momentum ($\Delta J = 0$) or linearly polarized laser field is used.

Acknowledgments: This study was supported by grant no. 09.1567 of the Latvian Council of Science and by European Social Fund project no. 2009/0223/1DP/1.1.1.2.0/09/APIA/VIAA/008.

References

- [1] B. J. Sussman *et al.*, PRA 71, 051401 (2005)
- [2] M. Wollenhaupt *et al.*, PRA 81, 053422 (2010)
- [3] O. Mishina *et al.*, Optics and Spectroscopy, Vol 108, Issue 2 (2010), pp.313-318
- [4] T. Kirova *et al.*, http://home.lu.lv/~mauzins/Papers/Kirova_09.pdf

A UV frequency-quadrupled diode laser system for the mercury co-magnetometer in the nEDM experiment

M. Fertl¹, the nEDM collaboration¹

¹Paul Scherrer Institute, Laboratory for Particle Physics, WMSA/B12, 5232 Villigen, Switzerland

Corresponding Author: martin.fertl@psi.ch, nedm.web.psi.ch

In this contribution the implementation of a ‘no light-shift’ lock for a UV frequency-quadrupled diode laser system based on the sub-Doppler DAVLL (dichroic atomic vapor laser lock) technique will be presented. The laser system is part of a free induction decay magnetometer based on a spin polarized ensemble of ¹⁹⁹Hg atoms. The magnetometer is employed to extract and survey the time stability ($\approx 10^{-8}$ over 100 s) of the magnetic field ($\approx 1\mu\text{T}$) in the neutron electric dipole moment (nEDM) experiment at the Paul Scherrer Institute, Switzerland (PSI). The nEDM experiment employs Ramsey’s method of separated oscillatory fields to detect a shift of the Larmor frequency of stored ultra-cold neutrons (UCN) in a parallel and an anti-parallel configuration of magnetic and electric fields. The spin polarized ensemble of ¹⁹⁹Hg atoms is added to the UCN storage chamber and acts as a co-magnetometer. The free spin precession of the ¹⁹⁹Hg atoms after a $\pi/2$ flip is detected as amplitude modulation of a circularly polarized UV light beam traversing the UCN/Hg storage volume in the spin precession plane. Off-resonant light (as currently used from a ²⁰⁴Hg discharge lamp) can induce vector light shifts and induce systematic frequency shifts correlated to necessary polarity reversals of the magnetic field. The Standard Model (SM) of Particle Physics predicts a nEDM, breaking time reversal and parity symmetry, several orders of magnitude below the current best experimental limit $d_n < 2.9 \times 10^{-26}$ ecm (90 % CL, [1]). However many extensions of the SM predict values for a nEDM on the level of the current experimental sensitivities. Thus the search for a nEDM probes the parameter space of the SM extensions. The experiment at the new UCN source at PSI aims at a factor five improved sensitivity and will place a limit of $d_n < 5 \times 10^{-27}$ ecm at 95 % CL in case no nEDM is found. In the next step the sensitivity will be improved by another order of magnitude, $d_n < 5 \times 10^{-28}$ ecm at 95 % CL in case no nEDM is found. This project is supported by the Swiss National Science Foundation under contract number 200021_126562.

References

[1] C. A. Baker *et al.*, PRL **97**, 131801 (2006)

Dark resonances for systems with large J studied in potassium diatomic molecules

M. Auzinsh¹, R. Ferber¹, I. Fescenko¹, L. Kalvans¹, and M. Tamanis¹

¹Laser Centre, The University of Latvia, 19 Rainis Boulevard, LV-1586 Riga, Latvia

Corresponding Author: iliafes@gmail.com

We have studied experimentally as well as theoretically nonlinear magneto-optical resonances in K_2 molecules in the electronic ground state with large values of the angular momentum quantum number $J \sim 100$. At zero magnetic field, the absorption transitions are suppressed because of population trapping in the ground state due to Zeeman coherences between magnetic sublevels of this state along with depopulation pumping [1]. The destruction of such coherences in an external magnetic field was used to study the resonances in this work. Well pronounced dark resonances were observed (see, for example, Fig. 1) in the intensities of the linearly polarized components of the laser-induced fluorescence (LIF) detected in the Hanle configuration. The intensities of

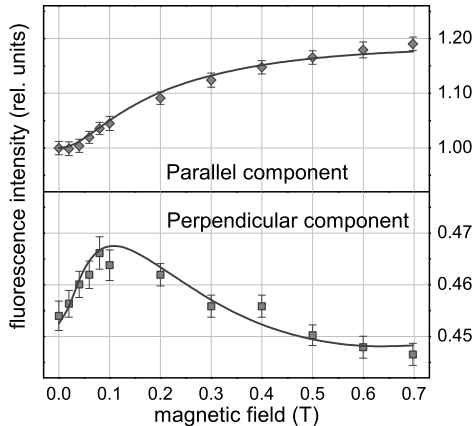


Figure 1: Experimental (scattered dots) LIF intensities and versus magnetic field observed in K_2 dilute vapour for Q -type excitation. The solid lines are the result of simulations.

the LIF components were detected for different experimental parameters, such as laser power density and vapor temperature, in order to compare them with numerical simulations that were based on the optical Bloch equations for the density matrix[2]. We report good agreement of our measurements with numerical simulations. Narrow dark resonances in perpendicular component of the LIF intensity were detected and explained [3].

This work has been supported by the European Social Fund within the project Support for Doctoral Studies at University of Latvia. Support from ERAF Grant No. 2010/0242/2DP /2.1.1.1.0/10/ APIA/VIAA/036 is gratefully acknowledged.

References

- [1] M. Auzinsh and R. Ferber, *Optical Polarization of Molecules* (Cambridge University Press, Cambridge, UK, 1995)
- [2] M. Auzinsh, D. Budker, and S. M. Rochester, *Optically Polarized Atoms: Understanding Light-Atom Interactions* (Oxford University Press, Oxford, New York, 2010)
- [3] M. Auzinsh *et al.*, Phys. Rev. A **85**, 013421 (2012)

Statistical multimode resonant annihilation of positrons in molecules

A. C. L. Jones¹, J. R. Danielson¹, M. R. Natisin¹, C. M. Surko¹, and G. F. Gribakin²

¹Physics Department, University of California, San Diego, La Jolla California 92093, USA

²School of Mathematics and Physics, Queen's University, Belfast BT7 1NN, UK

Corresponding Author: g.gribakin@qub.ac.uk

It is well established now that large positron annihilation rates in polyatomic molecules result from positron capture in vibrational Feshbach resonances [1]. The energies of the resonances ε_ν are related to the vibrational excitation energies ω_ν and positron-molecule binding energy ε_b via $\varepsilon_\nu = \omega_\nu - \varepsilon_b$. For most molecules the resonances observed in the normalised annihilation rate Z_{eff} correspond to individual vibrational modes, which allows measurements of ε_b .

In this work we examine positron annihilation on molecules such as CBr_4 , in which the positron binding energy is greater than all the vibrational fundamentals. In spite of the absence of mode-based resonances, we observe strongly enhanced Z_{eff} due to direct positron capture into a dense quasicontinuous spectrum of multimode vibrational excitations, see Fig. 1 (left). The corresponding annihilation rate is compared with the predictions of the *statistical multimode resonant annihilation* (SMRA) model [2] for positron energy ε (in atomic units),

$$Z_{\text{eff}}^{\text{(stat)}}(\varepsilon) = \pi F \sqrt{\frac{\varepsilon_b}{\varepsilon}} \frac{\rho(\varepsilon + E_v + \varepsilon_b)}{N(\varepsilon + E_v)}, \quad (1)$$

where $F \approx 0.66$, E_v is the thermal energy of the target molecule, $\rho(\varepsilon + \varepsilon_b + E_v)$ is the energy density of multimode vibrational states, and $N(E) = \int_0^E \rho(E') dE'$ is the total number of open inelastic escape channels. To achieve agreement with experiment the SMRA contribution needs to be scaled down by an empirical factor η (possibly, to account for incomplete vibrational mixing). For CHBr_3 the SMRA contribution provides a background on which individual resonances of the C-H bonds can be seen (Fig. 1 left). Turning to larger molecules, hexane (C_6H_{14}) and decane ($\text{C}_{10}\text{H}_{22}$), we observe that the SMRA appears to be of *ubiquitous* nature (Fig. 1 right, $\eta = 0.25$), underpinning the contribution of resonances at all positron energies [3].

The research at UCSD is supported by the U.S. NSF, Grant No. PHY 10-68023.

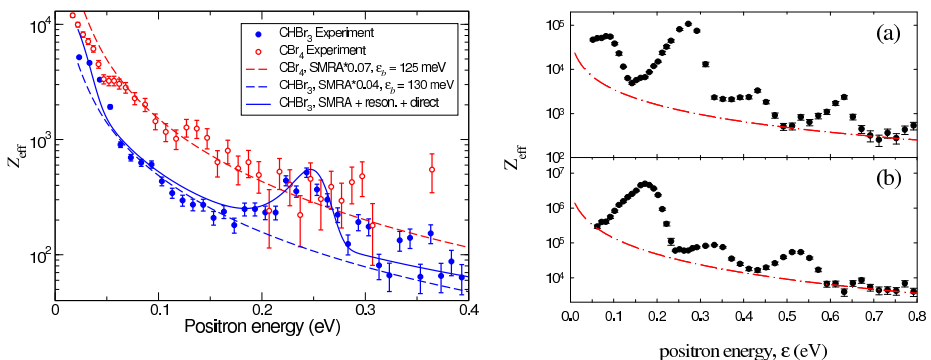


Figure 1: Left: measured Z_{eff} for CBr_4 and CHBr_3 and theoretical fits of the data.

Right: measured Z_{eff} (●) for hexane (a) and decane (a) and SMRA predictions.

References

- [1] G. F. Gribakin, J. A. Young, and C. M. Surko, Rev. Mod. Phys. **82**, 2557 (2010)
- [2] G. F. Gribakin and C. M. R. Lee, Eur. Phys. J. D **51**, 51 (2008)
- [3] A. C. L. Jones, J. R. Danielson, M. R. Natisin, C. M. Surko, and G. F. Gribakin, Phys. Rev. Lett. **108**, 093201 (2012)

Modeling of coherent atomic excitation including energy distribution within laser profile

U. Kalinsh¹, L. Kalvans¹

¹*Laser Centre, University of Latvia, Riga, Latvia*

Corresponding Author: uldis.kalinsh@gmail.com

The traditional approach for modeling of coherent atomic excitation is to use averaged laser power in numerical calculations of laser induced fluorescence. At laser power below saturation this model gives results which are in good agreement with experimental data, but, for laser power that exceeds saturation, the traditional model begins to deviate from experimental data. This can be explained with the “wings” of energy distribution within laser profile where laser power is below saturation and continues to increase fluorescence after the average laser power has reached saturation. Possible solutions to the problem are either introducing effective Rabi frequency[1] or adding energy distribution within laser profile to the theoretical model.

In this study we expand the theoretical model based on Optical Bloch equations[2] to incorporate realistic (Gaussian) energy distribution within laser profile. To do this, we divide the laser profile in multiple sectors, calculate the individual fluorescence intensities for each sector and then calculate the average intensity over all sectors. Results obtained with this model are then compared to results of the model with averaged laser power.

References

- [1]M. Auzinsh *et al.*, Phys. Rev. A 85, 013421 (2012)
- [2]K. Blushs & M. Auzinsh, Phys. Rev. A 69, 063806 (2004)

Optical cesium magnetometers for high precision magnetic field measurements

H.-C. Koch^{1,2}, Z. D. Grujić¹, M. Kasprzak¹, P. Knowles¹, A. Kraft², W. Heil², and A. Weis¹

¹Department of Physics, University of Fribourg, CH-1700 Fribourg, Switzerland

²Department of Physics, University Mainz, Staudingerweg 7, 55124 Mainz, Germany

Corresponding Author: hans-christian.koch@unifr.ch

The search for a nonzero neutron electric dipole moment (nEDM) is one of the very important high precision experiments in low energy particle physics. Such an experiment using the vacuum Ramsey method on stored ultracold neutrons has been constructed at the SUNS neutron source at the Paul Scherrer Institut (PSI) in Villigen, Switzerland, and in mid-2012 it will start taking data. To achieve its design sensitivity to nEDM's of order 10^{-28} e · cm, the experiment requires very precise control of a $1 \mu\text{T}$ magnetic field and its spatial and temporal gradients at levels equal or better than $100 \text{ fT}/\sqrt{\text{Hz}}$ in a volume of approximately 25 liters. For this purpose an array of a state-of-the-art vacuum-compatible optically-pumped double-resonance Cs magnetometers have been developed at Fribourg University and installed in the experiment at PSI. In a continuing research effort, we are investigating performance improvements for the existing magnetometers and developing new methods for precision magnetic field measurements.

A combination of the double-resonance (i.e., rf driven) Cs sensors with the free induction decay magnetometry of polarized ^3He nuclei is intended. Polarized ^3He gas will be introduced into dedicated large-volume glass cells surrounding the neutron precession chamber. The free induction decay (FID) of the ^3He nuclei is recorded by measuring the oscillation and decay of the weak ^3He -generated magnetic field using an array of Cs sensors. First measurements under realistic conditions have been made, using an array of Cs magnetometers to both directly measure the field and its gradients and to detect the ^3He FID. This contribution outlines the Cs magnetometry system and its operation in the current nEDM experiment at PSI, and gives an overview of the results of the latest ^3He -Cs magnetometry studies.

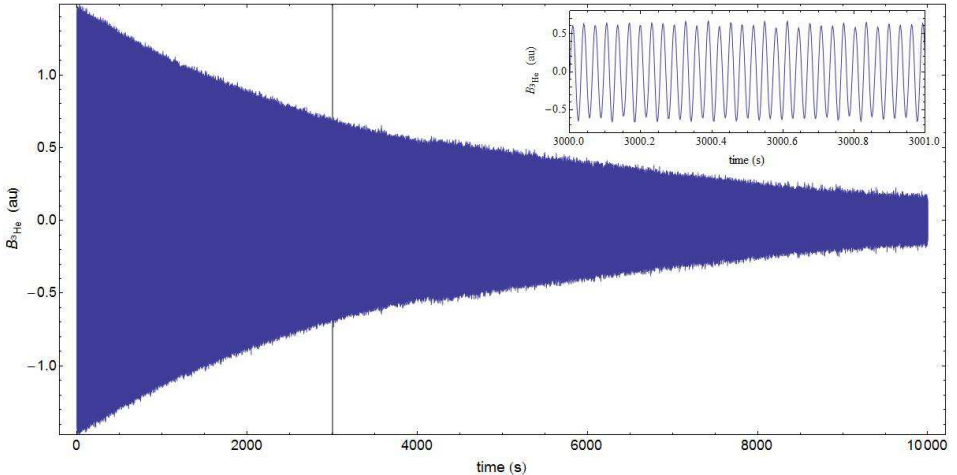


Figure 1: Free induction decay of ^3He field measured by Cs sensor. Inset: blown-up view of FID in region of 3000 to 3001 s.

Coherent and non-coherent magneto-optical effects in the $5P_{3/2}$ state of atomic Rubidium

M. Auzinsh¹, A. Berzins¹, R. Ferber¹, F. Gahbauer¹, L. Kalvans¹, and A. Mozers¹

¹*Laser Centre, University of Latvia, Rainis blvd. 19, Riga, Latvia, LV-1586*

Corresponding Author: linards.kalvans@lu.lv

The resonant magneto-optical properties of atoms have been studied extensively since the historical paper by Wilhelm Hanle [1], for whom a whole class of coherent effects in atoms has been named. A magneto-optical resonance that can be observed in the (resonant) laser induced fluorescence as a function of an external magnetic field is a manifestation of the Hanle effect [2]. It is common to distinguish between the ground and excited state Hanle effects. The width of the ground state Hanle resonance is several orders of magnitude less than that of the excited state Hanle resonance, which corresponds to lower rates of relaxation in the ground state. Therefore, the ground state resonances have been studied more extensively. Nevertheless, there are effects in the excited state that reveal intriguing properties of the atomic systems. For example, the recently reported sign change of the magneto-optical resonance with the increase of excitation power density at Rb D_2 excitation is caused by redistribution among the orthogonal components of the fluorescent light [3]. At larger magnetic field values crossings of the magnetic sublevel's energies within the hyperfine structure of the excited state may occur raising the non-zero field magneto-optical resonances [4].

Here we report an extensive experimental and theoretical study of the broad structure that accompanies the narrow ground-state resonance (Fig. 1) when Rubidium atoms are excited at the D_2 line in the presence of an external magnetic field. A theoretical model that is based on the optical Bloch equations and includes both mixing of the atomic hyperfine states in the magnetic field and averaging over the Doppler profile is employed to reveal details about how the broad structure is formed. Three causes for this structure can be identified: the influence of different atomic velocity groups, the shift in transition frequencies caused by the magnetic field, and the change in transition probabilities caused by the magnetic field.

This study is supported by ERAF project No. 2010/0242/2DP/2.1.1.1.0/10/APIA/VIAA/036.

References

- [1] W. Hanle, *Zeitschrift für Physik A* **30**, 93–105 (1924)
- [2] D. Budker *et al.*, *Reviews of Modern Physics* **74**, 1153–1201 (2002)
- [3] M. Auzinsh *et al.*, *Physical Review A* **84**, 033418 (2012)
- [4] Alnis *et al.*, *Journal of Physics B*, **36**, 1161–1173 (2003)

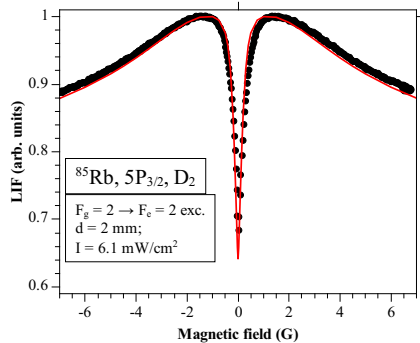


Figure 1: Intensity of laser induced fluorescence versus magnetic field showing both a narrow and a broad structure.

Radiative parameters for lowly charged tungsten ions of interest in fusion plasma research

P. Quinet^{1,2}, E. Biémont^{1,2}, P. Palmeri¹, and S. Enzonga Yoca³

¹*Astrophysique et Spectroscopie, Université de Mons - UMONS, B-7000 Mons, Belgium*

²*IPNAS, Université de Liège, B-4000 Liège, Belgium*

³*Département de Physique, Faculté des Sciences, Université Marien Ngouabi, BP 69
Brazzaville, Congo*

Corresponding Author: Pascal.Quinet@umons.ac.be

Radiative decay rates have been obtained for allowed (E1) and forbidden (M1, E2) transitions in Lu-like (W IV), Yb-like (W V) and Tm-like (W VI) tungsten. Our calculations, motivated by strong interest for low-density plasmas and fusion research, illustrate in a convincing way the importance of core-valence correlation effects which substantially increase the lifetimes and, accordingly, decrease the transition probabilities of these heavy ions. Due to the lack of experimental data, the reliability of the theoretical A -values can only be tested by comparison of numerical results obtained with independent methods such as the relativistic Hartree-Fock (HFR) approach [1] including core-polarization corrections (HFR+CPOL) [2], multiconfiguration Dirac-Fock (MCDF) method [3,4] and the Flexible Atomic Code (FAC) [5] well suited for investigating the atomic structure of heavy ions.

From detailed comparisons between these different approaches, the accuracy of the computed transition probabilities and oscillator strengths has been estimated. It has been shown that some line strengths are particularly sensitive to level mixings which are expected to be better estimated when using semi-empirical methods. The new set of radiative data reported in this work for allowed and forbidden lines in W IV, W V and W VI should be useful for plasma diagnostics in future fusion reactors where tungsten will be used as plasma facing material.

References

- [1] R. D. Cowan, *The Theory of Atomic Structure and Spectra* (University of California Press, Berkeley, 1981)
- [2] P. Quinet *et al.*, Mon. Not. R. Astr. Soc. **307**, 934 (1999)
- [3] I. P. Grant *et al.*, Comput. Phys. Commun. **21**, 207 (1980)
- [4] B. J. McKenzie, I. P. Grant, and P. H. Norrington, Comput. Phys. Commun. **21**, 233 (1980)
- [5] M. F. Gu, Astrophys. J. **582**, 1241 (2003)

Sensitivity optimization of an optically pumped magnetometer with miniaturized Cs cell at earth's magnetic field strength

T. Scholtes¹, R. IJsselsteijn¹, S. Woetzel¹, V. Schultze¹, and H.-G. Meyer¹

¹*Institute of Photonic Technology, Albert-Einstein-Strasse 9, D-07745 Jena, Germany*

Corresponding Author: theo.scholtes@ipht-jena.de

The application of optically pumped magnetometers for geomagnetic measurements calls for optimized sensor operation in the range of the earth's magnetic field strength. To this end we investigate the performance of a 2x2 array of miniaturized Cs vapour cells ($V = 50\text{mm}^3$) sharing a central Cs metal reservoir. The array is incorporated into a thick ($d = 4\text{mm}$) Si wafer and additionally filled with a sufficient amount of nitrogen buffer gas [1]. The temperature of the whole cell array is set conveniently by off-resonant heating laser radiation, fiber-coupled directly on the Si wafer's side walls.

Optimization of the shot-noise limited sensitivity by the variation of the magnetometer's operational parameters (like pump laser power and frequency, rf-field strength and cell temperature) is carried out at $B_0 = 50\mu\text{T}$. A light-narrowed (LN) mode [2] using detuned and very intense pumping light is compared to the common M_x mode not only in terms of sensitivity (i.e. magnetic resonance width and strength), but also with respect to challenges like the Zeeman light shift and the magnetic field orientational dependence of the signal. Consequences for future unshielded operation are discussed and possible sensor concepts are presented.

References

- [1] S. Woetzel *et al.*, Rev. Sci. Instrum. **82**, 033111 (2011)
- [2] T. Scholtes *et al.*, Phys. Rev. A **84**, 043416 (2011)

Atomic magnetometer pumped with intensity-modulated light

V. Schultze¹, R. IJsselsteijn¹, T. Scholtes¹, S. Woetzel¹, and H.-G. Meyer¹

¹*Institute of Photonic Technology, Albert-Einstein-Strasse 9, D-07745 Jena, Germany*

Corresponding Author: volkmar.schultze@ipht-jena.de

We present an all-optical chip-scale atomic magnetometer. It uses pump-light intensity modulation (IM) like the original Bell-Bloom (BB) magnetometer [1], combining pumping, phase synchronization of the spins, and measurement in one laser beam. In contrast to the BB setup, where only the secular change of the transmission was evaluated, we detect the resulting modulation of the transmitted light-signal phase-sensitive. Various pump-light modulation patterns were tested, revealing rectangular modulation with 100% modulation depth and 50% duty cycle as the best choice for high magnetic field resolution. Figure 1 shows the resulting signals.

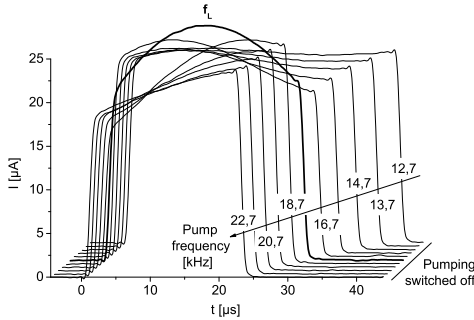


Figure 1: Dependence of the photocurrent I behind the cesium vapor cell on the modulation frequency. The signal at the Larmor frequency $f_L = 17.7\text{kHz}$ clearly stands out.

In array setups, one single laser source can be used for multiple channels. As an example, we show the noise-reduction by the subtraction of the signal of a reference magnetometer cell from the measurement channel. In this way, the shot-noise limit of the magnetic field resolution ($220 \frac{\text{fT}}{\sqrt{\text{Hz}}}$ in our 50 mm^3 cesium cells) is approached for measurements even in the micro-tesla field range. In the IM configuration, various errors which may occur in the common M_x method (phase errors due to misalignment between pump-light and B_1 -field direction, crosstalk between various channels in magnetometer arrays) are excluded *per se*.

References

- [1] W. E. Bell and A. L. Bloom, Phys. Rev. Lett. **6**, 280–281 (1961)

NICE-OHMS – A Spectroscopic Technique for Detection of Molecular Species Down to the 10^{-12} cm^{-1} Range

I. Silander¹, P. Ehlers¹, J. Wang¹, and O. Axner¹

¹*Department of Physics, Umeå University, SE-901 87 Umeå, Sweden*

Corresponding Author: isak.silander@physics.umu.se

Noise-Immune Cavity-Enhanced Optical Heterodyne Molecular Spectrometry (NICE-OHMS) is a technique for ultra-sensitive detection of molecules in gas phase that is based upon a combination of Frequency Modulated Spectroscopy (FMS), for reduction of noise, and Cavity Enhanced Absorption Spectroscopy (CEAS), for prolongation of the interaction length. By matching the modulation frequency to the free-spectral range (FSR) of the cavity, all components of the FM-triplet will be transmitted through the cavity in an identical manner. This implies that technique attains an immunity to laser frequency-to-amplitude noise conversion. The linewidth can be limited down to the mechanical stability of the cavity, whereas the transmitted intensity is stabilized by the lifetime of the cavity. It can detect both absorption and dispersion signals and provide Doppler-broadened as well as sub-Doppler signals. This implies that the technique can be realized in a multitude of manners and acquire a detection sensitivity that has the potential to supersede those of most other detection techniques.

The technique was first developed for high precision frequency standard applications at JILA in Boulder CO in the mid-90tes, addressing narrow sub-Doppler signal of molecular overtone transitions in the near-infrared. The first demonstration of Doppler-broadened NICE-OHMS for gas detection was performed in 1999 by L. Gianfrani et al. who detected O_2 . In 2003 we initiated a programme aimed at investigating the possibilities to simplifying the realization of NICE-OHMS. The project has so far resulted in two set-ups, one based upon an Er-doped fiber-laser and one a narrow linewidth distributed feedback (DFB) laser, both working in the $1.5 \mu\text{m}$ region, with impressive detection powers.

Recently the fiber-laser based system was subjected to four improvements. *i*) Optical components have been placed at so called etalon immune distances (EID), which correspond to distances at which the FM signals disappear [1, 2]. *ii*) The mechanical insulation of the set-up was increased by the use of a two-layer air-suspended optical table in the Lexan enclosure [2]. *iii*) Active feedback of the electro optical modulator (EOM) was used for minimization of the background signals (by regulation) [1, 3]. *vi*) The locking of the laser to the cavity was improved by the use of an acousto optic modulator (AOM). With these improvements implemented, the system is capable of Doppler-broadened detection of C_2H_2 down to an absorbance per unit length of $1.8 \times 10^{-12} \text{ cm}^{-1}$ (over 10 s), a few times from the shot noise level [2].

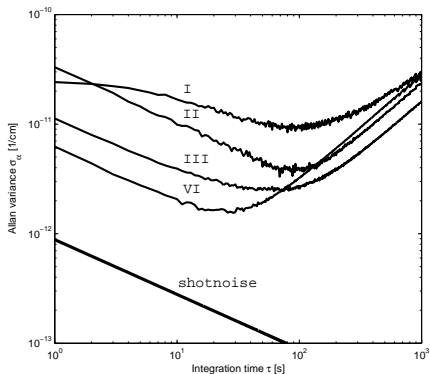


Figure 1: Allan deviation of measured Doppler-broadened NICE-OHMS signals for the four improvements; I) Etalon immune distances; II) Mechanical insulation of cavity and EID; III) Active feedback of EOM and EID; IV) Improved cavity locking, mechanical insulation and EID.

References

- [1] A. Foltynowicz, I. Silander, and O. Axner, *J. Opt. Soc. Am. B* **28**(11), 2797-2805 (2011)
- [2] P. Ehlers *et al.*, *J. Opt. Soc. Am. B*, Doc. ID 160011 (posted 29 february 2012, in press)
- [3] I. Silander *et al.*, *J. Opt. Soc. Am. B*, Doc. ID 156948 (posted 18 january 2012, in press)

Electron-impact study of B_2 molecule: R -matrix method

J. Singh^{1,2}, K.L. Baluja²

¹*Keshav Mahavidyalaya, University of Delhi, Pitam pura, Delhi-110034, India.*

²*Department of Physics and Astrophysics, University of Delhi, Delhi-110007, India.*

Corresponding Author: rajvanshi_jasmeet@yahoo.co.in

The results of *ab-initio* scattering calculations for low-energy electron collisions with B_2 molecule using the R -matrix method [1–2] have been presented. The differential and momentum-transfer cross sections are calculated using the POLYDCS program of Sanna and Gainturco [3], along with effective collision frequencies over a wide electron temperature range (300 - 30000 K) are computed at one-state close-coupling level. The ionization cross sections (Figure 1) are calculated in the binary-encounter Bethe (BEB) model [4] in which Hartree-Fock molecular orbitals at a self-consistent level are used to calculate kinetic and binding energies of the occupied molecular orbitals (Table 1).

The molecule B_2 is an open-shell system that has ground state $X^3\Sigma_g^-$ in the $D_{\infty h}$ point group which is reduced to the D_{2h} point group when the symmetry is lowered. In this work 61-state close-coupling calculations are performed to compute the integral cross sections (elastic and excitations), and results are compared with previous work [5–7]. We investigated five resonances; two core-excited resonances of $^2\Pi_u$ and $^2\Sigma_u^-$ symmetries, and three shape resonances of $^2\Pi_g$, $^4\Pi_g$ and $^4\Sigma_g^-$ symmetries. The Born-correction for the allowed transition ($X^3\Sigma_g^-$ to $A^3\Pi_u$) has been carried out to account for the contribution of partial waves higher than g wave ($l = 4$) upto which the R -matrix scattering calculations are carried. We have detected a stable anionic bound state $^2\Pi_u$ of B_2^- having configuration $1\sigma_g^2 2\sigma_g^2 1\sigma_u^2 2\sigma_u^2 1\pi_u^3$. We have also evaluated scattering length (6.8 a_0) of B_2 molecule at one state close-coupling level.

Molecular orbital	$ B $ (eV)	U (eV)	N
$1\sigma_g(1a_g)$	209.80	297.17	2
$1\sigma_u(1b_{1u})$	209.78	297.46	2
$2\sigma_g(2a_g)$	19.07	28.92	2
$2\sigma_u(2b_{1u})$	10.09	26.95	2
$1\pi_u(1b_{2u}/1b_{3u})$	9.54	18.07	2

Table 1: B_2 molecular orbital binding ($|B|$, in eV) and average kinetic energies (U , in eV) for DZP basis set at equilibrium geometry, N is occupation number.

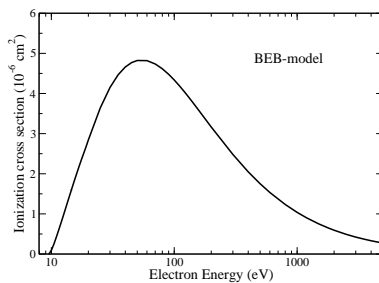


Figure 1: Electron-impact BEB ionization cross sections of the B_2 molecule.

References

- [1] J. Tennyson, Phys. Rep. **491**, 29 (2010).
- [2] P. G. Burke, R-Matrix Theory of Atomic Collisions: Application to Atomic, Molecular and Optical Processes, (Springer, 2011).
- [3] N. Sanna and F. A. Gianturco, Comput. Phys. Commun. **114**, 142 (1998)
- [4] Y. K. Kim and M. E. Rudd, Phys. Rev. A **50**, 3954 (1994).
- [5] S. R. Langhoff and C. W. Bauschlicher, Jr., J. Chem. Phys. **95**, 5882 (1991).
- [6] M. Hachey, S. P. Karna and F. Grein, J. Phys. B: At. Mol. Opt. Phys. **25**, 1119 (1991).
- [7] T. Muller *et al.*, Theor. Chem. Acc. **105**, 227 (2000).

Level-crossing spectroscopy of atomic rubidium at D_2 excitation in the presence of a non zero magnetic field

M. Auzinsh¹, A. Berzins¹, R. Ferber¹, F. Gahbauer¹, L. Kalvans¹, A. Mozers¹, and
A. Spiss¹

¹*Laser Centre. University of Latvia, 19 Rainis Boulevard, Riga, Latvia, LV-1586*

Corresponding Author: Agris.Spiss@gmail.com

The four hyperfine levels of the alkali metal $nP_{3/2}$ states are split into even more components in the presence of an external magnetic field according to the nonlinear Zeeman effect. Consequently, when a particular hyperfine component is excited by a laser, absorption and fluorescence decrease for magnetic fields larger than a few Gauss, an effect known as the excited state Hanle effect. Nevertheless, peaks in the absorption and fluorescence signals can be registered at certain nonzero magnetic field values at which magnetic sublevels cross. At linearly polarized excitation, when the polarization vector and magnetic field direction are mutually perpendicular (Hanle geometry), such resonances can be observed at $\Delta m = 2$ crossings. When the excitation and observation geometry differs from the Hanle configuration, resonance can be observed at $\Delta m = 1$ crossings.

In this study we revisit earlier work on such resonances at D_2 ($5S_{1/2} - 5P_{3/2}$) excitation of atomic Rubidium [1], aiming to describe a more accurate experiment with an expanded theoretical description that is based on the optical Bloch equations and has proven to be a reliable tool for describing zero-field resonances in alkali vapors [2]. The difference of two orthogonal, linearly or circularly polarized fluorescence components is registered experimentally and described numerically by the theoretical model.

The support from ERAF Project Nr. 2010/0242/2DP/2.1.1.1.0/10/APIA/VIAA/036 is gratefully acknowledged.

References

- [1] 1. J. Alnis *et al.*, J. Phys. B: At. Mol. Opt. Phys. **36** (2003) 11611173
- [2] 2. M. Auzinsh *et al.*, Phys. Rev. A **79**, 053404 (2009)

Dicke Narrowing and Speed-dependent Effects in Dispersion Mode of Detection – Theory and Experimental Verification by NICE-OHMS

J. Wang¹, P. Ehlers¹, I. Silander¹, and O. Axner¹

¹Department of Physics, Umeå University, SE-901 87 Umeå, Sweden

Corresponding Author: junyang.wang@physics.umu.se

Line shapes of molecules in gas phase are often described by the Voigt line shape function, which results from an assumption that the Doppler and pressure broadening are independent processes. However, measured spectra often deviate from the Voigt line shape due to two mechanisms: Dicke narrowing, which results from velocity-changing collisions and leads to a narrower Doppler distribution, and speed-dependent effects (SDEs), which originate from the velocity dependence of the collision cross section.

During the years, both these effects have been extensively investigated, and are found to be essential to perform accurate assessments of spectroscopic parameters or species concentrations. However, according to the authors' knowledge, all the demonstrations and investigations have been based on absorption spectrometry. Their influences on dispersion line shapes have not yet been generally known. The dispersion line shape is the basis for techniques relying on interference between two or several modes of light, e.g., frequency modulation spectroscopy (FMS), and thereby noise-immune cavity-enhanced optical heterodyne molecular spectroscopy (NICE-OHMS) and Faraday modulation or rotation spectrometry (FAMOS or FRS).

Expressions for Dicke narrowing [1] and SDEs [2] for the dispersion mode of detection are for the first time proposed and verified by the NICE-OHMS technique using an isolated transition of C_2H_2 at around $1.55 \mu m$. We also provide, for the first time, a comparison of the two phenomena in the absorption and dispersion modes of detection. It is shown that in the tens of Torr region the Dicke narrowing dispersive signal can be described by the dispersive counterparts to the conventional Galatry or Rautian absorption line shape functions, and that for pressures around and above 100 Torr SDEs in dispersion can be represented by the dispersive counterpart to the speed-dependent Voigt (SDV) model for absorption spectrometry. This opens up for accurate concentration assessments also in the pressure range where many techniques show their highest sensitivity. Spectroscopic parameters retrieved from the fits for the two modes of detection are shown to agree.

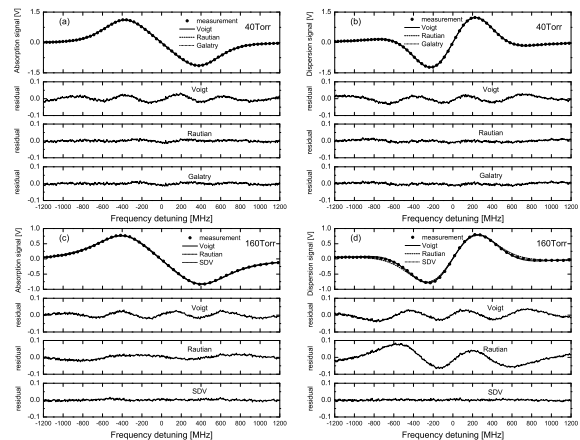


Figure 1: Fits of the measured NICE-OHMS signals based on various line shape functions (Voigt, Galatry, Rautian, and SDV), and the corresponding residuals. Top panels: 40 Torr, bottom panels: 160 Torr.

References

- [1] J. Wang *et al.*, Journal of the Optical Society of America B **28**, 2390–2401 (2011)
- [2] J. Wang *et al.*, In manuscript (2012)

Analytical expressions for fast real-time fitting of modulated dispersion line shapes

J. Westberg¹, J. Wang¹, and O. Axner¹

¹*Department of Physics, Umeå University, SE-901 87 Umeå, Sweden*

Corresponding Author: jonas.westberg@physics.umu.se

Laser-based spectroscopic techniques are nowadays frequently used for quantitative concentration measurements of various molecules in gas phase. The techniques are usually based on the ability of an analyte to absorb light, which accurately can be related to its concentration. By introducing a modulation, the influence of noise on the signals can be largely reduced, which leads to higher signal-to-noise ratios and consequently lower detection limits. The signals obtained by using a sinusoidal modulation together with phase-sensitive detection at a multiple of the modulation frequency can be modelled by using a theoretical description of the signals based on Fourier coefficients (Fc) [1]. This has proven to be a powerful tool for curve fitting to collisionally broadened absorption signals from techniques such as Wavelength Modulation Spectrometry (WMS), since it eliminates the need to numerically solve various integrals which allows for greatly improved computational efficiency.

Recently, however, the use of the dispersion mode of detection has become increasingly popular. Techniques such as Noise-Immune Cavity-Enhanced Optical Heterodyne Molecular Spectrometry (NICE-OHMS) and Faraday Modulation Spectrometry (FAMOS) are two examples of modulated techniques that rely on dispersion. In order to adopt the advantages of the Fc approach also to dispersion techniques a Fc-based description of modulated dispersion line shapes has been developed. By realizing that the expressions for the Fc for absorption and dispersion line shapes originate from a common complex molecular polarizability it was possible to provide an analytical expression for the Fc of also modulated dispersion line shape functions [2]. This implies that curve fitting to modulated dispersion techniques, such as FAMOS, can be made as swiftly as for absorption techniques, which enables fast and efficient real-time fitting.

However, the validity of the existing Fc description is restricted to the collisionally broadened regime, i.e. to gases under high pressure. It does not take into account the Doppler broadening which dominates at low pressure. This has so far limited the usefulness of the Fc curve fitting procedure when high accuracy is required.

The conventional way to include the Doppler broadening is by convoluting the Lorentzian profile with the Maxwell-Boltzmann velocity distribution, which yields the so called Voigt profile which can often be swiftly calculated by an FFT-algorithm. However, the use of modulation and phase-sensitive detection introduces numerically demanding integrals involving the Voigt profile that significantly increase the computational time. To avoid this, an alternative means to calculate modulated Voigt functions using a convolution of the Fc of modulated Lorentzian line shapes and the Maxwell-Boltzmann distribution has been developed. This provides an accurate representation (see Figure 1) of modulated Voigt line shapes while reducing computational time by roughly two orders of magnitude as compared to the conventional integral-based approach [3].

References

- [1] P. Kluczynski et al, *Spectrochim. Acta B* (56) 1277-1354 (2001)
- [2] J. Westberg et al, *JQSRT* (112) 14431449 (2011)
- [3] J. Westberg et al, *In manuscript* (2012)

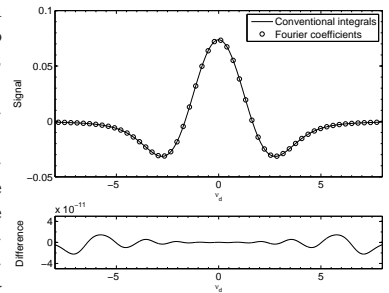


Figure 1: A comparison of modulated Voigt dispersion line shape calculated by the conventional approach and the Fc approach.

(see Figure 1) of modulated Voigt line shapes while reducing computational time by roughly two orders of magnitude as compared to the conventional integral-based approach [3].

Elastic scattering of electrons from Lithium and Potassium.

S. Y. Yousif Al-Mulla¹, L. Jönsson¹

¹ *University of Borås, College of Engineering, S-50190 Borås, Sweden.*

Corresponding Author: Yousif Al-Mulla

Electron collision with atoms and ions is one of the fundamental processes in nature and has attracted interest both experimentally and theoretically for a long time. The study of electron-atom collisions has served as a testing ground for our theoretical understanding of the important physical effects contributing to the behaviour of elementary quantum mechanical systems. In this work, the process of electron scattering from lithium and potassium is studied theoretically by calculating the differential cross sections for the elastic scattering of electrons from atoms at both low and intermediate incident energies. Local density approximations to the exchange and correlation potentials have been used in these calculations, and it is confirmed that Hara exchange coupled with a Hedin-Lundqvist electron-gas-type correlation potential joined to an adiabatic polarization potential gives good predictions for differential cross sections [1-4]. A comparison of the calculated results with other experimental and theoretical data are presented. For atomic scattering we consider two local-density approximations for the exchange-correlation potentials. One is obtained by incorporating Hara exchange [5] and Hedin-Lundqvist [6] correlation potential (HCC). In the second model we use Hara exchange and join the correlation potential of Hedin and Lundqvist with a polarisation potential (HCP).

References

- [1] J. A. D. Matthew and S. Y. Yousif, *Surf. Science* **152/153**, 38 (1985).
- [2] S. Y. Yousif and J. A. D. Matthew, *J. Phys. B: At. Mol. Phys.* **19**, 3305 (1986).
- [3] S. Y. Yousif and L. Jönsson, *Physica Scripta* **65**, 387 (2002).
- [4] S. Y. Yousif, *Eur. Phys. J. D* **42**, 11 (2007).
- [5] S. Hara, *J. Phys. Soc. Japan* **22** 710 (1967).
- [6] L. Hedin and B. I. Lundqvist, *J. Phys. C : Solid State Phys.* **4**, 2064 (1971).
- [7] D. H. Madison, R. P. McEachran and M. Lehmann, *J. Phys. B: At. Mol. Opt. Phys.* **27**, 1807 (1994).
- [8] W. Williams, S. Trajmar and D. Bozinis, *J. Phys. B: At. Mol. Phys.* **9**, 1529 (1976).
- [9] D. H. Madison *et al.*, *J. Phys. B: At. Mol. Opt. Phys.* **28**, 105 (1995).
- [10] L. Vuskovic and S. K. Srivastava, *J. Phys. B: At. Mol. Phys.* **13**, 4849 (1980)

Highly correlated multi-state and multi-reference *ab initio* study of the potential energy surface for the $N(^2D) + CH_4$ reaction

Ch.-M. Ouk¹, N. Zvereva-Loëte², B. Bussery-Honvault², Y. Scribano², and V. Boudon²

¹*Institut UTINAM, UMR6213, CNRS-UFC, 25030 Besançon cedex, France*

²*ICB, Burgundy University, 9, Av. A. Savary, BP4870, 21078, Dijon, France*

Corresponding Author: Natalia.Loete@u-bourgogne.fr

The study of the $N(^2D) + CH_4$ reaction is very important for various fields such as combustion chemistry, atmospheric chemistry and the atmosphere of other planets. The presence of nitriles in Titan's atmosphere, which was demonstrated by the Cassini-Huygens mission, suggests the existence of reactive mechanisms involving nitrogen in its activated forms [1-3]. The exit channels of the $N(^2D) + CH_4(^1A_1)$ reaction are now clearly defined and well characterized by the work of Kurosaki et al. [4] and by a recent crossed molecular beams (CMB) study of Balucani et al. [5]. But the mechanisms for this reaction have not been fully explored and discrepancies remain among theorists and experimentalists.

Multi-reference single and double configuration interaction (MRCI) calculations including Davidson (+Q) or Pople (+P) corrections have been conducted in present work for the reactants, products and extrema of the doublet ground state potential energy surface involved in the $N(^2D) + CH_4$ reaction. Such highly correlated *ab initio* calculations are then compared with previous PMP4, CCSD(T), W1 and DFT/B3LYP studies. Large relative differences are observed in particular for the transition state in the entrance channel resolving the disagreement between previous *ab initio* calculations. We confirm the existence of a small but positive potential barrier in the entrance channel of the title reaction. The correlation is seen to change significantly the energetic position of the two minima and five saddle points of this system together with the dissociation channels but not their relative order. In addition, we studied and highlighted the various reaction mechanisms to characterize and to understand all possible channels of the $CH_4 + N(^2D)$ potential energy surface. The minimum energy pathway (MEP) were calculated by the intrinsic reaction coordinate (IRC) theory for four transition states. TST (Transition State Theory) of thermal rate constant and RRKM (Rice Ramsperger Kassel Marcus) calculations were performed for comparison with experimental results [5,6]. RRKM calculations have been carried out for values of the energy corresponding to the surface temperature of Titan (94 K), to the stratospheric temperature of Titan (175 K), to the room temperature and to the collision energies used in the CMB experiments [5]. Our results for the rate constants k (T) are very close to experimental ones.

References

- [1] H. B. Niemann, S. K. Atreya, S. J. Bauer, G. R. Carignan, J. E. Demick, R. L. Frost, D. Gautier, J. A. Haberman, D. N. Harpold, D. M. Hunten, G. Israel, J. I. Lunine, W. T. Kasprzak, T. C. Owen, M. Paulkovich, F. Raulin, E. Raaen and S. H. T. Way, *Nature*, **438**, 779–784 (2005)
- [2] Vuitton, V. and Yelle, R. V. and Anicich, V. G., *Astrophys J.*, **647**, 175–178 (2006)
- [3] A. Coustenis, D. E. Jennings, C. A. Nixon, R. K. Achterberg, P. Lavvas, S. Vinatier, N. A. Teanby, G. L. Bjoraker, R. C. Carlson, L. Piani, G. Bampasidis, F. M. Flazar, P. N. Romani, *Icarus*, **207**, 461–476 (2010)
- [4] Y. Kurosaki, T. Takayanagi, K. Sato, S. Tsunashima, *J. Phys. Chem. A*, **102**, 254–259 (1998)
- [5] N. Balucani, D. Skouteris, M. Rosi, *J. Phys. Chem. A*, **113**, 11138–11152 (2009)
- [6] T. Takayanagi and Y. Kurosaki, K. Sato, K. Misawa, Y. Kobayashi, and S. Tsunashima, *J. Phys. Chem. A*, **103**, 250–255 (1999)



Cold atoms, Molecules, Ions and Quantum Gases

Transition rates for states of the $2s^22p^5$ and $2s2p^6$ configurations in fluorine-like ions between Si VI and W LXVI

P. Jönsson¹, A. Alkauskas², and G. Gaigalas^{3,2}

¹*School of Technology, Malmö University, 20506 Malmö, Sweden*

²*Department of Physics and Information Technologies, Lithuanian University of Educational Sciences, Studentų g. 39, LT-08106 Vilnius, Lithuania*

³*Vilnius University, Institute of Theoretical Physics and Astronomy, A. Goštauto 12, LT-01108 Vilnius, Lithuania*

Corresponding Author: andriusalkauskas@gmail.com

E1, M1, E2 transition rates from relativistic configuration interaction calculations are reported for the states of the $(1s^2)2s^22p^5$ and $2s2p^6$ configurations in all fluorine-like ions between Si VI and W LXVI. Valence, core-valence, and core-core correlation effects were accounted for through single-double expansions to increasing sets of active orbitals.

The present transition rates are compared with rates from multiconfiguration Breit-Pauli calculations by Froese Fischer and Tachiev [1], CIV3 calculations by Blackford and Hibbert [2] and by MCDF calculations by Jonauskas et al. [3]. Starting with Si VI we see that the rates for the E1 transitions differ from those by Froese Fischer and Tachiev by 1.7%. The agreement is even better with the values by Blackford and Hibbert. For values for the M1 and E2 transitions between the fine-structure levels of the $2s^22p^5$ are almost identical to the ones by Froese Fischer and Tachiev. Turning to Fe XVIII and the E1 transitions we again have a good agreement with the values presented by Blackford and Hibbert. The agreement with the MCDF calculation is less good and the difference reaches 7.5% for the $1/2 - 1/2$ transition. For the M1 and E2 transitions there is very good agreement with the values by Jonauskas et al. Overall, the agreement between different theoretical approaches is very satisfactory.

States		Type	This work A_B	CIV3 [2]	MCHF BP [1]	MCDF [3]
Upper	Lower					
Si VI						
$2s2p^6 \ ^2S_{1/2}$	$2s^22p^5 \ ^2P_{3/2}^o$	E1	1.808e+10	1.797e+10	1.777e+10	
$2s2p^6 \ ^2S_{1/2}$	$2s^22p^5 \ ^2P_{1/2}^o$	E1	8.664e+09	8.600e+09	8.517e+09	
$2s^22p^5 \ ^2P_{1/2}^o$	$2s^22p^5 \ ^2P_{3/2}^o$	M1	2.374e+00		2.376e+00	
$2s^22p^5 \ ^2P_{1/2}^o$	$2s^22p^5 \ ^2P_{3/2}^o$	E2	1.536e-05		1.541e-05	
Fe XVIII						
$2s2p^6 \ ^2S_{1/2}$	$2s^22p^5 \ ^2P_{3/2}^o$	E1	7.784e+10	7.740e+10		8.313e+10
$2s2p^6 \ ^2S_{1/2}$	$2s^22p^5 \ ^2P_{1/2}^o$	E1	2.824e+10	2.744e+10		3.035e+10
$2s^22p^5 \ ^2P_{1/2}^o$	$2s^22p^5 \ ^2P_{3/2}^o$	M1	1.933e+04			1.905e+04
$2s^22p^5 \ ^2P_{1/2}^o$	$2s^22p^5 \ ^2P_{3/2}^o$	E2	1.939e+00			1.941e+00

Table 1: Comparison of transition rates in s^{-1}

References

- [1] C. Froese Fischer and G. Tachiev, *At. Data Nucl. Data Tables* **87**, 1–184 (2004)
- [2] H.M.S. Blackford and A. Hibbert, *At. Data Nucl. Data Tables* **58**, 101–164 (1994)
- [3] V. Jonauskas *et al.*, *Astronomy Astrophysics* **416**, 383–389 (2004)

Transport properties of Li(2s) and Li(2p) diffusing in ground sodium

M.T. Bouazza¹, K. Alioua², N. Lamoudi³, L. Reggami⁴, F. Talbi⁴, and M. Bouledroua⁴

¹*Physics Department, Badji Mokhtar University, Annaba, Algeria*

²*L.P.R., Badji Mokhtar University, Annaba, Algeria*

³*Physics Department, Badji Mokhtar University, Annaba, Algeria*

⁴*L.P.R., Badji Mokhtar University, Annaba, Algeria*

Corresponding Author: tahar23000@yahoo.fr

In the present work, using the Chapman-Enskog method for dilute gases [1], we have calculated the diffusion coefficients D of ground Li(2s) and excited Li(2p) lithium atoms in a very weakly ionized buffer gas of ground sodium atoms in function of temperature T . The calculations are carried out quantum mechanically. The study begins by the construction of the potential-energy curves of the two possible molecular symmetries, namely, $X^1\Sigma^+$ and $a^1\Sigma^+$, through which a Li(2s) approaches Na(3s), and the singlet states A and B and the triplet states b and c through which Li(2p) interact with Na(3s). The data points upon which the construction is made are smoothly connected to the long- and short-range forms. They are supposed to behave analytically like $1/R^n$ and $\alpha \exp(-\beta R)$, respectively. The spectroscopic data, R_e and D_e , are in accordance with what is available in literature [2 – 4]. The second virial coefficients with quantum corrections are also calculated for several temperatures. Besides, we have investigated the variation law with temperature T of the diffusion coefficients D . We have found that, for temperatures ranging from 200K to 3000K, the results of D can be reproduced by simple formulas of the form $AT^b \exp(-c/T)$. Generally, the results of the transport properties with temperature show an excellent agreement with the available data.

References

- [1] S. Chapman and T.G. Cowling, *The Mathematical Theory of Non-Uniform Gases*, (Cambridge University Press, Cambridge, 1952)
- [2] M. Aubert-Frécon, private communication (2011)
- [3] AN. Mabrouk and H. Berriche, *J. Phys. B* **41**, 155101 (2008)
- [4] I. Schmidt-Mink, W. Müller, and W. Meyer, *Chem. Phys. Lett.* **112**, 120 (1984)

Towards a quantum gas of polar YbCs molecules

K. L. Butler¹, S. A. Hopkins¹, and S. L. Cornish¹

¹*Department of Physics, University of Durham, South Road, Durham, DH1 3LE, UK*

Corresponding Author: k.l.butler@durham.ac.uk

The formation and study of ultracold polar molecules leads to many fascinating areas of study, including quantum computation and the behaviour of degenerate quantum gases of molecules. This experiment aims to produce ground state YbCs molecules, using techniques such as magneto-association across Feshbach resonances [1] and Stimulated Raman Adiabatic Passage (STIRAP) [2]. The extra valence electron in ytterbium means that YbCs will have both electric and magnetic dipole moments in the ground state, unlike bi-alkali molecules which have just an electric dipole moment. This additional degree of freedom in experiments makes it possible to explore interesting phenomena such as spin dependent interactions in lattices [3,4]. We present progress towards the development of the two-species apparatus, as well as some theoretical background to the project.

References

- [1] P. S. Zuchowski, J. Aldegunde, and J. M. Hutson, *Phys. Rev. Lett.* **105**, 153201 (2010)
- [2] K. Bergmann, H. Theuer, and B. W. Shore, *Rev. Mod. Phys.* **70**(3), 1003 (1998)
- [3] A. Micheli *et al.*, *Phys. Rev. A* **76**, 043604 (2007)
- [4] A. Micheli, G. K. Brennen, and P. Zoller, *Nature Physics* **2**(5), 341 (2006)

A Centrifuge Molecular Decelerator for Polar Molecules

S. Chervenkov¹, X. Wu¹, A. Rohlfes¹, J. Bayerl¹, C. Sommer¹, M. Zeppenfeld¹, and G. Rempe¹

¹*Max-Planck-Institut für Quantenoptik, Hans-Kopfermann-Straße 1, 85748 Garching, Germany*

Corresponding Author: sotir.chervenkov@mpq.mpg.de

We present a novel and a versatile technique for deceleration of continuous beams of neutral polar molecules, which employs the centrifugal potential in a rotating frame. The idea is to inject and electrically guide [1] a beam of polar molecules from the periphery to the center of a rotating disk along a spiral trajectory. Thus the molecules climb up the centrifugal potential hill and get decelerated as they propagate. Since the rotational speed is tunable, the centrifuge decelerator is well-suited for a large range of input velocities. Moreover, in combination with our cryogenic source [2,3], internally cold molecules will be decelerated. For our design simulations show that output beams of ammonia molecules with velocities below 20 m/s and with fluxes of 10^9 molecules/s are feasible. The outcoming quasi-continuous slow and dense molecular beams provide an ideal source of cold and slow molecules for various experiments and applications, in particular, for trapping and subsequent opto-electrical cooling [4].

References

- [1] S. A. Rangwala *et al.*, Phys. Rev. A **67**, 043406 (2003)
- [2] L. D. van Buuren *et al.*, Phys. Rev. Lett. **102**, 033001 (2009)
- [3] C. Sommer *et al.*, Faraday Discuss. **142**, 203 (2009)
- [4] M. Zeppenfeld *et al.*, Phys. Rev. A **80**, 041401 (2009)

Complete ionisation of the neutral gas: why there are so few detections of 21-cm hydrogen in high redshift radio galaxies and quasars

S. J. Curran¹, M. T. Whiting²

¹*Sydney Institute for Astronomy, School of Physics, The University of Sydney, NSW 2006, Australia*

¹*ARC Centre of Excellence for All-sky Astrophysics (CAASTRO)*

²*CSIRO Astronomy and Space Science, PO Box 76, Epping NSW 1710, Australia*

Corresponding Author: sjc@physics.usyd.edu.au

Cool neutral gas provides the raw material for all of the star formation in the Universe, and yet, from a survey for this in the hosts of high redshift radio galaxies and quasars, we find a complete dearth of atomic gas, as traced through the hydrogen 21-cm spin-flip transition [1]. This runs contrary to the expectation that at these redshifts (look-back times $\gtrsim 11.5$ Gyr) much of the gas has yet to be consumed by star formation, meaning that we would expect its abundance to be many times higher than in the present day Universe. Upon a thorough analysis of the optical photometry, however, we find that *all* of our targets have ionising (i.e. at $\lambda \leq 912$ Å) ultra-violet continuum luminosities of $L_{1216} \gtrsim 10^{23}$ W Hz⁻¹. We therefore attribute the deficit to the traditional optical selection of targets biasing surveys towards the most ultra-violet luminous objects in the Universe, where the intense radiation excites neutral gas to the point where it cannot engage in star formation [2]. However, this hypothesis does not explain why there is a critical luminosity, rather than a continuum where the detections gradually become fewer and fewer as the harshness of the radiation increases.

We show that by placing a quasar within a galaxy of gas there is *always* an ultra-violet luminosity above which *all* of the gas in the galaxy is excited, thus explaining the critical value above which neutral gas cannot be detected in absorption. We also show that the observed critical UV luminosity of $L_{1216} \sim 10^{23}$ W Hz⁻¹ is just sufficient to ionise/excite *all* of the gas in a large spiral galaxy, such as our own. This demonstrates that these galaxies are truly devoid of star-forming material rather than this being at abundances below the sensitivity limits of current radio telescopes.

References

- [1] S. J. Curran, et al., Monthly Notices of the Royal Astronomical Society **391**, 765 (2008)
- [2] S. J. Curran & M. T. Whiting, The Astrophysical Journal **712**, 303 (2010)

Formation of Feshbach resonance in laser radiation field in case of two interconnected resonance phases.

E. Gazazyan¹, A. Gazazyan¹, and V. Chaltykyan¹

¹*Institute for Physical Research, NAS of Armenia, Ashtarak-2 0203, Armenia*

Corresponding Author: EmilGazazyan@gmail.com

We consider collision of atoms with formation of the Feshbach resonance in the field of the laser radiation, which couples two molecular levels with the interaction Ω and the molecular level of the ground state with continuum with the interaction Ω_E (see figure). In this case two scattering channels are seen, and weak coupling between those channels may lead to strong mixing between them. On the other hand the one-photon transition from the upper level to other continuum (inelastic channel) takes place, where the molecule decays under the action of laser radiation with the interaction Ω'_E into two excited atoms, which fly away to infinity. We obtained cross-sections for elastic and inelastic resonance scattering, and showed that they are determined by two coupled (interconnected) phases of resonance scattering, which pass in respective limits to the corresponding expressions reported in [1, 2]. Their dependence on intensity of the laser radiation is studied, and plots of these cross-sections versus the center-of-mass energy of colliding particles are given and analyzed. An expression for the scattering length in collision of two cold atoms in the laser radiation field is obtained.

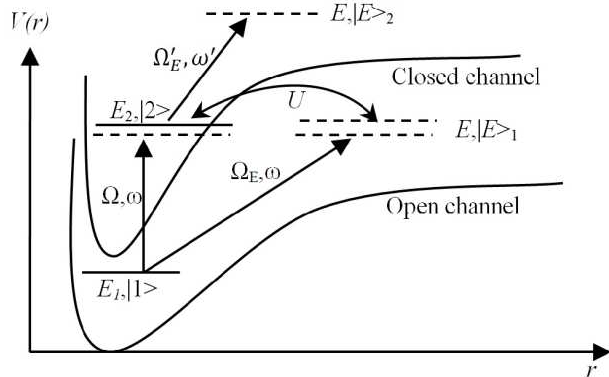


Figure 1: Diagram of formation of Feshbach resonance in the field of laser radiation.

References

- [1] A. Gazazyan, E. Gazazyan and V. Chaltykyan, Proc. SPIE 7998, 79980Y, doi:10.1117/12.890508 (2010); Europhysics conference abstracts, 43rd European Group for Atomic System (EGAS), University of Fribourg, Fribourg, Switzerland, June 28 - July 2, volume 35C, page 93 (2011).
- [2] E. A. Gazazyan, A. D. Gazazyan, and V. O. Chaltykyan, Journal of Contemporary Physics (Armenian Academy of Sciences), Vol. 46, No. 5, pp. 204-210 (2011).

Inelastic quantum diffraction of slowed atoms near a surface

M. Hamamda¹, T. Taillandier-Loize¹, G. Dutier¹, F. Perales¹, M. Boustimi²,
V. Bocvarski³, J. Baudon¹, and M. Ducloy¹

¹Laboratoire de Physique des Lasers, CNRS-UMR 7538, University Paris 13, Villetaneuse, France

²Umm Al-Qura University, Makkah, Saudi Arabia

³Institute of Physics, University of Belgrade, Serbia

Corresponding Author: mehdi.hamamda@univ-paris13.fr

Van der Waals-Zeeman transitions are inelastic atom-surface processes caused by the quadrupolar part of the van der Waals potential [cf. Eq. (1)] among magnetic sub-levels of metastable rare gas atoms Ne*, Ar* and Kr* (³P₂) [2] in the presence of a magnetic field.

$$V_{vdW} = -\frac{1}{4\pi\epsilon_0} \frac{\epsilon - 1}{\epsilon + 1} \frac{1}{4z^3} \left[\frac{D^2}{3} + \frac{1}{4} \left(D_z^2 - \frac{D^2}{3} \right) \right] \quad (1)$$

We investigate theoretically and experimentally those processes using a Zeeman slower providing metastable argon atoms with various velocities ranging from 170 to 560 m/s. This leads to measure with an accuracy of 20% the range of the interaction (3-12nm) [3-4], as well as the effect of atom polarisation on the sharing out of the M states.

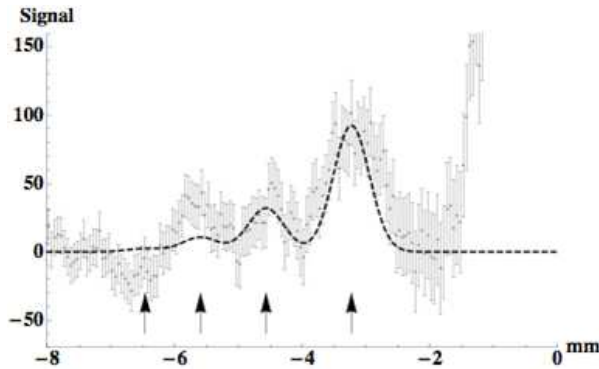


Figure 1: Inelastic spectrum obtained using the position-sensitive detector, for non-polarised (³P₂) metastable atoms at thermal velocity, i.e. $v = 560$ m/s for Ar*. Dashed curve is the theoretical inelastic peaks calculated via coupled-equation resolution.

References

- [1] J. -C. Karam *et al.*, *van der Waals - Zeeman transitions of metastable neon atoms passing through a micro-slit copper grating*, Europhys. Lett. **74** (1), 36-42
- [2] M. Hamamda, PhD Thesis, University Paris 13, (2011)
- [3] M. Hamamda *et al.*, *Inelastic transitions of atoms and molecules induced by van der Waals interaction with a surface*, Nucl. Instr. Meth. B, (2011)
- [4] M. Hamamda *et al.*, *Atom close to a surface, in a magnetic field: van der Waals - Zeeman transitions*, Europhys. Lett., To be published (2012)

Characterization and dynamics of rubidium magneto-optical trap induced by pushing beam

G. Kregar¹, N. Santic¹, and T. Ban¹

¹*Institute of Physics, HR-10 000 Zagreb, Croatia*

Corresponding Author: gordanak@ifs.hr

Since its first experimental realization by Raab et al. [1] in 1987, magneto-optical trap (MOT) has become the most reliable source of cold atoms. The properties of the trap can be modeled by Doppler and sub-Doppler cooling mechanisms. By applying an external force onto the atom cloud, we can observe the trap dynamics and conclude about the cooling processes and the trap parameters [2].

We have worked on ⁸⁷Rb MOT in standard six beams configuration. We have characterized the main parameters of our trap and have investigated how the number of trapped atoms changes with the trapping beam intensity, detuning and magnetic field gradient of the trap. We are studying time-dependent center of mass oscillation of rubidium cold cloud induced by on-resonance pushing beam. This chopped pushing beam presents an external force which acts on atoms translating the atom cloud along one horizontal direction. Induced trap oscillations are monitored through changes in the probe beam absorption. By fitting the free oscillation signals the values of damping coefficient and the spring constant can be determined and subsequently the temperature of the cloud. Further investigations are based on parametric resonance of the rubidium MOT.

PO

References

- [1] E. L. Raab, M. Pretniss, A. Cable, S. Chu and D. E. Pritchard, Phys. Rev. Lett. **59**, 2631 (1987)
- [2] X. Xu, T. H. Loftus, J. L. Hall, A. Gallagher and J. Ye, Phys. Rev. A **65**, 041401 (2002)

1b₂ study in (e,3e) oriented water molecule

A. Mansouri¹, I. Kada¹, C. Dal Cappello², and C. Champion²

¹Laboratoire de Physique quantique et systèmes dynamiques, Département de Physique, Faculté des Sciences Université Ferhat Abbas, Sétif 19000, Algeria

²Université Paul Verlaine-Metz, Laboratoire de Physique Moléculaire et des Collisions, ICPMB (FR 2843), Institut de Physique, 1 rue Arago, 57078 Metz Cedex 3, France

Corresponding Author: azmansouri@yahoo.com

An isolated water molecule fixed in space is studied in the double ionization by 250 eV electron impact. Calculations are made within a theoretical approach based on the first and the second Born approximation. Electron angular distributions from the 1b₂ state have been studied for particular kinematical conditions where the ts2 mechanism is isolated and studied.

To describe the initial state of the molecule we use a single-center molecular wave function[1].

The final state wave function describing the two ejected electrons is the approximate BBK wave function[2].

Whereas Champion *et al.* have found that the 6DCS were null when considering the 1b₂ molecular state [3] - what means that the SO and the TS1 mechanisms give *no contribution for this particular target orientation* - we here observe non negligible 6DCS (see Figure 1), what reveals - for the first time - a "pure" contribution of the TS2 mechanism.

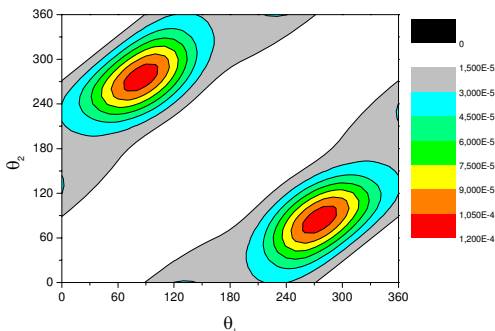


Figure 1: 6fold differential cross sections for the double ionization the second Born approximation of the water molecule (1b₂), oriented in the direction for and as a function of the ejected angles and relative to the incident electron. The ejected energies are eV .

References

[1] R. Moccia, J. Chem. Phys. A 40 (1964) 2186

[2] Mansouri A, Dal Cappello C, Houamer S, Charpentier I and Lahmam-Bennani A 2004 J. Phys.B: At. Mol. Opt. Phys. **37** 1203

[3] C Dal Cappello, C Champion ,I Kada, and A Mansouri, Phys. Rev.A83,062716(2011)

Fourier transform spectroscopy, direct potential fit, and radiative properties calculation on the shelf-like $E(4)^1\Sigma^+$ state of RbCs molecule

O. Docenko¹, V. Zuters¹, M. Tamanis¹, R. Ferber¹, V. Meshkov², E. Pazyuk², and A. Stolyarov²

¹*Laser Center, Department of Physics, University of Latvia, 19 Rainis blvd, Riga LV-1586, Latvia*

²*Department of Chemistry, Moscow State University, 119991, Moscow, Leninskie gory 1/3, Russia*

Corresponding Author: meshkov@laser.chem.msu.ru

We present results of high-resolution experimental study, direct potential fit and radiative properties calculation on the RbCs $E(4)^1\Sigma^+$ state converging to Rb(5^2S) + Cs(5^2D) atomic limit; such shelf-like states [1,2] are of particular interest for searching optical paths suitable for STIRAP producing of stable ultracold polar molecules. The collisionally enhanced laser induced fluorescence (LIF) spectra corresponding to both spin-allowed $E(4)^1\Sigma^+ \rightarrow X(1)^1\Sigma^+$ and spin-forbidden $E(4)^1\Sigma^+ \rightarrow a(1)^3\Sigma^+$ transitions of RbCs were recorded in visible region by Fourier Transform Spectrometer (Bruker IFS 125HR) with the instrumental resolution of 0.03 cm^{-1} . Overall about 2300 rovibronic term values of the $E(4)^1\Sigma^+$ state of $^{85,87}\text{RbCs}$ isotopologues were determined in the energy range [16750, 18170] cm^{-1} above the minimum of the ground X -state. Experimental data field is limited by vibrational levels $v' \in [3, 88]$ with rotational quantum numbers $J' \in [2, 276]$. The closed analytical form for potential energy curve (PEC) based on Chebyshev polynomial expansion was implemented to a direct potential fit of the experimental term values of the most abundant $^{85}\text{RbCs}$ isotopologue. The mass-invariant properties of the empirical PEC were tested by the prediction of rovibronic term values of the $^{87}\text{RbCs}$ isotopologue. The absorption and emission Einstein coefficients were predicted in a wide range of vibrational v and rotational J quantum numbers for both singlet-singlet $E - X$ and singlet-triplet $E - a$ rovibronic transitions along with radiative lifetimes of the upper E -state and branching ratios of spontaneous emission into the low lying electronic states, including both bound-bound and bound-continuum parts of the spectra. The required spin-allowed $E^1\Sigma^+ - X; A; C^1\Sigma^+; B^1\Pi$ transition dipole moments were obtained in the framework of quasi-relativistic electronic structure calculations. The regular spin-orbit coupling effect with the nearest $^3\Pi$ states is found to be sufficient to induce the spin-forbidden $E^1\Sigma^+ - a; c^3\Sigma^+; b^3\Pi$ transitions by borrowing probabilities of the relevant $^3\Pi - ^3\Pi$ transitions. Reliability of the derived empirical E -state PEC and *ab initio* $E - X; a$ transition dipole moments is additionally confirmed by good agreement between the calculated and experimental relative intensity distributions in the long $E(v') \rightarrow X(v'')$ and $E(v') \rightarrow a(v'')$ LIF progressions.

The Moscow team is grateful to the Russian Foundation for Basic Researches for support by the grant 10-03-00195-a. The support from the Latvian Science Council grant 09.1567 is greatly acknowledged by Riga team.

References

- [1] A.F. Nogueira, C.E.Fellows, and T.Bergeman, J. Chem. Phys. **129**, 136101 (2008)
- [2] L. Busevica *et al.*, J. Chem. Phys. **134**, 104307 (2011)

Collisional quenching of Rydberg atomic states by the ground-state alkaline-earth atoms

E. S. Mironchuk¹, A. A. Narits^{2,1}, and V. S. Lebedev^{2,1}

¹Moscow Institute of Physics and Technology, 9 Institutskiy per., 141700 Dolgoprudnyy, Moscow Region, Russian Federation

²P. N. Lebedev Physical Institute, 53 Leninskiy prospect, 119991 Moscow, Russian Federation

Corresponding Author: myolena@yandex.ua

The processes of quenching of Rydberg nl -states of atoms in slow collisions with alkaline-earth atoms with small electron affinities have been studied. Particular attention is paid to the analysis of the effects associated with the long-range part of interaction. We consider two possible mechanisms of quenching. According to the first mechanism [1], the depopulation of Rydberg states occurs through the formation of temporary weakly-bound negative ion and its subsequent decay in the field of positive ion. The second mechanism corresponds to the scattering of a quasifree electron of Rydberg atom on the perturbing particle. For the former mechanism the calculations were done using the Landau-Zener approach combined with the decay model. The important feature of the present calculations consists in the exact evaluation of the ionic-covalent coupling. This allows us to describe correctly the effects of the long-range electron-perturber interaction that are essential for the reactions involving highly polarizable targets. The quenching cross sections associated with the mechanism of quasifree electron scattering on a perturbing atom were determined on the basis of the theory of inelastic transitions between the highly excited states [2,3] using the momentum space electron wave function and *ab initio* data on the phase-shifts of electron-alkaline-earth atom scattering.

We have performed the calculations of the quenching cross sections in thermal collisions of various highly-excited atoms with ground-state Ba, Sr and Ca atoms. The contributions of the two mechanisms into the total quenching cross section have been evaluated in a wide range of principal quantum number for different values of relative collision velocity. The results for collisions of Rydberg neon atoms with Sr are plotted in Fig. 1.

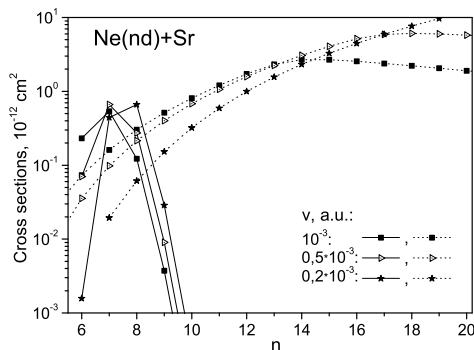


Figure 1: Quenching process cross sections for collision system $Ne(nd) + Sr$. Solid lines, resonant mechanism; dashed lines, mechanism of quasifree electron-perturber scattering.

References

- [1] I.I. Fabrikant, V.S. Lebedev, J. Phys. B **33**, 1521 (2000).
- [2] V.S. Lebedev, V.S. Marchenko, J. Phys. B **20**, 6041 (1987).
- [3] V.S. Lebedev, I.I. Fabrikant, Phys. Rev. A **54**, 2888 (1996).

Controlling large molecules at kHz repetition rates

T. Mullins¹, S. Trippel¹, N. Mller¹, K. Dugocki¹, and J. Kpper^{1,2}

¹Center for Free-Electron Laser Science, DESY, Notkestrasse 85, 22607 Hamburg, Germany

²Department of Physics, University of Hamburg, Luruper Chaussee 149, 22761 Hamburg, Germany

Corresponding Author: terry.mullins@cfel.de

Our motivating goal is to study ultrafast chemical dynamics of large and complex molecules directly in the molecular frame. It is accessed by using a combination of AC and DC electric fields to strongly align and orient the molecules to a fixed laboratory frame [1]. In addition, the selection of internal quantum states, conformers, or isomers of polar molecules is available using inhomogeneous electric fields [2,3]. Such experiments have, so far, typically been carried out at relatively low repetition rates, limited primarily by the pulsing rate of high power Nd:YAG lasers, and by the difficulties involved in producing cold supersonic beams of complex molecules at such high rates [4,5], resulting in long measurement times.

Our benchmark experiments will be presented in which we image the molecular frame at 1 kHz. We begin with a supersonic, cold beam of prototypical iodobenzene (C_6H_5I) molecules from an Even-Lavie valve [4]. These molecules are quantum-state selected and, subsequently, adiabatically laser aligned using a strongly chirped broadband pulse from a high power Ti:Sa laser and mixed-field oriented with an additional weak DC electric field. The resulting strongly aligned and oriented molecular samples are characterised by strong-field ionization using femtosecond laser pulses and velocity-map imaging of the product ions to derive the angular distribution of the molecules in the lab frame.

Such a system, showing large degrees of alignment even at the highest repetition rates, is highly advantageous for investigating weakly interacting molecular processes that require good statistics to avoid the signal being lost in the noise. Our immediate future prospects include investigating of molecular-frame photoelectron angular distributions [6,7] to reveal the dynamics of molecular orbitals as the molecule undergoes conformational isomerization.

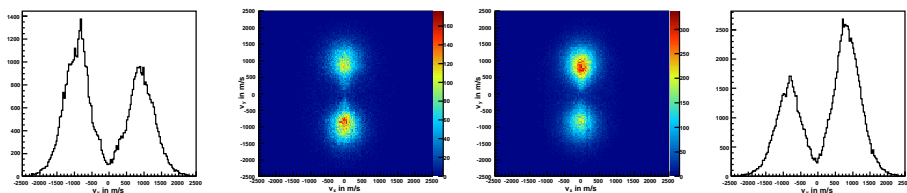


Figure 1: Mixed field orientation at 1 kHz with angles of $\pm 45^\circ$ between the DC electric field and the linearly polarised picosecond laser pulse.

References

- [1] L. Holmegaard *et al.*, Phys. Rev. Lett. **102**, 023001 (2009)
- [2] F. Filsinger *et al.*, Phys. Rev. Lett. **100**, 133003 (2008)
- [3] F. Filsinger *et al.*, Angew. Chem. Int. Ed. **48**, 6900-6902 (2009)
- [4] U. Even *et al.*, J. Chem. Phys. **112**, 8068 (2000)
- [5] D. Irimia *et al.*, Phys. Chem. Chem. Phys. **11**, 3958-3966 (2009)
- [6] L. Holmegaard *et al.*, Nat. Phys. **6**, 428 (2010)
- [7] J. L. Hansen *et al.*, Phys. Rev. Lett. **106**, 073001 (2011)

The revised deperturbation analysis of the $A \sim b$ complex of the Cs_2 dimer based on Fourier transform measurements

H. Cerins¹, O. Nikolayeva¹, M. Tamanis¹, R. Ferber¹, E. Pazyuk², and A. Stoloyarov²

¹Laser Center, Department of Physics, University of Latvia, 19 Rainis blvd, Riga LV-1586, Latvia

²Department of Chemistry, Moscow State University, 119991, Moscow, Leninskie gory 1/3, Russia

Corresponding Author: pazyuk@phys.chem.msu.ru

We accomplished the systematic high resolution Fourier transform measurements of the rovibronic term values of cesium dimer belonging to the spin-orbit coupled singlet $A^1\Sigma_u^+$ and triplet $b^3\Pi_u$ states. To perform unambiguous vibrational assignment of fully mixed states of the $A \sim b$ complex the particular attention was paid to probe low-lying levels located in the vicinity of a minimum of the singlet A -state. The Cs_2 molecules were formed in a heatpipe oven containing admixture of Rb and Cs atoms at 550 K as well as in glass-cell containing only Cs metal and buffer Ar gas. The collisionally enhanced laser induced $A^1\Sigma_u^+ \sim b^3\Pi_u \rightarrow X^1\Sigma_g^+$ fluorescence (LIF) spectra were excited by tunable diode lasers and recorded by Fourier transform spectrometer (Bruker IFS 125HR operating with InGaAs detector) with the instrumental resolution of 0.03-0.05 cm^{-1} . More than 1900 rovibronic term values of the Cs_2 $A \sim b$ complex were obtained in the energy range [9630, 12650] cm^{-1} above the minimum of the ground state. The relative intensity distribution measured for the lowest vibrational levels of the singlet state $A(v') \sim b \rightarrow X(v'')$ confirms the breakdown of the 1D oscillation theorem for strongly coupled diatomic states [1].

The present experimental data were then involved (simultaneously with the preceding experimental data available from the several sources [2]) in the rigorous 4×4 coupled-channel deperturbation treatment based on Hund's coupling case (a) basis set. Besides of the dominating spin-orbit coupling (SOC) effect between the crossing A and b states the elaborated model also takes into account the weak regular perturbations by the remote electronic states. The robust nonlinear weighting fitting procedure [3] was used to diminish the influence of incorrectly assigned terms as well.

The resulting empirical diabatic potential energy curves and relevant SOC functions reproduce about 94% of the overall experimental term values with a standard deviation of 0.007 cm^{-1} which becomes close to the uncertainty of the experiment. The achieved accuracy of deperturbation parameters is sufficient to provide reliable predictions for optical pathways leading to the efficient formation of ultracold molecules.

The Moscow team is grateful to the Russian Foundation for Basic Researches for support by the grant 10-03-00195-a. The support from the Latvian Science Council grant 09.1567 is greatly acknowledged by Riga team.

References

- [1] V. I. Pupyshev *et al.*, Phys. Chem. Chem. Phys. **12**, 4809 (2010)
- [2] J. Bai *et al.*, Phys. Rev. A **83**, 032514 (2011)
- [3] I.Dabrowski, D.W.Tokaryk, and J.K.G.Watson, J.Mol.Spectrosc. **189**, 95 (1998)

Vibrational quantum defect coupled to improved LeRoy-Bernstein formula for a precise analysis of photoassociation spectroscopy

L. Pruvost¹, H. Jelassi²

¹*Laboratoire Aimé Cotton, CNRS II, Univ Paris sud, 91405 Orsay, France*

²*CNSTN, Pôle Technologique. 2020 Sidi Thabet, Tunisia*

Corresponding Author: laurence.pruvost@lac.u-psud.fr

Laser photoassociation (PA) of cold atoms creates excited, weakly-bound molecules, which are key intermediates in the most of schemes that allow the formation of cold molecules in the ground state.

For that reason the spectroscopy of these weakly bound molecules is one of the tools to know, not only the energy position of the levels but also if it exists their mixings with neighboring levels. Indeed, the mixings determine the wavefunction shapes, especially at short internuclear distance, and thus the Franck-Condon factors required for molecule formation.

We show that, for an accurate analysis of the PA spectroscopy data, the LeRoy-Bernstein formula has to be improved [1]. Furthermore we show that the use of vibrational quantum defects and of Lu-Fano graphs provide efficient tools to determine and measure the couplings [2–4].

References

- [1] Reexamination of the LeRoy-Bernstein formula for weakly bound molecules, Haikel Jelassi, Bruno Viaris de Lesegno, and Laurence Pruvost, *Phys. Rev. A* **77**, 062515 (2008)
- [2] Photoassociation spectroscopy of $^{87}\text{Rb}_2(5s_{1/2} + 5p_{1/2})0_g^-$ long-range molecular states: Analysis by Lu-Fano graph and improved LeRoy-Bernstein formula, H. Jelassi, B. Viaris de Lesegno, and L. Pruvost, *Phys. Rev. A* **73**, 032501 (2006)
- [3] Spin effects in $(6s_{1/2} + 6p_{1/2})0_u^+ \text{}^{133}\text{Cs}_2$ weakly bound molecules analyzed by using the Lu-Fano method coupled to the improved LeRoy-Bernstein formula, H. Jelassi, B. Viaris de Lesegno, and L. Pruvost, M. Pichler, W. C. Stwalley, *Phys. Rev. A* **78**, 022503 (2008)
- [4] Weakly bound $(6s_{1/2} + 6p_{1/2})0_g^- \text{}^{133}\text{Cs}_2$ levels analysed using the vibrational quantum defect. Detection of two deeply bound $(6s_{1/2} + 6p_{3/2})0_g^-$ levels, L. Pruvost and H. Jelassi, *J. Phys. B: At. Mol. Opt. Phys.* **43**, 125301 (2010).

On the energy difference between $1s^22s^22p^2\ ^2P^o$ and $1s^22s2p^2\ ^4P$ terms in Boron

P. Rynkun¹, S. Verdebout², P. Jönsson³, G. Gaigalas^{4,1}, C. Froese Fischer⁵, and M. Godefroid²

¹*Department of Physics and Information Technologies, Lithuanian University of Educational Science, Studenty 39, LT-08106 Vilnius, Lithuania*

²*Service de Chimie Quantique et Photophysique, CP160/09, Université Libre de Bruxelles, Av. F. D. Roosevelt 50, B-1050 Brussels, Belgium*

³*School of Technology, Malmö University, 20506 Malmö, Sweden*

⁴*Vilnius University, Institute of Theoretical Physics and Astronomy, A. Goštauto 12, LT-01108 Vilnius, Lithuania*

⁵*National Institute of Standards and Technology, Gaithersburg, MD 20899-8420, USA*

Corresponding Author: pavel.rynkun@gmail.com

In this work we present calculations of the energy separation between $1s^22s^22p^2\ ^2P^o$ and $1s^22s2p^2\ ^4P$ terms using the multiconfiguration Hartree-Fock (MCHF) [1] and the Partitioned Correlation Function Interaction (PCFI) [2] methods. Calculations are made in two different ways: simultaneous and separate optimizations of the two terms. In both approaches, the configuration expansions are obtained by single and double (SD) excitations to orbital active sets with principal quantum numbers $n = 4 \dots 10$ and angular symmetries s, p, d, f, g, h from all shells of the multi-reference (MR) set.

In the PCFI approach, independent sets of correlation orbitals, embedded in the partitioned correlation function (PCFs), are produced from separate MCHF calculations. These non-orthogonal functions span configuration state function spaces that are coupled to each other by solving the associated generalised eigenproblem. The Hamiltonian and overlap matrix elements are evaluated using the biorthonormal orbital transformations and efficient counter-transformations of the configuration interaction eigenvectors. Two sets of results are compared in the Table 1, with the estimations of Edlén *et al.* [3] and Kramida and Ryabtsev [4]. As seen in the table the energy convergence is definitely faster using the PCFI method than with the usual MR-SD-MCHF approach.

n	MR-SD-MCHF		MR-PCFI	
	simult. opt.	separ. opt.	simult. opt.	separ. opt.
4	28449.26	28296.53	28538.16	28457.67
5	28471.05	28394.99	28773.89	28765.42
6	28688.74	28643.74	28846.86	28847.01
7	28779.43	28761.27	28867.18	28866.65
8	28822.39	28818.40	28875.94	28875.63
9	28849.68	28845.24	28879.69	
10	28862.23	28859.74		
Edlén <i>et al.</i> [3]	28866 ± 15			
KR [4]	28644.27			

Table 1: Energy separation between $^2P^o$ and 4P terms in cm^{-1} .

References

- [1] C. Froese Fischer *et al.* Comp. Phys. Commun **176**, 559 (2007)
- [2] S. Verdebout *et al.* J. Phys. B: At. Mol. Opt. Phys. **43**, 74017 (2010)
- [3] B. Edlén *et al.* Solar Physics **9**, 432 (1969)
- [4] A. E. Kramida and A. N. Ryabtsev Physica Scripta **76**, 544 (2007)

Buffer gas cooling of YbF molecules

, S. M. Skoff, N. E. Bulleid, D. Nohlmans, R. J. Hendricks, B. E. Sauer, D. M. Segal, E. A. Hinds, and M. R. Tarbutt
Centre for Cold Matter, Blackett Laboratory, Imperial College London, London SW7 2BW, United Kingdom

Corresponding Author: s.skoff07@imperial.ac.uk

Using a cryogenic buffer gas source, with both continuous and pulsed helium flow, we have produced cold, slow beams of YbF molecules. The flux exceeds 10^{10} ground state molecules per shot per steradian. The translational and rotational temperatures are 4 K and the center of mass velocity can be tuned from 130m/s to 320m/s by exploiting different flow regimes. We use absorption imaging of atoms and molecules inside the buffer gas cell to learn about the flow dynamics and its impact on the extraction efficiency [1]. This new cold and intense beam of YbF molecules will be used to increase the sensitivity of the next measurement of the electron's electric dipole moment [2]. Another route that we are currently pursuing is buffer gas cooling of molecules and atoms directly in a permanent magnetic trap. For this purpose we have designed a quadrupole trap using NdFeB magnets, which give a trap depth of 0.5 K for YbF molecules. Inside this trap the molecules are created via laser ablation and are cooled with helium gas that is pulsed into the trapping region through a solenoid valve. The cold tail of the Boltzmann distribution is then trapped in the magnetic field minimum at the center of the trap. We will present our recent results on the beam and the magnetic trap.

References

- [1] S. M. Skoff, *et al.*, Phys. Rev. A **83**, 023418 (2011)
- [2] J. J. Hudson *et al.*, Nature **473**, 493 (2011)

Theoretical determination of the potassium far-wing photo-absorption spectra

F. Talbi¹, K. Alioua², N. Lamoudi³, L. Reggami⁴, M.T. Bouazza⁴, and M. Bouledroua⁴

¹*Physics Department, Badji Mokhtar University, Annaba, Algeria*

²*L.P.R., Badji Mokhtar University, Annaba, Algeria*

³*Physics Department, Badji Mokhtar University, Annaba, Algeria*

⁴*L.P.R., Badji Mokhtar University, Annaba, Algeria*

Corresponding Author: fftalbi@yahoo.fr

This theoretical work reports full quantum-mechanical analysis of the potassium far-wing photo-absorption spectra. The accuracy of adopted K_2 potential-energy curves and transition dipole moments is established by computing the vibration-rotation levels and the radiative lifetimes of the excited molecular states. The pressure-broadening calculations revealed that the photo-absorption spectra have, in the temperature range 850 – 2000K, a satellite structure characterized by the presence of three peaks around 718.7nm in the blue wings and 1048.1 and 1100.8nm in the red wings. This theoretical work could in particular point out the occurrence in the blue wing of satellite originating from the bound-free $B \leftarrow X$ transition near 731.5nm. All these results agree quite well with the experimentally measured values [1, 2]. The temperature effect on the satellite and its amplitude has also been investigated and the results are compared with recent experimental data [1].

References

- [1] C. Vadla , R. Beuc, V. Horvatic, M. Movre, A. Quantmeier, and K. Niemax, Eur. Phys. J. D 37, 37 (2006)
- [2] Y. Hasegawa, H. Yamasaki, S. Kabashima, and S. Shioda, J. Quant. Spectrosc. Radiat. Transfer 48, 1 (1992)

Cryogenic Paul trap for experiments on cold HCIs

O. O. Versolato¹, M. Schwarz¹, A. Windberger¹, J. Ullrich^{2,3}, P. O. Schmidt^{2,3},
A. K. Hansen⁴, A. D. Gingell⁴, M. Drewsen⁴, and J.R. Crespo López-Urrutia¹

¹Max-Planck-Institut für Kernphysik, D-69116 Heidelberg

²Physikalisch-Technische Bundesanstalt, Bundesallee 100, D-38116, Braunschweig

³Institut für Quantenoptik, Leibniz Universität Hannover, D-30167 Hannover

⁴Department of Physics and Astronomy, University of Aarhus, DK-8000 Aarhus C

Corresponding Author: oscar.versolato@mpi-hd.mpg.de

Highly charged ions (HCIs) are of particular interest for metrology and fundamental physics. For example, the highest sensitivity for a changing fine structure constant ever predicted for an atomic system is found in Ir¹⁷⁺ [1]. Optical clocks based on HCIs are impervious to detrimental field shifts such as the blackbody Stark effect. Such high-accuracy studies laser spectroscopy of HCIs [2] are possible only when HCIs are cooled down from the MK temperatures present in an electron beam ion trap -where the HCIs are created and studied- to the mK range. These low temperatures can be obtained by means of sympathetic cooling in a linear Paul trap. Storage and cooling of HCIs requires ultra-high vacuum levels obtainable by cryogenic methods. We have developed a linear Paul trap operating at 4 K with external ion injection capabilities [3] and optical access ports for the laser light. Exposure to black body radiation (BBR) is minimized in our design. Measurements with molecular ions (MgH⁺) were performed in Aarhus which exploit in particular this low exposure to BBR [4]. An all-solid state laser system at 313 nm has been set up for the Doppler laser cooling of Be⁺ ions that will serve as sympathetic coolants of HCIs [3]. A laser system with two SHG stages to provide laser light at 235 nm wavelength is being set up for the loading of Be⁺ ions by means of photo-ionization. Ion optical elements for ion extraction from the Heidelberg Hyper-EBIT into CryPTE_x are currently being constructed.

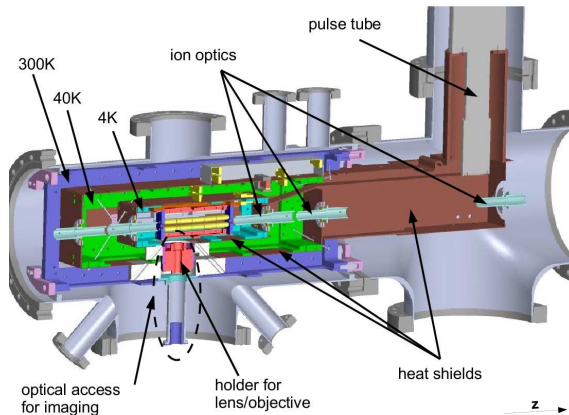


Figure 1: A set-up for Cryogenic Paul Trap Experiments.

References

- [1] J.C. Berengut *et al.*, Phys. Rev. Lett. **106** (2011) 210802.
- [2] Mäckel *et al.*, Phys. Rev. Lett. **107** (2011) 143002.
- [3] M. Schwarz *et al.*, Rev. Sci. Instr., submitted.
- [4] M. Schwarz *et al.*, in preparation.

Bose-Einstein condensation of ^{85}Rb by direct evaporation in an optical dipole trap

, T. P. Wiles, A. L. Marchant, S. Händel, S. A. Hopkins, M. M. H. Yu, and S. L. Cornish

Department of Physics, University of Durham, South Road, Durham, DH1 3LE, UK

Corresponding Author: timothy.wiles@durham.ac.uk

We report a simple method for the creation of Bose-Einstein condensates of ^{85}Rb by direct evaporation in a crossed optical dipole trap [1]. The independent control of the trap frequencies and magnetic bias field afforded by the trapping scheme permits full control of the trapped atomic sample, enabling the collision parameters to be easily manipulated to achieve efficient evaporation in the vicinity of the 155 G Feshbach resonance. We produce nearly pure condensates of up to 4×10^4 atoms and demonstrate the tunable nature of the atomic interactions.

We describe a plan to transfer the condensate into an optical waveguide in order to produce bright matter wave solitons [2-4]. These self-stabilizing wave packets are well localized due to attractive atom-atom interactions and hence show great potential as surface probes for the study of short-range atom-surface interactions [5]. Our apparatus includes a super-polished Dove prism for use in such experiments. There is also much scope for the study of binary soliton collisions and the scattering of solitons from barriers. We present these schemes utilizing bright matter wave solitons with the aim of studying atom interferometry.

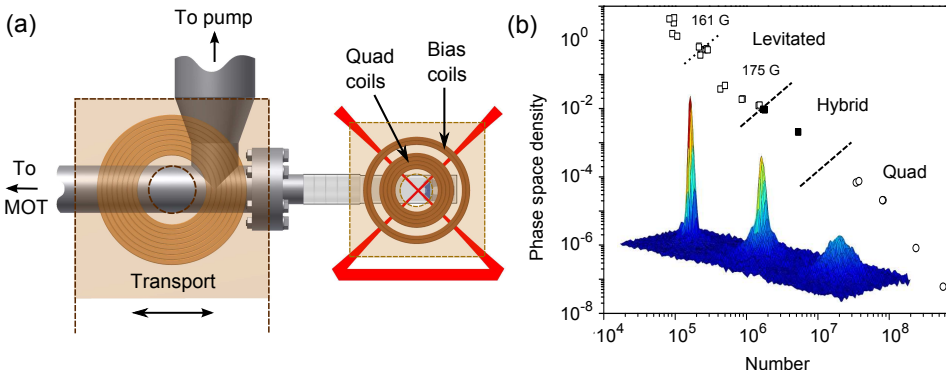


Figure 1: (a) Experimental setup showing the arrangement of coils around the UHV cell and the beam geometry used to create the crossed dipole trap. (b) Evaporation trajectory to reach BEC. RF evaporation occurs in a magnetic quadrupole trap before the atoms are loaded into an optical dipole trap for evaporation to degeneracy.

References

- [1] A. L. Marchant *et al.*, Submitted to Phys. Rev. A (2012), arXiv:1203.6598.
- [2] S. L. Cornish, S. T. Thompson, and C. E. Wieman, Phys. Rev. Lett. **96**, 170401 (2006).
- [3] K. E. Strecker *et al.*, Nature (London) **417**, 150 (2002).
- [4] L. Khaykovich *et al.*, Science **296**, 1290 (2002).
- [5] S. Cornish *et al.*, Physica D: Nonlinear Phenomena **238**, 1299 (2009).

High-resolution Spectroscopy

Energy structure and transition rates in the Ne-like sequence from relativistic CI calculations

P. Bengtsson¹, J. Ekman¹, S. Gustafsson¹, P. Jönsson¹, L.B. Karlsson¹, and G. Gaigalas²

¹*Group for Materials Science and Applied Mathematics, School of Technology, Malmö University, 205 06 Malmö, Sweden*

²*Vilnius University, Institute of Theoretical Physics and Astronomy, A. Goštauto 12, LT-01108 Vilnius, Lithuania*

Corresponding Author: peter.bengtsson@mah.se

Atomic data are important in astrophysical applications and transition rates can be used in the determination of element abundances and plasma diagnostics [1,2]. To provide for the extensive data needs a number of general computer codes such as SUPERSTRUCTURE, CIV3, and ATSP2K have been developed. As an alternative to these codes, which all rely on the Breit-Pauli approximation, the fully relativistic GRASP2K code [3,4] can be used. GRASP2K is based on the multiconfiguration Dirac-Hartree-Fock method and implements a bi-orthogonal transformation method that permits initial and final states in a transition array to be optimized separately, which, in many cases, leads to more accurate values of the resulting rates [5]. The GRASP2K package also contains modules to compute diagonal and off-diagonal hyperfine interaction constants, isotope shifts, Landé gJ factors, and splittings of magnetic sub-state in intermediate and strong magnetic fields. In this work, GRASP2K has been applied to provide highly accurate spectroscopic data for ions in the Ne-like sequence between Mg III and Kr XXVII [6]. Valence, core-valence, and core-core correlation effects were accounted for through SD-MR expansions to increasing sets of active orbitals. In Mg III, Al IV, Si V, P VI, S VII, and Ar IX, for which experimental energies are known to high accuracy, the mean error in the calculated energies is only 0.011%. For ions with no available experimental energy levels the calculated values should be most valuable in various applications. The high accuracy of the calculated energies makes it possible, in some cases, to point out experimental values that are in error. Babushkin (length) and Coulomb (velocity) forms of transition rates are computed and agree to within a few percent for the majority of the allowed transitions. Computed lifetimes for states belonging to the $2p^33s$ and $2p^53d$ configurations are in good agreement with values from beam-foil measurements as well as from accurate MCHF Breit-Pauli calculations.

References

- [1] C. Jupén, Nucl. Instr. Meth. B31 (1988) 166.
- [2] P. Beiersdorfer, J. Clementson, J. Dunn, M. F. Gu, K. Morris, Y. Podpaly, E. Wang, M. Bitter, R. Feder, K. W. Hill, D. Johnson, and R. Barnsley J. Phys. B: At. Mol. Opt. Phys. 43(14) (2010) 144008.
- [3] P. Jönsson, X. He, C. Froese Fischer, and I.P. Grant, Comput. Phys. Commun. 177 (2007) 597.
- [4] P. Jönsson, G. Gaigalas, J. Bieroń, C. Froese Fischer, and I.P. Grant, Comput. Phys. Commun. to be submitted (2012).
- [5] J. Olsen, M. Godefroid, P. Jönsson, P.Å. Malmqvist, and C. Froese Fischer, Phys. Rev. E 52 (1995) 4499.
- [6] P. Jönsson *et al.*, At. Data and Nucl. Data Tables, accepted (2012).

Searching for cosmological spatial variations in values of fundamental constants using laboratory measurements

J.C. Berengut¹, V.V. Flambaum¹

¹*School of Physics, University of New South Wales, Sydney 2052, Australia*

Corresponding Author: jcb@phys.unsw.edu.au

The results of a very large study of around 300 quasar absorption systems using data from both the Keck telescope and the Very Large Telescope provide hints that there is a spatial gradient in the variation of the fine structure constant, $\alpha = e^2/\hbar c$ [1, 2]. In one direction on the sky α appears to have been smaller in the past, while in the other direction it appears to have been larger. The data from both telescopes give the same direction and magnitude for the α -gradient. A remarkable result such as this must be independently confirmed by complementary searches.

We discuss how terrestrial measurements of time-variation of the fundamental constants in the laboratory, meteorite data, and analysis of the Oklo nuclear reactor can be used to corroborate the spatial variation observed by astronomers [3]. In particular we can expect the yearly variation of α in laboratory measurements to be

$$\dot{\alpha}/\alpha = 1.35 \times 10^{-18} \cos \psi \text{ yr}^{-1}$$

where ψ is the angle between the motion of the Sun and the dipole, approximately $\cos \psi \sim 0.07$ according to the best-fit quasar data. This signal will be modulated by the annual motion of the Earth around the Sun. The required accuracy is two orders of magnitude below current atomic clock limits, but there are several proposals that could enable experiments to reach it. These include nuclear clocks and transitions in highly-charged ions that would have the highest sensitivity to variation of the fine-structure constant ever seen in atomic systems.

References

- [1] J. K. Webb *et al.*, Phys. Rev. Lett. **107**, 191101 (2011)
- [2] J. C. Berengut *et al.*, Phys. Rev. D **83**, 123506 (2011)
- [3] J. C. Berengut and V. V. Flambaum, Europhys. Lett. **97**, 20006 (2012)

Testing time-variation of fundamental constants using Th and U nuclear clocks

J.C. Berengut¹, V.V. Flambaum¹

¹*School of Physics, University of New South Wales, Sydney 2052, Australia*

Corresponding Author: jcb@phys.unsw.edu.au

The low-energy (7.6 eV) transition in Th-229 could provide a reference for an optical clock of extremely high accuracy [1–3]. Nuclear clocks would be very sensitive probes of any potential changes to the values of fundamental constants of nature [4, 5]. The 76 eV isomeric transition of U-235 has some potential advantages over the Th-229 transition, not least that its properties (energy, line width) are well known. With recent advances in high-UV frequency combs using high-harmonic generation [6] the transition may come within laser range in the foreseeable future. We present results of nuclear and atomic calculations that show a U-235 nuclear clock would have comparable accuracy to the Th-229 clock, and an absolute sensitivity to variation of fundamental constants that is larger than any other proposed laboratory reference standard.

References

- [1] E. Peik and Chr. Tamm, *Europhys. Lett.* **61**, 181 (2003)
- [2] S. G. Porsev *et al.*, *Phys. Rev. Lett.* **105**, 182501 (2010)
- [3] C. J. Campbell *et al.*, Accepted to *Phys. Rev. Lett.* (2012) (arXiv:1110.2490)
- [4] V. V. Flambaum, *Phys. Rev. Lett.* **97**, 092502 (2006)
- [5] J. C. Berengut *et al.*, *Phys. Rev. Lett.* **102**, 210801 (2009)
- [6] A. Cingöz *et al.*, *Nature* **482**, 68 (2012)

Modelling of electromagnetic radiation group velocity reduction

L. Busaite¹, L. Kalvans¹

¹*Laser Centre, University of Latvia, 19 Rainis Boulevard, Riga, Latvia, LV-1586*

Corresponding Author: laima.busaite@gmail.com

The reduction of group velocity is a process related to electromagnetically induced transparency (EIT), when considering propagation effects of pulses [1]. In atomic vapor this process typically is described using dispersion profiles for simplified three-level atomic system.

In this research theoretical model for group velocity reduction in atomic vapor, based on optical Bloch equations, is developed. We use high intensity pump field, which interacts with the system creating coherences between ground- and excited-state Zeeman sublevels.

Simultaneously to that interaction with weak probe field is considered to be present. Assuming that the probe field does not change the density matrices, we obtain its susceptibility and absorption as a function of frequency in the atomic medium polarized by the pump field. The susceptibility and absorption are then used to calculate group velocity.

References

[1] M. Feischauer, A. Imamoglu, and J. P. Marangos, Electromagnetically induced transparency: Optics in coherent media **77**, 633–673 (2005)

Development of perturbed relativistic coupled-cluster theory for the calculation of dipole polarizability of closed-shell systems

S. Chattopadhyay¹, B. K. Mani², and D. Angom¹

¹*Physical Research Laboratory, Ahmedabad-380009, Gujarat, India*

²*Department of Physics, University of South Florida, Tampa, Florida 33620, USA*

Corresponding Author: sidhu@prl.res.in

The coupled-cluster theory is one of the most reliable quantum many-body theory [1–3]. It has been used with great success in atomic, nuclear, molecular and condensed matter physics calculations[4–8]. In the present work, we have developed perturbed relativistic coupled-cluster (PRCC) theory to incorporate the effect of external electric field as a perturbation in the atomic many-body calculations. For this, the coupled-cluster equations for singles and doubles cluster operators are derived and the contributing diagrams are examined. These diagrams are further evaluated using the angular momentum algebra[9]. The PRCC operators, obtained by solving the coupled non-linear coupled-cluster equations, are then used for the dipole polarizability calculation of closed-shell systems. In this poster, we will present results of electric dipole polarizability for noble gas atoms Ne, Ar, Kr and Xe, using the PRCC theory.

References

- [1] F. Coester, Nucl. Phys. **7**, 421 (1958).
- [2] F. Coester and H. Kümmel, Nucl. Phys. **17**, 477 (1960)
- [3] R. J. Bartlett and M. Musial, Rev. Mod. Phys. **79**, 291 (2007)
- [4] H. S. Nataraj *et al.*, Phys. Rev. Lett. **101**, 033002 (2008)
- [5] R. Pal *et al.*, Phys. Rev. A **75**, 042515 (2007)
- [6] G. Hagen *et al.*, Phys. Rev. Lett. **101**, 092502 (2008)
- [7] T. A. Isaev *et al.*, Phys. Rev. A **69**, 030501(R) (2004)
- [8] R. F. Bishop *et al.*, Phys. Rev. B **79**, 174405 (2009)
- [9] I. Lindgren and J. Morrison, *Atomic Many-Body Theory* (Springer-Verlag, Heidelberg, 1986)

Relativistic calculations of the transition rates for the Be-like and the Zn-like ions

H.-S. Chou³, H.-C. Chi¹

³*Institute of Optoelectronic Sciences, National Taiwan Ocean University, Keelung, Taiwan 202, Republic of China*

¹*Department of Physics, National Dong Hwa University, Hualien, Taiwan 974, Republic of China*

Corresponding Author: hschou@mail.ntou.edu.tw

We have performed relativistic many-body perturbation theory (RMBPT) calculations up to second order to study the transition amplitudes, Einstein A coefficients, and oscillator strengths for the spin-allowed electric-dipole transitions in the Be-like [1–4] and the Zn-like [5] ions. The calculations start with a V^{N-2} Dirac-Fock potential and include correlation corrections systematically. Multiconfiguration reference states are employed to account for the valence-valence correlations within the valence shell and perturbation theory is applied to systematically improve upon the wave functions. The transition amplitudes obtained in different gauges are in excellent agreement. The transition amplitudes from the RMBPT calculations agree well with experiment for all ions except for the neutral Be and Zn atoms.

References

- [1] H. S. Chou, Phys. Rev. A **62**, 042507-1–042507-14 (2000)
- [2] H. S. Chou, Phys. Scr. **64**, 140–143 (2001)
- [3] H. S. Chou, Chin. J. Phys. **39**, 41–49 (2001)
- [4] P. Bogdanovich and H. S. Chou, Lithuanian J. of Phys. **47**, 387–395 (2007)
- [5] H. C. Chi and H. S. Chou, Phys. Rev. A **82**, 032518-1–032518-9 (2010)

Semiempirical procedure of parametrization of the oscillator strengths for electric dipole transitions

J. Dembczyński¹, M. Elantkowska¹, and J. Ruczkowski¹

¹*Chair of Quantum Engineering and Metrology, Faculty of Technical Physics, Poznań University of Technology, Nieszawska 13B, 60-965 Poznań, Poland*

Corresponding Author: jerzy.dembczynski@put.poznan.pl

In this work, semiempirical procedure of parametrization of the oscillator strengths for electric dipole transitions, in the case of Ti II, is presented.

In order to parametrize the oscillator strength, the matrix of angular coefficients of the possible transitions in multiconfiguration system were calculated. In the same configuration system, the fine structure eigenvectors for both parities were obtained, using our semiempirical method, which taken into account also the second order effects, resulting from the excitations from electronic closed shells to open shells and from open shells to empty shell, described in [1].

The correctness of the fine structure wave functions was verified by the comparison of calculated and experimental hyperfine structure constants A , B , available in the literature [2,3].

The least square fit to experimental values for some transitions, published in the NIST Atomic Spectra Database [4], allow to obtain the values of radial parameters and parametrize the oscillator strengths.

This work was supported by The National Centre for Science under the project N N519 650740

References

- [1] J. Dembczyński *et al.*, J. Phys. B: At. Mol. Opt. Phys **43**, 065001 (20pp) (2010)
- [2] N. Berrah-Mansour, *et al.*, Phys. Rev. A **46**, 5774–5780 (1992)
- [3] Z. Nouri, *et al.*, Phys. Scr. **81**, 065301 (8pp) (2010)
- [4] Yu. Ralchenko, A. E. Kramida, J. Reader, and NIST ASD Team (2011). NIST Atomic Spectra Database (ver. 4.1.0), [Online]. Available: <http://physics.nist.gov/asd> [2012, March 29]. National Institute of Standards and Technology, Gaithersburg, MD

Study of the spin-orbit coupled $A^1\Sigma_u^+ \sim b^3\Pi_u$ states of the Rb_2 dimer: laser spectroscopy and refined coupled-channel treatment

A. Drozdova^{1,2}, A. Stolyarov¹, A. Ross², P. Crozet², A. Brasovs³, M. Tamanis³, and R. Ferber³

¹*Department of Chemistry, Moscow State University, 119991, GSP-1, Leninskie gory 1/3, Moscow, Russia*

²*Université Lyon 1 and CNRS (LASIM UMR 5579), Campus La Doua, 69622, Villeurbanne, France*

³*Department of Physics, University of Latvia, 19 Rainis blvd, Riga LV-1586, Latvia*

Corresponding Author: asya@laser.chem.msu.ru

Two excitation schemes, $A^1\Sigma_u^+ \sim b^3\Pi_u \leftarrow X^1\Sigma_g^+$ and $(2)^1\Pi_g \leftarrow A^1\Sigma_u^+ \sim b^3\Pi_u \leftarrow X^1\Sigma_g^+$, were used to extend the set of rovibrational energies of the $A \sim b$ complex used in [1], particularly to probe energy levels lying 13000 - 16500 cm^{-1} above the minimum of the electronic ground state. These data are required to give an accurate picture of the complex of spin-orbit coupled states, $A \sim b$, sharing the same dissociation limit, $\text{Rb}(5s) + \text{Rb}(5p)$, which should be able to provide predictions for optical mechanism leading to the formation of ultracold molecules.

Rubidium dimers were formed in a heatpipe oven around 500 K and excited with single-mode emission from (a) Ti:sapphire laser(s) operating between 10600 and 11600 cm^{-1} . Double resonance excitation was detected as enhanced fluorescence at wavelengths > 1.1 micron. Promising signals were then recorded between 6000 and 10000 cm^{-1} on an FT spectrometer (InGaAs detector) at resolution of 0.04 - 0.08 cm^{-1} , using optical filters to eliminate laser scatter, and to attenuate strong $A \rightarrow X$ emission.

We also included a few hundred energies of low vibrational levels obtained as Rb_2 impurity signals in spectra recorded (at University of Latvia) to investigate RbCs . $A \sim b \rightarrow X$ fluorescence was excited by tunable diode laser, $\lambda = 980$ nm, and recorded on an FT spectrometer Bruker IFS 125HR. The instrumental resolution was set at 0.03 cm^{-1} .

Term energy data for the $^{85}\text{Rb}_2$ and $^{85}\text{Rb}^{87}\text{Rb}$ isotopologues were then treated simultaneously in the framework of coupled-channel deperturbation model by means of the 4×4 Hamiltonian constructed in Hund's coupling case (a) basis functions, taking into account spin-orbit interaction between the $A^1\Sigma_u^+$ and $b^3\Pi_u(\Omega=0,1,2)$ states. The initial potential energy curves (PECs) and spin-orbit coupling (SOC) functions were extracted from quasi-relativistic *ab initio* calculations using small (9-electrons) effective core pseudo-potential of Rb atom.

63 fitting parameters corresponding to the analytically represented diabatic PECs and SOC functions were required to reproduce 4500 term values (representing 98% of all available data, covering 93% of the $A^1\Sigma_u^+$ potential energy well) of the $A \sim b$ complex in $^{85}\text{Rb}_2$ and $^{85}\text{Rb}^{87}\text{Rb}$ with a standard deviation of 0.005 cm^{-1} which is consistent with the uncertainty of the experiment of 0.008 cm^{-1} . The term values predicted by our model for rovibronic energies of the $^{87}\text{Rb}_2$ isotopologue confirmed reliability of derived mass-invariant parameters.

The Moscow team is grateful to the Russian Foundation for Basic Researches for support by the Grant 10-03-00195-a. The support from the Latvian Science Council Grant N 09.1567 is greatly acknowledged by Riga's team.

References

[1] H. Salami *et al.*, Phys. Rev. A **80**, 022515 (2009)

Spectral properties of In II, Sn III, Sb IV, and Te V in the Cd-sequence from large scale MCDHF and RCI calculations

S. Verdebout¹, J. Grumer², J. Ekman³, and P. Jönsson³

¹*Chimie Quantique et Photophysique, CP160/09, Université Libre de Bruxelles, , Av. F.D. Roosevelt 50, B-1050 Brussels, Belgium*

²*Department of Physics, Lund University, Sweden*

³*Group for Materials Science and Applied Mathematics, School of Technology, Malmö University, 205 06 Malmö, Sweden*

Corresponding Author: jorgen.ekman@mah.se

We report on extensive relativistic multiconfiguration Dirac-Hartree-Fock and relativistic configuration interaction spectrum calculations for In II, Sn III, Sb IV, and Te V in the Cd-sequence [1]. For each ion, energies, LS-composition, and Landé gJ -factors for up to 60 odd and even parity states are computed along with lifetimes and E1 and M1 rates for transitions between these states. Results for the $5s^2\ ^1S_0 \rightarrow 5s5p\ ^3P_0^o$ hyperfine induced transition are also presented. Valence and core-valence electron correlation effects are accounted for by explicit configuration interaction. The calculated energies are based on expansions with several hundred thousand configuration state functions (CSFs), and agree well with recent experiment [2,3], but the labeling of some of the odd states are ambiguous due to close degeneracies between several configurations. Calculated lifetimes of the excited states are in good agreement with values from cascade corrected beam-foil measurements.

References

- [1] S. Verdebout, J. Grumer, J. Ekman and P. Jnsson, manuscript in preparation for J. Phys. B (2012).
- [2] T. Rana, A. Tauheed, and Y.N. Joshi, Physica Scripta 63 (2001) 108.
- [3] T. Rana, Y.N. Joshi, and A.F. Zafaran, Physica Scripta 62 (2000) 316.

New classifications of unclassified lines in Niobium Fourier transform spectra

A. Er¹, I.K. Öztürk¹, Gö. Başar¹, S. Kröger², A. Jarmola³, R. Ferber³, and M. Tamanis³

¹*Istanbul University, Faculty of Science, Physics Department, Tr-34134 Vezneciler, Istanbul, Turkey*

²*Hochschule für Technik und Wirtschaft Berlin, Fachbereich 1, Wilhelminenhofstr. 75A, D-12459 Berlin, Germany*

³*Laser Centre, The University of Latvia, Rainis Boulevard 19, LV-1586, Riga, Latvia*

Corresponding Author: alever@istanbul.edu.tr

Niobium, with atomic number 41, has one stable isotope ⁹³Nb which is characterized by a broad hyperfine structure caused by the nuclear spin $I = 9/2$ and by the large nuclear magnetic dipole moment $\mu_I = 6.1705(3) \mu_N$ [1]. The comparatively small value of the nuclear electric quadrupole moment $Q = -0.36(7) \text{ b}$ [1] leads only to very weak deviations of the hyperfine splitting from the interval rule, which is mostly not observable in FT spectra.

The niobium spectrum was produced with a hollow cathode discharge lamp, which was cooled with liquid nitrogen. The discharge ran in an argon atmosphere at a pressure of around 1.7 mbar and with a discharge current of about 110 mA. The spectrum was recorded in the wavelength range from 330 nm to 1000 nm using high-resolution *Bruker IFS 125HR* Fourier transform (FT) spectrometer in the Laser Centre of the University of Latvia.

In previous studies [2, 3], we analysed the hyperfine structure of 275 lines of Niobium and determined from these spectra new magnetic dipole hyperfine structure constants A for 67 energy levels.

In this work, the remaining unclassified lines in the Fourier transform spectra are investigated. Several lines of Nb I and Nb II, which were unclassified in reference [4], could be classified using the classification programme [5]. All lines were fitted with a Voigt profile using the programme Fitter [6]. As a result new magnetic dipole hyperfine structure constants A of Nb I could be determined.

References

- [1] C. M. Lederer, V. S. Shirley, *Tables of Isotopes*, 7th edn. Wiley, New York (1978).
- [2] S. Kröger *et al.*, *Astronomy & Astrophysics* **516**, **A70**, (2010)
- [3] A. Er *et al.*, *Journal of Physics B: Atomic, Molecular and Optical Physics* **44**, (2011)
- [4] C. I. Humphreys, W. F. Meggers, *J. Res. Natl Bur. Stand.*, **34**, 478 (1945)
- [5] L. Windholz, G. H. Guthöhrlein, *Physica Scripta*, **T105**, 55 (2003)
- [6] G. H. Guthöhrlein, *Universität der Bundeswehr Hamburg*, unpublished (2004)

Astrophysical evidences for the variation of fundamental constants and proposals of laboratory tests

V.V. Flambaum¹

¹*School of Physics, University of New South Wales, Sydney 2052, Australia*

Corresponding Author: v.flambaum@unsw.edu.au

I present a review of recent results on a search for space-time variation of the fundamental constants. There are new results for the variation of the fine structure constant α , based on the quasar absorption spectra data. These results indicate the variation of α in space [1]. The spatial variation can explain the fine-tuning of the fundamental constants which allows humans (and any life) to appear. We appeared in the area of the Universe where the values of the fundamental constants are consistent with our existence. There is an agreement between the results obtained using different telescopes and different redshifts. Also, now there are no contradictions between the results obtained by different groups. These astrophysical results may be used to predict the variation effects for atomic clocks which are very small and require improvement of the sensitivity by 1-2 orders of magnitude. This improvement may be achieved using ^{229}Th nuclear clocks where the effect of the variation is hugely enhanced [2]. There are also enhanced effects in ions, and certain atomic and molecular transitions - see, e.g. [3-5] and review [6].

References

- [1] J.K. Webb, J.A. King, M.T. Murphy, V.V. Flambaum, R.F. Carswell, M.B. Bainbridge, *Phys. Rev. Lett.* **107**, 191101 1-5 (2011).
- [2] V.V. Flambaum, *Phys. Rev. Lett.* **97**, 092502 1-3 (2006).
- [3] V. V. Flambaum, M. G. Kozlov, *Phys. Rev. Lett.* **99**, 150801 1-4 (2007).
- [4] M.T. Murphy, V.V. Flambaum, S. Muller, C. Henkel, *Science*, **320**, 1611-1613 (2008).
- [5] V. V. Flambaum, M. G. Kozlov, *Phys. Rev. Lett.* **99**, 1508010 1-9 (2007).
- [6] J. C. Berengut, V. V. Flambaum, *J. Phys. CS* **264**, 012010 1-9 (2011).

Parity and time reversal violation in atoms and search for physics beyond the Standard Model

V.V. Flambaum¹

¹*School of Physics, University of New South Wales, Sydney 2052, Australia*

Corresponding Author: v.flambaum@unsw.edu.au

This review covers three different topics:

1. Measurements of Cs weak charge by C. Wieman group allowed to test the Standard Model predictions. We performed calculations of parity violation in Cs (also for other atoms of experimental interest like Tl, Fr, Ra+, Ba+) including all-orders summation of dominating diagrams in many-body theory and strong Coulomb field radiative corrections. The theoretical error was reduced two times. Conclusions for the Standard Model and possible "new physics" will be discussed.
2. Atomic and molecular experiments can also be used to detect nuclear anapole moment - magnetic multipole which violates fundamental symmetries: parity (P) and charge conjugation (C).
3. Measurements of atomic electric dipole moments (EDM) present a possibility to search for physics beyond the Standard model. We explain different mechanisms generating atomic EDM, screening theorems for neutral atoms, ions and molecules, and present results of recent measurements testing models of CP violation. New generation of experiments with enhanced effects will put popular models (e.g. supersymmetry) to crucial test.

References

- [1] J.S.M. Ginges, V.V. Flambaum. *Phys. Rep.* **397** 63-154 (2004).
- [2] V. V. Flambaum, A. Kozlov, *Phys. Rev. A* **85**, 022505 1-7 (2012).

Theoretical determination of the transition energies and probabilities in spectra of EuI and HgII

T. A. Florko¹

¹*Odessa State University-OSENU, P.O.Box 24a, 65009, Odessa-9, Ukraine*

Corresponding Author: quantflo@mail.ru

The experimental and theoretical studying of the radiation transition characteristics of a whole number of atomic systems is of a great importance and interest from the point of view of as the quantum electronics and atomic physics as plasma physics and thermonuclear fission science. It is also very important for search the optimal candidates and conditions for realization of the X-ray lasing. We have carried out calculating energies and probabilities of the radiative transitions for the complex heavy single ionized atom of Hg and neutral Eu atom on the basis of the combined energy approach [1] and relativistic many-body perturbation theory [2]. In all calculations we used the optimized Dirac-Kohn-Sham potential with defining its parameter within an initio QED procedure [1b]. The new data on the energies and probabilities of the 5d107p(P1/2,P3/2)-5d106s(S1/2), 5d107p(P1/2,P3/2)-5d107s(S1/2) transitions in the singly-ionized atom of Hg and 4f7(8S)6s(2)- 4f7(8S)6snp (n=6-8) transitions in spectrum of neutral EuI are listed. For comparison we listed in this table the theoretical Hartree-Fock (HF), Dirac-Fock (DF) and DF (with fitting to experimental transition energies) values [3] and experimental data by Moore (NBS, Washington). Our approach provides physically reasonable agreement with experiment and significantly more advantageable in comparison with standard Dirac-Fock method and the Hartree-Fock approximation approach. It has been checked that all results for oscillator strengths, obtained within our approach in different photon propagator gauges (Coulomb, Babushkon, Landau) are practically equal, that is provided by using an effective QED energy procedure [1b]. It has been confirmed a great role of the interelectron correlation effects of the second and higher PT orders. Some mistakes have been found in data on the table energies and radiation transition probabilities for neutral EuI.

References

- [1] E. P. Ivanova, L. N. Ivanov, L. Knight, **48**, 4365 (1993); A. Glushkov, L. Ivanov, **A170**, 33 (1992)
- [2] A. V. Glushkov *et al.*, In: *Frontiers in Quantum Systems in Chemistry and Physics*, Eds.S. Wilson, P. Grout, J. Maruani, G. Delgado-Barrio, P. Piecuch (Springer, Berlin, 2008) **18**, 505-522; S. V. Malinovskaya, A. V. Glushkov, T. A. Florko *et al.*, *Int.J.Quant.Chem.***109**, 3325 (2009)
- [3] M. Kunisz, *Acta Phys.Pol.* **62**,285 1982); V. N. Ostrovsky, S. Sheynerman, *Opt. Spectr.* **67**, 16 (1989)

Critical analysis of the methods of interpretation in the hyperfine structure for the chromium atom

P. Głowacki¹, A. Krzykowski¹, A. Jarosz¹, J. Ruczkowski¹, M. Elantkowska¹, and J. Dembczyński¹

¹*Chair of Quantum Engineering and Metrology, Faculty of Technical Physics, Poznań University of Technology, Nieszawska 13B, 60-965 Poznań, Poland*

Corresponding Author: przemyslaw.glowacki@put.poznan.pl

In this work, we analyse the experimental data, both own and available in the literature [1–3], for the even configurations of chromium atom using the semi-empirical calculations.

We use the method of quantitative determination of two-body contributions to the fine and the hyperfine structure, resulting from the excitations from electronic closed shells to open shells and from open shells to empty shell, described in [4].

Hyperfine structure intervals for levels belongs to the configurations $3d^44s^2$ and $3d^54s$ of the chromium atom were precisely measured with the use of the ABMR-LIRF method. Magnetic dipole hyperfine interaction constants (A) and electric quadrupole (B) constants for the measured electron levels have been determined with the accuracy of few kHz.

Application of the method of energy matrix diagonalization in the basis $SLJF$ allows to describe the observed hyperfine structure intervals with the use of the constants A , B and C within the experimental accuracy. The corrected values of A and B were used to parametrization of the hyperfine structure and to determine the value of the nuclear electric quadrupole moment.

This work was performed within the framework of the project DS 63-029/12.

References

- [1] W. J. Childs, L. S. Goodman, and D. von Ehrenstein, Phys. Rev. **132**, 2128–2135 (1963)
- [2] W. Ertmer, U. Johann, and R. Mosmann, Z. Phys. A **309**, 1–4 (1982)
- [3] A. Jarosz *et al.*, J. Phys. B: At. Mol. Opt. Phys **40**, 2785–2797 (2007)
- [4] J. Dembczyński *et al.*, J. Phys. B: At. Mol. Opt. Phys **43**, 065001 (20pp) (2010)

Relativistic effects on the hyperfine structures of $2p^4(^3P)3p^2D^o$, $^4D^o$ and $^2P^o$ in F I

M. Godefroid¹, M. Nemouchi², J. G. Li¹, and T. Carette³

¹Chimie Quantique et Photophysique, Université Libre de Bruxelles, B-1050 Brussels, Belgium

²Faculté de Physique, Laboratoire d'Électronique Quantique, USTHB, Algiers, Algeria

³Department of Physics, Stockholm University, SE-106 91 Stockholm, Sweden

Corresponding Author: Michel.Godefroid@ulb.ac.be

The evaluation of hyperfine interaction structures (hfs) for atomic states provides a good opportunity to study the interplay between the correlation and relativistic effects. For light atomic systems, the relativistic effects are usually included with success in the Breit-Pauli approximation [1,2]. It is worthwhile to investigate if this method is consistent with the fully relativistic approach.

In this work, the hyperfine interaction constants of the $2p^4(^3P)3p^2D^o$, $^4D^o$ and $^2P^o$ levels in neutral fluorine are investigated theoretically. Large-scale calculations are carried out using the atsp2k [3] and grasp2k [4] packages based on the multiconfiguration Hartree-Fock (MCHF) and Dirac-Fock (MCDF) methods, respectively. In both non-relativistic and relativistic models, the set of many-electron states selected to form the total wave function is constructed systematically using the “single and double multireference” approach. In the framework of MCHF, the relativistic effects are taken into account, either in the Breit-Pauli (BP) approximation using the MCHF orbitals or through relativistic configuration interaction (RCI) calculations, in which the non-relativistic one-electron basis is converted to Dirac spinors using the Pauli approximation [2].

Preliminary results are presented in table 1. In the case of $^2D^o_{5/2}$, $^4P^o_{3/2}$ and $^4P^o_{5/2}$, relativistic effects play a significant role on the hyperfine structures. Furthermore, the good agreement between the MCHF-BP, RCI and MCDF results illustrates that these three methods are valid to capture relativistic effects in a system like F I. The remaining discrepancies between experiment and theory arise from higher-order electron correlation and relativistic corrections.

Term	A_J	MCHF	MCHF-BP	RCI	MCDF	Exp [5]
$2p^4(^3P)3p^2D^o$	$A_{3/2}$	1715	1768	1765	1789	1857(2.1)
	$A_{5/2}$	2040	1691	1679	1666	1746(1.5)
$2p^4(^3P)3p^4D^o$	$A_{1/2}$	2114	2100	2107	2060	
	$A_{3/2}$	930	837	839	818	
	$A_{5/2}$	1103	1095	1100	1111	1148(1)
	$A_{7/2}$	1561	1542	1540	1526	1564(1)
$2p^4(^3P)3p^4P^o$	$A_{1/2}$	-1682	-1620	-1620	-1606	
	$A_{3/2}$	1374	1745	1735	1784	
	$A_{5/2}$	788	1007	1004	1002	

Table 1: Theoretical and experimental hyperfine interaction constants (in MHz).

References

- [1] C. Froese Fischer and G. Tachiev, Atomic Data and Nuclear Data Tables **87**, 1 (2004).
- [2] T. Carette and M. R. Godefroid, Phys. Rev. A **83**, 062505 (2011).
- [3] C. F. Fischer *et al.*, Comput. Phys. Comm. **176**, 559 (2007).
- [4] P. Jönsson *et al.*, Comput. Phys. Comm. **177**, 597 (2007).
- [5] D. A. Tate and D. N. Aturaliye, Phys. Rev. A **56**, 1844 (1997).

Isotope shift parameters, hyperfine interaction constants and Landé factors along the Be, B, C and N isoelectronic sequences

C. Nazé¹, S. Verdebout¹, P. Rynkun², P. Jönsson³, G. Gaigalas^{2,4}, and M. Godefroid¹

¹*Chimie Quantique et Photophysique, Université Libre de Bruxelles, B-1050 Brussels, Belgium*

²*Department of Physics and Information Technologies, Lithuanian University of Educational Science, Studentu 39, LT-08106 Vilnius, Lithuania*

³*School of Technology, Malmö University, 20506 Malmö, Sweden*

⁴*Research Institute of Theoretical Physics and Astronomy, Vilnius University, LT-01108 Vilnius, Lithuania*

Corresponding Author: michel.godefroid@ulb.ac.be

The mass shift parameters, the electron density at the origin, the hyperfine interaction constants and the g_J Landé factors are computed along the beryllium, boron, carbon and nitrogen isoelectronic sequences. The calculations on B- and C-like ions are based on the wave functions described in [1-4]. The many-electron wave functions corresponding to the Be and N isoelectronic sequences are obtained using the new version of the GRASP2K multiconfiguration Dirac-Fock package [5], following similar optimization strategies.

A new program [6], hereafter referred as RIS and designed as a module of GRASP2K, calculates the mass shift parameters and the electron density at the origin within the relativistic framework. For estimating the mass shift, RIS considers the expectation value of the following operator [9]

$$H_{\text{MS}} = \frac{1}{2M} \sum_{i,j}^N \left(\mathbf{p}_i \cdot \mathbf{p}_j - \frac{\alpha Z}{r_i} \left(\boldsymbol{\alpha}_i + \frac{(\boldsymbol{\alpha}_i \cdot \mathbf{r}_i) \mathbf{r}_i}{r_i^2} \right) \cdot \mathbf{p}_j \right), \quad (1)$$

that is more complete than the one calculated in SMS92 [7]. The one-body part ($i = j$) of the first term of equation (1) is responsible for the observed breakdown of the Dirac kinetic energy operator often used to evaluate the isotope normal mass shift [8]. The second term of equation (1) takes the nuclear recoil corrections into account at the (αZ) order [9]. The programs RIS and RHFS2 [5] allow the storage of the angular coefficients to reduce the cpu time when calculations are performed along a given isoelectronic sequence.

References

- [1] P. Jönsson *et al At. Data Nucl. Data Tables* **96** 271 (2010)
- [2] P. Jönsson and J. Bierón *J. Phys. B* **43** 074023 (2010)
- [3] P. Jönsson *et al At. Data Nucl. Data Tables* **97** 648 (2011)
- [4] P. Rynkun *et al At. Data Nucl. Data Tables* **98** 481 (2012)
- [5] P. Jönsson *et al Comp. Phys. Commun.* **177** 597 (2007)
- [6] C. Nazé *et al Comp. Phys. Commun.* work in progress (2012)
- [7] P. Jönsson *et al Comp. Phys. Commun.* **100** 81 (1997); P. Jönsson *et al, Ibid.*, in preparation.
- [8] J. Li *et al Eur. Phys. J. D* in preparation (2012)
- [9] V. M. Shabaev and A. N. Artemyev. *J. Phys. B*, **27** 1307 (1994).

A Partitioned Correlation Function approach for atomic properties

S. Verdebout⁵, P. Rynkun¹, P. Jönsson², G. Gaigalas^{2,4}, C. Froese Fischer⁴, and M. Godefroid¹

⁵*Chimie Quantique et Photophysique, Université Libre de Bruxelles, B-1050 Brussels, Belgium*

¹*Department of Physics and Information Technologies, Lithuanian University of Educational Science, Studentu 39, LT-08106 Vilnius, Lithuania*

²*School of Technology, Malmö University, S-20506 Malmö, Sweden*

³*Research Institute of Theoretical Physics and Astronomy, Vilnius University, LT-01108 Vilnius, Lithuania*

⁴*National Institute of Standards and Technology, MD 20899-8420 Gaithersburg, United States of America*

Corresponding Author: michel.godefroid@ulb.ac.be

Variational methods are used for targeting specific correlation effects by tailoring the configuration space. Independent sets of correlation orbitals, embedded in partitioned correlation functions (PCFs), are produced from multiconfiguration Hartree-Fock (MCHF) and Dirac-Hartree-Fock (MCDHF) calculations [1,2]. These non-orthogonal functions span configuration state function (CSF) spaces that are coupled to each other by solving the associated generalized eigenvalue problem. The Hamiltonian and overlap matrix elements are evaluated using the biorthonormal orbital transformations and efficient counter-transformations of the configuration interaction eigenvectors [3]. This method was successfully applied for describing the total energy of the ground state of beryllium [4]. Using this approach, we demonstrated the fast energy convergence in comparison with the conventional SD-MCHF method optimizing a single set of orthonormal one-electron orbitals for the complete configuration space.

In the present work, we investigate the Partitioned Correlation Function Interaction (PCFI) approach for the two lowest states of neutral lithium, i.e. $1s^2 2s \ ^2S$ and $1s^2 2p \ ^2P^o$. For both states, we evaluate the total energy, as well as the expectation values of the specific mass shift operator, the hyperfine structure parameters and the transition probabilities using different models for tailoring the configuration space. We quantify the “contraction effect” due to the use of fixed PCF eigenvector compositions and illustrate the possibility of a progressive decontraction, up to the non-orthogonal configuration interaction limit case.

Even if the lithium atom is a three electron system that can be described accurately by a single orthonormal orbitals set, the PCFI method leads to an impressive improvement in the convergence pattern of all the spectroscopic properties. As such, this system constitutes a perfect benchmark for the PCFI method. For larger systems, it becomes hopeless to saturate a single common set of orthonormal orbitals and the PCFI method is a promising approach for getting high-quality correlated wave functions. The present study constitutes a major step in the current developments of both ATSP2K and GRASP2K packages [1,2] that adopt the biorthonormal treatment for estimating energies, isotope shifts, hyperfine structures and transition probabilities.

References

- [1] C. Froese Fischer *et al.* *Comp. Phys. Commun.* **176** 559 (2007)
- [2] P. Jönsson *et al.* *Comp. Phys. Commun.* **177** 597 (2007)
- [3] J. Olsen *et al.* *Phys. Rev. E* **52** 4499 (1995)
- [4] S. Verdebout *et al.* *J. Phys. B: At. Mol. Opt. Phys.* **43** 74017 (2010)
- [5] S. Verdebout *et al.* *J. Phys. B: At. Mol. Opt. Phys.*, in preparation.

The $A^1\Sigma^+$ electronic state of KLi molecule

A. Grochola⁵, J. Szczepkowski¹, W. Jastrzębski², and P. Kowalczyk¹

⁵*Institute of Experimental Physics, University of Warsaw, Hoża 69, 00-681 Warsaw, Poland*

¹*Institute of Physics, Polish Academy of Sciences, Al. Lotników 32/46, 02-668 Warsaw, Poland*

Corresponding Author: Anna.Grochola@fuw.edu.pl

Investigations on the KLi molecule have been impeded for a long time by difficulties in production of molecular vapour of concentration sufficient for spectroscopic experiments. However, since construction of the injection heat pipe ovens and dual temperature heat pipes [1], pretty much information has been gathered on its low lying electronic states. The two lowest singlet and triplet states, $X^1\Sigma^+$ and $a^3\Sigma^+$ were characterized with high accuracy in a series of studies [2,3]. Several experiments were performed on the excited states accessible in one-photon transitions from the ground state, including the $B(1)^1\Pi$, $C^1\Sigma^+$, $D(2)^1\Pi$, $4^1\Sigma^+$, $4^1\Pi$, $6^1\Pi$ and $7^1\Pi$ states [4–9]. In the last decade the interest in KLi has been additionally stimulated by the cold physics community. Although KLi is not particularly well suited for photoassociation from cold atoms, its isotopic forms offer all possible boson/fermion pair combinations. Samples of ultracold $^{40}\text{K}^{6}\text{Li}$ molecules were produced using Feshbach resonances [10] and, very recently, also by photoassociation [11]. In view of the raising interest in KLi, it is rather surprising that the first excited state of singlet symmetry, $A^1\Sigma^+$, has never been observed, particularly that it is involved in a direct and supposedly strong transition from the molecular ground state. The reason for this neglect may be that the $A^1\Sigma^+ \leftarrow X^1\Sigma^+$ band system is placed in a near infrared part of the spectrum.

In this contribution the $A^1\Sigma^+ \leftarrow X^1\Sigma^+$ band system in the $^{39}\text{K}^7\text{Li}$ molecule is investigated by the polarisation labelling spectroscopy technique. The excited state is characterised by a set of Dunham coefficients describing rovibrational levels $v = 0 - 34$, $J = 9 - 73$ and the corresponding potential energy curve is constructed with the Rydberg-Klein-Rees method. The main equilibrium constants are $T_e = 12097.11(3) \text{ cm}^{-1}$ (with respect to the minimum of the electronic ground state), $\omega_e = 137.0821(131) \text{ cm}^{-1}$, $R_e = 3.9466(3) \text{ \AA}$.

References

- [1] V. Bednarska, I. Jackowska, W. Jastrzębski, and P. Kowalczyk, *Meas. Sci. Technol.* 7 (1996) 1291
- [2] V. Bednarska, A. Ekers, P. Kowalczyk, and W. Jastrzębski, *J. Chem. Phys.* 106 (1997) 6332
- [3] E. Tiemann, H. Knöckel, P. Kowalczyk, W. Jastrzębski, A. Pashov, H. Salami, and A.J. Ross, *Phys. Rev. A* 79 (2009) 042716
- [4] A. Pashov, W. Jastrzębski, and P. Kowalczyk, *Chem. Phys. Lett.* 292 (1998) 615
- [5] W. Jastrzębski, P. Kowalczyk, and A. Pashov, *J. Mol. Spectrosc.* 209 (2001) 50
- [6] A. Grochola, W. Jastrzębski, P. Kowalczyk, A. Ross, and P. Crozet, *Chem. Phys. Lett.* 372 (2003) 173
- [7] J. Szczepkowski, A. Grochola, W. Jastrzębski, and P. Kowalczyk, *Chem. Phys. Lett.* 499 (2010) 36
- [8] A. Grochola, W. Jastrzębski, P. Kertyka, and P. Kowalczyk, *Mol. Phys.* 102 (2004) 1739
- [9] Z. Jędrzejewski-Szmek, D. Lubiński, P. Kowalczyk, and W. Jastrzębski, *Chem. Phys. Lett.* 458 (2008) 64
- [10] A.-C. Voigt, M. Taglieber, L. Costa, T. Aoki, W. Wieser, T.W. Hänsch, and K. Dieckmann, *Phys. Rev. Lett.* 102 (2009) 020405
- [11] A. Ridinger, S. Chaudhuri, T. Salez, D. R. Fernandes, N. Bouloufa, O. Dulieu, C. Salomon and F. Chevy, *EPL*, 96 (2011) 33001

Algebraic model and experimental verification of magnetic resonance induced by amplitude-modulated light

Z. D. Grujić¹, E. Breschi¹, H.-C. Koch^{1,2}, M. Kasprzak¹, P. Knowles¹, and A. Weis¹

²*Department of Physics, University of Fribourg, CH-1700 Fribourg, Switzerland*

¹*Department of Physics, University Mainz, Staudingerweg 755124 Mainz, Germany*

Corresponding Author: zoran.grujic@unifr.ch

In the early 1960s, Bell and Bloom [1,2] reported measurements in which magnetic resonance in an atomic vapour exposed to a magnetic field was created by intensity-modulated light at frequencies close to the Larmor frequency. They observed resonances in the time-averaged power of a circularly [1] or linearly [2] polarized light beam traversing the vapour cell. In recent times this idea has been refined and led to magnetometers using frequency [3,4] or amplitude [5] modulated light together with phase-sensitive detection of the transmitted intensity or its polarization.

Here we address magnetic resonance based on light amplitude-modulation (AM). We model the AM-driven magnetic resonance by a two step model. In a first step, we solve the Bloch equations that take optical pumping, precession and relaxation into account. In a second step the absorption of the same (modulated) light field by the medium whose spin orientation is given by the steady-state oscillations of the Bloch vector components, is evaluated. By applying this procedure to each Fourier component of the incident light field, we obtain algebraic expressions for the in-phase and quadrature components of the transmitted light power. The results are valid for arbitrarily-shaped periodic modulation profiles and can be applied to ground state levels of arbitrary angular momenta in the lowest order (quadratic) light power limit. The particular case of a square wave modulation with an arbitrary duty cycle will be discussed in detail.

Experiments were done in an evacuated paraffin-coated glass cell containing room-temperature Cs vapour excited by circularly-polarized laser light, frequency-locked to the $4 \rightarrow 3$ hyperfine component of the D_1 transition. The amplitude of a magnetic field, orthogonal to the laser beam, is scanned while the modulation frequency is held constant. The photodiode signal is analyzed by a lock-in amplifier at the fundamental and higher harmonics of the modulation frequency. At each harmonic, multiple resonances are observed and their relative amplitudes and shapes are compared to the theoretical model. Implications for the use of an array of such magnetometers in the new generation neutron electric dipole moment experiment are discussed.

References

- [1] W. Bell, and A. Bloom, Phys. Rev. Lett. **6**, 280–281 (1961)
- [2] W. Bell, and A. Bloom, Phys. Rev. Lett. **6**, 623–624 (1961)
- [3] D. Budker, D. F. Kimball, V. V. Yashchuk, and M. Zolotarev, Phys. Rev. A **65**, 055403 (2002)
- [4] Ch. Andreeva, G. Bevilacqua, V. Biancalana, S. Cartaleva, Y. Dancheva, T. Karaulanov, C. Marinelli, E. Mariotti and L. Moi, Appl. Phys. B **76**, 667–675, (2003)
- [5] W. Gawlik, L. Krzemień, S. Pustelny, D. Sangla, J. Zachorowski, M. Graf, A. O. Sushkov, and D. Budker, Appl. Phys. Lett. **88**, 131108 (2006)

Experimental determination of magnetic dipole hyperfine structure constants for levels of the configuration $3d^44p$ of atomic Vanadium

F. Güzelçimen¹, G. Demir¹, Gö. Başar¹, I.K. Öztürk¹, S. Kröger², R. Ferber³,
A. Jarmola³, M. Tamaniš³, and Gü. Başar⁴

¹*Faculty of Science, Physics Department, Istanbul University, Tr-34134 Vezneciler, Istanbul, Turkey*

²*Hochschule für Technik und Wirtschaft Berlin, Wilhelminenhofstr. 75A, D-12459 Berlin, Germany*

³*Laser Centre, The University of Latvia, Rainis Boulevard 19, LV-1586 Riga, Latvia*

⁴*Faculty of Science and Letters, Physics Engineering Department, Istanbul Technical University, 34469 Maslak, Istanbul, Turkey*

Corresponding Author: feyzag@istanbul.edu.tr

This study is a continuation of our previous work on the $3d$ -shell transition metal Vanadium [1]. A systematic study of the Fourier Transform (FT) spectra of V shows that the hyperfine structure of several high-lying energy levels of atomic V is not known up to now.

High-resolution FT Spectroscopy was applied at the Laser Centre of the University of Latvia to record the spectra of a Vanadium hollow cathode discharge in the wavelength range from 360 nm to 660 nm. In the present work, particular focus is put on transitions including levels of the configuration $3d^44p$. The search for such lines was done with a classification program [2], confirming the classifications given in reference [3].

In the overview of the FT spectra, the corresponding spectral lines have low intensities. Therefore, the optical bandpass interference filters have been inserted in the set-up of the FT Spectrometer to increase the signal to noise ratio.

In total, 46 spectral lines have been investigated. Due to a Doppler limited experimental method, most of these lines show totally unresolved or partially unresolved hyperfine structure. We were able to determine the magnetic dipole hyperfine structure constants A for levels of the configuration $3d^44p$ only, because we used for our analysis the known A values of the levels of even parity previously published in [4 - 9].

As a result, 23 new magnetic dipole hyperfine structure constants A are presented for the high-lying multiplets 4P , 6F , 6D , 2G , 4I , 4H of the odd parity configuration $3d^44p$. In some cases, more than one spectral line is available to determine the hyperfine structure constant A for a level; thence using uncertainty as weight, the weighted mean value A_{mean} is calculated.

References

- [1] F. Güzelçimen *et al.* 2011 *J. Phys.B: At. Mol. Opt. Phys.* **44** 215001
- [2] Windholz L and Guthöhrlein G H 2003 *Phys. Scripta T* **105** 55
- [3] Thorne AP, Pickering JC, Semeniuk J 2011 *Astrophys J Suppl* **192** 1
- [4] Childs W J and Goodman LS 1967 *Phys. Rev.* **156** 64
- [5] Childs W J, Poulsen O, Goodman LS, Crosswhite H 1979 *Phys. Rev. A* **19** 168
- [6] Unkel P, Buch P, Dembczynski J, Ertmer W, Johann U 1989 *Z. Phys.* **11** 259
- [7] Palmeri P, Biemont B, Aboussaid A, Godefroid M 1995 *J. Phys.B: At. Mol. Opt. Phys.* **28** 3741
- [8] Palmeri P, Biemont E, Quinet P, Dembczynski J, Szawiola G 1997 *Phys. Scripta* **55** 586
- [9] Lefebvre PH, Garnir HP, Biemont E 2002 *Phys. Scripta* **66** 363

Investigations of VUV transitions of iron for astrophysical applications using synchrotron radiation

H. Hartman^{1,2}, H. Nilsson², S. Hultdt², T. Lennartsson², E. Bäckström³,
S. Mannervik³, and S. Ristinmaa Sörensen⁴

¹Group for Materials Science and Applied Mathematics, School of Technology, Malmö University, 205 06 Malmö, Sweden

²Lund Observatory, Lund University, Box 43, SE-22100 LUND, SWEDEN

³Department of Physics, Stockholm University, SE-106 91 STOCKHOLM, Sweden

⁴Department of Physics, Lund University, SE-221 00 LUND, Sweden

Corresponding Author: Henrik.Hartman@mah.se

We have developed an experimental station at the gas-phase branch line at the 6.65 m normal incidence beam line at I3, MAX-lab, Sweden. It is used to investigate free metal atoms and ions in plasma phase, and their spectral properties. The sample ions are produced in a hollow cathode discharge lamp, which is illuminated by the synchrotron radiation producing absorption when in resonance with the atomic lines. The synchrotron light is scanned in energy building up an absorption spectrum. From relative absorptions for transitions with common levels transition rates are derived. Contributions from intrinsic light of the discharge are minimized through geometrical, spectral and temporal filters.

The projects major goal is to measure transition rates (or oscillator strengths) for specific lines in the spectrum of ionized iron, Fe II lines, at vacuum UV wavelengths, 100-130 nm. These transitions are important for many astrophysical applications, e.g. in objects where line fluorescence is prominent, as well as stars observed in the ultraviolet FUSE and HST/STIS region. Level mixing make several of these levels uncertain to calculate. In this wavelength region many other iron-group element ions have important transitions, which will be measured in future projects.

Iron lines are of great importance in analyses of stars, nebulae and the interstellar medium, not only for abundance studies, but also for diagnostics of the plasma conditions and derivation of physical properties such as temperature, electron density and radiation field.

We describe the experimental setup at the I3 beam line at MAX III, the reduction technique and the early results from neutral iron, FeI.

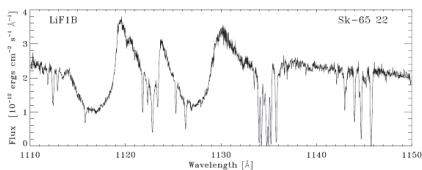


Figure 1: FUSE spectrum showing narrow iron absorption from interstellar clouds.

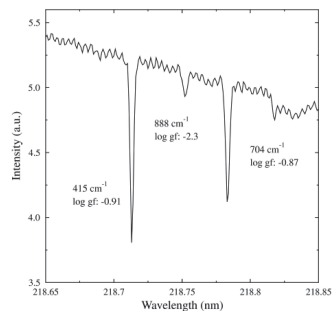


Figure 2: Absorption from iron atoms in the discharge lamp.

Towards a ${}^3\text{H}/{}^3\text{He}$ Mass-Ratio Measurement with THE-Trap

J. Ketter¹, T. Eronen¹, M. Höcker¹, S. Streubel¹, R. S. Van Dyck, Jr.², and K. Blaum¹

¹*Max-Planck-Institut für Kernphysik, 69117 Heidelberg, Germany*

²*University of Washington, Seattle, WA 98195-1560, USA*

Corresponding Author: jochen.ketter@mpi-hd.mpg.de

Penning-trap mass spectrometry has the prospect of complementing the determination of the electron antineutrino's mass by KATRIN [1], the Karlsruhe Tritium Neutrino Experiment. KATRIN employs a retardation spectrometer for electrons to investigate the kinematics of the beta-decay of tritium. A more accurate independent determination of the decay's Q -value by measuring the masses of ${}^3\text{H}$ and its daughter ${}^3\text{He}$ will help pin down the endpoint of the electron spectrum, where a nonzero neutrino mass leaves its mark.

In a Penning trap, which consists of the superposition of a strong magnetic field and a quadrupolar electrostatic potential, the mass of an ion is linked to a measurement of its mass-dependent eigenfrequencies, from which the free-space cyclotron frequency can be recovered. A specialized experiment is required in order to meet the challenges of a mass-ratio measurement of ${}^3\text{H}$ and ${}^3\text{He}$ with a relative uncertainty of 10^{-11} .

Originally developed at the University of Washington in Seattle, the UW-PTMS (University of Washington Penning Trap Mass Spectrometer) was moved to the Max Planck Institute for Nuclear Physics in Heidelberg in 2008, where the experiment has been commissioned in a dedicated laboratory. Special safety precautions had to be taken in order to obtain an official permission to handle a gaseous tritium source. The lab features temperature stabilization and the extremely stable superconducting magnet system rests on a vibrationally isolated platform. The helium level and pressure inside the magnet's bore are stabilized to limit magnetic field fluctuations caused by the temperature-dependent magnetic susceptibility of the materials surrounding the traps. Furthermore, a flux-gate magnetometer controls a Helmholtz coil used to compensate for fluctuations of external magnetic fields.

In contrast to its single-trap closed-system predecessor, THE-Trap, formerly known as the MPIK/UW-PTMS [2], combines two hyperbolic Penning traps with an external ion source, yet retaining the possibility to load the traps by ionizing rest gas with electrons from a field emission point inside the trap envelope. External ion loading is expected to reduce the number of unwanted species trapped and to minimize the risk of contaminating the trap electrodes with radioactive tritium. By swapping the ions-of-interest (${}^3\text{H}$, ${}^3\text{He}$) between the two traps without having to reload the trap, the total measurement cycle will be shortened, thereby reducing the influence of magnetic field drifts, while also allowing to accumulate more statistics within the same amount of measurement time. However, the transfer between the two traps through small holes in the endcaps in single-pass mode requires the use of a well-timed sequence of transfer pulses on various electrodes that has yet to be demonstrated.

The non-destructive ion detection relies on the image currents the moving ions induce in the trap electrodes. These currents in the femtoamp range cause a voltage drop across a tuned circuit. This ion signal is subsequently amplified by a cryogenic differential amplifier and processed with room-temperature electronics. The detection scheme is based on a triggered sweep technique which monitors the ion's response to an external drive. By sharing drive and signal lines for both traps, a full replication of the whole drive and detection system for the additional trap is avoided. A novel voltage source [3] based on a cascade of voltage-references replaces the previously used Weston cells.

Details about the experimental setup and recent progress will be given.

References

- [1] E. W. Otten *et al.*, Int. J. Mass Spectrom. 251 (2006) 173–178
- [2] C. Diehl *et al.*, Hyperfine Interactions (2011) 199:291–300
- [3] D. B. Pinegar *et al.*, Rev. Sci. Instrum. 80, 064701 (2009)

Quantum structure of electro-weak interaction in heavy atomic systems and Parity nonconservation effect

O. Yu. Khetselius¹

¹*Odessa State University-OSENU, P.O.Box 24a, 65009, Odessa-9, Ukraine*

Corresponding Author: nuckhet@mail.ru

During the past two decades, the nuclear and atomic-optical experiments to detect parity non-conservation (*PNC*) have progressed to the point where *PNC* amplitudes can be measured with accuracy on the level of a few percents in certain heavy atoms and significantly worse in some nuclei (*Mossbauer* spectroscopy). Nowadays the *PNC* in atoms has a potential to probe a new physics beyond the standard model. In our paper we systematically apply the nuclear-relativistic many-body perturbation theory formalism [1,2] to precise studying *PNC* effect in heavy atoms with account for nuclear, correlation and QED corrections. There are determined the *PNC* radiative amplitudes for a set of nuclei (atoms): ^{133}Cs , $^{137}\text{Ba}^+$, ^{205}Tl , ^{173}Yb with account of exchange-correlation, Breit, weak e-e interactions, QED and nuclear (magnetic moment distribution, finite size, neutron skin) corrections, nuclear-spin dependent corrections due to anapole moment, Z-boson ($(A_n V_e)$ current) exchange, hyperfine -Z exchange ($(V_n A_e)$ current). The most exciting result is the weak charge for ^{173}Yb . Using the experimental value $E^{PNC}/\beta=39\text{mV/cm}$ (Tsigutkin et al, 2009) and our calculated amplitude value ($9.707 \cdot 10^{-10}$ ea) one could find for ^{173}Yb ($Z=70$, $N=103$) the weak charge value $Q_W=-92.31$ (the SM gives $Q_W=-95.44$). The received data are compared with known earlier and recent results by Flambaun-Dzuba et al, Johnson-Safronova et al, by Johnson-Sapirstein-Blundell et al (look [3,4] and refs. therein). The role of the nuclear effects contribution, spatial distribution of magnetization in a nucleus and non-accounted high order QED corrections and at last the dynamical enhancement of the weak e-N, N-N interaction are analyzed. Some perspective lanthanides isotopes are proposed for future studying.

References

- [1] O. Yu. Khetselius, Phys.Scripta **T135**, 014023 (2009)
- [2] O. Yu. Khetselius, Int.J.Quant.Chem. **109**, 3330-3336 (2009)
- [3] W. R. Johnson, M. S. Safronova, U. I. Safronova, Phys.Rev. **A69**, 062106 (2003)
- [4] V. V. Flambaun, J. S. Ginges, Phys.Rev. **A72**, 052115 (2005)

Laser electron-gamma-nuclear spectroscopy of heavy atoms and NEET effect in heavy atomic/nuclear systems.

O. Yu. Khetselius¹

¹*Odessa State University-OSENU, P.O.Box 24a, 65009, Odessa-9, Ukraine*

Corresponding Author: nuckhet@mail.ru

In the resonant process of nuclear excitation by electron transition (NEET) or electron capture (NEEC) an electron is captured into a bound atomic shell with the simultaneous excitation of the nucleus [1,2]. The excited nucleus can then decay radiatively or by internal conversion. In the latter case, a resonant inelastic electron scattering on the nucleus occurs. Here we present consistent, relativistic approach to calculation of the probabilities of the different cooperative laser electron-gamma-nuclear processes in atoms, ions, nuclei and resonant NEET (NEEC) processes in heavy nuclei, based on the relativistic optimized Dirac-Fock-Woods-Saxon formalism and energy approach (S-matrix formalism of Gell-Mann and Low) [3]. Decay and excitation probability is linked with the imaginary part of energy of the excited state for the electron shell-nucleus-photon system. For radiate decays it is manifested as effect of retarding in interaction and self-action and calculated within QED theory. We firstly present data about intensities of the electron satellites in gamma-spectra of nuclei in the neutral (low lying transitions) and multicharged O- and F-like ions for isotopes ⁵⁷Fe, ¹³³Cs, ¹⁷³Yb and discover an effect of the giant increasing electron satellites intensities under transition from the neutral atoms to multicharged ions. There are presented new data about NEET probabilities in the nuclei of ¹⁸⁹Os, ¹⁹⁷Au (comparison with exp. data of Argonne Nat.Lab. and Japan synchrotron Centre) [2] and firstly for nuclei of ²³⁵U, ²⁶⁸Mt.

References

- [1] M. Morita, *Progr.Theor.Phys.***49**, 1574 (1973); V. S. Letokhov, V. I. Goldanskii, *JETP*, **67**, 513 (1974); V. I. Goldanskii, V. A. Namiot, *Phys. Lett.B* **62**,393 (1976); L. N. Ivanov, V. S. Letokhov, *JETP*,**93**, 396 (1987); . Glushkov, L. Ivanov, V. Letokhov, Preprint ISAN NAS-1, Moscow-Troitsk (1991)
- [2] E. V. Tkalya, *Phys.Rev.A*,**75**, 022509 (2007); I. Ahmad *et al.*, *Phys. Rev. C* **61**, 051304 (2000); S. Kishimoto *et al.*, *Nucl.Phys.A* **748**, 3 (2005); *Phys.Rev. C* **74**, 031301 (2006)
- [3] O. Yu. Khetselius, *Phys.Scripta* **T34**, 014023 (2009); *Int.J.Quant.Chem.* **109**, 3330 (2009); *In: Progress in Theoretical Chem. and Phys.*, Eds.K. Nishikawa, J. Maruani, E. Brandas, G. Delgado-Barrio, P. Piecuch (Springer, Berlin, 2012) **24**, 51

Rovibrational levels of hydrohelium cation

K. Pachucki¹, J. Komasa²

¹*Institute of Theoretical Physics, University of Warsaw, Hoża 69, 00-681 Warsaw, Poland*

²*Faculty of Chemistry, A. Mickiewicz University, Grunwaldzka 6, 60-780 Poznań, Poland*

Corresponding Author: komasa@man.poznan.pl

Dissociation energies of bound rovibrational states of hydrohelium cation (HeH^+) in the ground electronic state have been calculated by including nonadiabatic, relativistic, and quantum electrodynamic effects.

The energy levels have been evaluated using an expansion of the energy in powers of the fine structure constant, α

$$E = E^{(0)} + \alpha^2 E^{(2)} + \alpha^3 E^{(3)} + \alpha^4 E^{(4)} + \dots$$

The individual terms of this expansion have a clear physical interpretation: the first term represents the nonrelativistic energy, $\alpha^2 E^{(2)}$ is the leading relativistic contribution, terms proportional to α^3 and α^4 are the QED effects of the leading and higher order, respectively. The nonrelativistic energy $E^{(0)}$ is composed of the adiabatic energy corrected for the presence of the nonadiabatic effects. The nonadiabatic correction has been obtained by means of a recently developed perturbation theory [1], which introduces variable nuclear reduced masses and a radial correction to the adiabatic potential energy curve. The α^2 relativistic effects have been computed as an expectation value of the Breit-Pauli Hamiltonian. Also the effect of the final size of the nuclear charge has been taken into account. Rigorous evaluation of the Bethe logarithm and the Araki-Sucher term enabled a complete treatment of the α^3 and $\alpha^3 \log \alpha$ QED effects [2]. In addition, an approximate α^4 QED correction, based on the so-called one-loop term, has been evaluated.

References

- [1] K. Pachucki and J. Komasa, *J. Chem. Phys.* **130**, 164113 (2009).
- [2] J. Komasa, K. Piszczatowski, G. Lach, M. Przybytek, B. Jeziorski, and K. Pachucki, *J. Chem. Theory Comput.* **7**, 3105 (2011).

Hyperfine-resolved polarizability measurement of the Cs $9s\ ^2S_{1/2}$ state

A. Kortyna¹, H. Weaver¹

¹*Department of Physics, Lafayette College, Easton, PA 18042, U.S.A.*

Corresponding Author: kortynaa@lafayette.edu

We report the first polarizability measurement of atomic cesium's $9s\ ^2S_{1/2}$ hyperfine states. We use two single-mode external-cavity diode lasers: one locked to a $6s\ ^2S_{1/2}(F'') \rightarrow 6p\ ^2P_{1/2}(F')$ transition and the second stepped across the $6p\ ^2P_{1/2}(F') \rightarrow 9s\ ^2S_{1/2}(F)$ manifold. Two spectra are generated concurrently. One is a laser-induced-fluorescence spectrum from a collimated effusive beam in a region of uniform electric field (Fig. 1 upper panel). The electric field strengths are calibrated by measuring the $6s\ ^2S_{1/2} \rightarrow 6p\ ^2P_{1/2}$ polarizability and comparing it to a previous high-precision measurement [1]. For frequency calibration, we also record an absorption spectrum in a field-free vapor cell with the $6p\ ^2P_{1/2} \rightarrow 9s\ ^2S_{1/2}$ laser phase modulated (Fig. 1 lower panel). The modulation frequency is directly reference to a rubidium frequency standard and the resulting modulation sidebands provide frequency markers.

The $9s\ ^2S_{1/2}$ Stark shift measurements show the expected electric-field-squared dependence. A total of 40 Stark shift measurements are used to compute the $9s\ ^2S_{1/2}$ scalar polarizability as 144660 ± 610 au and the magnetic dipole contact interaction as 630 ± 110 au. The scalar polarizability does not agree with recent relativist all order calculations (153700 ± 1100 au [2]). We are currently evaluating the accuracy of our apparatus by measuring the $8s\ ^2S_{1/2}$ scalar polarizability, which will be compared to previous measurements [3].

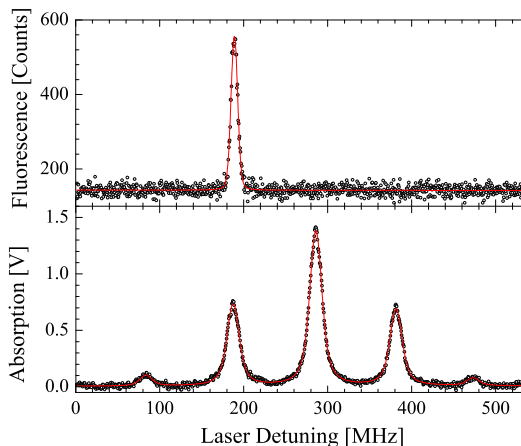


Figure 1: Concurrent Cs $6p_{1/2} \rightarrow 9s_{1/2}(F=4)$ spectra (circles) and fitted Voigt profiles (lines). Upper panel: fluorescence from an effusive beam at 2.55 ± 0.02 kV/cm. Lower panel: absorption in a field-free vapor cell with 110 MHz phase modulation for frequency calibration.

References

- [1] L. Hunter *et al.*, *Opt. Comm.* **94**, 210 (1992).
- [2] J. Mitroy, M. S. Safronova, and C. W. Clark, *J. Phys. B* **43**, 202001 (2010).
- [3] D. Antypas and E. Elliott, *Phys. Rev. A* **83**, 062511 (2011).

Polarisation labelling spectroscopy of the $2^1\Pi$ state of NaLi

N. H. Bang¹, D. X. Khoa¹, N. T. Dung¹, J. Szczepkowski², W. Jastrzębski², and
P. Kowalczyk³

¹*Vinh University, 182 Le Duan Str., Vinh City, Vietnam*

²*Institute of Physics, Polish Academy of Sciences, Al. Lotnikow 32/46, Warsaw, Poland*

³*Institute of Experimental Physics, Department of Physics, University of Warsaw, Hoza 69,
Warsaw, Poland*

Corresponding Author: Pawel.Kowalczyk@fuw.edu.pl

An interest in alkali dimers has increased considerably in recent years because of spectacular progress in ultracold physics. Heteronuclear alkali molecules are of particular importance here because their permanent electric dipole moments allow to manipulate them by external electric fields. NaLi molecule is the lightest among these species.

The knowledge of electronic states of NaLi molecule has been recently extended to the $7^1\Pi$ and $10^1\Sigma^+$ states [1,2]. However, one of the low excited states, $2^1\Pi$, was still known only at vibrational resolution [3]. The potential curve of this state was predicted theoretically to be of rather unusual shape because of small potential barrier towards dissociation, arising from an interplay between the repulsive van der Waals interaction and attractive exchange forces [4].

In the present experiment we employ the polarisation labelling spectroscopy method [5] to investigate the $2^1\Pi \leftarrow X^1\Sigma^+$ band system in NaLi under rotational resolution. We observe all bound vibrational levels contained in the $2^1\Pi$ state potential, thus exploring the molecular state up to the barrier. The potential energy curve is constructed from the experimental data, using a fitting procedure (Inverted Perturbation Approach) developed in our group [6].

References

- [1] N. H. Bang *et al.*, J. Chem. Phys. **130**, 124307 (2009)
- [2] I. D. Petsalakis *et al.*, Chem. Phys. **362**, 130 (2009)
- [3] M. M. Kappes, *et al.*, Chem. Phys. Lett. **107**, 6 (1984)
- [4] N. Mabrouk, and H. Berriche, J. Phys. **B41**, 155101 (2008)
- [5] W. Jastrzębski and P. Kowalczyk, Phys. Rev. **A51**, 1046 (1995)
- [6] A. Pashov, W. Jastrzębski, and P. Kowalczyk, Comput. Phys. Commun. **128**, 622 (2000)

Measurements of Stark Widths of Fe II lines by laser induced breakdown spectroscopy

J. Manrique¹, J.A. Aguilera², and C. Aragón²

¹*Facultad de Farmacia, Universidad San Pablo CEU, Urbanización Montepríncipe, Boadilla del Monte, E-286 68 Madrid, Spain*

²*Departamento de Física, Universidad Pública de Navarra, Campus de Arrosadía, E-310 06 Pamplona, Spain*

Corresponding Author: jamanros@ceu.es

Stark broadening parameters are widely used for plasma physics and atomic structure studies. Namely the emission observed from the Sun and hotter stars depends on the opacity produced by ionized iron and some other elements [1]. Despite its relevance, the available experimental and calculated data of Stark widths of ionized iron are scarce.

In the present work, we report new experimental Stark widths of Fe II lines including weak and intense lines belonging to 24 multiplets. The measurements have been performed using laser-induced plasmas as spectroscopic sources with two sets of Fe-Cu and Fe-Ni samples with variable iron concentration (0.2-22 %). The detector is a photomultiplier tube, whose signal is amplified and captured by a digital oscilloscope. A home-made program controls the movement of the grating and the data acquisition [2]. From the stored signal the software averages out nine acquisitions and obtains the spectra at selected time windows of the plasma evolution ranging from 0.84 μs to 3.6 μs . As a consequence, the Stark widths have been determined at electron densities in the range $(1.6-7.4)\times 10^{17}\text{ cm}^{-3}$ corresponding to the selected intervals [3]. The electron density is determined from the Stark broadening of the H_{α} line. For this type of plasma, the existence of optically thin conditions is specially relevant as self-absorption leads to distortion of the line profiles, which results in larger width (Fig. 1). The curve of growth methodology [4] has been applied to avoid self absorption in the Stark width measurements.

For some of the measured lines, the selected iron concentration and the Stark widths obtained are shown in Table 1.

Wavelength (\AA)	C (wt. %)	w(\AA)
2585.88	0.2	0.0411
2382.04	0.5	0.038
2444.52	1.5	0.046
2430.08	5.0	0.044
2469.52	10.0	0.046

Table 1: Stark width (FWHM) normalized at the electron density $N_e=10^{17}\text{ cm}^{-3}$ of Fe II lines for a temperature range 12900-15200 K.

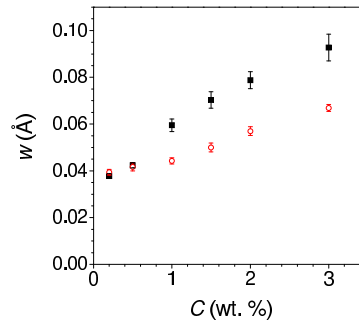


Figure 1: Normalized Stark widths of 2382.04 \AA (solid squares) and 2585.88 \AA (open circles) Fe II lines as a function of the iron concentration in the sample.

References

- [1] J. Gurell, H. Hartman, R. Blackwell-Whitehead, H. Nilsson, E. Bäckström, L. O. Norlin, P. Royen, and S. Mannervik, *Astron. Astrophys.* **508**, 525–529 (2009)
- [2] C. Aragón, P. Vega, and J. A. Aguilera, *J. Phys. B* **44**, 055002 (2011)
- [3] J. A. Aguilera, J. Manrique, and C. Aragón, *J. Phys. B* **44**, 245701 (2011)
- [4] C. Aragón, F. Peñalba, and J. A. Aguilera, *Spectrochimica Acta Part B* **60**, 879 (2005)

Modification of Initially Forbidden Atomic Transitions of Rb D_2 line in Magnetic Field

R. Mirzoyan^{1,2}, G. Hakhumyan^{1,2}, C. Leroy¹, Y. Pashayan-Leroy¹, and D. Sarkisyan²

¹Laboratoire Interdisciplinaire Carnot de Bourgogne, UMR CNRS 6303, Universite' de Bourgogne, 21078 Dijon Cedex, France

²Institute for Physical Research, NAS of Armenia, Ashtarak 0203, Armenia

Corresponding Author: rafayelm@gmail.com

Atom located in a magnetic field undergoes shifts of the energy levels and changes in transition probabilities, therefore precise knowledge of these behaviors are very important. Recently it was shown that spectrally narrow velocity-selective optical pumping (VSOP) resonances located exactly at the positions of atomic transitions appear in the transmission spectrum of a one-dimensional nanometric-thin cell (NTC) with the thickness of Rb atomic vapor column $L = \lambda$, where $\lambda = 780$ nm is the wavelength of the laser radiation resonant with D_2 line. When the NTC is placed in a magnetic field, the VSOPs are split into several components with the amplitudes and frequency positions depending on the B -field, which makes it convenient to study separately each individual atomic transition and thus this technique may be called λ -Zeeman technique (λ -ZT) [1]. By the exploration of the λ -ZT we reveal for the first time a strong modification of probability of the ^{87}Rb D_2 line $F_g=1 \rightarrow F_e=0, 1, 2, 3$ atomic transitions, including initially forbidden transition $(1, m_F = 0) \rightarrow (1, m_F = 0)'$ labeled 5 and transition $(1, m_F = -1) \rightarrow (3, m_F = -1)'$ labeled 3 in the range of magnetic field 100 - 1100 G. For π -polarized exciting diode laser radiation, transitions 5 and 3 at $B > 150$ G are among the strongest in the transmission spectra shown in Fig. 1. Also the frequency shifts of the individual hyperfine transitions vs magnetic field are presented: particularly, transition labeled 8 has a unique behavior, since its frequency remains practically unchanged in the range of 100 - 1100 G. The theory well describes the experiment.

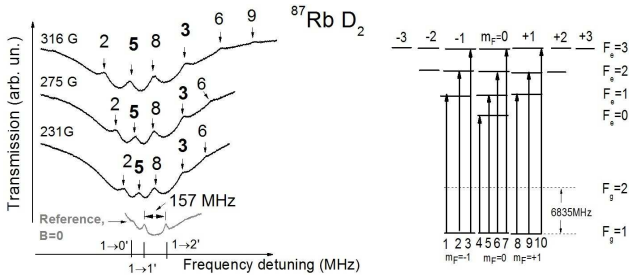


Figure 1: Transmission spectra (shown in the left side) from the Rb NTC $L = 780$ nm for transitions $F_g=1 \rightarrow F_e=0, 1, 2, 3$ vs magnetic field. VSOPs numbers denote the corresponding transitions depicted in the right side. Initially forbidden transitions labeled 3 and 5 are among the strongest atomic transitions, when magnetic field is $B > 150$ G. The lower grey curve is the transmission spectrum from the reference Rb NTC $L = \lambda$. The spectra are shifted vertically for convenience. Diagram of the ^{87}Rb , D_2 line (shown in the right side) transitions for π -polarized excitation ($m_F = 0$) is shown.

The research leading to these results has received funding from the European Union FP7/2007-2013 under grant agreement n° 205025 - IPERA. Research conducted in the scope of the International Associated Laboratory IRMAS (CNRS-France & SCS-Armenia).

References

[1] A. Sargsyan, G. Hakhumyan, A. Papoyan, et al., Appl. Phys. Lett. 93, 021119 (2008).

Fourier Transform Spectroscopy of $B^1\Pi$ State in RbCs

I. Birzniece¹, O. Docenko¹, O. Nikolayeva¹, M. Tamanis¹, and R. Ferber¹

¹*Laser Center, Department of Physics, University of Latvia, 19 Rainis blvd., LV-1586, Riga, Latvia*

Corresponding Author: onikolay@latnet.lv

The lowest $^1\Pi$ state of the RbCs molecule, the $B^1\Pi$ state, was studied using a diode lasers for inducing fluorescence that was resolved by a high resolution Fourier-transform spectrometer (FTS) Bruker IFS - 125HR. RbCs molecules were produced in a linear heat-pipe filled with 10 g of rubidium (natural isotope mixture) and 7 g of cesium at temperature about 280°C and were excited in transition $B(1)^1\Pi(v', J') \leftarrow X(v'', J'' = J', J' \pm 1)$. Back-scattered laser induced fluorescence (LIF) was sent onto input aperture of FTS by a pierced mirror. Spectra were recorded by FTS at resolution 0.03 cm⁻¹. A diode laser with 705 nm or 730 nm laser diode installed in a home-made external resonator was used for excitation. Laser frequency used in the experiment varied from 13610 to 13860 cm⁻¹ for 730 nm diode and from 14063 to 14223 cm⁻¹ for 705 nm diode. As a detector mainly InGaAs photodiode operating at room temperature was used (over 80% of recorded spectra), but in some cases it was replaced by silicon photodiode operating at room temperature. The assignment of the LIF progressions in the $B \rightarrow X$ spectra was straightforward from measured vibrational and rotational spacings exploiting to accurate ground state potential [1]. The term values of the rovibronic levels of the $B^1\Pi$ state giving rise to $B \rightarrow X$ LIF were obtained by adding the corresponding ground state level energy to a transition wave number. The presence of argon buffer gas yielded rich rotational relaxation spectra allowing to enlarge the data set for the $B(1)^1\Pi$ state, to obtain Λ -splitting and to reveal numerous local perturbations. The uncertainty of measured lines position is 0.1 from spectrum resolution, that is the 0.003 cm⁻¹. Due to the Doppler profile of the absorption transition uncertainty of upper state energy is 0.01 cm⁻¹.

Data covering a large number of adjacent J' were obtained for $v' \in [0; 3]$. Rotational constant $B_{v'}$ has been calculated as dependent on J' ; $B_{v'}$ values falling out from the smooth behavior indicated the presence of local perturbations. The respective levels were omitted from the fit. Point-wise potential energy curve (PEC) and Dunham-type constants were obtained describing non-perturbed or weakly perturbed f -levels up to $v' = 2$ with standard deviation of 0.15 cm⁻¹. Such accuracy, being worse than experimental uncertainty indicates presence of strong perturbations. For weakly perturbed levels with $v' = 0$ and 1 included in the fit, the differences between experimental term values and the ones calculated from the PEC do not exceed 0.03 cm⁻¹.

The support from ESF grant Nr. 2009/0223/1DP/1.1.1.2.0/09/APIA/VIAA/008 is gratefully acknowledged.

References

- [1] O. Docenko *et al.*, Phys. Rev. A **83**, 052519 (2011)

Semiempirical calculation of energies spectra configurations 2p3p4p CI, 3p4p5p SiI and PII, 4p5p6p GeI and gyromagnetic ratios

G.P. Anisimova¹, O.A. Davlatova¹, and V.A. Polischuk¹

¹*Department of Physics, Saint Petersburg State University, 199034, 7-9 Universitetskaya nab.,
Russia*

Corresponding Author: vpvova@rambler.ru

Fine structure parameters, energy of excitation of levels, expansion coefficient of wave in the LS-coupling basis and gyromagnetic ratios are obtained by semiempirical method (with zero differences between calculation and experiment). For a phosphorus ion and atom germanium gyromagnetic ratios were calculated, which comparison with analogous experimental data.

Parameters of fine structure it is unknown sizes which in semiempirical calculation are defined from the decision of system of the nonlinear equations which are received from analytical reduction not diagonal hermitian matrixes of the operator of energy to a diagonal kind.

$$|\varepsilon\rangle = U^{-1}|E\rangle U, \quad (1)$$

where $|\varepsilon\rangle$ - a diagonal matrix (experimentally measured levels of thin structure), E - not diagonal matrix of the energy operator, U -it factors of decomposition of wave functions of real communication on wave functions of any vector type of communication

The system of the equations for numerical calculation of parameters of fine structure is received on the basis of analytical reduction of not diagonal matrix of the operator of energy to a diagonal kind and added by the equations normalization orthogonality of factors of communication.

The matrix of the energy operator was obtained by using formulas of the general form taken from [1]. In a matrix of the operator of energy following interactions are considered: electrostatic, backs - an orbit, backs-another's an orbit, backs-backs, an orbit-orbit. Last three interactions are small in comparison with two first, but give the contribution to energy of levels of thin structure, providing zero are nonviscous. It is very important at theoretical research of considered systems in external fields, in particular magnetic that gives the chance to receive gyromagnetic ratios on splitting of levels in linear area of a magnetic field for atoms and ions at which g-factors aren't measured yet, for example for atom of carbon and the silicon considered in work.

References

[1] A. P. Yutsis, A. Yu. Savukinas., *Mathematical Foundations of Atomic Theory*. Mintis, Vilnius, 1973

Calculations of energy levels of the beryllium atom

J. Komasa¹, M. Puchalski¹, and K. Pachucki²

¹*Department of Chemistry, Adam Mickiewicz University, Poznań, Poland*

²*Faculty of Physics, University of Warsaw, Warsaw, Poland*

Corresponding Author: mariusz.puchalski@amu.edu.pl

Accurate results for nonrelativistic energy, relativistic, quantum electrodynamics and finite nuclear mass corrections are obtained for the ground state 2^1S and the excited 2^1P state of the beryllium atom. A basis set of correlated Gaussian functions is used, with exponents optimized against nonrelativistic binding energies [1]. Obtained results for Bethe logarithms [2] demonstrate the availability of high precision theoretical predictions for light four-electron atomic systems within the NRQED theory [3], with expansion terms ordered in powers of the fine structure constant α . Several results for the beryllium, including 2^1P-2^1S transition and ionization energy will be presented, which are few order of magnitude more accurate than obtained previously [4,5].

References

- [1] J. Komasa, J. Rychlewski, and K. Jankowski, *Phys. Rev. A* **65**, 042507 (2002).
- [2] C. Schwartz, *Phys. Rev.* **123**, 1700 (1961).
- [3] K. Pachucki, *Phys. Rev. A* **71**, 012503 (2005).
- [4] K. Pachucki, and J. Komasa, *Phys. Rev. Lett.* **92**, 213001 (2004).
- [5] S. Bubin, and L. Adamowicz, *Phys. Rev.* **79**, 022501 (2009).

Hyperfine Paschen-Back regime study using Rb Nano-Thin Cell

A. Sargsyan¹, G. Hakhumyan^{1,2}, C. Leroy², Y. Pashayan-Leroy², A. Papoyan¹, and D. Sarkisyan¹

¹*Institute for Physical Research, NAS of Armenia, Ashtarak 0203, Armenia*

²*Laboratoire Interdisciplinaire Carnot de Bourgogne, UMR CNRS 6303, Universite' de Bourgogne, 21078 Dijon Cedex, France*

Corresponding Author: sarmeno@mail.ru

The implementation of the so-called λ -Zeeman technique (λ -ZT) allows us to obtain Hyperfine Paschen-Back (HPB) regime of Rb atoms in a strong magnetic field in the range of 0.5-0.7T [1]. λ -ZT is based on narrow velocity selective optical pumping (VSOP) resonances formation in nanometric thin cell (NTC) transmission spectrum of thickness $L = \lambda$, where $\lambda = 794$ nm is the resonant wavelength of Rb D_1 line. The VSOP resonance is split into several components in a magnetic field; their frequency positions and transition probabilities depends on B -field. NTC allows to apply permanent magnets facilitating significantly the creation of strong magnetic field [2]. The magnetic field required to decouple the nuclear and electronic spins is given by $B \gg A_{hfs}/\mu_B$ (~ 0.07 T) for ^{85}Rb , where A_{hfs} is the ground-state hyperfine coupling coefficient and μ_B is the Bohr magneton. For this case the eigenstates of the Hamiltonian are described in a uncoupled basis of J and I projections ($m_J; m_I$). In Fig. 1a, six transitions labeled 1–6, are shown in the case of σ^+ polarized laser excitation for the HPB. The B -field dependence of frequency shift is shown in Fig. 1b (solid lines: HPB theory; symbols: experiment). Rb NTC could be implemented for mapping strongly inhomogeneous magnetic fields by local submicron spatial resolution.

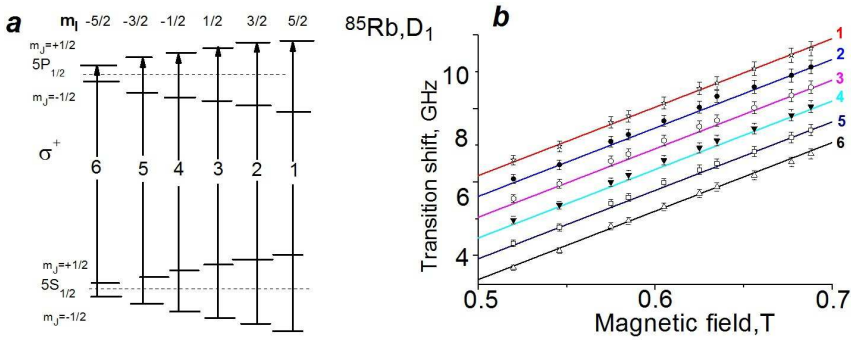


Figure 1: a) Diagram of the ^{85}Rb ($I = 5/2$) transitions for σ^+ laser excitation for the case of HPB regime. b) Atomic transitions shift labeled 1 - 6 vs B field: solid lines- HPB theory, symbols - experiment.

The research leading to these results has received funding from the FP7/2007-2013 under grant agreement n^o 205025 - IPERA. Research conducted in the scope of the International Associated Laboratory IRMAS (CNRS-France and SCS-Armenia).

References

- [1] A. Sargsyan, G. Hakhumyan, C. Leroy, Y. Pashayan-Leroy, A. Papoyan, D. Sarkisyan, accepted, Optics Letters (2012).
- [2] A. Sargsyan, G. Hakhumyan, A. Papoyan, et al., Appl. Phys. Lett. 93, 021119 (2008).

N-Resonance Formation in Micrometric-Thin Cell Filled with Rubidium and Buffer Gas

A. Sargsyan¹, R. Mirzoyan^{1,2}, C. Leroy², Y. Pashayan-Leroy², and D. Sarkisyan¹

¹Institute for Physical Research, NAS of Armenia, Ashtarak 0203, Armenia

²Laboratoire Interdisciplinaire Carnot de Bourgogne, UMR CNRS 6303, Université de Bourgogne, 21078 Dijon Cedex, France

Corresponding Author: sarmeno@mail.ru

High interest to coherent population trapping (CPT) and the related electromagnetically induced transparency (EIT) phenomena is caused by a number of important applications [1]. Recently, it was demonstrated that N -resonance is a promising alternative to CPT- and EIT-resonances [2]. From the application point of view it is important to reduce the dimensions of a cell where the N -resonance is formed, while keeping the resonance parameters good. To perform the relevant study, we have designed a multi region (MR) high-temperature optical cell having several regions with the following thicknesses L : 2 mm, 0.5 mm, and the region of 3-90 μm . The MR cell was filled with Rb and Ne gas with 200 Torr pressure. For the EIT- and N -resonance formation and comparison two diode lasers (forming the coupling ν_C and probe ν_P beams) with $\lambda \approx 794$ nm and 1 MHz line-width are used. The diagram in Fig. 1 a) shows the configuration of ν_C and ν_P for N -resonance formation, while for the EIT-resonance formation one needs to switch ν_C to $\nu_{C2} = \nu_C + 2\Delta_{HFS}$. Fig. 1 b) shows N -resonance for $L = 500$ μm (upper curve, contrast 20%, line-width 5 MHz) and $L = 50$ μm (middle curve contrast 4%, line-width 7 MHz). Disk sizes indicate the corresponding atomic level population N_3 and N_2 . Due to the inversion $N_2 - N_3 > 0$, N -resonance is formed by two-photon absorption from $F_g = 2$ to $F_g = 3$. The lower grey curve is the reference. The lasers powers P_C and P_P are 30 mW and 1 mW, correspondingly, the cell temperature $\sim 100^\circ\text{C}$. N -resonance has better parameters for ~ 1 -cm long cell [2], meanwhile for L reduced down to 3 μm , it is EIT that has better parameters and 40% EIT contrast for $L = 800$ nm is demonstrated in [3]. The results on N -resonance splitting in external magnetic field will be presented.

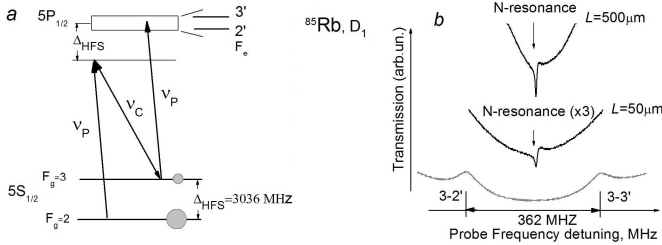


Figure 1: a) the configuration of ν_C and ν_P for N -resonance formation, b) upper and middle curves show N -resonance for the thickness $L = 500$ and 50 μm , correspondingly (N -resonance on D_1 has dispersive profile [2]), the lower grey curve is the reference.

The research leading to these results has received funding from the European Union FP7/2007-2013 under grant agreement n^o 205025 - IPERA. Research conducted in the scope of the International Associated Laboratory IRMAS (CNRS-France & SCS-Armenia).

References

- [1] M. Fleischhauer, A. Imamoglu, J. P. Marangos, Rev. Mod. Phys. 77, 633 (2005).
- [2] I. Novikova, D. F. Phillips, A. S. Zibrov et al., Opt. Lett. 31, 2353 (2006).
- [3] A. Sargsyan, C. Leroy, Y. Pashayan-Leroy et al., Appl. Phys. B 105, 767 (2011).

Fourier transform spectroscopy of KCs and potential construction of ground $X^1\Sigma^+$ and $a^3\Sigma^+$ states at large internuclear distance

O. Nikolayeva³, M. Tamanis³, R. Ferber³, and E. Tiemann¹

³Laser Center, Department of Physics, University of Latvia, 19 Rainis blvd., LV-1586, Riga, Latvia

¹Institute of Quantum Optics, Leibniz University Hannover, Germany

Corresponding Author: tamanis@latnet.lv

The KCs molecule is expected to be a promising candidate to produce the ultracold gas of polar molecules, and accurate potentials of the ground and excited states would be prerequisites of such experiments. Recent Fourier transform spectroscopy (FTS) of KCs exploiting $(A(2)^1\Sigma^+ - b(1)^3\Pi) \rightarrow X^1\Sigma^+$ and $B^1\Pi \rightarrow X^1\Sigma^+, a^3\Sigma^+$ transitions yielded accurate empirical potential energy curves (PECs) up to about 13 Å for the ground states $X^1\Sigma^+$ and $a^3\Sigma^+$ [1,2]. The highest vibrational levels observed in [1,2] were $v''_X = 97$ and $v''_a = 29$ being about 7.5 and 2.8 cm^{-1} respectively below the atomic asymptotic limit $K(4s)+Cs(6s)$.

We report an observation of the vibrational levels of the $X^1\Sigma^+$ and $a^3\Sigma^+$ states substantially closer to the dissociation limit by laser induced fluorescence (LIF) spectra of the $(4)^1\Sigma^+ \rightarrow X^1\Sigma^+$ transition. $(4)^1\Sigma^+$ state is not of pure singlet character, thus otherwise spin - forbidden transitions to $a^3\Sigma^+$ state can be observed along with transitions to $X^1\Sigma^+$ from the same upper level. The highest levels were observed when $v' = 44$ of the $(4)^1\Sigma^+$ state was excited. Knowledge of accurate PEC of this electronic state [3] greatly facilitated the experiment.

The experiment has been performed by FTS of LIF using a Bruker IFS125HR spectrometer with 0.03 cm^{-1} resolution. The KCs molecules were produced in a heat - pipe containing K and Cs metals at 560K. A single mode ring dye laser Coherent 699-21 with Rhodamine 6G dye was used for excitation, frequencies varied between 17750 cm^{-1} and 17820 cm^{-1} . Different combinations $v' = 44, J' \leftarrow v'', J''$ of excitation transitions were tried to ensure maximal excitation selectivity. Furthermore, long acquisition time and narrow bandpass filter were applied to improve signal-to-noise ratio. As a result the highest observed v''_X and v''_a are 102 and 32, respectively being about 0.2 - 0.3 cm^{-1} below the dissociation limit.

Coupled - channels calculations were required for obtaining accurate experiment based de-perturbed PECs up to 20 Å internuclear distances. Remarkable, that this type spectroscopy has reached the asymptotic range where systematic strong hyperfine interaction between $X^1\Sigma^+$ and $a^3\Sigma^+$ states takes place (the gap of the last observed level to the dissociation energy is comparable to the Cs hyperfine interaction). Thus the above mentioned vibrational quantum numbers indicate only the main contribution of the radial wavefunction of the singlet or triplet channel. Because of strong mixing the determination of counting the nodes could lead to a different naming of the level by vibrational quantum numbers.

The support from ERAF grant 2010/0242/2DP/2.1.1.1.0/10/APIA/ VIAA/036008 is gratefully acknowledged by Riga team.

References

- [1] R. Ferber *et al.*, J. Chem. Phys. **128**, 244316 (2008)
- [2] R. Ferber *et al.*, Phys. Rev. A **80**, 062501 (2009)
- [3] L. Busevica *et al.*, J. Chem. Phys. **134**, 104307 (2011)

Electron-impact excitation of the $(4p^5 4d5s)^4P_J$ autoionizing states in Rb atoms

V. Roman¹, R. Tymchyk¹, A. Kupliauskiene², and A. Borovik¹

¹*Department of Electron Processes, Institute of Electron Physics, Uzhgorod, 88017, Ukraine*

²*Institute of Theoretical Physics and Astronomy, Vilnius University, Vilnius, LT-01108, Lithuania*

Corresponding Author: sasha@aborovik.uzhgorod.ua

The quartet states from the p^5sd and p^5sp lowest configurations in Na, K, Rb and Cs atoms form the main part of the autoionizing level manifold lying below the first excited ionic levels and give the bulk of the autoionization contribution to the total single electron-impact ionization of alkali atoms [1]. In the present work, we report the ejected-electron excitation functions for the $(4p^5 4d5s)^4P_J$ states of Rb atoms and their spectroscopic parameters calculated by using the FAC code [2]. The apparatus and experimental procedure were described in detail elsewhere [3]. Briefly, the ejected-electron excitation functions for each J-component were obtained by measuring the normalized intensities of corresponding lines in ejected-electron spectra measured at different incident electron energies. The data were obtained at an incident electron energy resolution of 0.2 eV and an observation angle of 54.7° .

Level	E_{exc}	$\sigma _{26.24eV}$	A^a
$^4P_{1/2}$	16.647	4.78	$9.10+08$
$^4P_{3/2}$	16.768	9.35	$6.00+07$
$^4P_{5/2}$	16.961	12.83	$1.92+09$

Table 1: Calculated energies (E_{exc} , eV), cross sections (σ , 10^{-18}cm^2) at 26.24 eV impact energy and autoionization probabilities (A^a , s^{-1}) for the $(4p^5 4d5s)^4P_J$ levels in Rb atoms.

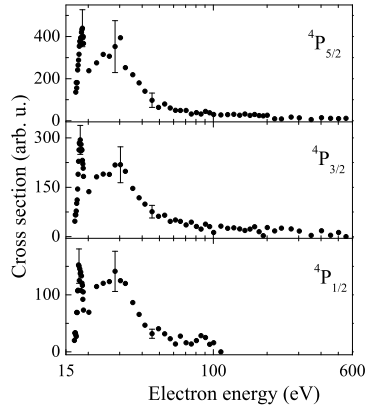


Figure 1: Ejected-electron excitation functions for the $(4p^5 4d5s)^4P_J$ states in Rb atoms.

Figure 1 and Table 1 represent, respectively, the experimental ejected-electron excitation functions and the calculated parameters for the $(4p^5 4d5s)^4P_J$ states. As can be seen, all excitation functions are similar in shape and characterized by the presence of two maxima of the cross section at 18 eV and 27 eV. The first maximum is due to effective formation of the negative ions where the second one reflects the spin-exchange character of electron transitions $^2S_{1/2} \rightarrow ^4P_J$. At 26.24 eV impact energy, both experimental and calculated cross sections fit well with the statistical ratio of 3:2:1.

References

- [1] A. A. Borovik, A. B. Kupliauskiene, J. Phys. B. **42**, 165202–165207 (2009)
- [2] M. F. Gu <http://kipc-tree-stanford.edu/fac>
- [3] A. A. Borovik et al., J. Phys. B. **38**, 1081–1092 (2005)

Rotationally resolved predissociation lifetimes of the $c^3\Pi_u^+$ state of D_2

X. Urbain¹, T. Depret¹, and J. Lecointre²

¹*Institute of Condensed Matter and Nanosciences, Université catholique de Louvain, 1348 Louvain-la-Neuve, Belgium*

²*Haute École Namur-Liège-Luxembourg HENALLUX, Département Ingénieur Industriel, Pierrard, Rue d'Arlon 112, B-6760 Virton, Belgium*

Corresponding Author: Xavier.Urbain@uclouvain.be

The $c^3\Pi_u^+$ state of molecular hydrogen is subject to rotational predissociation to the repulsive $b^3\Sigma_u^+$ state, yielding a pair of ground state atoms. This process is hindered by the poor Franck-Condon overlap with the vibrational continuum of the dissociative state, resulting in lifetimes of the order of 10 to 100ns for the lower rotational levels of the $c^3\Pi_u^+$ vibrational ground state of the D_2 molecule, as predicted by Comtet and De Bruijn [1].

In order to restrict the population to a few rovibrational levels, a (3+1) REMPI scheme involving the $C^1\Pi_u$ state is applied to create D_2^+ ions in specified v^+ , N^+ levels. These ions are accelerated and formed into a 2 keV beam, that crosses at right angle an effusive potassium beam emerging from a capillary array. The resonant capture of an electron from an alkali target allows for an efficient population of the $a^3\Sigma^+$ and $c^3\Pi_u$ states. The dissociation products fly apart and strike a pair of position and time sensitive detectors operating in coincidence. This time and position information univocally determines the total kinetic energy released in the process, provided the location of the dissociation is known.

The predissociation lifetime causes the dissociation to occur further downstream, hence the KER to be underestimated, producing a low-energy tail in the spectrum (Fig. 1). A full analysis has been performed that incorporates both the exact energy and predissociation lifetimes of specific rovibrational levels. Combined with the known selectivity of the REMPI process [2], these spectra indicate a strong propensity for the charge transfer to populate the $c^3\Pi_u^+$ state with $J=N^+ \pm 1$, pointing to the induced-dipole character of the charge transfer process [3].

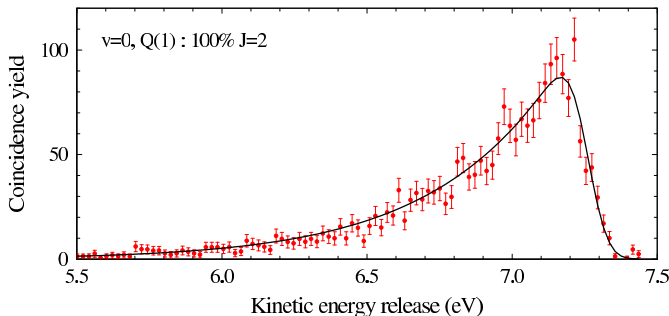


Figure 1: Kinetic energy release spectrum for $v^+=0$, $N^+=1$ ions prepared by (3+1) REMPI via a $Q(1)$ transition to the $C^1\Pi_u$ state. The full line takes into account the $v=0$, $J=2$ predissociation lifetime of the $c^3\Pi_u^+$ state and the energy resolution (100 meV FWHM).

References

- [1] G. Comtet, and D. P. de Bruijn, *Journal* **65**, 445–469 (1942)
- [2] S. T. Pratt, P. M. Dehmer, and J. L. Dehmer, *J. Chem. Phys.* **85**, 3379–3385 (1986)
- [3] V. Sidis, and D. P. de Bruijn, *Chem. Phys.* **85**, 201–214 (1984)

New odd levels of Pr I

R. Zafar¹, R. Sikandar², Z. Uddin^{2,3,4}, I. Siddiqui^{2,3}, and L. Windholz³

¹*NED University, Karachi, Pakistan*

²*University of Karachi, Pakistan*

²*Technical University Graz, Austria*

²*University of Karachi, Pakistan*

²*Yanbu University College, KSA*

Corresponding Author:

The investigation of a high resolution Fourier transform (FT) spectrum [1] has been continued in order to find new levels from unclassified lines of Pr. Some odd levels of Pr I have been discovered in this study, most of them are low lying upper levels. One even lower levels has also been discovered. The hyperfine (hf) structure patterns of the investigated unclassified lines were fitted and information about lower and upper levels involved in the transition were extracted. On the basis of this information the new levels are found. The confirmation of a new levels is made by comparing predicted hf patterns with corresponding structures in the FT spectrum with respect to wave number and shape.

The list of new levels discovered in this study are given in Table 1. The spectral line through which the level was discovered, angular momentum, parity, and magnetic dipole constant are also given along with the energy of the new levels.

Table 1: List of new level of Pr I

<i>Level Discovered via Spectral line/Å</i>	<i>Angular momentum</i>	<i>Parity</i>	<i>New Level Energy/cm⁻¹</i>	<i>Magnetic dipole hf constant</i>
6564.640	2.5	<i>e</i>	11664.79	667
9081.700	3.5	<i>o</i>	19328.33	696
8090.893	7.5	<i>o</i>	24606.74	320
5604.709	5.5	<i>o</i>	22703.72	715
8112.152	5.5	<i>o</i>	29302.83	588
4863.589	7.5	<i>o</i>	30300.66	659
5264.440	3.5	<i>o</i>	32431.93	1103
7894.381	6.5	<i>o</i>	32582.51	637

References

[1] B.Gamper, Z.Uddin, M.Jahangir, O.Allard, H.Knöckel, E.Tiemann, and L.Windholz; J. Phys. B: At. Mol. Opt. Phys. 44 (2011) 045003

Precision Spectroscopy of Highly Charged Ions in Penning Traps

M. Vogel¹, G. Birkel¹, W. Nörtershäuser², Z. Andjelkovic³, W. Quint³,
D. von Lindenfels³, M. Wiesel³, S. Bharadia⁴, D. M. Segal⁴, and R.C. Thompson⁴

¹Institut für Angewandte Physik, TU Darmstadt, 64289 Darmstadt, Germany

²Institut für Kernchemie, Universität Mainz, 55099 Mainz, Germany

³Helmholtz-Zentrum für Schwerionenforschung GSI, 64291 Darmstadt, Germany

⁴Department of Physics, Imperial College London, SW7 2AZ London, UK

Corresponding Author: m.vogel@gsi.de

We present Penning trap experiments for precision spectroscopy of highly charged ions nearly at rest. Both the SPECTRAP and the ARTEMIS experiments are designed for capture, confinement and cooling of low-energy highly charged ions as will be available in the framework of the HITRAP project at GSI, Germany. Precision spectroscopy in the optical and microwave domain allows studies of fine and hyperfine structure transitions in a wide range of few-electron ions such as for example $^{208}\text{Pb}^{81+}$ [1]. With a combination of laser and microwave spectroscopy, magnetic moments of bound electrons can be determined with ppb accuracy or better [2]. At the same time, the magnetic moments of the ionic nuclei can be measured with ppm accuracy [2]. Since in few-electron ions diamagnetic shielding is negligible, such measurements allow a model-free determination of nuclear magnetic moments. Precision spectroscopy furthermore allows stringent tests of bound-state QED calculations of electrons in the extreme fields close to the nucleus [3]. We present the status of the experiments and show first results of spectroscopy with singly charged ions which have been captured, confined and laser-cooled close to the Doppler limit where evidence for formation of ion crystals has been observed. We also give results of spectroscopy with singly charged ions which have been driven to form a plasma by the 'rotating wall' technique which will be applied to form dense targets of highly charged ions for laser spectroscopy on a well-defined and cooled ensemble [4].

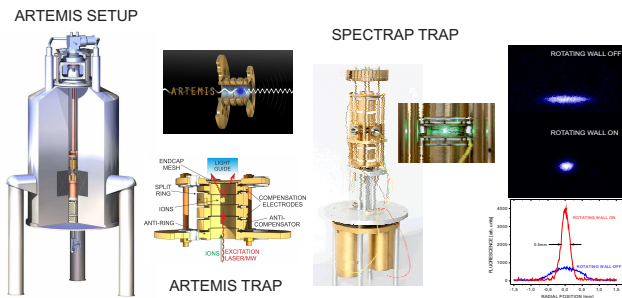


Figure 1: Illustration of ARTEMIS and SPECTRAP experimental setups.

References

- [1] M. Vogel and W. Quint, *Physics Reports* **490** (2010) 1-47.
- [2] W. Quint, D. Moskovkhin, V.M. Shabaev and M. Vogel, *Phys. Rev. A* **78** (2008) 032517.
- [3] M. Vogel, *Contemporary Physics* **50** (2009) 437.
- [4] S. Bharadia, M. Vogel, D.M. Segal and R.C. Thompson, *Appl. Phys. B* (2012) DOI 10.1007/s00340-012-4871-6.

Investigation of the hyperfine structure of the configuration $3d^3 4s 4p$ of atomic Vanadium with Fourier transform spectroscopy

B. Yapıcı¹, F. Güzelçimen¹, Gö. Başar¹, I.K. Öztürk¹, S. Kröger², R. Ferber³,
A. Jarmola³, M. Tamaniš³, and Gü. Başar⁴

¹*Faculty of Science, Physics Department, Istanbul University, Tr-34134 Vezneciler, Istanbul, Turkey*

²*Hochschule für Technik und Wirtschaft Berlin, Wilhelminenhofstr. 75A, D-12459 Berlin, Germany*

³*Laser Centre, The University of Latvia, Rainis Bulevard 19, LV-1586 Riga, Latvia*

⁴*Faculty of Science and Letters, Physics Engineering Department, Istanbul Technical University, 34469 Maslak, Istanbul, Turkey*

Corresponding Author: berinyapici@gmail.com

Vanadium with the atomic number of 23 has one stable isotope ^{51}V and a long-living isotope ^{50}V , with abundance of 99.75% and 0.25%, respectively. The predominant stable isotope ^{51}V has nuclear spin $I = 7/2$ [1]. The atomic spectra of Vanadium is characterized by the large hyperfine structure of the isotope ^{51}V due to large nuclear magnetic dipole moment $\mu_I(^{51}\text{V}) = 5.1574 \mu_N$ [2]. Although many experimental investigations of the hyperfine structure of atomic Vanadium with different spectroscopic techniques have been done in the past (see [3] and references cited therein) for many energetically higher lying levels the hyperfine structure is still unknown.

Hyperfine structure investigations of iron-group elements, like Vanadium, are important for the determination of physical parameters in astrophysics. The aim of this study is to determine the magnetic dipole hyperfine structure constants A for energetically high-lying levels of the odd parity configuration $3d^3 4s 4p$.

A plasma containing Vanadium is produced in a hollow cathode discharge lamp which is cooled with liquid nitrogen in order to reduce Doppler broadening. The spectra of atomic Vanadium were recorded using by a high-resolution Bruker IFS 125HR Fourier transform (FT) spectrometer (resolution of 0.025 cm^{-1}) in the wavenumber interval from 15 000 to 28 500 cm^{-1} at the Laser Centre of the University of Latvia. In the experimental setup, optical bandpass interference filters were inserted into the beam path between the hollow cathode discharge and the FT spectrometer to reduce the background caused by the intensity noise.

In total, 43 spectral lines have been investigated. The classifications of these lines have been done with a classification program [4], which confirms the classifications given in reference [5]. For all transitions, the A values of lower levels are well-known from the literature and have been fixed during the fitting procedure. Magnetic dipole hyperfine structure constants A for the upper levels are determined, 16 of which has been measured for the first time. The magnetic dipole hyperfine constants A of the high-lying multiplets 6P , 4P , 4F and 4S of the odd parity configuration $3d^3 4s 4p$ are described completely.

References

[1] NIST Physical Reference Data:

<http://physics.nist.gov/PhysRefData/Handbook/Tables/vanadiumtable1.htm>

[2] J. Emsley, *The Elements* (Oxford Chemistry Guides, New York: Oxford University Press, 1995) and references therein

[3] F. Güzelçimen *et al.*, J. Phys. B: At. Mol. Opt. Phys. **44** (2011) 215001 (6pp)

[4] Windholz L and Guthöhrlein G H 2003 *Phys. Scripta* T **105** 55

[5] Thorne A P, Pickering J C, Semeniuk J 2011 *Astrophys J Suppl* **192** 1

The KCs and RbCs $A \sim b$ complex revisited by means of extensive FT high resolution spectroscopy

A. Kruzins¹, K. Alps¹, O. Docenko¹, O. Nikolayeva¹, I. Klincare¹, M. Tamanis¹,
R. Ferber¹, E. Pazyuk², and A. Stolyarov²

¹Laser Center, Department of Physics, University of Latvia, 19 Rainis blvd, Riga LV-1586, Latvia

²Department of Chemistry, Moscow State University, 119991, Moscow, Leninskie gory 1/3, Russia

Corresponding Author: avstol@phys.chem.msu.ru

We present results of systematic high resolution Fourier transform study and direct deperturbation fit performed for the lowest excited $A^1\Sigma^+$ and $b^3\Pi$ states of KCs and RbCs molecules converging to $K(4^2S)+Cs(6^2P)$ and $Rb(5^2S)+Cs(6^2P)$ dissociation limits, respectively. Such strongly spin-orbit coupled singlet and triplet states are of continual interest for selecting optimal optical paths for producing and monitoring cold polar diatomic molecules.

The collisionally enhanced laser induced fluorescence (LIF) spectra corresponding to the $A^1\Sigma^+ \sim b^3\Pi \rightarrow X^1\Sigma^+$ and $E^1\Sigma^+ \rightarrow A^1\Sigma^+ \sim b^3\Pi$ transitions of both molecules were recorded by Fourier Transform Spectrometer (Bruker IFS 125HR) with the instrumental resolution of 0.03-0.05 cm^{-1} . More than 4600 rovibronic term values assigned to the $A \sim b$ complex of $^{85}\text{RbCs}$ isotopologue were obtained in the energy range [10066, 12857] cm^{-1} above the minimum of the ground state. The experimental data set of the KCs $A \sim b$ complex currently consists of 5900 term values which covers even wider energy interval [9190, 13560] cm^{-1} .

Data of the both molecules were treated in the framework of the 4×4 coupled-channel deperturbation Hamiltonian constructed in Hund's coupling case (a) basis functions. The elaborated model takes into account explicitly: (1) direct spin-orbit coupling between A -state and $b^3\Pi_{\Omega=0}$ components of the b -state; (2) indirect spin-orbit-electronic-rotational interaction between the A -state and $b^3\Pi_{\Omega=1}$ component; (3) spin-rotational interaction between the $\Omega = 0, 1, 2$ components of the triplet state. The required initial potential energy curves (PECs) and spin-orbit coupling (SOC) functions were extracted from a large scale quasi-relativistic *ab initio* calculations. The resulting analytically defined empirical PECs and SOC functions reproduce about 96% of the experimental term values with a standard deviation of 0.005 cm^{-1} which is consistent with 0.003-0.01 cm^{-1} of the uncertainty of the experiment upper limited by the Doppler effect.

The Moscow team is grateful to the Russian Foundation for Basic Researches for support by the Grant 10-03-00195-a. The support from the Latvian Science Council grant 09.1567 is greatly acknowledged by Riga team.

References

- [1] A. Kruzins *et al.*, Physical Review A **81**, 042509 (2010)
- [2] O. Docenko *et al.*, Physical Review A **81**, 042511 (2010)

Mesoscopic Systems

Heat capacity of nanoconfined ideal gas

D.U. Matrasulov¹, I.Kh. Ibragimov¹, A.A. Saidov¹, and V.E. Eshniyazov¹

¹ *Turin Polytechnic University in Tashkent, 100095 Tashkent, Uzbekistan*

Corresponding Author: dmatrasulov@gmail.com

Study of the properties of the nanoscale confined matter is of fundamental and practical importance. From the fundamental viewpoint the role of quantum size confinement effects may lead to crucial changing of such macroscopic properties as heat conductance, heat capacity, dielectric permeability and others. Such properties can be used as underlying principle in construction of different nanoscale devices. Therefore, investigation of quantum size and confinement effects is of importance for newly emerging area, nanotechnologies. Especially size and shape induced effects are important in this context. From the viewpoint of quantum mechanics the quantum confinement effects are caused by changing of the boundary conditions in the Schrodinger equation describing system under consideration. In most of the cases microscopic properties of the bulk matter is described by the Schrodinger equation whose boundary conditions given at (positive or negative) infinity. Then macroscopic characteristics (e.g. heat capacity, heat and electric conductance, dielectric permeability etc) are calculated by proper averaging over the large number of particles or subsystems. If a matter is confined, a subsystem or structural unit should be treated by re-solving the Schrodinger equation with the boundary conditions describing size and geometric shape of the confinement. Averaging should be done for such "recalculated" characteristics. In this work we demonstrated such a prescription for an ideal gas confined in a nanoscale cavity. Namely, we calculated heat capacity of such system. Calculations are performed by considering gas molecules as the non-interacting harmonic oscillators using the prescription as that in the Ref. [1]. Harmonic oscillators are treated as being confined in a box of size L and energy levels of the oscillators are calculated by solving Schrodinger equation with the box boundary conditions as it is done in the Refs. [2,3]. The results show that heat capacity of a confined gas is much higher than that of bulk one. Also, jump-like decreasing of the heat capacity can be observed by increasing of the box size.

References

- [1] R. P. Feynman, *Statistical Mechanics* (Westview Press, 1998).
- [2] Lj. Stevanovic and K. D. Sen, *J. Phys. B* **41**, 225002 (2008).
- [3] N. Aquino, *J. Phys. A: Math. Gen.* **30**, 2403 (1997).

Modeling of plasmon-molecule interaction based on nano-particles of sphere, bar, and cube shapes

H. Nadgaran¹, A. Ahmdai¹, and A. Noormandi¹

¹*Department of Physics, Shiraz University, Shiraz 71454, Iran*

Corresponding Author: nadgaran@susc.ac.ir

The interaction of localized surface plasmons (LSP) with molecules is an important issue in organic and bio sciences [1]. In this work a comprehensive physical model describing this interaction will be proposed. The LSPs are assumed to be generated from gold and silver nanoparticles and their interaction with non-absorbing molecules of sphere, bar, and cube shapes were investigated for the first time. By analyzing a frequency shift noticed in the plasmonic resonance frequencies, we report the dependencies of this frequency shift on the shape, size, and molecular properties. The results of the modeling were compared with experimental works and very good agreements were realized in that the model exactly predicts the range of the LSP resonance frequencies together with the frequency shift interval.

References

- [1] H.J. Chen *et al.*, *Langmuir* **24**, 5233 (2008)
- [2] H. Chen *et al.*, *Nano Today* **5**, 494 (2010)
- [3] B. N. Khlebtsov, N. G. Khlebtsov, *Journal of Quantative Spectroscopy and Radiative Transfer* **106**, 154 (2007)
- [4] K. S. Lee, M. A. El-Sayed, *J. Phys. Chem.* **B 110**, 19220 (2006)

Interaction of electromagnetic waves with carbon nano tubes (CNT)

H. Nadgaran¹, A. Noormandi¹, and A. Ahmdai¹

¹*Department of Physics, Shiraz University, Shiraz 71454, Iran*

Corresponding Author: nadgaran@susc.ac.ir

The invention of carbon nano tubes (CNT) has made them very attractive in science and technology [1] due to their unique electrical, mechanical, chemical, and optical properties. One of the most important issues in CNT studies is the understanding of the physics behind the interaction of electromagnetic waves with CNTs and the extent of interaction. This work uses the scattering theory of electromagnetic waves from infinite length cylinders [2] and its concise and compact expression to report a physical model for the scattering of electromagnetic waves from finite cylinders with different diameters and lengths in nanoscale regime. The results were then applied to finite cylinders of CNTs to achieve more understanding of the mutual interaction between the electromagnetic waves and these nanoscale materials. Finally coated CNTs with different substances were brought into our consideration to analyze the effects of the coated substances on the nature of interaction and scattering mechanisms.

References

- [1] S. Iijima, *Nature* **354**, 6348 (1991)
- [2] C. F. Bohren, D. R. Huffman, *Absorption and Scattering of Light by Small Particles* (Wiley-Interscience, New York, 1983)
- [3] T. Leung, J. A. Kong, K. H. Ding, *Scattering Of Electromagnetic Waves* (John Wiley and Sons, New York, 2000)
- [4] P. M. Morse, H. Feshback, *Methods of Theoretical Physics* (McGrawHill , New York, 1953)

Energy losses of fast highly charged ions in the collisions with carbon nanotubes

Kh.Yu. Rakhimov^{1,2}, O.V. Karpova², F.Sh. Matyakubov², and V.I. Matveev³

¹*Department of Physics, National University of Uzbekistan, 100174 Tashkent, Uzbekistan*

²*Turin Politechnic University in Tashkent, 100095 Tashkent, Uzbekistan*

³*Pomor State University, 4 Lomonosov St., 163002 Arkhangelsk, Russia*

Corresponding Author: kh.rakhimov@gmail.com

Collisions of highly charged ions with low-dimensional nanostructures is of considerable fundamental and practical importance. From the fundamental viewpoint in such collisions one can explore behavior of confined atomic electrons under the influence of strong external fields, while practical aspect of the problem is related to that of constructing low-dimensional functional materials and advanced devices with needed electronic, mechanical and thermal properties. In addition, nanoparticles can be used for stripping of multi-electron, heavy ions which is important for creation of highly charged ion beams in modern accelerators [1–3].

Unlike to the case of collisions with atomic targets, in collision of highly charged ions with atomic systems, such as molecules and nanoparticles, the cross section depends on the collision multiplicity and the displacement of atoms with respect of the direction of collision velocity. For example in case of collisions of highly charged ion with a diatomic molecule the cross section for projectile electron loss is highly sensitive to the direction of the molecular axis with respect to the direction of projectile motion [3].

In this work we study inelastic transitions in the projectile electron states in the collision of fast highly charged ions with carbon nanotubes. In particular, we calculate energy losses of the fast Fe^{10+} - projectile in its collisions with C_{300} and C_{640} carbon nanotubes. In particular, we have calculated energy loss of such ions as a function of the angle between the directions of atomic displacements and projectile's motion. We found that energy loss strongly depends on this angle when the target atoms have regular (ordered) displacement, while for chaotic displacement of the atoms with respect to projectile's motion the cross section doesn't depend on this angle.

References

- [1] A. B. Voitkiv and J. Ullrich, *Relativistic collisions of structured atomic particles* (Springer-Verlag, Berlin, 2008).
- [2] V. I. Matveev, S. V. Ryabchenko, D. U. Matrasulov, *et al.*, Phys. Rev. A **79**, 042710 (2009).
- [3] V. I. Matveev, D. N. Makarov, and Kh. Yu. Rakhimov, Phys. Rev. A **84**, 012704 (2011).

Nonlinear Dynamics of the Kicked Screened Atom

D.M. Otajanov¹, F. Khoshimova², and Kh.Yu. Rakhimov^{1,3}

¹*Turin Politechnic University in Tashkent, 100095 Tashkent, Uzbekistan*

²*Novoi State Mining Institute, 27 Janubiy Str., 106800 Novoi, Uzbekistan*

³*Department of Physics, National University of Uzbekistan, 100174 Tashkent, Uzbekistan*

Corresponding Author: kh.rakhimov@gmail.com

Periodically driven dynamical systems is an important topic in nonlinear dynamics and quantum chaos theory [1–3]. Microwave driven or delta-kicked atoms are of special importance among such systems. Remarkable feature of periodically driven atom is so-called chaotic ionization that occurs due to the diffusion of atomic electron over the orbits. Unlike multiphoton ionization? Chaotic (or diffusive ionization) occurs during relatively long time-period. Underlying reason for such ionization is chaotization of the electron motion caused by external driving force. Critical value of the external field strength can be estimated from the resonance overlap criterion [3]. Classical and quantum dynamics of periodically driven atoms have been explored from the viewpoint nonlinear dynamics and quantum chaos theory by many authors (see., e.g. [3]).

In this work we study similar problem for the atom with screened nuclear (Coulomb) potential. Classical equations of motion are solved numerically. Analysis of phase space portraits is done and Lyapunov exponent is calculated for different values of the kicking parameter and screening coefficient. The critical value of the external kicking strength at which chaotization will occur is estimated using Chirkov's resonance overlap criterion. In particular, it is found that for smaller values of the screening coefficient the system is more stable than that for higher values.

References

- [1] G. M. Izrailev, Phys. Rep. **196**, 299 (1990).
- [2] D. F. Escande, Phys. Rep. **121**, 167, (1985).
- [3] R. V. Jensen, S. M. Susskind, and M. M. Sanders, Phys. Rep. **201**, 1 (1991).

Photoionization/Photodetachment, anions

Spectroscopic analysis of the blue light emitted from Middleton type Cesium sputter negative ion sources.

P. Andersson¹, M. Martschini¹, A. Priller¹, P. Steier¹, R. Golser¹, and O. Forstner¹

¹University of Vienna, Faculty of Physics, Isotope Research, AT-1090 Wien, Austria

Corresponding Author: pontus.andersson@univie.ac.at

Negative ions of atoms and molecules are widely used in both fundamental and applied research. The possibility to provide intense beams of negative ions is especially important in negative ion research [1], fusion development [2] and nuclear physics performed with tandem accelerators [3]. A special case of the last is ultra rare isotope analysis by Accelerator Mass Spectrometry (AMS) [4]. Sputter ion sources of the Middleton type [5] have since 1977 been the main tool used to create stable, intense negative ion beams for injection into AMS machines. However, the theory behind negative ion formation in Middleton type cesium sputter sources is yet not fully agreed upon [6,7,8,9]. When this type of source is run under conditions that provide medium to high output currents, a blue light can often be seen emanating from, or just in front of the sputter target surface [10]. As a part of the work in trying to unravel the mechanisms of hard sputtering in a cesium rich environment, we have resolved the spectrum of the blue light emitted from three different cathodes; A carbon filled copper cathode, a pure aluminum cathode and a pure copper cathode. All cathodes were analyzed under the same source conditions but with different total current output. A fiber coupled spectrometer was used to detect light in the wavelength region 200 to 1100 nm and the blue glowing region was observed from a distance of 3 meters through a view port with a straight line of sight onto the cathode. The spectra showed clear differences depending on the cathode material. The emitted light from the carbon consists almost entirely of lines from neutral cesium and no lines from ionized cesium. A weak, broad feature was also seen between 470 and 510 nm. This feature was not seen in the two metallic cathodes. Both displayed several lines originating from positively ionized cesium. For the copper cathode the intensity of the spectrum was much smaller than for the other two cathodes. These results may suggest different mechanisms of negative ion formation in the ion source depending on the cathode material. As a side effect of the measurement it proved relatively easy to determine the source temperature to 1185 ± 30 K from the black body radiation in the spectra. This was verified by spectra from a temperature controlled combustion oven.

References

- [1] T. Andersen, Phys. Rep.-Rev Sect. Phys Lett. **394** (4-5),157-313 (2004)
- [2] R. Hemsworth, H. Decamps, J. Graceffa, *et al.* Nucl. Fusion **4**, 045006(2009)
- [3] D. A. Bromley, Nuclear Instruments and Methods **122** 1-34 (1974)
- [4] A. E. Litherland, X-L. Zhao And W. E. Kieser, Mass Spectrometry Reviews, DOI: 10.1002/mas.20311 (2010)
- [5] R. Middleton, Nucl. Instr. & Meth.in Phys. Res. **214** (2-3),139-150(1983)
- [6] K. Wittmaack, Ion Beam Science. Solved and Unsolved Problems, Part II pp 465-495 (2007)
- [7] H.Gnaser, Phys. Rev. B **54** (23) 16 456 (1996)
- [8] G. Doucas, Int. J. Mass Spectrom. Ion Processes **25** (1) 71 (1977)
- [9] J. S.Vogel, J. A. Giacomo, S. R. Dueker, Submitted to Nucl. Instr. Meth B , Private communication
- [10] Middleton R., A Negative Ion Cookbook, University of Pennsylvania, USA, 1989 (unpublished) Available (2011) at www.pelletron.com/cookbook.pdf

Vibrationally resolved photoionization spectra of small molecules

D. Ayuso¹, E. Plésiat¹, L. Argenti¹, A. Palacios¹, P. Decleva², and F. Martín^{1,3}

¹*Departamento de Química, Módulo 13, Universidad Autónoma de Madrid. 28049 Madrid, Spain*

²*Dipartimento di Scienze Chimiche, Università di Trieste, 34127 Trieste, and CNR-IOM, Trieste, Italy*

³*Instituto Madrileño de Estudios Avanzados en Nanociencia (IMDEA-Nanociencia), Cantoblanco, 28049 Madrid, Spain*

Corresponding Author: david.ayuso@uam.es

We present our latest results in the theoretical study of the vibrationally resolved cross sections for the photoionization of small molecules, such as BF_3 or CF_4 , at both low and high photoelectron energies.

We employ the B-spline static-exchange Density Functional Theory (DFT) method [1–3], which makes use of the Kohn-Sham DFT to describe the molecular ionic states and the Garlekin approach to evaluate the continuum electron wave function in the field of the corresponding Kohn-Sham density. Results obtained using time-independent (TI) and time-dependent (TD) DFT are compared. In the region of low energies, where features as shape resonances appear, TD-DFT based methods are expected to be more accurate.

The nuclear motion is included by solving the nuclear Schrödinger equation in a basis set of B-spline functions within a fixed box size [4]. To study valence shell photoionization, high accuracy ab initio methods can be used to evaluate the potential energy curves that take into account the symmetric stretching modes for the ground state of the neutral molecule and for the first excited states of the cation. Convergence studies using Coupled Cluster and the multi-reference methods CASPT2 and MRCI, based on the active space approximation, have been performed. In the case of k-shell ionization, reliable Morse potential energy curves available in the literature [5] are employed for the electronic states of the cation containing a hole in the core.

The vibrationally resolved photoionization cross section is then evaluated to first order perturbation theory within the Born-Oppenheimer approximation [6–8]. The advent of third generation synchrotron radiation sources, in combination with high energy-resolution detection techniques allow us to compare our theoretical spectra with the experimental ones.

References

- [1] M. Stener, G. Fronzoni and P. Decleva, *Chem. Phys. Lett.* **351**, 469–474 (2002)
- [2] M. Stener and P. Decleva, *J. Chem. Phys.* **112**, 10871 (2000)
- [3] D. Toffoli *et al.*, *Chem. Phys.* **276**, 2543 (2002)
- [4] H. Bachau *et al.*, *Rep. Prog. Phys.*, **64**, 18151942 (2001)
- [5] T. D. Thomas *et al.*, *J. Chem. Phys.* **127-24**, 244309 (2007)
- [6] Sophie E. Canton *et al.*, *PNAS* **108**, 7302-7306 (2011)
- [7] E. Plésiat *et al.*, *Phys. Rev. A*, **85**, 023409 (2012)
- [8] L. Argenti *et al.*, *New J. Phys.* **14**, 033012 (2012)

Evolution of the accuracy of electron affinity measurements

C. Blondel¹, C. Drag¹, and M. Vandevraye¹

¹*Laboratoire Aimé Cotton, Centre national de la recherche scientifique, bâtiment 505, université Paris-sud, F-91405 Orsay, France*

Corresponding Author: christophe.blondel@u-psud.fr

Two techniques are presently used to measure electron affinities, both relying on a measurement of the photodetachment threshold of the negative ion species. One is the laser photodetachment threshold (LPT) technique, which consists in monitoring the photodetachment signal as the excitation wavenumber is scanned through the threshold. The other one is laser photodetachment microscopy (LPM), which is an interferometric version of the older laser photodetachment electron spectroscopy (LPES) technique.

Photodetachment microscopy has now produced electron affinity measurements for 13 years [1], and set a new standard for the accuracy of electron affinity measurements. Uncertainties yet had to be overcome, such as the possible offset due to the presence of a residual magnetic field, which led to a progressive improvement in the accuracy of the measured electron affinities. The electron affinity of Sulfur was e.g. measured several times. The data themselves were revisited when the robustness of the measurements with respect to magnetic perturbations could be recognized. The last revision [2] produced the up-to-date value of $1\,675\,297.53(41)\text{ m}^{-1}$ or $2.0771040(6)\text{ eV}$ for the electron affinity of ^{32}S , which is the record in accuracy and even makes it possible to investigate the isotope shift of the electron affinity of this element [3].

A more recent measurement was the electron affinity of the element just below Sulfur, Selenium: $1\,629\,727.6(9)\text{ m}^{-1}$, or $2.020\,604\,6(11)\text{ eV}$ [4]. The accuracy, of the order of $1\text{ }\mu\text{eV}$ in both cases, is to be compared to the typical accuracy of classical electron spectrometry techniques, of the order of 1 meV .

Both LPT and LPM techniques, however, better apply when photodetachment releases an electron into an s-wave. Today's challenge is to apply photodetachment microscopy to the case of p-wave photodetachment, which has much smaller cross-sections at low energies above the detachment threshold. This would nevertheless produce a greater variety of electron interferograms, with an additional degree of freedom to be explored varying the polarization of the laser. Possible solutions to enhance near-threshold photodetachment will be discussed at the conference.

References

- [1] C. Blondel, C. Delsart, F. Dulieu, and C. Valli, *Eur. Phys. J. D* **5**, 207–216(1999)
- [2] W. Chaibi, R. J. Peláez, C. Blondel, C. Drag, and C. Delsart, *Eur. Phys. J. D* **58** 29–37. (2010)
- [3] T. Carette, C. Drag, O. Scharf, C. Blondel, C. Delsart, C. Froese Fischer, and M. Godefroid, *Phys. Rev. A* **81**, 042522(10 pp)(2010)
- [4] M. Vandevraye, C. Drag, and C. Blondel, *Phys. Rev. A* **85** 015401 (2012)

Velocity-Map Imaging spectroscopy of negative ion photodetachment

K.C. Chartkunchand¹, K. Carpenter¹, V. T. Davis¹, P. Neill¹, J. S. Thompson¹, and A. M. Covington¹

¹*Department of Physics and Nevada Terawatt Facility, University of Nevada, Reno, Nevada, 89557, USA*

Corresponding Author: kiattichartc@gmail.com

Fixed and tunable photon sources have been utilized for photodetachment of fast-moving anion beams and the resulting photoelectrons studied using the technique of Velocity-Map Imaging (VMI) spectroscopy. Digital images produced by the VMI spectrometer have been used to determine anion structure from photoelectron kinetic energy spectra. Photoelectron angular distributions are measured simultaneously and give insight into the dynamics of the photon-ion collision process as well. Results from investigations of a number of atomic and molecular anions are presented.

Wavelength dependence of Photoelectron Angular Distributions from four- and five-photon ionization of Mg in the vicinity of the 4-photon excited $3p^2\ ^1S_0$ state

A. Dimitriou¹, S. Cohen¹, and A. Lyras¹

¹*Department of Physics, University of Ioannina, 45110 Ioannina, Greece*

Corresponding Author: adimitr@cc.uoi.gr

Electron Energy Analysis and Photoelectron Angular Distributions (PADs) from multiphoton ionization are valuable tools for the study of laser-coupled autoionizing states of Alkaline Earth atoms, particularly when the highly correlated $mp^2\ ^1S_0$ levels are involved. That was recently demonstrated for the case of four-photon excitation of the $3p^2\ ^1S_0$ state of Mg¹ with linearly polarized light. The recorded four-photon PADs were fitted to an expression of the form of Eq. (1):

$$S(\omega, \theta) = \sum_{k=1}^N \beta_{2k}^{(N)} P_{2k}(\cos\theta) \quad (1)$$

(with $N = 4$ the number of absorbed photons), where $P_{2k}(\cos\theta)$ are the Legendre polynomials. The energy variation of the fitted parameters showed a significant red-shift of the resonance position, verifying earlier theoretical results as well as experimental ones². The shift stems from the laser-induced strong one-photon coupling of this state with a multitude of levels located near the third (bound) and the fifth photon (autoionizing) - (Fig. 1) (a). Nevertheless, that earlier study¹ was carried out by employing such a laser intensity ($< 2 \times 10^{11}$ W/cm²) that was unable to saturate four-photon ionization². The present work extends these measurements to a wider wavelength range and with a laser intensity which is higher by about a factor of three. This fact allowed for the recording of PADs from five-photon ionization ($N = 5$). The latter stems from the first above-threshold-absorbed photon ((Fig. 1) (a)). As it is evident from ((Fig. 1) (b)) the asymmetry parameters $\beta_{10}^{(5)} \approx \beta_8^{(5)} \approx 0$ over the whole studied energy range. Thus, out of the $J = 1^\circ, 3^\circ$ and 5° available continua, the $J = 5^\circ$ one is not excited³. Furthermore, the considerable variation of $\beta_6^{(5)}$ implies the presence of a $J = 3^\circ$ resonance while, since the value of $\beta_2^{(5)}$ is quite large over the whole energy range, the $J = 1^\circ$ continua are always excited. The four- and five-photon data, along with their discussion with respect to the aforementioned coupling are to be presented in the conference. Acknowledgements: This research has been co-financed by the European

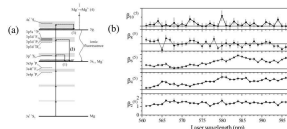


Figure 1: (a) Energy level diagram of Mg and excitation scheme (b) Laser wavelength dependence of five-photon asymmetry parameters extracted from the fits of the relevant PADs.

Union (European Social Fund ESF) and Greek national funds through the Operational Program "Education and Lifelong Learning" of the National Strategic Reference Framework (NSRF) - Research Funding Program: Heracleitus II. Investing in knowledge society through the European Social Fund.

References

- [1] A. Dimitriou, S. Cohen, and A. Lyras, *J. Phys. B: At. Mol. Opt. Phys* **44**, 135001 (2011)
- [2] I. Liontos, A. Bolovinos, S. Cohen, and A. Lyras, *Phys. Rev A* **70**, 033403 (2004)
- [3] L. L. Nikolopoulos, *Phys. Rev. A* **71**, 033409-1 (2005)

Renner-Teller Coupling In H_2S^+ : Partitioning The Rovibronic And Spinorbit Coupling Hamiltonian

G. Duxbury¹, Ch. Jungen², and A Alijah³

¹*Department of Physics, SUPA, John Anderson Building, University of Strathclyde, 107 Rottenrow, Glasgow G4 0NG, Scotland, UK*

²*LAC, 1Laboratoire Aim Cotton du CNRS, Universite de Paris-Sud, 91405 Orsay, France*

³*GSMA, UMR CNRS 6089, Universit de Reims Champagne-Ardenne, B.P. 1039, 51687 Reims Cedex 2, France*

Corresponding Author: g.duxbury@strath.ac.uk

In the family of dihydride molecules such as NH_2 or H_2O^+ , which are derived from a $^2\Pi$ state of a linear molecule, the two potential energy curves for bending are degenerate when the molecule is linear, and split into two well resolved components as the molecule bends. H_2S^+ behaves in the same way. The strong interaction between the two half states, the X^2B_1 and A^2A_1 , occurs once the levels belonging to the X^2B_1 state begin to interleave those of the A^2A_1 state [1]. As the spin-orbit coupling in H_2S^+ , ca. 400 cm^{-1} , is much larger than in the water ion, the resultant perturbations may become very large. This transition from small amplitude motion in the lowest bending levels of the ground state to the large amplitude motion close to the barrier to linearity was first described in detail by Hougen, Bunker and Johns [2]. They demonstrated that the vibration-rotation Hamiltonian required to be partitioned so that the A-axis rotation is included in the vibrational problem, as when the molecule becomes linear it correlates with the angular part of the two dimensional bending vibration. However, the end-over-end rotation about the b- and c- axes may be modelled by a k-dependent rotational model as shown by Jungen and Merer [3]. This partitioning of the ro-vibronic Hamiltonian is included in the stretch-bender approach.

The stretch-bender reference-frame for a symmetric triatomic molecule, [4] and [5], was as chosen so that as the molecular bends the reference geometry follows the minimum in the potential energy surface, thus minimising the size of the displacements required to reach the instantaneous axis geometry. This allows the separation of large amplitude bending motion and symmetric stretching. It has been used to calculate the effect of vibrational resonances such as Fermi resonance, the effects of spin-orbit coupling, and of overall rotation. Its use allows the block factorisation of the Renner-Teller interaction super matrix.

We wish to show the utility of this approach when two different approaches by Dixon and Duxbury [6], and Jungen and Merer [3], are used to minimise the effects of the large amplitude bending upon the Renner-Teller interaction in H_2S^+ . The overall structure of the interaction super-matrix is the same in either approach, although the wavefunctions used to construct the super matrix are slightly different. The super-matrix may be set up for vibronic coupling only, or including the effects of overall rotation. Use of the super-matrix approach allows the effects of large amplitude motion on the rotational structure to be calculated, including the switchover from bent to linear behaviour, and the effects of the large spin-orbit coupling of the sulphur, ca 400 cm^{-1} ,

References

- [1] G. Duxbury, Ch. Jungen and J. Rostas, *Molec. Phys.* 48, 719 (1983)
- [2] J. T. Hougen, P. R. Bunker and J. W. C. Johns. *J. Mol. Spectrosc.* 34, 136 (1970)
- [3] Ch. Jungen and A. J. Merer *Molec. Phys.* 40,1(1981))
- [4] G. Duxbury *et al.*, *J. Chem. Phys.* 108,2336 (1998))
- [5] A. Alijah and G. Duxbury *J. Mol. Spectrosc.* 211,7 (2002))
- [6] G. Duxbury and R. N. Dixon *Molec. Phys.* 43,255(1981))

Strong-field photodetachment of C_2^-

M. Eklund^{1,2}, H. Hultgren^{1,2}, D. Hanstorp², H. Helm¹, and I. Yu. Kivan³

¹Physikalisches Institut, Albert-Ludwigs-Universität, 79104 Freiburg, Germany

²Department of Physics, Gothenburg University, 412 96 Gothenburg, Sweden

³Helmholtz-Zentrum für Materialien und Energie, 12489 Berlin, Germany

Corresponding Author: mikael eklund@physik.uni-freiburg.de

We present results from experiments on strong-field photodetachment of C_2^- . A beam of diatomic carbon anions is intersected by a pulsed infrared laser inside an electron imaging spectrometer operating in the velocity mapping regime [1]. The velocity and direction of electrons emitted by strong-field detachment are detected. The momentum distribution of the electrons are compared with simulations of the molecular strong-field approximation. This approximation exists in two versions, a dressed version where the laser field is taken into account for the initial state of the ion, and an undressed version where the laser field is neglected [2]. Measurements have been performed on laser wavelengths of 2055 and 1310 nm. Fig. 1 shows the electron momentum distribution along the laser polarization at a wavelength of 2055 nm. The simulations show that for the ground state of C_2^- there is little difference between the dressed and undressed versions. Both versions of the theory successfully predict that a maximum occurs around a momentum of 0.4 atomic units.

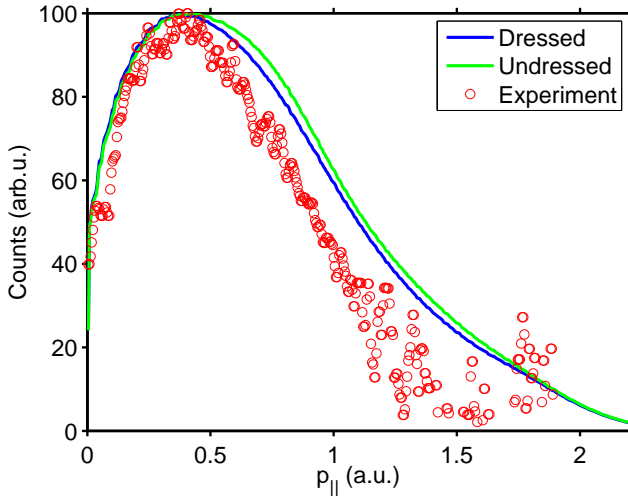


Figure 1: Measurement and simulations of momentum distribution of photoelectrons along laser polarization axis for $\lambda = 2055\text{nm}$

References

- [1] Boris Bergues et al. Phys. Rev. A **75**, 063415 (2007)
- [2] D.B. Milosevic, Phys. Rev. A **74**, 063404 (2006)

Non-dipole effects in $(\gamma, 2e)$ processes caused by photon momentum

A.G. Galstyan¹, O. Chuluunbaatar², Yu.V. Popov³, and B. Piraux⁴

¹Physics Faculty, Moscow State University, Moscow, Russia

²Joint Institute for Nuclear Research, Dubna, Russia

³Skobeltsyn Institute of Nuclear Physics, Moscow State University, Moscow, Russia

⁴Institute of Condensed Matter and Nanosciences, Université catholique de Louvain, B-1348 Louvain-la-Neuve, Belgium

Corresponding Author: galstyan@physics.msu.ru

In dipole approximation, vector potential $\vec{A}(\vec{r}, t)$ is considered as independent on \vec{r} at characteristic atomic distances of interaction. However, for very high frequencies, the vector potential may vary significantly over typical atomic distances. In these conditions, it is important to take explicitly into account the dependence of \vec{A} on the position vector \vec{r} in its the simplest form $\vec{A} \sim \vec{e}[\exp(i\vec{k}\vec{r} - i\omega t) + c.c.]$ with polarization \vec{e} and photon momentum \vec{k} , $\vec{k} \perp \vec{e}$.

We study the influence of the photon momentum \vec{k} on triple differential cross section (TDCS) of $(\gamma, 2e)$ processes. Such effects were first considered by Amusia *et al* in [1] and recently were found experimentally [2].

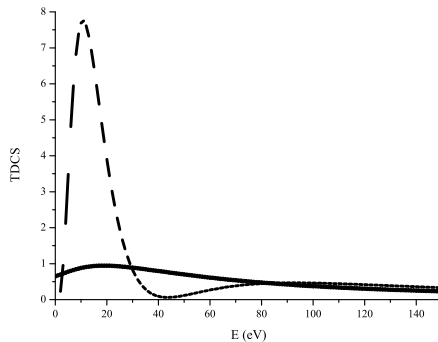


Figure 1: Averaged TDCS ($\text{mb eV}^{-1} \text{sr}^{-2}$) vs energy of one electron, back-to-back emission. The dashed line is the 3C correlated final-state wave function, and the solid line the 2C uncorrelated one.

These effects are very weak (Figure 1) because of small magnitude of photon momentum. Thus they can be obtained only in special kinematic conditions such as back-to-back emission with equal energy sharing, where the dipole approximation gives zero of TDCS.

Rather unexpectedly, absolute TDCS dependence on photon energy reaches its maximum at low energies. But this effect appears only when we take account electron correlations in the final state wave function. The dependence of maximum of TDCS for different light K -ions on their charge of nucleus was also studied and corresponding electron energies were obtained [3].

References

- [1] M. Ya. Amusia *et al.*, J. Phys. B **8**, 1248 (1975).
- [2] M. S. Schöffler *et al.*, Abstracts of XXVII ICPEAC, Th132 (2011)
- [3] A. G. Galstyan *et al.*, Phys. Rev. A **85**, 023418 (2012)

2D momentum distribution of electron in transfer ionization of helium atom by fast proton

M.S. Schöffler¹, J. Titze¹, L.Ph.H. Schmidt¹, H. Schmidt-Böcking¹, R. Dörner¹, O. Chuluunbaatar², A.A. Gusev², S. Houamer³, A.G. Galstyan⁴, and Yu.V. Popov⁵

¹*Institut für Kernphysik, University Frankfurt, D-60438 Frankfurt, Germany*

²*Laboratory of Information Technologies, Joint Institute for Nuclear Research, Dubna, Moscow Region 141980, Russia*

³*Laboratoire de Physique Quantique et Systèmes Dynamiques, Département de Physique, Faculté des Sciences, Université Ferhat Abbas, Sétif 19000, Algeria*

⁴*Faculty of Physics, Moscow State University, Moscow 119991, Russia*

⁵*Nuclear Physics Institute, Moscow State University, Moscow 119991, Russia*

Corresponding Author: galstyan@physics.msu.ru

The momentum distribution of the electron in the reaction $p+\text{He}\rightarrow\text{H}+\text{He}^{2+}+e$ is measured for the projectile energy $E_p = 300$ keV and very small (fractions of mrad) hydrogen scattering angle. Mainly, (k_z, k_\perp) plots are obtained in the scattering plain formed by the proton velocity vector \vec{v}_p (z -axis) and the hydrogen velocity vector \vec{v}_H . Experimental results are presented in Fig.1 (left panel).

Theoretical calculations were carried out within the plane wave first Born approximation (PWFB), which consists of three terms. Two of them correspond to the shake-off mechanism of the electron emission, while the third one describes the sequential mechanism of the proton interaction with both helium electrons [1]. The result close to the experimental one (see Fig.1, right panel) is obtained only with well correlated trial helium wave function [2]. $1s^2$ wave function gives quite different distribution.

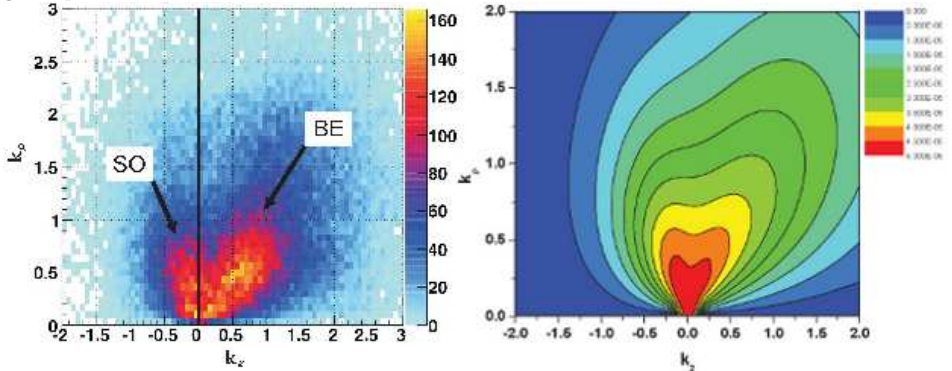


Figure 1: (k_z, k_\perp) momentum distribution of the emitted electron. Left panel, experiment; right panel, PWFB theory with highly correlated wave function

The forward emitted electrons might be associated with a two step process, where two independent interactions of the projectile with either electron leads to capture of one and ionization of the second one (binary encounter, BE). The second mechanism contributing to transfer ionization is single capture accompanied by a shake off (SO) of the second electron.

References

- [1] S. Houamer, Yu.V. Popov, and C. Dal Cappello, Phys. Rev. A **81**, 032703 (2010)
- [2] O. Chuluunbaatar O. *et al.*, Phys. Rev. A **74**, 014703 (2006)

Inner-shell photodetachment from O^-

N. D. Gibson¹, C. W. Walter¹, D. J. Matyas¹, A. N. Lebovitz¹, Y.-G. Li¹,
R. M. Alton¹, S. E. Lou¹, R. C. Bilodeau^{2,3}, N. Berrah², A. Aguilar³, and
D. Hanstorp⁴

¹*Department of Physics and Astronomy, Denison University, Granville, Ohio 43023, USA*

²*Department of Physics, Western Michigan University, Kalamazoo, Michigan 49008, USA*

³*Advanced Light Source, Lawrence Berkeley National Laboratory, Berkeley, California 94720, USA*

⁴*Department of Physics, Gothenburg University, SE-412 96 Gothenburg, Sweden*

Corresponding Author: gibson@denison.edu

Negative ions are of fundamental interest since they are found in a wide variety of physical situations including terrestrial and stellar atmospheres and electrical discharges and plasmas. The extra electron in a negative ion is bound predominantly by electron correlation effects and therefore negative ions provide a fertile testing ground for state-of-the-art atomic physics calculations regarding these multi-body interactions. We have used inner-shell photodetachment of oxygen negative ions to investigate correlations in short-lived negative ion resonances. The ground state configuration of O^- is $(1s^2 2s^2 2p^5)$. Photoexciting an inner-shell electron to fill the single vacancy in the $2p$ shell forms a strongly bound Feshbach resonance due to the extra stability of the now full $2p^6$ shell [1].

The K-shell photodetachment spectrum of O^- was measured using the merged ion-photon beam photodetachment technique. O^- ions were produced in a Cs sputtered negative ion source (SNICS II) on a Movable Ion Photon Beamline while the photons were produced by the undulator on the Advanced Light Source Beamline 8.0.1. Positive oxygen ions formed by multiple detachment were detected as a function of photon energy. Photoexcitation of a $1s$ electron to fill the $2p$ shell leads to a short-lived Feshbach resonance ~ 3 eV below the $1s$ detachment threshold. Energy calibration of the incoming photons, using an inline gas cell, leads to precise energy level assignments for the observed states. The Feshbach resonance is observed near 525 eV in the O^+ , O^{2+} and O^{3+} channels. Comparisons to inner-shell photoionization of O will be discussed for both experiment [2] and theory [3].

This material is based in part on work supported by the National Science Foundation under Grant Nos. 0757976 and 1068308, and by the US Department of Energy, Office of Science, Basic Energy Sciences, Chemical, Geoscience, and Biological Divisions. The ALS is funded by the DoE, Scientific User Facilities Division. D.H. acknowledges support from the Swedish Research Council.

References

- [1] R. C. Bilodeau *et al.*, Phys. Rev. A **72**, 050701(R) (2005)
- [2] W. C. Stolte *et al.*, J. Phys. B **30**, 4489 (1997)
- [3] T. W. Gorczyca and B. M. McLaughlin, J. Phys. B **33**, L589 (2000)

Measuring positron-atom binding energies through laser-assisted photorecombination

C. M. Surko¹, J. R. Danielson¹, G. F. Gribakin², and R. E. Continetti³

¹Physics Department, University of California, San Diego, La Jolla California 92093, USA

²School of Mathematics and Physics, Queen's University, Belfast BT7 1NN, UK

³Department of Chemistry and Biochemistry, University of California, San Diego, La Jolla California 92093, USA

Corresponding Author: g.gribakin@qub.ac.uk

In this work we propose and verify the feasibility of a new experiment aimed to measure positron-atom binding energies. Positron binding to about ten atoms has been predicted in a number of sophisticated calculations [1], and binding to many more atoms is expected [2]. None of these predictions have been verified experimentally. This is in stark contrast to positron binding to molecules, where binding energies E_b for about sixty species have been measured by observing vibrational Feshbach resonances in the positron annihilation rate [3,4]. These measurements were enabled by the development of pulsed positron beam from a buffer-gas positron accumulator. To measure positron-atom binding, we propose to combine this set-up with a collinear laser beam and a “hot cell” to provide sufficient density of atomic vapours (see Fig. 1) [5]. Laser pulses will be used to *stimulate* positron-atom recombination (and hence, positron annihilation). The condition for the photo-enhanced process is $\hbar\omega = \varepsilon + \varepsilon_b$, where the incident positron energy ε can be tuned to this resonance. The photorecombination cross section is estimated using the zero-range potential model. Other parameters are taken from positron-molecule annihilation experiments. The positron beam will be compressed radially using a rotating electric field. The assumed laser parameters are based on a LaserVision optical parametric oscillator/amplifier pumped by a Continuum Surelite EX Nd:YAG laser, capable of 12 mJ pulses at a 10 Hz rate for photon energies in the range 0.35–0.8 eV. The signal expected for zinc atoms with a predicted binding energy $\varepsilon_b = 0.10$ eV [1] and an estimated vapor pressure $\sim 3.5 \times 10^{-5}$ torr at 235° C, for $\hbar\omega = 0.35$ eV, is 0.0016 s⁻¹. Resolving the resonant enhancement with 10 points in energy at 50 counts per point at the peak, the expected time for a spectrum will be ~ 3.5 days.

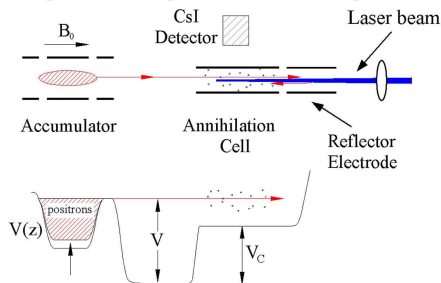


Figure 1: Schematic diagram of the experimental arrangement (top), and the corresponding electrical potential profile along the magnetic axis (bottom).

The research at UCSD is supported by the U.S. NSF, Grant PHY1068023 and PHY1002435.

References

- [1] J. Mitroy, M. W. J. Bromley, and G. G. Ryzhikh, *J. Phys. B* **35**, R81 (2002)
- [2] V. A. Dzuba, V. V. Flambaum, and G. F. Gribakin, *Phys. Rev. Lett.* **105** 203401 (2010)
- [3] J. R. Danielson, J. A. Young, and C. M. Surko, *J. Phys. B* **42**, 235203 (2009)
- [4] G. F. Gribakin, J. A. Young, and C. M. Surko, *Rev. Mod. Phys.* **82**, 2557 (2010)
- [5] C. M. Surko *et al.*, *New J. Phys.* **14**, 065004 (2012)

Two- and Three-Photon Atomic Double Ionization by Intense FEL Pulses

A. N. Grum-Grzhimailo¹, E. V. Gryzlova¹, S. Fritzsche², and N. M. Kabachnik^{1,3}

¹*Skobel'syn Institute of Nuclear Physics, Lomonosov Moscow State University, 119991 Moscow, Russian Federation*

²*GSI Helmholtzzentrum für Schwerionenforschung, D-64291 Darmstadt, Germany and Department of Physics, University of Oulu, PO Box 3000, Fin-90014, Finland*

³*European XFEL GmbH, Albert-Einstein-Ring 19, D-22607 Hamburg, Germany*

Corresponding Author: algrgr1492@yahoo.com

With the advent of Free-Electron Lasers (FELs) operating in the short-wavelength regime and generating extremely intense femtosecond pulses, nonlinear processes in the XUV and X-ray wavelength range are now accessible experimentally [1,2]. In this range, the energy of a single photon is already enough to ionize the target. When the photon energy is higher than the ionization threshold of the ion, it appears that sequential two-photon double ionization (2PDI) dominates in which the first photon produces an ion which is subsequently ionized by the second photon from the same pulse. For the photon energies between the atomic and ionic ionization thresholds, the second-step ionization proceeds via two-photon absorption, leading to three-photon double ionization (3PDI). In sequential 2PDI and 3PDI, the individual energy of each of the two emitted electrons is fixed by energy conservation. Studies of 2PDI and 3PDI, the simplest nonlinear reactions in the XUV, are at their beginning. They can provide a wealth of new information on photoionization amplitudes, cross-sections and transition probabilities in ions, allocate ionic autoionizing states, reveal dynamic correlations between two sequentially emitted photoelectrons, etc. The talk overviews developments in this new field. The following points are addressed: angular distributions and correlations of photoelectrons in sequential 2PDI and 3PDI [3–6], effects of alignment and coherency of the intermediate ionic states [6], resonant [7] and doubly resonant [8] sequential 3PDI. Theoretical predictions, based on statistical tensor approach combined with multi-configurational Hartree-Fock and Dirac-Fock calculations, are illustrated by first experimental data [1,7–9].

It is known that already at photon energies of a few hundreds eV, the photoelectron angular distribution in atomic single-photon ionization can be affected significantly by interferences between the electric dipole (E1) and electric quadrupole (E2) photoionization amplitudes. Thus, nondipole effects should show up also in the XUV/X-ray nonlinear atomic processes, first of all presumably in the angular distributions of emitted electrons. The nondipole effects in nonlinear photoprocesses in XUV is so far an opened field. First theoretical predictions will be presented of nondipole effects in the 2PDI.

This research is partly supported by the Russian President grant MK-6509.2012.2

References

- [1] M. Braune *et al.*, *XXV Int. Conf. on Photonic, Electronic and Atomic Collisions* (Freiburg, Germany, 2007), Abstracts, Fr034 and private communications
- [2] A. Rudenko *et al.*, *J. Phys. B* **43**, 194004 (2010)
- [3] A.S. Kheifets, *J. Phys. B* **40**, F313 (2007)
- [4] S. Fritzsche *et al.*, *J. Phys. B* **41**, 165601 (2008); *ibid* **42**, 145602 (2009); *ibid* **44**, 175602 (2011)
- [5] A.N. Grum-Grzhimailo *et al.*, *J. Phys. Conf. Ser.* **194**, 012004 (2009)
- [6] E.V. Gryzlova *et al.*, *J. Phys. B* **43**, 225602 (2010)
- [7] H. Fukuzawa *et al.*, *J. Phys. B* **43**, 111001 (2010)
- [8] E.V. Gryzlova *et al.*, *Phys. Rev. A* **84**, 063405 (2011)
- [9] M. Kurka *et al.*, *J. Phys. B* **42**, 141002 (2009)

Levitation and manipulation of aerosol particles by radiation pressure.

O. Isaksson^{1,2}, V. Mattiasson Ando², M. Karlsteen¹, and D. Hanstorp²

¹*Chalmers University of Technology, SE-412 96 Gothenburg, Sweden*

²*Department of Physics, Gothenburg University, SE-412 96 Gothenburg, Sweden*

Corresponding Author: oscar.isaksson@physics.gu.se

In the seventies, Arthur Ashkin [1,2] showed that particles can be levitated using radiation pressure. We have, using a similar technique, been able to levitate a single oil-drop for approximately 30 minutes. The drop was levitated just above the focus formed by a 30 mm lens in a vertically oriented laser beam. It was allowed to fall down through the laserbeam and it was trapped at the point where the radiation pressure balanced the gravitational force. This required a laser power of approximately 900 mW. The goal of our experiment is to show that we can measure the charge to mass ratio of the levitated oil drop. The levitation takes place inside a cell, Fig1. An electric field is applied between two electrodes in the bottom and the top of the cell. The charged drop is forced to oscillate by applying an AC electric field between the two electrodes. The movement is visualized by imaging the drop on a screen placed 1 m away from the cell, where the oscillations are magnified to an amplitude of a few millimetres. The intense scattering from the drop produces an image that is easily observable by the bare eye.

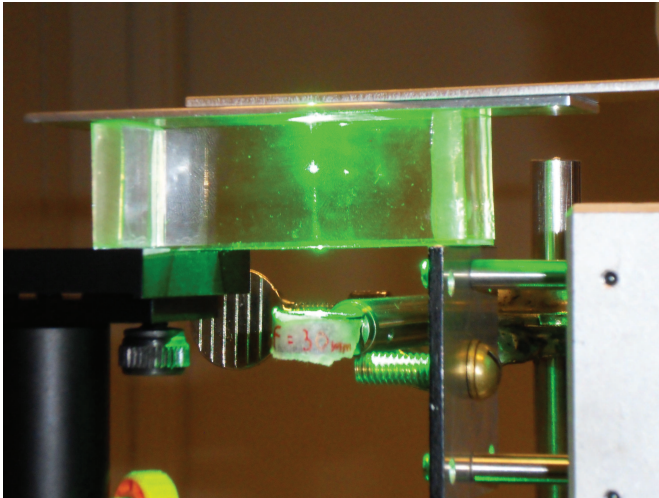


Figure 1: A picture of one levitated particle. The power of the laser is 900 mW and the wavelength is 532 nm.

References

- [1] A. Ashkin, Acceleration and trapping of particles by radiation pressure, *Physical Review Letters*, 24, s.156-159, (1970)
- [2] A. Ashkin, Optical Levitation by Radiation Pressure, *Applied Physics Letters*, 19, s. 283, (1971)

Suppression of endohedral cerium $4d \rightarrow 4f$ resonance in photoabsorption of Ce@C_{82}^+

G. Kashenock^{1,2}, S. Fritzsche¹

²*Department of Physics, Fi-90014 University of Oulu, Oulu, Finland*

¹*St.Petersburg Polytechnical University, St.Petersburg 195251, Russia*

Corresponding Author: galya.abroad@mail.ru

We present the first theoretical investigation of the single-photoionization spectrum for cerium in fullerene endohedron complex Ce@C_{82}^+ (in practice, $\text{Ce}^{3+@\text{C}_{82}^{2-}}$). The fullerene cage is modeled by a spherical jellium-shell [1,2]. With using multiconfiguration Dirac-Fock (MCDF) approach [3,4] we calculate the oscillator strengths within the $4d$ resonance region (100-160 eV) for phototransitions from the outermost shells of ion Ce^{3+} with and without account for influence of the potential generated by the fullerene cage. It is shown that integrated oscillator strengths have the main contribution from the Ce^{3+} : $4d \rightarrow 4f$ resonance photoexcitations and subsequent Auger decay which we consider within the two-step model. The photoabsorption is strongly suppressed for a $\text{Ce}^{3+@}$ ion embedded into a carbon cage C_{82}^{2-} compared with that for a "free" Ce^{3+} ion. Our calculations demonstrate that the resonance $f_{4d \rightarrow 4f}$ oscillator strength are changed (decrease) very slightly in the presence of the confining cage potential. On the contrary, the Auger transition linewidths are changed strongly (increase) due to change of photoelectron continuum wavefunctions behavior in scattering by the fullerene cage potential. We present the photoionization cross sections (Lorenzian profiles) for Ce^{3+} : $4d \rightarrow 4f$ "giant" resonance region calculated with the cage potential taken into account and with no account for it. It is shown that the main reason of changing in the resonance profile in the photoabsorption cross section curve (decreasing of the maximum values) is the increasing in Auger transition linewidths due to interaction of photoelectrons with cage electrons. The reduction of the integrated oscillator strength is demonstrated. Our results are in fair agreement with the recent experiment by Müller *et al.*[5].

References

- [1] V. K. Ivanov, G. Yu. Kashenock, R. G. Polozkov, and A. V. Solovyov, *J. Phys. B* **34**, L669 (2001)
- [2] V. K. Ivanov, G. Yu. Kashenock, R. G. Polozkov, and A. V. Solovyov, *JETP* **96**, 658 (2003)
- [3] F. A. Parpia, C. Froese Fischer, and I. P. Grant, *Comput. Phys. Commun.* **94**, 249 (1996)
- [4] S. Fritzsche *et al.*, *Nucl. Instrum. Methods Phys. Res. B* **205**, 93 (2003)
- [5] A. Müller *et al.*, *Phys. Rev. Lett.* **101**, 133001 (2008)

Photoionization from the deepest valence-band σ -shells of fullerenes C_{60} and C_{20} : δ -potential approach

G. Kashenock^{1,2}, R. Pratt¹

¹*Department of Physics and Astronomy, University of Pittsburgh, Pittsburgh, PA 15260, USA*

²*St.Petersburg Polytechnical University, St.Petersburg 195251, Russia*

Corresponding Author: galya.abroad@mail.ru

The nearly spherical cage form of carbon clusters such as fullerenes $C_{60}(I_h)$ and $C_{20}(C_i)$ or C_i point groups) in the first approximation might be considered as a spherical bubble. Then the potential energy is modeled by a spherical delta-function ("Dirac bubble") potential $V(r) = -A\delta(r - R)$, where A is the strength parameter, R is the fullerene radius. The quantum mechanical problem was considered by Blinder in 1979 [1]. Schrödinger equation are solved by exploiting the isomorphisms with free-particle partial-wave Green function. The δ -potential model was applied by Baltenkov [2] to description of an electron, bound or scattered, in the field of neutral C_{60} molecules, namely, to study of the extra, outermost-shell electron photodetachment from fullerene negative ion C_{60}^- . The goal of the present work is to investigate the ionisation by high-energy photons from the inner shells ($1s$ and $2p$) of the valence band (delocalized electrons) of the fullerenes C_{60} and C_{20} (the terminology usually used for modeling the planar graphite surface is accepted here). The whole energy spectra of σ orbitals and the behavior of valence shell wavefunctions within our model with the proper choice of the strength parameter values A (for given values $E_{1s}=29.5$ eV, $R=6.66$ au for C_{60} [3] and $E_{1s} = 27.9$ eV, $R = 3.86$ au for C_{20} [4]) are in good agreement with the other theoretical results for C_{60} [3] and C_{20} [4] systems.

Photoelectron (continuum) wave functions are specified in terms of phase shifts and normalizations. The dipole amplitudes are calculated numerically in the length gauge and analytically (with using the derivative of delta-function, δ' , formalism) in the acceleration gauge. The resonance features in photoionization are investigated. We analyze phaseshifts behaviour for s -, p -, d - partial waves which is of oscillation type. The energy dependence of the photoelectron phaseshifts is given. The calculated partial and total photoionization cross sections reveal a distinct "serrated" structures over the wide range of photon energies (1-6 au). The analytical expressions for l -partial $l \rightarrow l \pm 1$ phototransition cross sections are also written out.

The high-energy cross section asymptotics is deduced (k is an electron momentum, ω is a photon energy) - it is the inverse $5/2$ power fall off in energy, modulated by oscillating trig functions: $\sigma \sim \omega^{-5/2} \sin^2(kR)$.

References

- [1] B. M. Blinder, Chem. Phys. Lett. **64**, 485 (1979)
- [2] A. S. Baltenkov, Physics Letters A **254**, 203-209 (1999)
- [3] V. K. Ivanov, G. Yu. Kashenock, R. G. Polozkov, and A. V. Solovyov, JETP **96**, 658 (2003)
- [4] F. A. Gianturco, G. Yu. Kashenock, R. R. Lucchese, and N. Sanna, J. Chem. Phys. **116**, 2811 (2002)

Resonances and thresholds in negative ion photodetachment

A. O. Lindahl¹, J. Rohlén¹, H. Hultgren^{1,2}, H. Karlen¹, I. Yu. Kiyan², D. J. Pegg³,
C. W. Walter⁴, J. Welander¹, and D. Hanstorp¹

¹Department of Physics, Gothenburg University, SE-412 96 Gothenburg, Sweden

²Albert-Ludwigs-Universität, D-79104 Freiburg, Germany

³Department of Physics, University of Tennessee, Knoxville, Tennessee 37996, USA

⁴Department of Physics and Astronomy, Denison University, Granville, Ohio 43023, USA

Corresponding Author: Anton.Lindahl@physics.gu.se

Negative ions are of considerable interest in atomic physics since their properties are strongly influenced by electron-electron correlation. Experimental investigations can therefore serve as benchmarks for atomic many-body calculations. In this respect, two-electron processes in negative ions are of specific interest. Such processes include excitation and decay of doubly excited states and photodetachment into excited states of the residual atom.

We have recently presented a method [1, 2] where partial photodetachment cross sections to highly excited states in the residual atom can be measured. As discussed in [2], the possibility of observing the same resonance structures in multiple channels is a major advantage in the identification of the resonance parameters of the underlying doubly excited states.

Four partial cross sections for photodetachment of Cs⁻ are shown in Fig. 1. It is apparent from the data that the region contains many and partly overlapping resonances. Moreover, Fig. 1d represents the second observation ever of the 6h state in Cs [3]. In order to extract parameters for the overlapping resonances it is important to take the interference of the different resonances into account. A model for such parameter extraction will be described.

The new detection method led to the first observation of a new threshold behavior. It was recorded in the $K^- + h\nu \rightarrow K(5g) + e^-$ photodetachment channel and was attributed to the large and negative polarizability of the residual K(5g) atom [1]. In Cs⁻ the complex resonance structure impede any detailed investigation of the non resonant cross sections. However, an attempt to observe clean thresholds in Li⁻ photodetachment is underway. The progress of these experiments will be discussed together with possible implications of the data shown in Fig. 1.

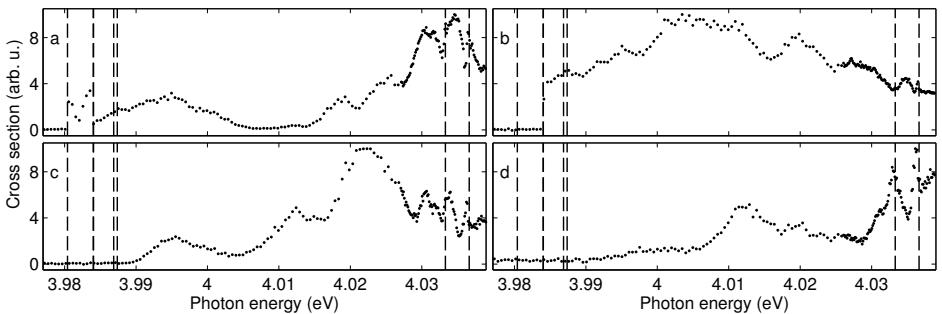


Figure 1: Partial photodetachment cross sections for Cs⁻ into the Cs(10s), Cs(6f), Cs(6g) and Cs(6h) channels in panels a, b, c and d, respectively. The vertical dashed lines mark the energies of the 10s, 6f, 6g, 6h, 10p($J=1/2$) and 10p($J=3/2$) states.

References

- [1] A. O. Lindahl *et al.*, Physical Review Letters **108**, 033004 (2012)
- [2] A. O. Lindahl *et al.*, Physical Review A **85**, 033415 (2012)
- [3] S. Civiš *et al.*, Journal of Physics B **44**, 225006 (2011)

The second Born approximation for the ionization of atoms

F. Menas^{1,2}, C. Dal Cappello³

¹Laboratoire de Physique et Chimie Quantique, Université Mouloud MAMMERI Tizi-Ouzou, BP 17,15000 Tizi-Ouzou, Algeria

²Ecole Nationale préparatoire aux Etudes d'Ingénierat, BP N5 ,Rouiba ,Algeria

³S.R.M.C. UMR 7565, Université de Lorraine,1 Boulevard Arago, 57078 Metz Cedex 3, France

Corresponding Author: menasferhat@mail.ummo.dz

Recently, Dal Cappello *et al.*[1] have shown that the second Born approximation fails for describing the ionization of atomic hydrogen by electrons when the energy of the ejected electrons is not small (for instance: an ejected energy of 50 eV and an incident energy of 250 eV). In this case the well-known BBK [2] model gives a good agreement with the experimental data [3].

Now, if we want to explain the ionization-excitation of helium by using the BBK model [4] the agreement is not good while the second Born approximation works very well [5].

In order to find a model which is able to give a good agreement in these two kinds of experiments we investigate the second Born approximation by including the BBK model. It means that the final state (the scattered electron , the ejected electron and the nucleus) is described by the BBK model and that the collision is a two-step process in any case.

We start to study the single ionization of atomic hydrogen in the plane of the collision and out the plane. For describing the intermediate state (as required in the second Born approximation) we use a basis including 32 discrete states and pseudo-states [1] and are able to reduce the 12-dimensional integrals in a 5-dimensional integral by using the well-known method of Roy *et al* [6] and that of Brauner *et al* [2] and a lot of derivations following the works of Hafid *et al* [7] and those of Cheikh *et al* [8].

Results will be presented at the conference.

References

- [1] C. Dal Cappello *et al.*, J. Phys. B: At. Mol. Opt. Phys. **44** , 015204 (2011)
- [2] M. Brauner, J. S. Briggs and H. Klar, J. Phys. B: At. Mol. Opt. Phys. **22** , 2265 (1989)
- [3] E. Weigold *et al.*, J. Phys. B: At. Mol. Opt. Phys. **12** , 291 (1979)
- [4] C. Dal Cappello *et al.*, NIMB, **266**, 570 (2008)
- [5] N. Watanabe *et al.*, Phys. Rev. A. **75**, 052727 (2007)
- [6] A. Roy, K. Roy and N. C. Sil, J. Phys. B: At. Mol. Opt. Phys. **13** , 3443 (1980)
- [7] H. Hafid, B. Joulakian and C. Dal Cappello, J. Phys. B: At. Mol. Opt. Phys. **26** , 3415 (1993)
- [8] R. Cheikh, J. Hanssen and B. Joulakian, Eur. Phys. J. D, **2** , 203 (1998)

Electron collisional spectroscopy of neutral atoms and multicharged ions in plasma within combined energy and Debae shielding approach

A. V. Loboda¹

¹*Odessa State University-OSENU, P.O.Box 24a, 65009, Odessa-9, Ukraine*

Corresponding Author: andmolec@mail.ru

The problem of diagnostics for the collisionally pumped plasma and search of the optimal plasma parameters of X-ray lasing are studied. Two principal theoretical problems must be solved in order to develop a special code adequate to predict the plasma parameters needed to generate a soft-X-ray or extreme UV amplified spontaneous emission: i). accurate calculation of electron-collision excitation cross-sections, rate coefficients for elementary processes in the plasma that are responsible for the formation of emission lines spectra; ii). kinetics calculation to determine level populations, inversions, line intensities, gain coefficients at definite plasma parameters. We present the generalized energy approach, formally based on the relativistic many-body perturbation theory (PT) [3] for the calculation of electron collision strengths and rate coefficients in a multicharged ions (in a collisionally pumped plasma). An account for the plasma medium influence is carried out within a Debae shielding approach. The aim is to study, in a uniform manner, elementary processes responsible for emission-line formation in plasmas. The electron collision excitation cross-sections and rate coefficients for some plasma Ne- and Ar-like multicharged ions are calculated. To test the results of calculations we compare them with other authors' calculations and with available experimental data [1,3]. Besides, we are studying the functions, which describe the population distribution within each Rydberg series dependent on the Rydberg electron energy for ions investigated. These functions bear the plasma diagnostic information. It is presented an electron collisional spectroscopy of neutral Ne atom too.

References

- [1] E. P. Ivanova, L. N. Ivanov, L. Knight, **48**, 4365 (1993)
- [2] A. V. Glushkov and L. N. Ivanov, *Phys. Lett.* **A170**, 33 (1992)
- [3] S. V. Malinovskaya, A. V. Glushkov, A. V. Loboda *et al.*, *Int.J.Quant.Chem.* **111**, 288 (2011)

Resonance states of atomic hydrogen in combined ac and dc fields

M. Pawlak¹, M. Bylicki², N. Moiseyev³, and M. Sindelka³

¹*Faculty of Chemistry, Nicolaus Copernicus University, Gagarina 7, 87-100 Toruń, Poland*

²*Institute of Physics, Nicolaus Copernicus University, Grudziądzka 5, 87-100 Toruń, Poland*

³*Schulich Faculty of Chemistry, Department of Physics and Minerva Center of Nonlinear Physics of Complex Systems, Technion-Israel Institute of Technology, Haifa, 32000, Israel*

Corresponding Author: teomar@chem.umk.pl

The influence of an external static dc field on atomic hydrogen in a monochromatic ac field is theoretically investigated. It is shown that by varying the strength of the dc field, the photoionization rate of decay is dramatically affected. An enhancement of the photoionization rate results from the photoexcitation of the ground state of atomic hydrogen to one of the excited Stark resonance states. A suppression of the photoionization rate arises because of the sum of the contributions of the adjacent Stark resonances. The analysis was conducted using the complex scaled Floquet method within basis of square integrable functions. Moreover our calculations show that even when the ac field intensity is high, the second-order perturbation theory explains quantitatively how the photoionization rate is enhanced or suppressed by the static field.

Spectroscopic analysis of the blue light emitted from Middleton type Cesium sputter negative ion sources.

P. Andersson¹, M. Martschini¹, A. Priller¹, P. Steier¹, R. Golser¹, and O. Forstner¹

¹University of Vienna, Faculty of Physics, Isotope Research, AT-1090 Wien, Austria

Corresponding Author: pontus.andersson@univie.ac.at

Negative ions of atoms and molecules are widely used in both fundamental and applied research. The possibility to provide intense beams of negative ions is especially important in negative ion research [1], fusion development [2] and nuclear physics performed with tandem accelerators [3]. A special case of the last is ultra rare isotope analysis by Accelerator Mass Spectrometry (AMS) [4]. Sputter ion sources of the Middleton type [5] have since 1977 been the main tool used to create stable, intense negative ion beams for injection into AMS machines. However, the theory behind negative ion formation in Middleton type cesium sputter sources is yet not fully agreed upon [6,7,8,9]. When this type of source is run under conditions that provide medium to high output currents, a blue light can often be seen emanating from, or just in front of the sputter target surface [10]. As a part of the work in trying to unravel the mechanisms of hard sputtering in a cesium rich environment, we have resolved the spectrum of the blue light emitted from three different cathodes; A carbon filled copper cathode, a pure aluminum cathode and a pure copper cathode. All cathodes was analyzed under the same source conditions but with different total current output. A fiber coupled spectrometer was used to detect light in the wavelength region 200 to 1100 nm and the blue glowing region was observed from a distance of 3 meters through a view port with a straight line of sight onto the cathode. The spectra showed clear differences depending on the cathode material. The emitted light from the carbon consists almost entirely of lines from neutral cesium and no lines from ionized cesium. A weak, broad feature was also seen between 470 and 510 nm. This feature was not seen in the two metallic cathodes, which both also displayed several lines originating from positively ionized cesium. For the copper cathode the intensity of the spectrum was much smaller than for the other two cathodes. These results may suggest different mechanisms of negative ion formation in the ion source depending on the cathode material. As a side effect of the measurement it proved relatively easy to determine the source temperature to within $\pm 30^\circ$ from the black body radiation in the spectra. This was verified by spectra from a temperature controlled combustion oven.

References

- [1] T. Andersen, Phys. Rep.-Rev Sect. Phys Lett. **394** (4-5),157-313 (2004)
- [2] R. Hemsworth, H. Decamps, J. Graceffa, *et al.* Nucl. Fusion **4**, 045006(2009)
- [3] D. A. Bromley, Nuclear Instruments and Methods **122** 1-34 (1974)
- [4] A. E. Litherland, X-L. Zhao And W. E. Kieser, Mass Spectrometry Reviews, DOI: 10.1002/mas.20311 (2010)
- [5] R. Middleton, Nucl. Instr. & Meth.in Phys. Res. **214** (2-3),139-150(1983)
- [6] K. Wittmaack, Ion Beam Science. Solved and Unsolved Problems, Part II pp 465-495 (2007)
- [7] H.Gnaser, Phys. Rev. B **54** (23) 16 456 (1996)
- [8] G. Doucas, Int. J. Mass Spectrom. Ion Processes **25** (1) 71 (1977)
- [9] J. S.Vogel, J. A. Giacomo, S. R.Dueker, Submitted to Nucl. Instr. Meth B , Private communication
- [10] Middleton R., A Negative Ion Cookbook, University of Pennsylvania, USA, 1989 (unpublished) Available (2011) at www.pelletron.com/cookbook.pdf

Variation of photodissociation spectra of molecular anions with storage time in an electrostatic storage ring

T. Tanabe¹, M. Saito², K. Noda³, and E. B. Starikov⁴

¹High Energy Accelerator Research Organization (KEK), Tsukuba 305-0801, Japan

²Kyoto Prefectural University, Kyoto 606-8522, Japan

³National Institute of Radiological Sciences, Chiba 263-8555, Japan

⁴Chalmers University of Technology, SE-41296 Gothenburg, Sweden

Corresponding Author: tetsumi.tanabe@kek.jp

Photodissociation of fluorescein and its 5-carboxyfluorescein analogue monoanions was studied using an electrostatic storage ring (Fig. 1). Ions were produced by an electrospray ion source and stored in an ion trap. Ions were then injected into the ring after acceleration to 20 keV. Stored ions were irradiated by an OPO laser (wavelength: 410 - 600 nm) and neutral products were detected [1]. The storage time was variable up to the order of seconds.

The photodissociation neutral spectra as a function of time vary dependent on the storage time as well as the laser wavelength. By comparing the wavelength spectra obtained herein with absorption spectra reported recently [2,3], it was deduced that the spectra originated from various tautomers of fluorescein monoanions. Moreover, wavelength spectra vary during long-term storage in the storage ring. Origin of this phenomenon seems to come from an interconversion of tautomers. Further studies with quantum chemical calculations are now going on.

The same was also found for desodiated orange I monoanions, which consist of tautomers.

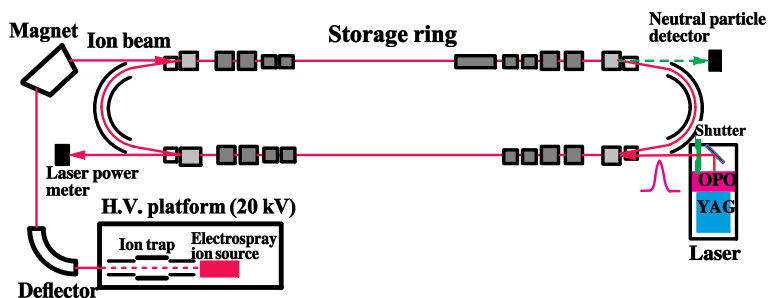


Figure 1: Experimental setup at KEK.

References

- [1] T. Tanabe, M. Saito, and K. Noda, *Eur. Phys. J. D* **62**, 191–195 (2011)
- [2] N. O. Mchedlov-Petrossyan *et al.*, *Chem. Lett.* **39**, 30–31 (2010)
- [3] P. D. McQueen *et al.*, *Angew. Chem. Int. Ed.* **49**, 9193–9196 (2010)

Autoionizing states of Ca in the problem of ionization of calcium atom by the electrons

V.M. Simulik¹, R. Tymchyk¹, and T.M. Zajac²

¹*Institute of Electron Physics, Ukrainian National Academy of Sciences, 21 Universitetska St., 88017 Uzhgorod, Ukraine*

²*Department of Engineering, Uzhgorod National University, 13 Kapitulna St., 88000 Uzhgorod, Ukraine*

Corresponding Author: romannetmail@gmail.com

The method of interacting configurations in complex numbers representation (MICCNR) has been developed in publications [1,2]. The first application for the problems of two-electron system ionization by photons has been realized. Excitation and decay of autoionizing states, which essentially contribute into ionization cross sections, were investigated.

In this abstract the possibility of using MICCNR for the investigation of autoionizing states of calcium is under consideration. The problem of ionization of Ca atom by the photons (electrons) is considered.

The results of our calculations, together with comparison of the energetic positions of some lowest 1P states with the similar results of other authors [3-5], are presented in the table. Here [3,5] are the experimental data and [4] is the theoretical calculation. We follow the classification suggested in [4].

<i>Configuration</i>	MICCNR, E	[3], E	[4], E	[5], E
<i>3d5p</i>	6.601	6.59	6.604	6.58
<i>3d6p</i>	7.033	7.02	7.038	7.02
<i>4p5s</i>	7.159	7.13	7.166	7.12
<i>3d5f</i>	7.240	7.25	7.248	7.25
<i>3d7p</i>	7.397	7.39	7.342	7.41

Table 1: *AIS of Ca atom in eV.*

References

- [1] S.M. Burkov et al., J. Phys. B: Atom. and Mol. Phys. **21**, 1195-1208 (1988)
- [2] S.M. Burkov et al., J. Phys. B: Atom. and Mol. Phys. **23**, 3677-3689 (1990)
- [3] J. E. Kontrosh, I.V. Chernyshova, and O.B. Shpenik, Optics and Spectroscopy **110** 500-507 (2011)
- [4] O.I. Zatsarinny, V.I. Lengyel, and E.A. Masalovich, Phys. Rev. A. **44**, 7343-7354 (1991)
- [5] NIST Atomic Spectra Database. <http://physics.nist.gov/cgi-bin/AtData>

Observation of bound-bound transitions in the negative ion of lanthanum

C. W. Walter¹, N. D. Gibson¹, D. J. Matyas¹, A. N. Lebovitz¹, K. J. Liebl¹, and J. Rohlén²

¹*Department of Physics and Astronomy, Denison University, Granville, Ohio 43023, USA*

²*Department of Physics, Gothenburg University, SE-412 96 Gothenburg, Sweden*

Corresponding Author: walter@denison.edu

Negative ions provide challenging problems and critical test cases for atomic theory because the added electron is bound to a neutral core, thus the influence of such effects as electron-electron correlation and core polarization is greatly enhanced relative to neutral atoms and positive ions. The short range attraction in negative ions leads to a shallow well that typically can support only a single bound state electron configuration. The lanthanides are particularly interesting and challenging because the large number of electrons and the presence of several open shells lead to strong correlation effects. Theoretical calculations by O'Malley and Beck [1] have predicted that the negative ion of lanthanum La^- has multiple bound states of both even and odd parity formed through attachment of either a $5d$ or $6p$ electron, respectively, to the neutral La atom ground state ($[\text{Xe}]5d6s^2$).

In the present study, La^- has been investigated using tunable infrared laser photodetachment spectroscopy. The relative signal of neutral atom production was measured with a crossed laser-ion beam apparatus over the photon energy range 0.29–0.50 eV. The spectrum reveals a number of sharp peaks that are interpreted as due to bound-bound electric-dipole transitions in La^- , observed here through a two-step process of excitation followed by photodetachment of the upper state. The transitions responsible for four of the peaks are identified through comparison to the theoretical calculations of energy levels and transition strengths [1,2]. The richness of the observed bound state spectrum of La^- is unprecedented for atomic negative ions.

This material is based on work supported by the National Science Foundation under Grant Nos. 0757976 and 1068308.

References

- [1] S. M. O'Malley and D. R. Beck, Phys. Rev. A **79**, 012511 (2009)
- [2] S. M. O'Malley and D. R. Beck, Phys. Rev. A **81**, 032503 (2010)

Spectral properties of fluorescence labels based on different sizes nanodimension-size structures

V.A. Polischuk¹, A.V. Baranov¹, A.V. Fedorov¹, and A.S. Zlatov¹

¹*Information optical technology center, National research university of information technologies, mechanics and optics, Saint Petersburg, Russia*

Corresponding Author: vpvova@rambler.ru

At the present time phosphors labels are commonly based at organic dyes and luminescent microparticles doped with rare earths. However, they have some significant shortcomings: the low quantum yield, the complex sources of radiation, fast fading and other.

The above-mentioned shortcomings are absent in semiconductor nanocrystals (quantum dots) [1], which makes semiconductor phosphors optimal material for creating fluorescent labels.

The objective was to investigate luminescent properties of different concentrations of quantum dots (QD) various sizes fluorescent QD-markers. To do this we have selected two QD compositions with an average particle size: first composition has 2.5 nm QD particles, second composition - 5 nm QD particles.

Figure 1: QD-markers fluorescence spectra's: 7 markers with different concentrations of QDs.

In this work we have established that larger-size QD particles effectively quenched smaller-size QDs fluorescence. When the concentration ratio of QD solutions with same values of extinction coefficients exceeded 4:1 (solution with particles of 2.5 nm to a solution with particles of 5 nm) fluorescence of 2.5 nm QD particles is completely extinguished. Thereby to create correctly working fluorescent QD labels necessary use QDs with same-size particles or scattered in space different-size particles.

References

[1] A.V. Baranov, V.G. Davydov, A.V. Fedorov, H.W. Ren, S. Sugou, and Y. Masumoto. *Heterostructure optical phonons in dynamics of quantum dot electronic excitations: new experimental evidences*. Proceedings of SPIE 5023,247-250 (2003)

PO

Quantum Optics

Harmonic generation on highly charged hydrogen-like ions at the multiphoton resonant interaction with x-ray laser

H.K. Avetissian¹, B.R. Avchyan¹, A.G. Ghazaryan¹, and G.F. Mkrtchian¹

¹*Centre of Strong Fields Physics, Yerevan State University,
1 A. Manukian Street, Yerevan, Armenia*

Corresponding Author: avetissian@ysu.am

The recent progress in x-ray free electron laser (FEL) technology [1] allows one to get coherent hard x-rays with peak brightness ten orders of magnitude exceeding ones in conventional synchrotron sources. The interaction of such powerful x-ray radiation with atomic/ionic systems has multiphoton character and opens up a wide research field where common atom-light interaction effects can be extended to high-energy transitions. For this propose atoms or ions with large enough nuclear charges are necessary, at which relativistic effects, particularly, the fine structure of atoms/ions should be taken into account.

In Ref. [2], on the basis of analytical solution of the Dirac equation the resonant multiphoton excitation of highly charged hydrogenlike ions in a strong high-frequency laser field has been investigated. Obtained results suggest that by the appropriate x-ray pulses when the rate of concurrent process of ionization is small, one can achieve various superposition states by multiphoton resonant transitions, which may lead to cooperative processes - such as superradiation, free-induction decay, photon-echo and etc.

In the present paper coherent x-ray scattering by a highly charged hydrogenlike heavy ions due to multiphoton resonant excitation is studied towards the harmonic generation implementation. The consideration is based on the Dirac equation, which allows to take into account the fine structure of ionic levels. The spectrum corresponding to harmonics radiation at the bound-bound transitions is investigated both analytically and numerically. To find out the radiation spectrum numerically, the Fast Fourier Transform algorithm has been applied.

Calculations show that one can achieve a quite large conversion efficiency for moderately large harmonics which is comparable to what one expects to achieve with resonant two-level systems possessed by permanent dipole moments [3,4]. The considered mechanism may serve as a promising scheme of superradiant source of coherent radiation with shorter wavelengths than the applied x-ray FEL.

This work was supported by State Committee of Science (SCS) of the Republic of Armenia.

References

- [1] P. Emma *et al.*, Nature Photonics **4**, 641 (2010)
- [2] H. K. Avetissian, G. F. Mkrtchian, and M. G. Poghosyan, Phys. Rev. A **73**, 063413 (2006)
- [3] H. K. Avetissian, B. R. Avchyan, and G. F. Mkrtchian, Phys. Rev. A **77**, 023409 (2008)
- [4] H. K. Avetissian, B. R. Avchyan, and G. F. Mkrtchian, J. Phys. B **45**, 025402 (2012)

All-Optical Toffoli gate in the solid

V. Chaltykyan¹, E. Gazazyan¹, and G. Grigoryan¹

¹*Institute for Physical Research, NAS of Armenia, Ashtarak-2 0203, Armenia*

Corresponding Author: EmilGazazyan@gmail.com

A universal reversible logic Toffoli gate was first introduced in 1980 year's work [1]. It has been shown that any reversible processor can be constructed using only circuits of this gate. The simplest three-bit Toffoli gate (CCNOT) has three inputs and three outputs. Two of the bits are control bits that are unaffected by the action of the Toffoli gate. The third bit is a target bit that is flipped in only cases when both control bits are set to 1. Due to its universality the Toffoli gate is important, not only in the classical calculations of conventional Boolean functions, but also in a quantum computer [3-4]. The quantum Toffoli gate recently has been successfully implemented experimentally in the ion trap [4].

In this paper we demonstrate a simple realization of all optical Toffoli gate in a resonant medium consisting of Λ -atoms. Proposed scheme based on the cyclic adiabatic population transfer by STIRAP and b-STIRAP methods, which are well studied both theoretically and experimentally, not only on individual atoms [5], but also in the medium [6]. As a solid state media can be used crystal $\text{Pr}^{3+}:\text{Y}_2\text{SiO}_5$, which has already been successfully used to construct a classical adder in the experiment [7]. The proposed scheme does not require any improvement of this experiment. It simply shows that one can construct all optical reversible processor in the same way. Note that all-optical logic elements, such as implemented in this experiment and using coherent resonant interaction of atoms with laser pulses, are a necessary intermediate step in the transition from classical to quantum calculating. At the same time, in order to transition directly from quantum logical schemes to classical, the last ones must contain only reversible elements, like the Toffoli gate [2].

References

- [1] T. Toffoli, "Reversible computing", Technical Report MIT/LCS/TM-151, Cambridge, Massachusetts, (1980)
- [2] M. Nielsen, I. C. Chuang, "Quantum Computation and Quantum Information", Cambridge University Press, Cambridge, UK (2000)
- [3] J. K. Pachos, P. L. Knight Phys. Rev. Lett. 91, 107902 (2003)
- [4] T. Monz, K. Kim, W. Hensel, M. Riebe, A. S. Villar, P. Schindler, M. Chwalla, M. Hennrich, R. Blatt, Phys. Rev. Lett. 102, 040501 (2009). [5] K. Bergman, H. Theuer, B. Shore, Rev. Mod. Phys. 70, 1003 (2004)
- [6] G. G. Grigoryan, G. Nikoghosyan, T. Halfmann, Y. T. Pashayan-Leroy, C. Leroy, S. Guerin, Phys. Rev. A 80, 033402 (2009)
- [7] F. Bell, T. Halfmann, F. Remacle, R. D. Levin, Phys. Rev. A 83, 033421 (2011)

Relativistic energy approach to atoms, ions and nuclei in a super strong laser field

A.-V. Glushkov^{1,2}

¹*Odessa State University-OSENU, P.O.Box 24a, 65009, Odessa-9, ukraine*

¹*ISAN, Russian Academy of Sciences, Troitsk, 142090, Russia*

Corresponding Author: glushkov@paco.net

A consistent relativistic energy approach [1-3] is applied to studying the interaction of the atoms and ions of plasma with an super intense electromagnetic (laser) field. Method bases on description of atom in a field by the k- photon emission and absorption lines. The lines are described by the QED moments of different orders, which can be calculated with the use of the Gell-Mann and Low S-matrix adiabatic formalism. In relativistic version the Gell-Mann and Low formulae expresses an imaginary part of the energy shift ImE through the QED scattering matrix, including interaction of atom with electromagnetic field and field of the photon vacuum. We present QED S-matrix energy formalism for calculation of the spectral lines shape in dense plasma. For any atomic level we calculate Im E as function of the laser pulse central frequency and further the moments of lines. Numerical modelling carried out for H, Cs, Ar, Yb, Tm atoms and H-, Li- and Ne-like ions. Especial interest attracts new relativistic treating of the drastic broadening effect of widths for the autoionization resonances in lanthanides. The direct interaction of super intense laser fields in the optical frequency domain with nuclei is studied and the AC Stark effect for nuclei is described within the operator perturbation theory and the relativistic mean-field model for the ground-state calculation of the nuclei 49Sc, 171Yb and compared with other available data

References

- [1] A. V. Glushkov *et al.*, In: *Frontiers in Quantum Systems in Chemistry and Physics*, Eds.S. Wilson, P. Grout, J. Maruani, G. Delgado-Barrio, P. Piecuch (Springer, Berlin, 2008) **18**, 505-558
- [2] A. V. Glushkov and L. N. Ivanov, *Phys. Lett.***A170**, 33 (1992)
- [3] A. V. Glushkov *et al.*, *Physica Scripta***T135**, 014022 (2009)

Manifestation of dark state formation in Na hyperfine level system

D. Efimov¹, N. N. Bezuglov^{1,2}, J. Ulmanis², M. Bruvelis², K. Miculis², T. Kirova², and A. Ekers²

¹*Faculty of Physics, St.Petersburg State University, 198904 St. Petersburg, Russia*

²*Laser Centre, University of Latvia, LV-1002 Riga, Latvia*

Corresponding Author: teo@lu.lv

We demonstrate experimentally the onset of the dark state formation upon strong coupling of atomic Na hyperfine energy levels. The $3S_{1/2}, F'' = 1, 2$ and the $3P_{1/2}, F' = 1, 2$ hyperfine levels are coupled by a strong laser field S with Rabi frequency Ω_S , leading to the formation of laser-dressed states [1]. The dressed states are monitored by recording the excitation spectrum upon scanning a weak probe field P across the $3P_{1/2}, F = 1, 2 \rightarrow 7D_{3/2}$ transition. The experiment is performed in a supersonic atomic beam with counter-propagating S and P laser fields while fluorescence from the $7D_{3/2}$ is registered by a photon counter. The excitation spectrum of the $7D_{3/2}$ state exhibits an intense main peak with side peaks with much smaller intensities (Fig. 1). The increase of Ω_S leads to no change in the position of the main peak, while the side peaks are shifted further apart. The results are confirmed by our theoretical model based on solving the density matrix equations of motion and the numerical simulations show a good agreement with the experimental data. These observations are explained in the dressed-states picture of the three level system consisting of Na ground state hyperfine level $F'' = 1$ or $F'' = 2$ (depending on S -field detuning) with the $F' = 1, 2$ levels of $3P_{1/2}$ coupled by Ω_S . Following the reasoning of Fano [2], we show that such system exhibits a visible "gray" state whose eigenvalue is weakly affected by the magnitude of Ω_S . This gray state evolves into a dark state at high Ω_S . We acknowledge support by the EU FP7 Centre of Excellence project FOTONIKA-LV and IRSES Project COLIMA.

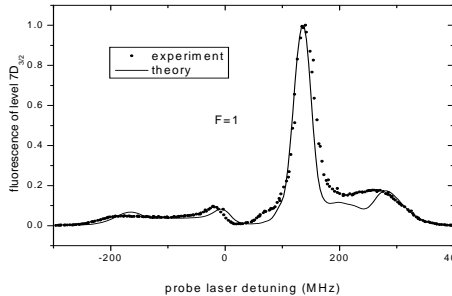


Figure 1: Fluorescence from the $7D_{3/2}$ level as a function of the probe laser detuning

References

- [1] C. Cohen-Tannoudji and S. Reynaud, J. Phys. B- At. Mol. Phys. **10**, 345–363 (1977)
- [2] U. Fano, Phys. Rev. **124**, 1866–1878 (1961)

First principle calculation on thermophysical and transport properties of alkali-rare gas systems

V. Meshkov¹, E. Pazyuk¹, and A. Stolyarov¹

¹*Department of Chemistry, Moscow State University, 119991, Moscow, Leninskie gory 1/3, Russia*

Corresponding Author: meshkov@laser.chem.msu.ru

There has been a long standing interest in developing optically pumped alkali atom lasers. Diode laser pumped alkali lasers (DPAL) hold considerable promise for efficient, scalable lasers in the visible range for Rb [1] and Cs [2] atoms. Theoretical basis and performance modeling for the DPAL systems apparently requires the extensive knowledge of thermophysical properties for the alkali-rare gas systems.

We present the results of high-level electronic structure calculations of the potential energy curves (PECs) for the ground state of van der Waals molecules MeRg (Me=Rb,Cs) as well as their well-bound MeRg⁺ cations. The energies were calculated in a wide range of internuclear distance using the coupled-cluster method with single, double and approximate triple excitations CCSD(T), with the *def2*-A(T/Q)ZV-PP basis sets for both atoms augmented by the bound functions centered on a middle of internuclear distance. The extrapolation to complete basis set was performed and the full counterpoise correction technique was employed to remove basis set superposition error.

The derived *ab initio* point-wise potentials have been approximated by the closed form based on Chebyshev polynomial expansion, and then, the resulting analytical PECs were used to estimate thermodynamic functions and transport properties of the Me-Rg pairs in the framework of classical, quasi-classical and quantum statistical approaches. The present results are obtained in a wide temperature range and compared systematically with available experimental data and preceding calculations. The full form of the interacting-particle partition function (including quasi-bound and continuum part of the spectra) is found to be essential to complete and correct calculation of the bulk properties of the systems studied.

The work is supported by the Russian Foundation for Basic Research, through the grant 11-03-00307-a.

References

- [1] B.V.Zhdanov and R.J.Knize, *Opt. Lett.*, **32**, 2167 (2007)
- [2] B.V.Zhdanov *et al.**Opt. Lett.*, **33**, 414 (2008)

Entanglement in Helium

J.S. Dehesa¹, T. Koga², R.J. Yáñez¹, A.R. Plastino^{1,3}, and R.O. Esquivel⁴

¹*Instituto Carlos I de Física Teórica y Computacional and Departamento de Física Atómica, Molecular y Nuclear, Universidad de Granada, 18071 Granada, Spain*

²*Applied Chemistry Research Unit, Graduate School of Engineering, Muroran Institute of Technology, Muroran, Hokkaido 050-8585, Japan*

³*National University La Plata, CREG-UNLP-CONICET, CC 727, La Plata 1900, Argentina*

⁴*Departamento de Química, Universidad Autónoma Metropolitana, 09340-México DF, Mexico*

Corresponding Author: dehesa@ugr.es

Quantum entanglement in systems consisting of N identical fermions has attracted considerable attention in recent years [1-5]. Here we have computed the amount of entanglement exhibited by the ground state and several singlet and triplet excited states of the helium atom using high-quality, state-of-the-art wavefunctions of the Kinoshita type. We found that the behaviour of the entanglement of the eigenstates of helium is consistent with that observed in the case of previously studied exactly soluble two-electron systems such as the Moshinsky model, the Crandall system and the Hooke atom. In particular, the amount of entanglement exhibited by the eigenstates tends to increase with energy. The present calculations therefore provide further evidence suggesting that this behaviour is universal in two-electron systems. It would be interesting to extend this investigation to atoms with more than two electrons.

State	Energy	Entanglement
Singlet 1s	-2.903724377	0.015914 ± 0.000044
Singlet 2s	-2.145974046	0.48866 ± 0.00030
Singlet 3s	-2.061271954	0.49857 ± 0.00097
Singlet 4s	-2.033586653	0.49892 ± 0.00052
Singlet 5s	-2.021176531	0.4993 ± 0.0019
Triplet 2s	-2.175229378	0.47778 ± 0.00027
Triplet 3s	-2.068689045	0.49342 ± 0.00045
Triplet 4s	-2.036512038	0.49746 ± 0.00055
Triplet 5s	-2.022618670	0.49955 ± 0.00098

Table 1: Entanglement and energies of helium eigenstates. Entanglement is dimensionless and energy is given in hartrees.

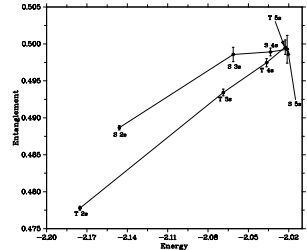


Figure 1: Entanglement against energy for both singlet and triplet states of helium.

References

- [1] J. S. Dehesa et al., J. Phys. B: At. Mol. Opt. Phys. **45**, 015504 (2012)
- [2] A.P. Majtey et al., J. Phys. A: Math. Theor. **45**, 115309 (11pp) (2012)
- [3] R.J. Yáñez et al., Eur. Phys. J. D **56**, 141 (2010)
- [4] D. Manzano et al., J. Phys. A: Math. Theor. **43** 275301 (2010)
- [5] K. Eckert et al., Ann. Phys. **299** 88 (2002)

An Ion Trap for Very Large Clouds

J. Pedregosa-Gutierrez¹, C. Champenois¹, M. Houssin¹, O. Morizot¹, G. Hagel¹, and M. Knoop¹

¹ *Universit e dAix-Marseille - CNRS, PIIM (UMR 7345), 13397 Marseille Cedex 20, France*
Corresponding Author: jofrat.pedregosa@univ-amu.fr

The trapping of large ion clouds or crystals is gaining interest for various applications. Quantum information processing and microwave metrology are only two of possible topics. Our group is setting up an experiment destined to the investigation of the dynamics and thermodynamics of trapped ions. In particular the use of very large ion clouds is a challenge allowing to reach interesting regimes for the study of phase transition, crystallization behaviour and long-range interactions. Our trapping device is composed of three zones aligned along a common z-axis. A quadrupole and an octupole linear trap are mounted in-line, the quadrupole part being separated in two zones by a center electrode. The geometry of trapping potentials has been optimized numerically [1]. The traps have been dimensioned to allow for the confinement of an ion cloud filling half the trap and reaching crystallization. The applied trapping voltages are of the order of several MHz with amplitudes of a couple of hundred volts (in order to trap Ca+ ions). Ions are created by photoionization from an atomic calcium beam crossing the first quadrupole zone. Clouds larger than 106 ions have been trapped and crystallized in the quadrupole part. These ion numbers correspond to a cloud size of $\approx 1/4$ with respect to the trap radius ($r_0 = 4\text{mm}$). Shuttling of the ions between the different zones of the device is one of the challenges. In view of the large number of parameters (voltage amplitudes, durations, switching functions and times), protocols have to be optimized numerically. While different solutions for shuttling have been proposed for quantum information processing, the present experiment has to take into account additional parameters, as for example the fact that the ion cloud is 3D, and the ratio of transport distance to the number of DC electrodes which is several orders of magnitude larger than in microtraps. Extended numerical simulations in 1D and 3D of such transports, together with experimental evidence will be reported.

References

- [1] [1] J. Pedregosa, C. Champenois, M. Houssin, M. Knoop, IJMS 290, 100-105 (2010)

$(e, 2e)$ ionization of molecular hydrogen

I. Tóth¹, L. Nagy¹

¹*Faculty of Physics, Babeş-Bolyai University, 400084 Cluj-Napoca, Romania*

Corresponding Author: istvan.toth@phys.ubbcluj.ro

$(e, 2e)$ studies for the ionization of atomic and molecular targets by electron projectiles have attracted much interest in the recent years due mainly to the development of new experimental techniques, which allowed for the detailed study of the ionization process. Such processes are described in terms of the triple or fully differential cross section (TDCS), which provides the angular distribution of the ejected electron of a given energy and for fixed momenta of the incident and scattered particles. Studies concerning the ionization of molecules are less abundant than for atomic targets due to the increased difficulties which arise when treating such complex structures. Experimentally is very difficult for example to separate the contributions of the electronic states with close energies, while for the theoretical treatment is challenging to take into account the multi-center nature of the targets.

Both experimental and theoretical $(e, 2e)$ studies have been performed in the last years for a relatively wide range of targets, from smaller molecules like H_2 [1-2] and N_2 [3] to larger targets such as $C_4H_4N_2$ [4]. Previously we have calculated TDCSs for N_2 , CH_4 and H_2O . These calculations were performed in the framework of the distorted-wave Born approximation (DWBA).

In our present study we calculate TDCSs for the ionization of the hydrogen molecule by electron impact for similar kinematical conditions as in case of the N_2 and CH_4 molecules. Our results are compared with the experimental data and the theoretical calculations presented in [1]. In this way a comparison of the TDCS for the different targets may be performed. Further, we calculate the TDCS for the ionization of the H_2 molecule as a function of the internuclear distance. In this case we compare our results with the experimental measurements and the theoretical TDCSs presented in [2]. In both cases the cross sections are determined within our TS (Total Screening) and TS* models. These models use distorted waves in order to describe the incident, scattered and ejected particles, while for the initial state of the target Gaussian type multi-center wavefunctions are employed. In the TS model we consider that the ejected electron moves in the spherically averaged potential field of the nuclei and the residual electrons, while the scattered electron experiences the effect of the spherically averaged nuclear potential and the field created by all electrons of the target. In the TS* model both outgoing electrons move in the same, spherically averaged field of the nuclei and the residual electrons.

This work was possible with the financial support of the Sectoral Operational Programme for Human Resources Development 2007-2013, cofinanced by the European Social Fund, under the project number POSDRU 89/1.5/S/60189 with the title "Postdoctoral Programs for Sustainable Development in a Knowledge Based Society" (I. Tóth) and of a grant of the Romanian National Authority for Scientific Research, CNCS-UEFISCDI, project number PN-II-ID-PCE-2011-3-0192 (L. Nagy)

References

- [1] E. M. Staicu Casagrande *et al.*, J. Phys. B: At. Mol. Opt. Phys. **41**, 025204 (2008)
- [2] A. Senftleben *et al.*, J. Phys. B: At. Mol. Opt. Phys. **45**, 021001 (2012)
- [3] A. Lahmam-Bennani *et al.*, J. Phys. B: At. Mol. Opt. Phys. **42**, 235205 (2009)
- [4] J. D. Builth-Williams *et al.*, J. Chem. Phys. **136**, 024304 (2012)

High-fidelity quantum information processing by composite pulses

B. T. Torosov¹, G. T. Genov¹, S. I. Ivanov¹, and N. V. Vitanov¹

¹*Department of Physics, Sofia University, 5 James Bourchier blvd, 1164 Sofia, Bulgaria*

Corresponding Author: vitanov@phys.uni-sofia.bg

The technique of composite pulses developed originally in nuclear magnetic resonance and optics is a powerful tool for quantum state manipulation. This technique replaces the single pulse used traditionally for driving a two-state quantum transition by a sequence of pulses with suitably chosen phases, which are used as a control tool for shaping the excitation profile in a desired manner. This technique combines the accuracy of resonant excitation with a robustness similar to adiabatic techniques. Composite pulses have therefore enjoyed increasing attention in the field of quantum computation, wherein ultrahigh fidelity of gate operations is required. We have developed a simple systematic approach, which allows the construction of composite sequences of pulses with smooth shapes that can create ultrahigh-fidelity excitation profiles [1]. Our method uses the SU(2) representation of the propagator of the two-state system, instead of the commonly used intuitive Bloch SO(3) rotations. We have designed arbitrarily accurate broadband, narrowband, passband and fractional- π composite pulses [1,2,3]. Composite sequences can reduce dramatically the addressing error in a lattice of closely spaced atoms or ions, and at the same time greatly enhance the robustness of qubit manipulations [2]. One can thus beat the diffraction limit, for only atoms situated in a small spatial region around the center of the laser beam are excited. We have used composite sequences of chirped pulses to optimize the technique of adiabatic passage between two quantum states: composite adiabatic passage (CAP) [4], in which nonadiabatic losses can be canceled to any desired order. We have also used composite pulses to design new, more efficient implementations of highly-conditional C^n -NOT gates, such as the Toffoli C^2 -NOT gate [5]. Finally, we have designed composite pulses suitable for manipulation of multistate systems [6], which allow to suppress unwanted transition channels [7].

References

- [1] B.T. Torosov and N.V. Vitanov, Phys. Rev. A **83**, 053420 (2011).
- [2] S.S. Ivanov and N.V. Vitanov, Opt. Lett. **36**, 1275 (2011).
- [3] N.V. Vitanov, Phys. Rev. A **84**, 065404 (2011).
- [4] B.T. Torosov, S. Guerin, and N.V. Vitanov, Phys. Rev. Lett. **106**, 233001 (2011).
- [5] S.S. Ivanov and N.V. Vitanov, Phys. Rev. A **84**, 022319 (2011).
- [6] G.T. Genov, B.T. Torosov, and N.V. Vitanov, Phys. Rev. A **84**, 063413 (2011).
- [7] G.T. Genov and N.V. Vitanov, to be published.

Electromagnetically induced transparency due to Zeeman coherence in buffer-gas cell - effects of laser radial profile and intensity

S. Nikolic¹, A. Krmpot¹, N. Lucic¹, B. Zlatkovic¹, M. Radonjic¹, and B. Jelenkovic¹

¹*Institute of Physics, University of Belgrade, 11080 Belgrade, Serbia*

Corresponding Author: stankon@ipb.ac.rs

Electromagnetically induced transparency (EIT), a narrow resonance in a laser transmission through coherent media, is essential for phenomena like slow and stored light, generation of correlated photon pairs, frequency mixing, Kerr nonlinearities. For many applications EIT line shape, amplitude and linewidths, are essential. In buffer gas cells optimum operating laser intensity and cell temperature for maximum EIT contrast and minimum linewidth may vary from cell to cell, depending on the cell geometry, type of buffer gas and its pressure.

We have investigated effects of laser intensity and cell temperature on Zeeman EIT for Rb cell with diameter of 25 mm and 8 cm of length, filled with 30 Torr Ne, at temperatures from 60 to 82 °C. We observed narrow, sub kHz EIT resonances due to Zeeman coherence in $Fg = 2$ hyperfine level of ⁸⁷Rb ground state using laser beams of different radial intensity distribution and of different radius.

For Gaussian laser radial profile variation of laser radius affects primarily the EIT contrast. Amplitudes for 6 mm and 1 mm beam diameter peak at laser intensity around 1.1 mW/cm² and 3.2 mW/cm² respectively and EIT contrast increased 2.2 folds for narrower laser beam. EIT line shapes for 1 mm laser beam radius also have non-Lorentzian profile. The line narrowing at the very center of the resonance is due to Ramsey effect occurring because coherently prepared atoms diffusing out, and then back to the laser beam, spend comparable time in and out of the laser beam [1].

At larger beam radius, for which the average diffusion time of an atom through the laser beam is much longer than the coherence life time (estimated at about several ms) EIT linewidth increases linearly with the laser intensity, throughout entire range covered in the experiment, from 0.01mW/cm² to 12 mW/cm². The slope of linear dependence of EIT linewidth is independent on cell temperature, for wider laser beam diameter. For higher intensities (over 2 mW/cm²) line contrast of the 6 mm laser beam increases several times when we block the central part of the laser beam cross section (diameter of blocked beam is also 6 mm) in front of the detector. Since the laser beam is well collimated, this eliminated contribution to observed EIT from the most intense laser region, and thus we detected EIT due to photons in the weak intensity large area laser wings.

References

- [1] Y. Xiao, I. Novikova, D. Phillips, R. L. Walsworth, *Opt. Express* **65**, 14128–14141 (2008)
- [2] A. Krmpot *et al.*, *Opt. Express* **17**, 22491–22498 (2009)

Op

Teaching Quantum Physics

Quantum entanglement in exactly soluble atomic models: the Moshinsky model with three electrons, and with two electrons in a uniform magnetic field

P.A. Bouvier¹, A.P. Majtey¹, A.R. Plastino^{1,2}, P. Sánchez-Moreno^{1,3}, and J.S. Dehesa¹

¹*Instituto Carlos I de Física Teórica y Computacional and Departamento de Física Atómica, Molecular y Nuclear, Universidad de Granada, 18071 Granada, Spain*

²*Universidad Nacional de La Plata, CREG-UNLP-Conicet, C.C. 727, 1900 La Plata, Argentina*

³*Departamento de Matemática Aplicada, Universidad de Granada, 18071 Granada, Spain*

Corresponding Author: bouvier@ugr.es

We investigate [1] the entanglement-related features of the eigenstates of two exactly soluble atomic models: a one-dimensional three-electron Moshinsky model, and a three-dimensional two-electron Moshinsky system in an external uniform magnetic field [2]. We analytically compute the amount of entanglement exhibited by the wavefunctions corresponding to the ground, first and second excited states of the three-electron model. We found that the amount of entanglement of the system tends to increase with energy, and in the case of excited states we found a finite amount of entanglement in the limit of vanishing interaction. We also analyze the entanglement properties of the ground and first few excited states of the two-electron Moshinsky model in the presence of a magnetic field. The dependence of the eigenstates entanglement on the energy, as well as its behaviour in the regime of vanishing interaction, are similar to those observed in the three-electron system. On the other hand, the entanglement exhibits a monotonically decreasing behavior with the strength of the external magnetic field. For strong magnetic fields the entanglement approaches a finite asymptotic value that depends on the interaction strength. For both systems studied here we consider a perturbative approach in order to shed some light on the entanglements dependence on energy and also to clarify the finite entanglement exhibited by excited states in the limit of weak interactions [3]. As far as we know, this is the first work that provides analytical and exact results for the entanglement properties of a three-electron model.

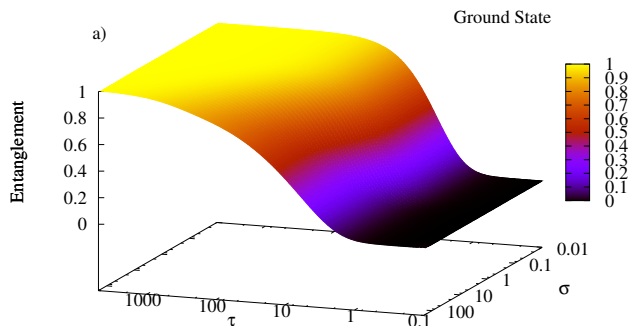


Figure 1: Entanglement of the ground state of the three-dimensional Moshinsky atom with two interacting (τ) electrons and a magnetic field (σ).

References

[1] P. A. Bouvier *et al.*, Eur. Phys. J. D **66**, 15 (2012)

[2] M. Moshinsky, Am. J. Phys. **36**, 52 (1968)

[3] M. Tichy, F. Mintert and A. Buchleitner, J. Phys. B At. Mol. Opt. Phys. **44**, 192001 (2011)

Undergraduate research: Laboratory experiments with many variables

M. Karlsteen⁴, J. Weidow⁴, A. Isacson⁴, I. Albinsson¹, A. Rosén¹, and A.-M. von Otter²

⁴*Department of Applied Physics, Chalmers, SE-412 96 Gothenburg, Sweden*

¹*Department of Physics, University of Gothenburg, SE-412 96 Gothenburg, Sweden*

²*Department of Pedagogical, Curricular and Professional Studies, University of Gothenburg, SE-405 30 Gothenburg, Sweden*

Corresponding Author: arne.rosen@physics.gu.se

The traditional approach to get experience in laboratory work in undergraduate education has been to perform experiments for determination of some constants as the gravitational constant, the refraction of index of the material in prism etc. The student has in most cases a laboratory instruction to follow with tables to fill in the recorded data. This is quite different from the problems the students will have to solve when they have finished the education.

The mission of the University is to provide opportunities for all students to be challenged and motivated, so that after graduation, they will be successful in their future careers. The biggest challenge is to prepare students for possible careers and/or further education, to make them see a direct link between the science and technology and their potential careers. We want to teach so that students think critically and provide them with the skills needed to see the many different solutions to problems.

In mid-seventies some students in physical engineering at Chalmers University of Technology went for a study trip to UK and visited Engineer M. J. Richards at Brunel University, who had introduced a different kind of laboratory course. Such a course had also been introduced at the Technical University at Trondheim Norway. Some students, teachers and an engineer from Gothenburg also made a trip to Trondheim to get experience of the laboratory work. We introduced this kind of experiments as the first introductory course in physics at Chalmers University of Technology and Gothenburg University in 1977/78. The course has since that time been given each year for many students.

The main goal of the experiments is to get a challenge to develop intellectual ability to solve different kind of problems. The students will for example have access to solid cylinders of different diameters and length, tubes of different inner and outer diameters and also length. The cylinders and tubes are also made of different materials as steel, aluminum or brass. The students have also access to an inclined plane, a clock and a ruler. The task for the student is to do experiments and determine a functional relation, which describes how long time it takes for a cylinder or tube to roll down on an inclined plane. The students have to find out which variables are important, decide which experiments should be done, do a number of experiments and fill in the data in tables, analyze the recorded data to find the final general functional relation. It is recommended that the students before doing the measurements make a dimensional analysis. The discussions, recorded data, tables, figures, analysis of the data should be recorded in a book. A report is written of the experiment.

References

[1] T. Eriksson, A. Rosén, *An Introduction to experimental problem solving* (Department of Physics, Chalmers and University of Gothenburg, Sweden, 1977)

Extended Cat Television Diagram (ECTD) for Quantum Physics in High School.

A.-S. Martensson¹

¹ *Institutionen fr pedagogik, Hogskolan i Boras, Sweden*

Corresponding Author: anne-sofie.martensson@hb.se

In this study the quantum physics content in swedish high school has been analysed using an Extended Cat Television Diagram, ECTD. In *Teaching Physics with the Physics Suite* Redish uses a diagram to illustrate the large number of different representations physicists use to describe events and processes in the real world. An extended version of this diagram, including both theoretical and experimental aspects, is in this work used to analyse what could be the central content in a physics course in e.g. high school.

In the picture below the experimental part of the diagram is shown. Experiments or observations are made to study some specific aspect of the real world, and the result is expressed in at least one of the representations to the right: spoken words, written words, equations, numbers, graphs, diagrams/pictures or physical models. To be able to make an experiment, knowledge of how to make measurements, how to use tools and how to vary parameters is necessary. Translation between different representations is a knowledge in its own as shown by arrows.

ECTD has now been used to analyse what parts of quantum physics are included in the swedish high school according to the curriculum, handbooks, textbooks and experienced teachers.

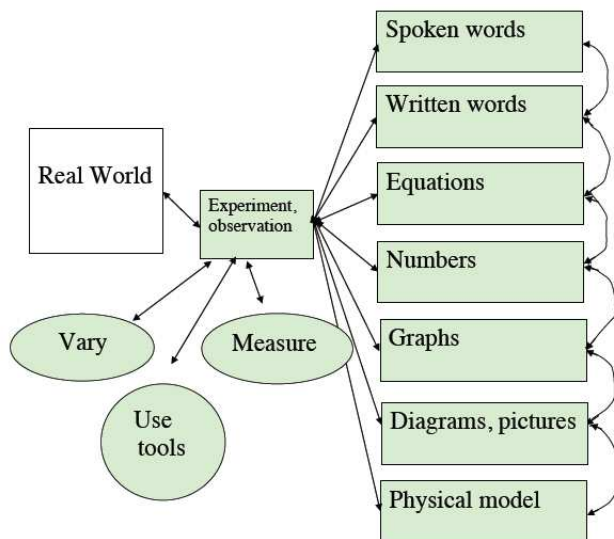


Figure 1: *Extended Cat Television Diagram, ECTD*

Ultrafast processes

Attoscience in Lund

C. L. Arnold¹, D. Guénot¹, D. Kroon¹, I. Balogh², E. P. Månsson¹,
S. Ristinmaa Sörensen¹, M. Gisselbrecht¹, and A. L'Huillier¹

¹*Department of Physics, Lund University, P.O. Box 118, 22100 Lund, Sweden*

²*Department of Optics and Quantum Electronics, University of Szeged, Dóm tér 9, 6720 Szeged, Hungary*

Corresponding Author: Cord.Arnold@fysik.lth.se

We report about a series of experiments which recently became possible after an improvement of the kHz attosecond pump-probe beam line at the Lund High-Power Laser Facility. We perform time-resolved interferometric attosecond pump-probe measurements, where XUV attosecond pulse trains (APTs), used as pump, are generated via high-order harmonic generation (HHG) by focusing intense ultrashort laser pulses into a dilute gas. The APTs are spatially overlapped with ultrashort IR probe pulses in the sensitive region of a magnetic bottle electron spectrometer (MBES) at variable attosecond to femtosecond delays. A needle valve provides detection gas and photo-electron energy is recorded as function of time delay. We recently improved the quality of our experimental configuration by actively stabilizing the arm length of the Mach-Zehnder interferometer, used to experimentally realize attosecond pump-probe delays. Experiments which require stable attosecond delay for long integration time, such as coincidence detection of photo-electrons, as well as experiments which rely on being able to reproducibly scan exactly the same delay range consecutively, benefit strongly from this improvement.

We were thus able to refine recent photo-ionization timing measurements of 3s and 3p valence electrons in Ar, revealing information on the temporal aspects of many-electron dynamics [1,2]. The principle of these experiments is based on the RABBIT method (Reconstruction of attosecond bursts by ionization of two-photon transitions) [3]. If RABBIT scans are performed using two different gases, the relative timing between the ionization processes can be extracted on attosecond time scale. We present results for the relative timing of valence electron photo-ionization for Kr, Ne, and Xe in reference to 3p photo-ionization in Ar.

The same kind of measurements allows to investigate the HHG process itself, which is a complicated combination of the microscopic single-atom response to a strong driving field and macroscopic phase-matching effects. By performing RABBIT scans we can quantify the relative walk-off between the fundamental IR driving pulse and the resulting APTs at different generation pressures.

We also investigated photo-double ionization in Xe by detecting pairs of photo-electrons in coincidence. By relating to the single photo-ionization signal (attoclock), measured simultaneously, we can identify temporal behavior of the different processes involved, namely direct non-sequential, indirect non-sequential, and indirect sequential photo-double ionization [4].

We conclude by describing the current laser sources and experimental setups used for attosecond experiments at the Lund High-Power Laser Facility. Our kHz femtosecond laser chain has recently been upgraded to deliver now sub-20 fs pulses with 5 mJ pulse energy. Its extraordinary wavelength tunability (>60 nm) is a perfect tool to investigate resonant processes in the XUV spectral region [5]. Finally, a novel OPCPA-based (Optical parametric chirped pulse amplification) laser, emitting pulses of <10 fs duration at >200 kHz repetition rate, enhances our activity in coincidence detection techniques as well as surface science with attosecond temporal resolution.

References

- [1] K. Klünder *et al.*, Phys. Rev. Lett. **106**, 143002 (2011)
- [2] A. S. Kheifets *et al.*, submitted.
- [3] P.-M. Paul *et al.*, Science **292**, 1689–1692 (2001)
- [4] O. Guyétand *et al.*, J. Phys. B: At. Mol. Opt. Phys. **41**, 065601 (2008)
- [5] M. Swoboda *et al.*, Phys. Rev. Lett. **104**, 103003 (2010)

Attosecond Tracing of Non-Sequential Double Ionization in a Single Laser Cycle

B. Bergues¹, M. Kübel¹, N. G. Johnson^{1,2}, B. Fischer³, N. Camus³, K. J. Betsch^{1,4},
 O. Herrwerth¹, A. Senftleben³, A. M. Saylor^{5,6}, T. Rathje^{5,6}, T. Pfeifer³,
 I. Ben-Itzhak², R. R. Jones⁴, G. G. Paulus^{5,6}, F. Krausz¹, R. Moshhammer^{3,3},
 J. Ullrich^{3,7}, and M. F. Kling^{1,2}

¹*Max-Planck-Institut fr Quantenoptik, D-85748 Garching, Germany*

²*J. R. Macdonald Laboratory, Department of Physics, Kansas State University, Manhattan, KS 66506, USA*

³*Max-Planck-Institut fr Kernphysik, D-69117 Heidelberg, Germany*

⁴*University of Virginia, Charlottesville, VA 22904, USA*

⁵*Institut fr Optik und Quantenelektronik, Friedrich-Schiller-Universitt, D-07743 Jena, Germany*

⁶*Helmholtz Institut Jena, D-07743 Jena, Germany*

⁷*Physikalisch-Technische Bundesanstalt, D-38116 Braunschweig, Germany*

Corresponding Author: boris.bergues@mpq.mpg.de

Non-sequential double ionization (NSDI) of atoms is a classical example for multi-electron dynamics in the presence of a strong laser field. In NSDI, the ionization of the second electron is triggered by the laser driven recollision of the first electron with the atomic core. Though NSDI has been extensively studied (for a recent review see Ref. [1] and references therein), the mechanism underlying its dynamics is not yet fully understood. On the one hand, NSDI in multi-cycle laser pulses usually involves multiple recollisions, which hamper the interpretation of experimental results. On the other hand, the exact theoretical modeling of NSDI in the multi-cycle regime remains a most difficult task, so that most of the predictions of the double ionization dynamics are restricted to a single cycle of a laser pulse (see e.g. [2,3]). A direct experimental test of these predictions, however, has been impeded so far by the lack of kinematically complete experimental data obtained with ultrashort pulses and precise knowledge of the electric field. We use a near-single-cycle laser pulse with appropriate carrier-envelope phase (CEP), to confine the double ionization dynamics of argon to a single laser cycle. This allows us to study NSDI in a clean experiment where the removal of the second electron is triggered by a single recollision event [4]. The measured two-electron spectrum shown in Fig. ?? exhibits a cross shaped structure that qualitatively differs from spectra recorded in all previous experiments using many-cycle pulses. This suggests that the transition from the multi-cycle to the near-single-cycle regime substantially modifies the dynamics of NSDI. With help of the CEP resolved two-electron momentum spectra, the correlated emission of two electrons is traced on sub-femtosecond timescales. In particular, we determine at which moment the second electron is released within the laser pulse. Our experimental results, which are discussed in terms of a semi-classical model provide strong constraints for the development of theories and lead us to revise common assumptions about the mechanism that governs double ionization.

References

- [1] C. Figueira de Morisson Faria and X. Liu, *J. Mod. Opt.* **58**, 1076-1131 (2011)
- [2] A. Staudte *et al.*, *Phys. Rev. Lett.* **99**, 263002 (2007)
- [3] T. Shaaran *et al.*, *Phys. Rev. A* **81**, 063413 (2010)
- [4] B. Bergues *et al.*, *Nature Communications* (in press).

Ionization of H by few-cycle XUV laser pulses: Spatial and temporal interference effects

S. Borbély¹, A. Tóth¹, K. Tőkési², and L. Nagy¹

¹*Faculty of Physics, Babeş-Bolyai University, Kogălniceanu 1, 400084 Cluj-Napoca, Romania*

²*Institute of Nuclear Research of the Hungarian Academy of Sciences (ATOMKI), P.O. Box 51, H-4001 Debrecen, Hungary*

Corresponding Author: sandor.borbely@phys.ubbcluj.ro

The interaction between atomic systems and ultrashort laser pulses is an interesting field of study with numerous applications. With the fast development of the laser technology the generation of few-cycle laser pulses became possible [1]. During the interaction of such a few-cycle laser pulse with an atomic system several competing processes occur leading to a complex pattern in the momentum distribution of photoelectrons (see **Figure ??**). If the underlying processes are understood in detail, valuable information regarding the structure and the temporal evolution of the target atom can be extracted from these complex electron distributions.

We have studied the interaction of few-cycle XUV laser pulses with the H atom in the tunneling and over-the-barrier ionization regime. We used the direct numerical solution of the time-dependent Schrödinger equation and classical trajectory Monte Carlo (CTMC) simulations. In our present case, the pattern shown on **Figure ??** is formed as a result of temporal and spatial interference between electron wave packets. During the temporal interference [2] electron wave packets emitted at different time moments (i.e. at different parts of the laser pulse) add up to an interference pattern built of concentric circles. Electrons originated from the same wave packet may follow different paths in the presence of the combined electric field generated by the core's Coulomb potential and the laser pulse. During recombination the different electron paths may interfere constructively or destructively depending on their relative phase [3]. This leads to the radial interference pattern observed on **Figure ??**, which is the holographic mapping [3] of the parent ion's state. In the present work, we have investigated the interplay between these interference mechanisms as a function of laser pulse parameters putting accent on the detailed understanding of the underlying mechanisms.

Acknowledgements: The present work was supported by the Sectoral Operational Programme for Human Resources Development 2007-2013, co-financed by the European Social Fund, under the project numbers POSDRU 89/1.5/S/60189 and POSDRU/107/1.5/S/76841, by a grant of the Romanian National Authority for Scientific Research, CNCS UEFISCDI, project number PN-II-ID-PCE-2011-3-0192.

References

- [1] F. X. Kärtner, Few-cycle laser pulse generation and its applications (Springer, Germany, 2004).
- [2] F. Lindner et. al. Phys. Rev. Lett. **95** (2005) 040401.
- [3] Y. Huismans et. al. Science **331** (2011) 61.

Iterative solution of the time-dependent Schrödinger equation

S. Borbély, G. Zs. Kiss, and L. Nagy

Faculty of Physics, Babeş-Bolyai University, Kogălniceanu Street No. 1, 400084 Cluj-Napoca, Romania

Corresponding Author: sandor.borbely@phys.ubbcluj.ro

The interaction between atomic systems and external electromagnetic fields (i.e ultrashort laser pulses) can be described most accurately by solving directly the time-dependent Schrödinger equation (TDSE). Each implementation of the direct solution is compute intensive and requires large amount of memory even in the framework of the single active electron approximation.

Recently, we have proposed [1] an approximate, much less compute intensive approach (momentum space strong field approximation - MSSFA) based on the first order iterative solution of the time-dependent Schrödinger equation in momentum space. It was shown [1], that the MSSFA model provides results with accuracy comparable to the direct solution of the TDSE in the half-cycle regime, where the net momentum transfer between the electromagnetic field and the electron is high. In contrast to this, in the multi-cycle regime the MSSFA model completely fails [2] leading to erroneous electron dynamics due to the underestimation (considered only as first order approximation) of the Coulomb interaction between the electron and the core.

To overcome this shortcomming (wrong electron dynamics), higher order iterations were included in the MSSFA model until convergence was achieved. This new, iterative approach is equivalent with the direct solution of the TDSE, and from this point on it will be called iTDSE model. During the implementation of the iTDSE model the coupling coefficients were calculated as integrals of highly oscillatory functions. These integrals were efficiently evaluated using Levin's [3] method leading to a fast numerical code.

In the present work the performance and accuracy of the iTDSE model is investigated, by comparing it with the direct momentum space [4] and coordinate space (time-dependent close-coupling method) solution of the TDSE.

Acknowledgements: The present work was supported by the Sectoral Operational Programme for Human Resources Development 2007-2013, co-financed by the European Social Fund, under the project number POSDRU 89/1.5/S/60189, by a grant of the Romanian National Authority for Scientific Research, CNCS UEFISCDI, project number PN-II-ID-PCE-2011-3-0192.

References

- [1] S. Borbély, K. Tókési and L. Nagy, Phys. Rev. A **77** (2008) 033412.
- [2] S. Borbély, D. G. Arbó, M.S. Gravielle, K. Tókési, J.E. Miraglia and L. Nagy, 10th ECAMP conference, Salamanca, Spain, 2010, poster 179
- [3] D. Levin, J. Comp. and Appl. Math. **78** (1997) 131.
- [4] S. Borbély, G. Zs. Kiss, and L. Nagy, Cent. Eur. J. Phys. **8** (2010) 249.

Harmonic Generation in Time Dependent R -Matrix Theory

A. C. Brown¹, D. R. Robinson¹, J. S. Parker¹, K. T. Taylor¹, and H.W. van der Hart¹

¹Centre for Theoretical Atomic, Molecular and Optical Physics, Queen's University Belfast, Belfast BT7 1NN, UK

Corresponding Author: abrown41@qub.ac.uk

In recent years, great advances have been made in the use of harmonic generation (HG) as a measurement tool. It has facilitated a series of very sensitive measurements of electronic dynamics in atoms and molecules [1, 2]. The sensitive nature of HG has made it increasingly important to develop accurate methods of modeling the process. When used to study electronic dynamics on ultrashort timescales it also becomes important to assess the influence of electron-electron interactions on HG.

In studying HG, many methods use the single active electron (SAE) model, a significant simplification which enables efficient computation of harmonic spectra. The relationship between atomic structure and HG can be approximated by the SAE to a good accuracy for many processes. For instance, the Cooper minimum in Argon has been successfully described with various SAE methods [3,4]. However, there are many processes which rely on the interaction of different electrons, and hence cannot be described in a SAE framework [1,2,5].

We have developed time dependent R -matrix (TDRM) theory to model the interaction of atoms with short, intense laser pulses, maintaining a full description of the multielectron dynamics involved [6,7]. We have extended TDRM to account for HG and have demonstrated how multielectron dynamics can influence harmonic spectra in Argon. Interference between pathways involving the excitation of a 3p electron into the continuum, and the excitation of a 3s electron to an np state was demonstrated to significantly influence the fifth harmonic yield at wavelengths between 200 and 240nm [5].

Although HG has been studied extensively over the past two decades, it is still an open question whether it is the expectation value of the dipole operator, dipole velocity operator or dipole acceleration operator that provides the best approximation to the HG yield. Recently it has been suggested that there is a natural link between HG and the dipole velocity operator [8, 9]. However, it is important to ensure that the computational approach used to evaluate these expectation values can actually do so accurately.

We have therefore extended the capability of the TDRM code to calculate harmonic spectra using the dipole length, velocity and acceleration operators. By comparing spectra from each, we can assess the reliability of the method and gain a greater understanding of the underlying process.

We apply TDRM to the test case of HG in Helium using various laser pulse profiles. We compare the results between each of the dipole length, velocity and acceleration operators, finding excellent consistency between the three approaches well into the cutoff regime. By varying the atomic basis, we assess the influence of atomic structure on the HG yields. Finally, we compare our HG yields with those obtained from the HELIUM code [10] and again find excellent agreement between the two methods.

References

- [1] O. Smirnova *et al.*, Nature **460**, 972 (2009)
- [2] A. D. Shiner *et al.*, Nat. Phys. **7**, 464 (2011)
- [3] H. J. Wörner *et al.*, Phys. Rev. Lett. **102** 103901 (2009)
- [4] J. Higuete *et al.*, Phys. Rev. A **83** 053401 (2011)
- [5] A. C. Brown *et al.*, Phys. Rev. Lett. **108** 063006 (2012)
- [6] M. A. Lysaght, H. W. van der Hart and P. G. Burke, Phys. Rev. A **79** 053411 (2009)
- [7] M. A. Lysaght, P. G. Burke and H. W. van der Hart, Phys. Rev. Lett, **102** 193001 (2009)
- [8] J. C. Baggese and L. B. Madsen, J. Phys. B. At. Mol. Opt. Phys. **44** 115601 (2011)
- [9] D. J. Diestler, Phys. Rev. A **78** 033814 (2008)
- [10] J. S. Parker *et al.*, Phys. Rev. Lett. **96** 133001 (2006)

High Harmonic Generation at 200 kHz repetition rate

E. Lorek¹, E. W. Larsen¹, C. M. Heyl¹, S. Carlström¹, D. Paleček², D. Zigmantas²,
and J. Mauritsson¹

¹*Department of Physics, Lund University, SE-221 00 Lund, Sweden*

²*Department of Chemistry, Lund University, SE-221 00 Lund, Sweden*

Corresponding Author: eleonora.lorek@fysik.lth.se

To study movements of electrons on their natural timescale attosecond laser pulses are used. These pulses are produced in a process termed "High Harmonic Generation" (HHG) [1],[2] which requires intensities on the order of 10^{14} W/cm². These high intensities puts a limit on the available repetition rates of the laser used for HHG experiments to a few kHz. Many experiments however, would benefit from higher repetition rates in order to achieve a high signal-to-noise ratio and avoid space charge effects [3]. Using tight focusing HHG at 100 kHz [4] and even 20 MHz [5] have recently been obtained.

We demonstrate high harmonic generation in Argon at repetition rates up to 200 kHz using a commercially available "turn-key" amplified laser system from Light Conversion with a tunable repetition rate. We use the system to investigate how the so-called "long-" and "short electron trajectories" are influenced by the ellipticity of the driving laser field. HHG using nanostructures [6] was also investigated in order to be able to increase the repetition rates even further in the future. The gold nanostructures were designed to maximize the plasmonic field enhancement between 170 nm sized bow tie elements spaced 30-60 nm apart.

In the near future a new CEP stabilized laser system with a central wavelength of 800 nm, sub-10 fs pulse duration and 10 μ J pulse energy at 200 kHz repetition rate will be installed at the Lund High-Power Laser Facility. Repetition rates up to 20 MHz will also be supported at the cost of pulse energy and duration.

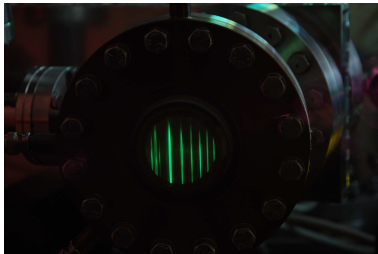


Figure 1: Harmonic spectrum on a phosphor screen.

References

- [1] P. M. Paul *et al.*, *Science*, **292**, 1689–1692 (2001)
- [2] M. Ferray *et al.*, *Journal of Physics B*, **21**, L31–L35 (1988)
- [3] A. Mikkelsen *et al.*, *Review of Scientific Instruments* **80**, 123703 (2009)
- [4] C. Heyl *et al.*, *Physical Review Letters*, **107**, 033903 (2011)
- [5] A. Vernaleken *et al.*, *Optics Letters*, **36**, 3428–3430 (2011)
- [6] S. Kim *et al.*, *Nature* **453**, 757–760 (2008)

Role of magnetic field in strong-field atomic stabilization

M. Yu. Emelin¹, M. Yu. Ryabikin¹, and L. A. Smirnov¹

¹*Institute of Applied Physics RAS, 46 Ulyanov Street, 603950 Nizhny Novgorod, Russia*

Corresponding Author: emelin@ufp.appl.sci-nnov.ru

Theory of atomic photoionization in very intense high-frequency laser field predicts the effect of stabilization, i.e., the saturation or even the decrease of ionization probability with increasing laser intensity (see, e.g., reviews [1, 2]). Although the basic mechanisms and many aspects of atomic stabilization have been rather well studied, some issues remain unresolved. One of them concerns the role of the magnetic field of the laser pulse. On the one hand, both the classical Monte Carlo simulations [3] and quantum-mechanical numerical experiments [4, 5] have indicated that stabilization can be observed only in a certain range of pulse intensities. Too high intensity leads to breakdown of stabilization, and the main reason is that the magnetic field pushes the electron in the laser pulse propagation direction. On the other hand, in [6] using the strong-field approximation (SFA) Reiss showed that stabilization can be observed at any level of pulse intensity and relativistic effects (including the magnetic-field effects) only enhance stabilization. As stated in [6], this interesting contradiction with results of [3–5] needs to be resolved. In this paper, we present the results of classical and quantum-mechanical simulations, which shed light on the above-mentioned contradiction.

Until recently, the computer capabilities did not allow extensive full-dimensionality numerical studies of strong-field phenomena in atomic and molecular systems, even in the single-electron approximation. That is why so far the numerical study of atomic stabilization beyond the dipole approximation has been made only for linearly polarized laser field. In this case, the 2D calculations [4, 5] are believed to give quite plausible results. The use of modern computer facilities makes possible the full-dimensional simulations, which allowed us to consider for the first time the problem of atomic stabilization in arbitrarily polarized field, including the magnetic-field effects, in full (3D) dimensionality. Moreover, it is very important that we were able to consider the long-term evolution of electron wave function, which is not limited to the time interval of about ten cycles of the laser field. Our study reveals two-stage electron wave-packet evolution in a pulses of short-wavelength ultraintense field. We will demonstrate the role of magnetic field of the laser pulse on each of these stages.

References

- [1] M. Gavrilin, *J. Phys. B: At. Mol. Opt. Phys.* **35**, R147–R193 (2002)
- [2] A. M. Popov, O. V. Tikhonova, and E. A. Volkova, *J. Phys. B: At. Mol. Opt. Phys.* **36**, R125–R165 (2003)
- [3] C. H. Keitel and P. L. Knight, *Phys. Rev. A* **51**, 1420–1430 (1995)
- [4] N. J. Kylstra *et al.*, *Phys. Rev. Lett.* **85**, 1835–1838 (2000)
- [5] M. Yu. Ryabikin and A. M. Sergeev, *Opt. Express* **7**, 417–426 (2000)
- [6] H. R. Reiss, *Opt. Express* **8**, 99–105 (2001)

Formation of extremely short pulses from resonant radiation in hydrogen-like medium: three-level model versus time-dependent Schrödinger equation

M. Yu. Emelin¹, V. A. Polovinkin¹, M. Yu. Ryabikin¹, and Y. V. Radeonychev¹

¹*Institute of Applied Physics RAS, 46 Ul'yanov Street, 603950 Nizhny Novgorod, Russia*

Corresponding Author: emelin@ufp.appl.sci-nnov.ru

In the last few years it was proposed to produce extremely short pulses from the resonant radiation in hydrogen-like medium irradiated by far-off-resonant low-frequency laser field [1-3]. The approach is based on the time-dependent perturbation of atomic energies over the optical cycle of the far-off-resonant laser field due to Stark effect and tunnel ionization from the excited atomic states. The pulses are formed from the incident VUV or XUV radiation, resonant to the quantum transition from the ground to the first excited states of hydrogen-like atoms, as a result of propagation of radiation through the medium and generation of spectral sidebands at the combination frequencies of the resonant and far-off-resonant fields.

In this paper we compare the results obtained within the three-level model of hydrogen-like medium, which takes into account only the resonant interaction of high-frequency radiation with atoms, with the results obtained via numerical integration of the time-dependent Schrödinger equation taking into account all the multiphoton processes in the system under consideration. This allows us to verify that the three-level model is valid in the large area of the parameter values as well as to determine the limitations of the three-level approximation. We show the possibility to produce extremely short femto- and attosecond few-cycle pulses from the resonant radiation for various intensities and frequencies of the resonant and far-off-resonant fields.

References

- [1] Y. V. Radeonychev, V. A. Polovinkin, O. Kocharovskaya, *Phys. Rev. Lett.* **105**, 183902 (2010)
- [2] V. A. Polovinkin, Y. V. Radeonychev, O. Kocharovskaya, *Opt. Lett.* **36**, 2296–2298 (2011)
- [3] Y. V. Radeonychev, V. A. Polovinkin, O. Kocharovskaya, *Las. Phys.* **21**, 1243–1251 (2011)

Cooperative muon-gamma-nuclear spectroscopy of atomic systems

A.-V. Glushkov^{1,2}

¹*Odessa State University-OSENU, P.O.Box 24a, 65009, Odessa-9, ukraine*

²*ISAN, Russian Academy of Sciences, Troitsk, 142090, Russia*

Corresponding Author: glushkov@paco.net

We have presented a generalized energy approach in the relativistic theory of discharge of a metastable nucleus with emission of gamma quantum and further muon conversion, which initiates this discharge. A negative muon captured by a metastable nucleus may accelerate the discharge of the latter by many orders of magnitude [1]. For a certain relation between the energy range of the nuclear and muonic levels a discharge may be followed by muon ejection and muon participates in discharge of other nuclei. The decay probability is linked with imaginary part of the "nucleus core+ external nucleon+muon" system energy [1,2]. One should consider 3 channels: 1). radiative purely nuclear 2j-poled transition (probability $P1$; this value can be calculated on the basis of known traditional formula); 2). Non-radiative decay, when a proton transits into the ground state and muon leaves a nucleus with energy $E = E(p - N1J1) - E(i)$, where $E(p - N1J1)$ is an energy of nuclear transition, $E(i)$ is the bond energy of muon in 1s state (P2); 3). A transition of proton to the ground state with muon excitation and emission of gamma quantum with energy $E(p-N1J1)-E(nl)$ (P3). Under condition $E(p - N1J1) > E(i)$ a probability definition reduces to calculation of probability of autoionization decay of 2-particle system. The numerical calculation of the corresponding probabilities is carried out for the Sc, Cs, Yb nuclei with using the Dirac-Woods-Saxon (DWS) and Dirac-Bloumkvist-Wahlborn models. The probabilities for some transitions for Sc are as follows: $P2=3.910^{15}$ 1/s (p1/2-p3/2) and $P2=3.110^{12}$ 1/s (p1/2-f7/2) (DWS model) [1]. The dipole transition 2p-1s occurs with $P3=1.9 \cdot 10^{13}$ 1/s. The detailed scheme of the possible high-power monochromatic gamma radiation source on the basis of examined processes is presented and its experimental realization is discussed.

References

- [1] V. S. Letokhov, V. I. Goldanskii, JETP.**67**, 513 (1974); L. N. Ivanov, V. S. Letokhov, JETP.**70**, 19 (1976); A. V. Glushkov, L. N. Ivanov, Phys. Lett.**A170**, 33 (1992); A. V. Glushkov, L. N. Ivanov, V. S. Letokhov, Preprint ISAN NAS-1, Moscow-Troitsk (1991)
- [2] A. V. Glushkov, O. Khetselius, A. Svinarenko, In: *Advances in the Theory of Quantum Systems in Chem. and Phys.*, Eds.P. Hoggan, E. Brandas, G. Delgado-Barrio, P. Piecuch (Springer, Berlin, 2011) **22**, 51-70

Resonant and non-resonant ionizations of xenon with 388 nm femtosecond laser pulses

K. Hansen¹, M. Goto¹

¹*Department of Physics, University of Gothenburg, SE-41296 Gothenburg, Sweden*

Corresponding Author: klavs.hansen@physics.gu.se

We report the ionization of xenon with a femtosecond 388 nm (3.2 eV) laser pulse with intensities below 38 TWcm^{-2} . The angular distributions were measured with a velocity imaging spectrometer.

We observe three ionization processes: resonant and non-resonant multi-photon ionization and autoionization. The relative yield of the first two was evaluated from the deconvolution of their angular distribution for the relevant electron energy, which includes the electron production via the $3h\nu-6s(^2P_{1/2} J=1)$ resonance. The non-resonant process gains in importance with increasing laser intensity and reaches 50% at 30 TW/cm^{-2} .

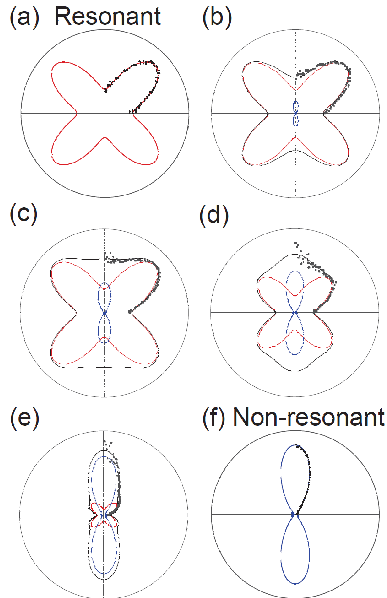


Figure 1: Polar plot of the angular distributions. The polarization is in the vertical direction. Frames (a)-(e) show the angular distributions for five different intensities: 2.1, 2.9, 5.3, 12 and 22 TWcm^{-2} , respectively. The energy interval used is from 0.60 to 0.66 eV

References

[1] M. Goto, and K. Hansen, *Physica Scripta* (submitted)

Enhanced High-Order Harmonic Generation using dual gas targets

C. M. Heyl¹, F. Brizuela¹, P. Rudawski¹, D. Kroon¹, L. Rading¹, P. Johnsson¹,
J. M. Dahlström², and A. L'Huillier¹

¹*Department of Physics, Lund University, P. O. Box 118, SE-22100 Lund, Sweden*

²*Atomic Physics, Fysikum, Stockholm University, AlbaNova University Center, SE-106 91 Stockholm, Sweden*

Corresponding Author: christoph.hey1@fysik.lth.se

High-order harmonic generation (HHG) in gases is nowadays well established and used for a variety of applications, in particular for the generation of attosecond pulses which give access to ultrafast phenomena in various fields of physics. This highly nonlinear light conversion process suffers, however, from a relatively low conversion efficiency. Several techniques have been implemented in order to enhance the efficiency, based on either improving phase matching or enhancing the single atom response. In this work, we investigate the possibilities of using a dual gas target in order to enhance the single atom response in the second target (generation cell) by driving the HHG process with an intense laser field and a superimposed harmonic field, generated in the first target (seeding cell). We demonstrate a significant enhancement of the harmonic signal (up to an order of magnitude), if an argon cell is placed in front of our low pressure neon cell. A similar effect has been observed earlier [1,2] involving an interpretation focusing on the role of the high-order harmonic field for controlling the ionization process in the generation cell. Our experimental results indicate that the enhancement happens due to low order harmonics which are efficiently generated in the seeding cell.

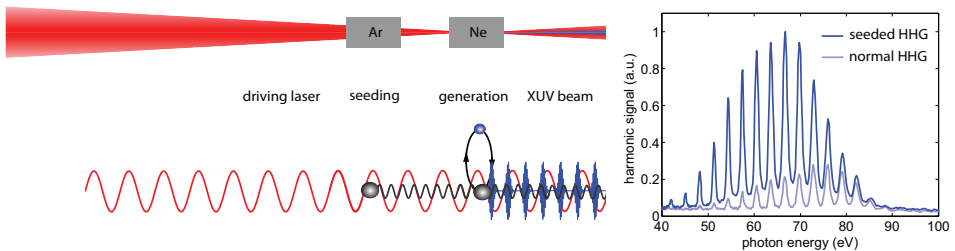


Figure 1: Principle of seeded high-order harmonic generation using dual gas targets.

This new HHG scheme has been implemented in our intense harmonics beamline which delivers high order harmonics at a μJ pulse energy level.

References

- [1] K. Ishikawa *et al.*, Phys. Rev. Lett. **91**, 043002 (2003)
- [2] A. Heinrich *et al.*, J. Phys. B. **39**, S275 (2006)

Study of Fano resonances with the Rabitt technique

A. Jiménez-Galán³, L. Argenti³, and F. Martín^{1,2}

³*Departamento de Química, Módulo 13, Universidad Autónoma de Madrid, 28049 Madrid, Spain*

¹*Instituto Madrileño de Estudios Avanzados en Nanociencia (IMDEA-Nanociencia), Cantoblanco, 28049 Madrid, Spain*

Corresponding Author: alvaro.jimenez@uam.es

We present a detailed theoretical study of the photoionization of the helium atom subject to a train of XUV attosecond pulses in conjunction with a strong near-IR probe pulse in the energy region of the first excitation threshold of the He⁺ parent ion. This pump-probe scheme extends the Rabitt technique (Reconstruction of Attosecond Beating by Interference of Two photon Transitions) [1] to the energy domain where resonances and inelastic thresholds appear. In the usual application of the Rabitt method, one assumes slowly varying atomic transition matrix elements to reconstruct, from the phaseshifts between consecutive sidebands in the photoelectron spectrum, the profile of an XUV train [2]. Conversely, if the phase relation between the harmonics in the XUV train is known, one can extract information on the intrinsic phases of the atomic transition amplitudes. This latter approach has already been employed to highlight the role of discrete intermediate states in the two-photon single ionization of helium [3]. Here, we apply the same scheme at higher energies to illustrate the effect of autoionizing states and threshold openings on continuum-continuum transitions.

To do so, we solve the time-dependent Schrödinger equation in a close-coupling B-spline basis with the Arnoldi propagator in a quantization box with a radius of 1200 Bohr radii. At the end of each simulation, the wave packet is projected on a complete set of multi-channel scattering states of the atom in order to extract channel-resolved, fully differential photoelectron distributions [4].

In the photoelectron spectrum we observe characteristic sideband phaseshifts associated to resonant and non-resonant multi-photon transitions as a function of the time delay between the XUV and the IR pulses, and a corresponding modulation of the Fano profiles (Fig. 1).

In addition, we observe shifts on resonance positions when the XUV pulse train is close to the maximum of the IR probe pulse. This effect is a signature of the dressing of the atom due to the interaction with the comparatively strong IR probe pulse.

References

- [1] P. M. Paul *et al.*, *Science* **292**, 1689–1692 (2001)
- [2] R. López-Martens *et al.*, *Phys. Rev. Lett.* **94**, 033001 (2005)
- [3] M. Swoboda *et al.*, *Phys. Rev. Lett.* **104**, 103003 (2010)
- [4] L. Argenti and E. Lindroth, *Phys. Rev. Lett.* **105**, 053002 (2010)
- [5] A. Bürgers, D. Wintgen, J. M. Rost, *J. Phys. B: At. Mol. Opt. Phys.* **28**, 3163–3183 (1995)

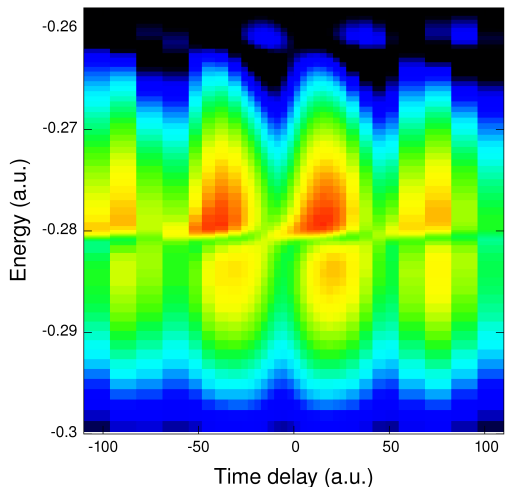


Figure 1: Detail of a sideband in the $2s\epsilon_s$ photoelectron spectrum of helium close to the $(3, 2)_4$ 1S doubly excited state [5].

Theory of resonant high-order harmonic generation by low-frequency laser field

M. Khokhlova^{1,2}, V. Strelkov²

¹Faculty of Physics, Lomonosov Moscow State University, Leninskie Gory, Moscow, Russia

²General Physics Institute of the Russian Academy of Science, 38 Vavilova st., Moscow, Russia

Corresponding Author: margaritkakhokhlova@gmail.com

Properties of resonant high-order harmonics generated in intense laser field are actively studied both experimentally [1, 2] and theoretically [2, 3]. Very efficient generation of the harmonic resonant with the transition from the bound to the autoionizing state of the generating particle was demonstrated recently in the experiments using plasma plumes [1] and Xe jet [4].

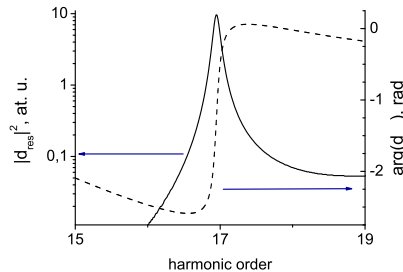


Figure 1: Squared absolute value and phase of the transition matrix element d_{res} vs. the harmonic number of 800 nm laser radiation. The values were calculated for the model Sn^+ ion.

In this paper we develop an analytical theory of the resonant HHG. We use the single-active electron approximation, and the role of the other electrons is reproduced with a model potential of the parent ion. We use double-barrier structure with a gap between the barriers as an approximation of this potential. The potential has one bound state and one quasi-stationary state, which reproduce the ground and the autoionizing states of the real atom (or ion), respectively. We derive analytically the wave function (both in the discrete and continuum spectrum) in such potential. We find the matrix element of the dipole moment of the continuum - ground state transition d_{res} . The absolute value and the phase of this matrix element for tin ion are shown in the figure. One can see that when the continuum state energy is close to that of the quasi-stationary state, the absolute value of the matrix element has a maximum corresponding to the strong enhancement of the harmonic generation efficiency; the phase of the matrix element varies rapidly in the vicinity of the resonance. This phase describes the additional phase shift of the harmonic close to the resonance. The rapid variation of the matrix element d_{res} near the resonance precludes the application of the stationary phase method used in the non-resonant HHG theories, for instance, in Ref. [5]. Applying different approximate integration methods, we find the time-dependent microscopic dipole moment.

References

- [1] R. A. Ganeev, J. Phys. B, **40**, R213 (2007)
- [2] R. A. Ganeev *et al.*, Phys. Rev. A **85**, 023832 (2012)
- [3] V. Strelkov, Phys. Rev. Lett. **104**, 123901 (2010)
- [4] A. D. Shiner *et al.*, Nature Physics **7**, 464 (2011)
- [5] M. Lewenstein *et al.*, Phys. Rev. A **49**, 2117-2132 (1994)

Timing measurements of an attosecond pulse train using a stabilized interferometer

D. Kroon¹, D. Guénot¹, I. Balogh², C. M. Heyl¹, A. L'Huillier¹, and C. L. Arnold¹

¹*Department of Physics, Lund University, SE-221 00 Lund, Sweden*

²*Department of Optics and Quantum Electronics, University of Szeged, Dóm tér 9, 6720, Szeged, Hungary*

Corresponding Author: David.Kroon@fysik.lth.se

High harmonic generation (HHG) refers to the nonlinear optical process where intense laser pulses interact with an atomic or molecular system to generate high order odd harmonics of the driving field frequency. Most commonly a target of dilute gas is used. In the temporal domain the generation will appear as repeated bursts of broadband electromagnetic radiation separated by half a period of the driving field. Under certain conditions these bursts can be compressed to have time duration of only a few hundreds of attoseconds. The emission consists then of a train of attosecond pulses (APT), separated by half a laser cycle. To be able to control this source of coherent broadband radiation it is important to understand the response of the single atom or molecule as well as the macroscopic propagation effects taking place as the harmonic fields are generated, i.e. phase-matching effects.

In this work we studied the effect of the target gas pressure on the relative spectral phases of the harmonic fields. The harmonic radiation was generated by focusing ultrashort laser pulses of 1.5 mJ pulse energy and 35 fs (FWHM) duration in a pulsed Ar gas jet. Using an interferometric technique, RABBIT (Reconstruction of attosecond bursts by ionization of two-photon transitions) [1], including a stabilized Mach-Zehnder interferometer, we observe how the phase locking between the consecutive harmonics is affected by varying the generation conditions. The long time stability of the interferometer also allow us to study how the generation conditions affect the phase locking between the APT and the generating field [2], which in the temporal domain corresponds to a relative time delay of the radiation bursts. Combined with computer simulations, these results might give an insight in the complex macroscopic space-time evolution of the HHG process.

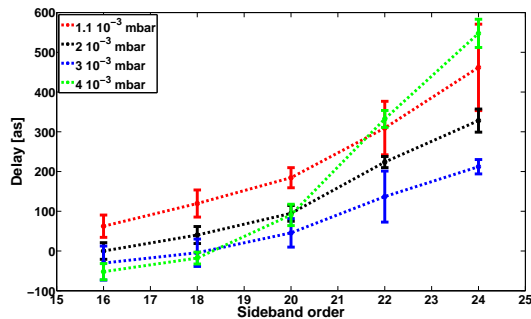


Figure 1: Relative group-delay of the harmonic fields as a function of the backing pressure in the generation vacuum chamber.

References

- [1] P. M. Paul *et al.*, Science **292**, 1689 (2001).
- [2] D. Kroon *et al.*, in preparation.

High Harmonic Generation at 200 kHz repetition rate

E. Lorek¹, E. W. Larsen¹, C. Heyl¹, S. Carlström¹, D. Palecek², D. Zigmantas², and J. Mauritsson¹

¹*Department of Physics, Lund University, SE-221 00 Lund, Sweden*

²*Department of Chemistry, Lund University, SE-221 00 Lund, Sweden*

Corresponding Author: eleonora.lorek@fysik.lth.se

To study movements of electrons on their natural timescale attosecond laser pulses are used. These pulses are produced in a process termed "High Harmonic Generation" (HHG) [1],[2] which requires intensities on the order of 10^{13} W/cm². These high intensities puts a limit on the available repetition rates of the laser used for HHG experiments to a few kHz. Many experiments however, would benefit from higher repetition rates in order to achieve a high signal-to-noise ratio and avoid space charge effects [3]. Using tight focusing HHG at 100 kHz [4] and even 1 MHz [5] have recently been obtained.

We demonstrate high harmonic generation in Argon at repetition rates up to 200 kHz using a commercially available "turn-key" amplified laser system from Light Conversion with a tunable repetition rate. We use the system to investigate how the so-called "long-" and "short electron trajectories" are influenced by the ellipticity of the driving laser field. HHG using nanostructures [6] was also investigated in order to be able to increase the repetition rates even further in the future. The gold nanostructures were designed to maximize the plasmonic field enhancement between 170 nm sized bow tie elements spaced 30-60 nm apart.

In the near future a new CEP stabilized laser system with a central wavelength of 800 nm, sub-10 fs pulse duration and 10 μ joule pulse energy at 200 kHz repetition rate will be installed at the Lund High-Power Laser Facility. Repetition rates up to 20 MHz will also be supported at the cost of pulse energy and duration.

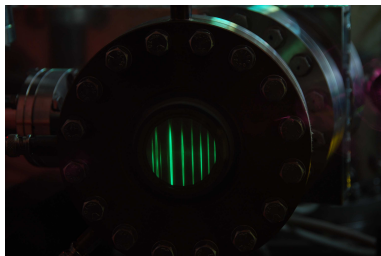


Figure 1: *Harmonic spectrum on a phosphor screen.*

References

- [1] P. M. Paul *et al.*, *Science*, **292**, 1689–1692 (2001)
- [2] M. Ferray *et al.*, *Journal of Physics B*, **21**, L31–L35 (1988)
- [3] A. Mikkelsen *et al.*, *Review of Scientific Instruments* **80**, 123703 (2009)
- [4] C. Heyl *et al.*, *Physical Review Letters*, **107**, 033903 (2011)
- [5] J. Bouillet *et al.*, *Optics Letters* **34**, 1489–1491 (2009)
- [6] S. Kim *et al.*, *Nature* **453**, 757–760 (2008)

An intense source of high-order harmonics

P. Rudawski¹, F. Brizuela¹, C. M. Heyl¹, J. Schwenke¹, P. Johnsson¹, L. Rading¹,
E. Mansten¹, R. Rakowski¹, and A. L'Huillier¹

¹*Department of Physics, Lund University, P. O. Box 118, SE-22100 Lund, Sweden*

Corresponding Author: Piotr.Rudawski@fysik.lth.se

High-order harmonic pulses focused with soft x-ray optics can reach intensities as high as 10^{14} W/cm². This leads to the possibility to study nonlinear processes in the soft X-ray region where, to date, only a limited number of experiments have been completed using free electron lasers and high-order harmonics [1-2]. We present a newly developed coherent source of intense high-order harmonics applicable for those studies. The high harmonic beam is generated by loosely focusing high energy Ti:Sapphire laser radiation into a gas cell filled with argon or neon. The obtained energy per pulse was optimized by an automatic control of the multiple parameters influencing the generation process. This optimization procedure allows us to obtain energies as high as 1,15 μ J and 0.23 μ J in argon and neon gas respectively. The spectra of the high-order harmonic beams generated in both gases are shown in Figure 1. The generated harmonic beams present a high degree of spatial coherence as measured using a two slit experiment. Our plan to reach a high focused intensity over a broad spectral range will be presented together with possible applications, e.g towards seeding of free electron lasers.

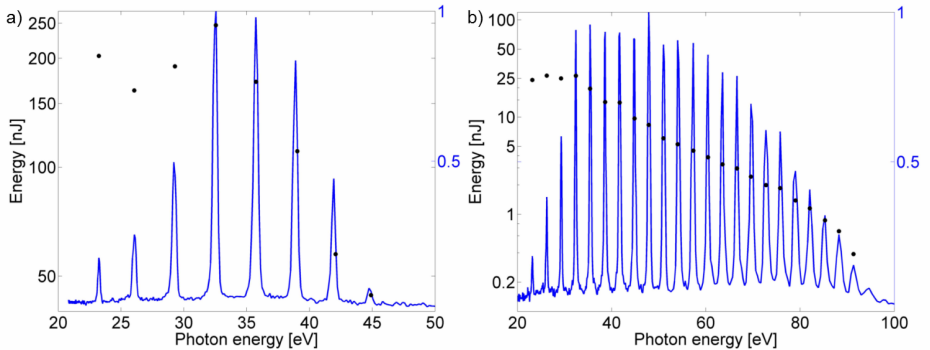


Figure 1: Spectra of High-order harmonic from Ar (a) and Ne (b) gas corresponding to total HH beam energies of up to 1 μ J and 0.2 μ J respectively. The pulse energy of individual harmonics, shown as dots, was obtained by combining the energy measurements with informations from a spectrometer calibrated for spectral response.

References

- [1] K. Ishikawa, *et al.*, Phys. Rev. A, **65** (2002).
- [2] E. P. Benis, *et al.*, Phys. Rev. A, **75** (2006).

Laser induced dynamics in the Shin-Metiu-Engel model: controlling singlet-triplet transition with the non-resonant Starck effect

P. Vindel-Zandbergen¹, I.R. Sola¹, M. Falge², and V. Engel²

¹*Departamento de Química Física I. Universidad Complutense de Madrid, 28040 Madrid, Spain*

²*Institut für Physikalische Chemie. Universität Würzburg, Am Hubland, 97074 Würzburg, Germany*

Corresponding Author: p.vindel.zandbergen@gmail.com

The control of chemical reactions by means of ultrashort laser pulses is an area of great interest. Over the past years significant developments have been made in using the quantum properties of light and matter to control the dynamics of molecular processes [1]. Using the properties of quantum interference we can achieve an unprecedented degree of control over the dynamics from simple atomic systems to complex biological molecules [2].

As a first approximation, we can view the control as the quest of frequencies and intensities of a laser pulse or a sequence of laser pulses that lead us to the desired products. For this end, multiple control schemes have emerged in which the laser can "drive" the system [3]. The non-resonant dynamic Stark effect (NRDSE) scheme is a simple but very general method that uses non-resonant electromagnetic fields to induce large time-dependent Stark-shifts in the energy levels. This scheme is used in many current experiments to hold and align molecules, to shape potential energy surfaces, influencing the outcome of photodissociation reactions at conical intersections [4]. As an interesting application of the NRDSE it is significant the optical control of the singlet-triplet transition, where the scheme is used to efficiently couple or decouple an intramolecular process that is not directly affected by the light [5]. In general, as the influence of the laser pulse is to second-order of the field, one needs to use quite strong laser pulses. It is thus important to evaluate the effect of multi-photon processes, and more importantly, the influence of tunneling ionization, which is rarely negligible with the use of strong low-frequency pulses.

In the present work, the NRDSE scheme is implemented to control the singlet-triplet transitions in a simple but very general model. The Shin-Metiu-Engel Hamiltonian [6,7] models the behavior of two electrons in an ion string with one moving ion, including spin exchange interactions between the singlet and triplet states. In spite of the simplicity of forcing one-dimensional (aligned) particle motion in screened Coulomb potentials, the model permits evaluating different levels of approximations. We implement the NRDSE scheme to stop or force the singlet-triplet transition working with very few potentials, with a large set of electronic potentials within the Born-Oppenheimer approximation, and by a full 3D Quantum propagation, including non-adiabatic couplings.

References

- [1] R. S. Judson, and H. Rabitz, *Phys. Rev. Lett.* **68**, 1500–1503 (1992)
- [2] T. Brixner *et al.*, *Nature* **434**, 625–628 (2005)
- [3] P. Brumer, and M. Shapiro, *Chemical Physics Letters* **126**, 541–546 (1986)
- [4] B. J. Sussman, D. Townsend, M. Y. Ivanov, and A. Stolow, *Science* **314**, 278–281 (2006)
- [5] J. Gonzalez-Vazquez, I. R. Sola, J. Santamaria, and V. S. Malinovsky, *J.Chem.Phys.* **125** 124315 (2006)
- [6] S. Shin, and H. Metiu, *J.Chem.Phys.* **102**, 9285–9295 (1995)
- [7] M. Erdmann, E. K. U. Gross, and V. Engel, *J.Chem.Phys.* **121**, 9666–9670 (2004)

Index by author

- Öztürk, I.K. 137, 147, 167
- Addis, C. R. J. 57
- Agueny, Hicham **63**
- Aguilar, A. 185
- Aguilera, J.A. 155
- Ahmdai, A. 171, 172
- Al-Shemmary, A. 14
- Albinsson, I. 215
- Alijah, A. 48, 181
- Alioua, K. 109, 124
- Alkaskas, A. **108**
- Alps, K. 168
- Alton, R. M. 185
- Andersson, J. 79
- Andersson, P. **176, 195**
- Andjelkovic, Z. 166
- Andler, G. 68
- Angom, D. 132
- Angonin, M.-C. 67
- Angulo, J.C. **82**
- Anisimova, G.P. 158
- Antolín, J. 82
- Aragón, C. 155
- Argenti, L. 177, 229
- Arita, Y. **46**
- Arndt, M. 47
- Arnold, C. L. 50
- Arnold, C. L. 34, **218, 231**
- Auzinsh, M. 91, 95, 101
- Avchyan, B.R. 202
- Avetissian, H.K. **202**
- Axner, O. 99, 102, 103
- Ayuso, D. **177**
- Bäckström, E. 148
- Bäck, T. 36
- Başar, Gö. 137, 147, 167
- Başar, Gü. 147, 167
- Başkan, H. 74, 75
- Bagudà, J. 45
- Bahri, H. **83**
- Bahri, M. 83
- Balogh, I. 218, 231
- Baluja, K.L. 84, 100
- Ban, T. 115
- Bang, N. H. 154
- Baranov, A.V. 199
- Barday, R. 36
- Bassi, M. **84**
- Baudon, J. 114
- Bayerl, J. 111
- Beaufils, Q. 67
- Ben-Itzhak, I. 219
- Bengtsson, P. **128**
- Benseny, A. **45**
- Berengut, J.C. **39, 129, 130**
- Bergschneider, Andrea 17
- Bergues, B. **219**
- Berrah, N. **3, 185**
- Berzins, A. 95, 101
- Betsch, K. J. 219
- Bezuglov, N. N. 205
- Bharadia, S. 166
- Biémont, E. 96
- Billy, J. **43**
- Bilodeau, R. C. 185
- Birkel, G. 166
- Birzniece, I. 157
- Bismut, G. 44
- Björkhage, M. 68
- Blaum, K. 26, 149
- Blom, M. 68
- Blondel, C. **178**
- Bocvarski, V. 114
- Bodart, Q. 52
- Bohachov, H. **85**
- Bolorizadeh, M. A. **86–88**
- Borbély, S. **220, 221**
- Borbely, Joe. **53**
- Borovik, A. 163
- Bouazza, M.T. **109, 124**
- Boudon, V. 105
- Bouledroua, M. 109, 124
- Boustimi, M. 114
- Bouvier, P.A. 82, **214**
- Brännholm, L. 68
- Brasovs, A. 135
- Breschi, E. 146
- Brizuela, F. 228, 233
- Brown, A. C. **222**
- Bruvelis, M. 205
- Bulleid, N. E. 123
- Busaite, L. **131**
- Bussery-Honvault, B. 105
- Butler, K. L. **110**

Bylicki, M.	194	Drozdova, A.	135
Cacciapuoti, L.	52	Dubois, Alain	63
Campbell, E.E.B.	4	Ducloy, M.	114
Camus, N.	219	Dung, N. T.	154
Cancio Pastor, P.	54	Dutier, G.	114
Carette, T.	35, 142	Duxbury, G.	48, 181
Carlström, S.	223, 232	Dzuba, V.A.	39, 65
Carpenter, K.	179	Dugocki, K.	119
Cederquist, H.	68	Efimov, D.	205
Cederwall, B.	36	Ehlers, P.	99, 102
Cerins, H.	120	Eikema, Kjeld	53
Chaltykyan, V.	113, 203	Ekers, A.	205
Champanois, C.	208	Eklund, M.	33, 182
Champion, C.	116	Ekman, J.	128, 136
Chartkunchand, K.C.	179	Eland, J.H.D.	51
Chattopadhyay, S.	132	Elantkowska, M.	134, 141
Chervenkov, S.	111	Emelin, M. Yu.	224, 225
Chi, H.-C.	133	Enders, J.	36
Chou, H.-S.	133	Engel, V.	234
Chuluunbaatar, O.	183, 184	Englert, B.G.U.	40
Cininch, A.	89	Enzonga Yoca, S.	96
Cohen, S.	62, 180	Er, A.	137
Consolino, L.	54	Ernst, Wolfgang E.	37
Constantin, Florin Lucian	59	Eronen, T.	149
Continetti, R. E.	186	Eshniyazov, V.E.	170
Cornish, S. L.	110, 126	Esquivel, R.O.	207
Covington, A. M.	179	Föhlisch, A.	79
Crespo López-Urrutia, J.R.	64, 125	Falge, M.	234
Crozet, P.	135	Fathi, R.	86–88
Curran, S. J.	112	Fedorov, A.V.	199
Dörner, R.	184	Feifel, R.	51
Dörre, N.	47	Ferber, R. 91, 95, 101, 117, 120, 135, 137, 147, 157, 162, 167, 168	
Düsterer, S.	14, 78	Fertl, M.	90
Dahlström, J. M.	34, 35 , 228	Fescenko, I.	91
Dal Cappello, C.	116, 192	Fischer, B.	219
Danared, H.	68	Flambaum, V.V. ...	39, 65 , 129, 130, 138 , 139
Danielson, J. R.	92, 186	Florko, T. A.	140
Davis, V. T.	179	Fordell, T.	34
Davlatova, O.A.	158	Forstner, O.	176, 195
De Natale, P.	54	Friedman, R.M.	20
Decleva, P.	177	Fritzsche, S.	19, 76, 187, 189
Dehesa, J.S.	207 , 214	Froese Fischer, C.	122, 144
Delsing, P.	10	Frolov, M. V.	56
Dembczyński, J.	134 , 141	Güzelçimen, F.	147 , 167
Demir, G.	147	Głowacki, P.	141
Depret, T.	164	Gahbauer, F.	95, 101
Dholakia, K.	46	Gaigalas, G. ...	42, 76, 108, 122, 128, 143, 144
Dicle, Y.	74 , 75	Galstyan, A.G.	183 , 184
Dimitriou, A.	62 , 180	Gazazyan, A.	113
Docenko, O.	117, 157, 168	Gazazyan, E.	113 , 203
Drag, C.	178		
Drewsen, M.	64, 125		

Gel'mukhanov, F.	79	Hilico, A.	67
Genov, G. T.	210	Hinds, E. A.	22, 123
Gensch, M.	14	Hogan, S. D.	38
Geyer, P.	47	Hoogerland, Maarten	53
Ghazaryan, A.G.	202	Hopkins, S. A.	110, 126
Gibson, N. D.	185 , 198	Houamer, S.	184
Gingell, A. D.	64 , 125	Houssin, M.	208
Gisselbrecht, M.	34, 35, 50, 80, 218	Hudson, J. J.	22
Gisufredi, G.	54	Huldt, S.	148
Glöckner, R.	40	Hultgren, H.	33 , 182, 191
Glushkov, A.-V.	204 , 226	Hundertmark, A.	14, 78
Godefroid, M.	76 , 122, 142–144	Hutchinson, S.	32
Golser, R.	176, 195		
Gonoskov, A.	55	Ibragimov, I.Kh.	170
Gonoskov, I.	55	IJsselsteijn, R.	97, 98
Gorceix, O.	44	Indelicato, P.	76
Goto, M.	227	Inguscio, M.	54
Gribakin, G. F.	65, 92 , 186	Ipek, N.	74, 75
Griesmaier, A.	43	Isacsson, A.	215
Grigoryan, G.	203	Isaksson, O.	188
Grimm, R.	7	Ivanov, S. I.	210
Grochola, A.	145		
Grujić, Z. D.	94, 146	Jönsson, P. 42, 76, 108, 122, 128, 136, 143, 144	
Grum-Grzhimailo, A. N.	19 , 187	Jönsson, L.	104
Grumer, J.	42 , 136	Jakubassa-Amundsen, D.	36
Gryzlova, E. V.	19, 187	Jarmola, A.	137, 147, 167
Guénot, D.	50	Jarosz, A.	141
Guénot, D.	34 , 35, 218, 231	Jastrzębski, W.	145, 154
Gusev, A.A.	184	Jelassi, H.	121
Gustafsson, S.	128	Jelenkovic, B.	211
		Jiménez-Galán, A.	229
Händel, S.	126	Jochim, Selim	17
Höcker, M.	149	Johnson, N. G.	219
Hagel, G.	208	Johnsson, P.	14 , 34, 78, 228, 233
Hakhumyan, G.	156, 160	Jona-Lasinio, M.	43
Hamamda, M.	114	Jones, A. C. L.	92
Hangst, J.	11	Jones, R. R.	219
Hansen, A. K.	125	Jungen, Ch.	48, 181
Hansen, K.	64, 227		
Hanstorp, D.	33, 182, 185, 188, 191	Kübel, M.	219
Harabati, C.	65	Kłosowki, L.	64
Hardy, J.	29	Kabachnik, N. M.	19, 77 , 78, 187
Hartman, H.	42, 148	Kada, I.	116
Haslinger, P.	47	Kadau, H.	43
Hedin, L.	51	Kalninsh, U.	93
Heil, W.	94	Kalvans, L.	91, 93, 95 , 101, 131
Helm, H.	182	Kara, D. M.	22
Hendricks, R. J.	123	Karlen, H.	191
Henn, E.	43	Karlsson, L.B.	128
Hennies, F.	79	Karlsteen, M.	188, 215
Herrwerth, O.	219	Karpova, O.V.	173
Hessman, D.	58	Karras, G.	49
Heyl, C.	232	Kashcheyevs, V.	89
Heyl, C. M.	223, 228 , 231, 233	Kashenock, G.	189 , 190

Kasprzak, M.	94, 146	Larsson, M.	68
Kaur, S.	84	Lebedev, V. S.	118
Kazansky, A. K.	77, 78	Lebovitz, A. N.	185, 198
Kellerbauer, Alban	16	Lecointre, J.	164
Kennedy, B.	79	Leiteritz, C.	26
Ketter, J.	149	Leitner, T.	14
Khaplanov, A.	36	Lennartsson, T.	148
Kheifets, A. S.	34	Leontein, S.	68
Khetselius, O. Yu.	150, 151	Leopold, T.	28
Khoa, D. X.	154	Leroy, C.	156, 160, 161
Khokhlova, M.	55, 230	Li, J. G.	76, 142
Khoshimova, F.	174	Li, Y.-G.	185
Kirova, T.	205	Liebl, K. J.	198
Kiss, G. Zs.	221	Lien, Y.-H.	52
Kiyan, I. Yu.	33, 182, 191	Liljebj, L.	68
Klinder, K.	34, 35	Lindahl, A. O.	191
Klapstein, D.	48	Lindroth, E.	34, 35
Klincare, I.	168	Lindstrøm, C.	27
Kling, M. F.	219	Linusson, P.	51
Klinkhamer, Vincent	17	Loboda, A. V.	193
Knoop, M.	208	Lompe, Thomas	17
Knowles, P.	94, 146	Lorek, E.	223, 232
Koch, H.-C.	94 , 146	Lou, S. E.	185
Koch, Markus	37	Lu, Z.T.	18
Koga, T.	207	Lucic, N.	211
Komasa, J.	152 , 159	Lyras, A.	62, 180
Kortyna, A.	153	Lysaght, M.A.	32
Kosmidis, C.	49	Löfgren, P.	68
Koussa, H.	83	Müller, S.	43
Kowalczyk, P.	145, 154	Mérot, J.	66
Kröger, S.	137, 147, 167	Månsson, E. P.	50 , 80, 218
Kracke, H.	26	Maier, J.-P.	48
Kraft, A.	94	Maier, T.	43
Kraus, P. M.	23	Majtey, A.P.	214
Krausz, F.	2 , 219	Makhoute, Abdelkader	63
Kregar, G.	115	Manakov, N. L.	56
Krmpot, A.	211	Mani, B. K.	132
Krois, Günter	37	Mannervik, S.	68, 148
Kroon, D.	34, 50, 218, 228, 231	Manrique, J.	155
Kruzins, A.	168	Mansouri, A.	116
Krzykowski, A.	141	Mansten, E.	233
Kuhn, R.	48	Maquet, A.	34, 35
Kupliauskiene, A.	163	Marchant, A. L.	126
Källberg, A.	68	Marechal, E.	44
Källersjö, G.	68	Marouani, S.	83
Kpper, J.	119	Martín, F.	177, 229
L'Huillier, A.	35, 50, 218, 228, 231, 233	Martensson, A.-S.	216
Laburthe-Tolra, B.	44	Martschini, M.	176, 195
Lackner, Florian	37	Matrasulov, D.U.	170
Laksman, J.	80	Mattiasson Ando, V.	188
Lamoudi, N.	109, 124	Matveev, V.I.	173
Lamour, E.	66	Matyakubov, F.Sh.	173
Larsen, E. W.	223	Matyas, D. J.	185, 198

Mauritsson, J.	34, 35, 223, 232	Palecek, D.	223, 232
Mazilu, M.	46	Palmeri, P.	96
Mazur, E.	9, 24	Papoyan, A.	160
Meijer, G.	5	Parker, J. S.	222
Menas, F.	192	Pashayan-Leroy, Y.	156, 160, 161
Merkt, F.	38, 60	Pasquiou, B.	44
Meshkov, V.	117, 206	Paulus, G. G.	219
Meyer, H.-G.	97, 98	Pawlak, M.	194
Meyer, M.	78	Pazyuk, E.	117, 120 , 168, 206
Mezdari, F.	66	Paál, A.	68
Miculis, K.	205	Pedregosa-Gutierrez, J.	208
Miranda, M.	34	Pedri, P.	44
Mironchuk, E. S.	118	Pegg, D. J.	191
Mirzoyan, R.	156 , 161	Pelle, B.	67
Mkrtchian, G.F.	202	Perales, F.	114
Moiseyev, N.	194	Pereira Dos Santos, F.	67
Mompart, J.	45	Petryla, A.	42
Mooser, A.	26	Pfau, T.	43
Morizot, O.	208	Pfeifer, T.	219
Moshammer3, R.	209	Pietzsch, A.	79
Mozers, A.	95, 101	Piroux, B.	183
Mucke, M.	51	Plésiat, E.	177
Mullins, T.	119	Plastino, A.R.	207, 214
Murmann, Simon	17	Poli, N.	41
Mårtensson-Pendriell, A.-M.	69	Polischuk, V.A.	158 , 199
Mller, N.	119	Polovinkin, V. A.	225
Nörtershäuser, W.	166	Poltoratska, Yu.	36
Nadgaran, H.	171, 172	Popov, A. M.	56
Nagy, L.	209, 220, 221	Popov, Yu.V.	183, 184
Narits, A. A.	118	Pratt, R.	190
Natisin, M. R.	92	Prehn, A.	40
Nazé, C.	76, 143	Prevedelli, M.	52
Neill, P.	179	Prigent, C.	66
Nemouchi, M.	142	Priller, A.	176, 195
Nikolayeva, O.	120, 157 , 162, 168	Pruvost, L.	121
Nikolic, S.	211	Puchalski, M.	159
Nilsson, H.	148	Quinet, P.	96
Nimmrichter, S.	47	Quint, W.	26, 166
Noda, K.	196	Röhlsberger, R.	25
Nohlmans, D.	123	Radcliffe, P.	78
Noormandi, A.	171, 172	Radeonychev, Y. V.	225
Ohlén, G.	58	Rading, L.	14, 78 , 228, 233
Ong, A.	39	Radonjic, M.	211
Oriols, X.	45	Rakhimov, Kh.Yu.	173, 174
Osmanoglu, Ş.	74, 75	Rakowski, R.	233
Osmanoglu, Y.E.	74, 75	Rathje, T.	219
Otajanov, D.M.	174	Reggami, L.	109, 124
Ouk, Ch.-M.	105	Reinhard, P.	68
Péllisson, S.	67	Rempe, G.	40, 111
Pachucki, K.	54, 152, 159	Rensfelt, K.-G.	68
Palacios, A.	177	Renström, R.	21
		Reuschl, R.	66

Ries, Martin	17	Seiler, Ch.	38
Ristinmaa Sörensen, S.	50, 80, 148, 218	Senftleben, A.	219
Robinson, D. R.	222	Shearer, S. F. C.	57
Rodegheri, C.	26	Shojaei-Akbarabad, F.	86–88
Rodewald, J.	47	Siddiqui, I.	165
Rohlén, J.	191, 198	Sikandar, R.	165
Rohlfes, A.	111	Silaeu, A. A.	56
Roman, V.	163	Silander, I.	99 , 102
Rosén, A.	215	Simonet, Juliette	53
Rosi, G.	52	Simonsson, A.	68
Ross, A.	135	Simulik, V.M.	197
Rosén, S.	68	Sindelka, M.	194
Rouzée, A.	14, 78	Singh, J.	100
Rozendaal, Roel	53	Skoff, S. M.	123
Rozet, J.-P.	66	Smallman, I. J.	22
Rubensson, J.-E.	79	Smirnov, L. A.	224
Ruczkowski, J.	134, 141	Sola, I.R.	234
Rudawski, P.	228, 233	Sommer, C.	111
Rupenyan, A.	23	Sorrentino, F.	52
Ryabikin, M. Yu.	55, 224, 225	Spiss, A.	101
Rynkun, P.	122 , 143, 144	Sprecher, D.	60
Sütçü, K.	74, 75	Starace, Anthony F.	56
Sánchez-Moreno, P.	214	Starikov, E. B.	196
Sadeghi, M.	86–88	Steier, P.	176, 195
Sahoo, B.	25	Steydli, S.	66
Saidov, A.A.	170	Stojanovic, N.	14
Saito, M.	196	Stolyarov, A.	117, 120, 135, 168 , 206
Sankari, A.	80	Strelkov, V.	55 , 230
Santic, N.	115	Streubel, S.	149
Santos, L.	43	Stringari, S.	6
Sargsyan, A.	160 , 161	Strocov, V. N.	79
Sarkisyan, D.	156, 160, 161	Sun, Y.-P.	79
Sauer, B. E.	22, 123	Surko, C. M.	92, 186
Sayler, A. M.	219	Surzhykov, A.	36
Schöffler, M.S.	184	Szczepkowski, J.	145, 154
Schässburger, K.-U.	36	Tóth, A.	220
Schioppo, M.	41	Tóth, I.	209
Schlage, K.	25	Tőkési, K.	220
Schlappa, J.	79	Taïeb, R.	34, 35
Schmidt, H. T.	68	Tackmann, G.	67
Schmidt, L.Ph.H.	184	Taillandier-Loize, T.	114
Schmidt, P. O.	125	Talbi, F.	109, 124
Schmidt-Böcking, H.	184	Tamanis, M.	91, 117, 120, 135, 137, 147, 157, 162 , 167, 168
Schmitt, A.	28	Tanabe, T.	196
Schmitt, M.	43	Tarbutt, M. R.	22 , 123
Schmitt, T.	79	Tarchouna, Y.	83
Schneider, J.	23	Tashenov, S.	36
Scholtes, T.	97 , 98	Tastevin, G.	15
Schultze, V.	97, 98	Tavella, F.	14
Schwarz, M.	64, 125	Taylor, K. T.	222
Schwenke, J.	233	Tennyson, Jonathan	8
Scribano, Y.	105	the nEDM collaboration,	90
Segal, D. M.	123, 166		

the SOC team,	41	Walsh, N.	80
Thomas, R. D.	68	Walter, C. W.	185, 191, 198
Thompson, J. S.	179	Walz, J.	26
Thompson, R.C.	166	Wang, J.	99, 102 , 103
Tiemann, E.	162	Weaver, H.	153
Tikhonova, O. V.	56	Weidow, J.	215
Tino, G. M.	41, 52	Weis, A.	94, 146
Titze, J.	184	Welander, J.	191
Torosov, B. T.	210	Wendt, K.D.A.	28
Trassinelli, M.	66	Wenz, Andre	17
Trippel, S.	119	Wernet, Ph.	14
Tymchyk, R.	85, 163 , 197	Westberg, J.	103
Uddin, Z.	165	Whiting, M. T.	112
Ullrich, J.	64, 125, 219	Wiesel, M.	166
Ulmanis, J.	205	Wiles, T. P.	126
Ulmer, S.	26	Wille, H. C.	25
Urbain, X.	164	Windberger, A.	64, 125
van der Hart, H.W.	32 , 222	Windholz, L.	165
Van Dyck, Jr., R. S.	149	Woetzel, S.	97, 98
van Rooij, Rob	53	Wolf, P.	67
Vandevraye, M.	178	Wu, X.	111
Vassen, Wim	53	Yáñez, R.J.	207
Verdebout, S.	42, 122, 136, 143, 144	Yapıcı, B.	167
Vernac, L.	44	Yerokhin, V.	36, 54
Vernhet, D.	66	Yousif Al-Mulla, S. Y.	104
Versolato, O. O.	64, 125	Yu, M. M. H.	126
Vindel-Zandbergen, P.	234	Zafar, R.	165
Vitanov, N. V.	210	Zajac, T.M.	197
Vogel, M.	166	Zeppenfeld, M.	40, 111
Volkova, E. A.	56	Zettergren, H.	68
von Lindenfels, D.	166	Zigmantas, D.	223, 232
von Otter, A.-M.	215	Zincircioğlu, B.	74, 75
Vracking, M. J. J.	14, 78	Zlatkovic, B.	211
Vujicic, N.	61	Zlatov, A.S.	199
Vvedenskii, N. V.	56	Zuters, V.	117
W. Larsen, E.	232	Zvereva-Loëte, N.	105
Wörner, H. J.	23	Zürn, Gerhard	17

